UNIVERSITY OF TROMSØ UIT

FACULTY OF SCIENCE AND TECHNOLOGY
DEPARTMENT OF GEOLOGY

Landform Assemblages in Inner Kongsfjorden, Svalbard: Evidence of Recent Glacial (Surge) Activity

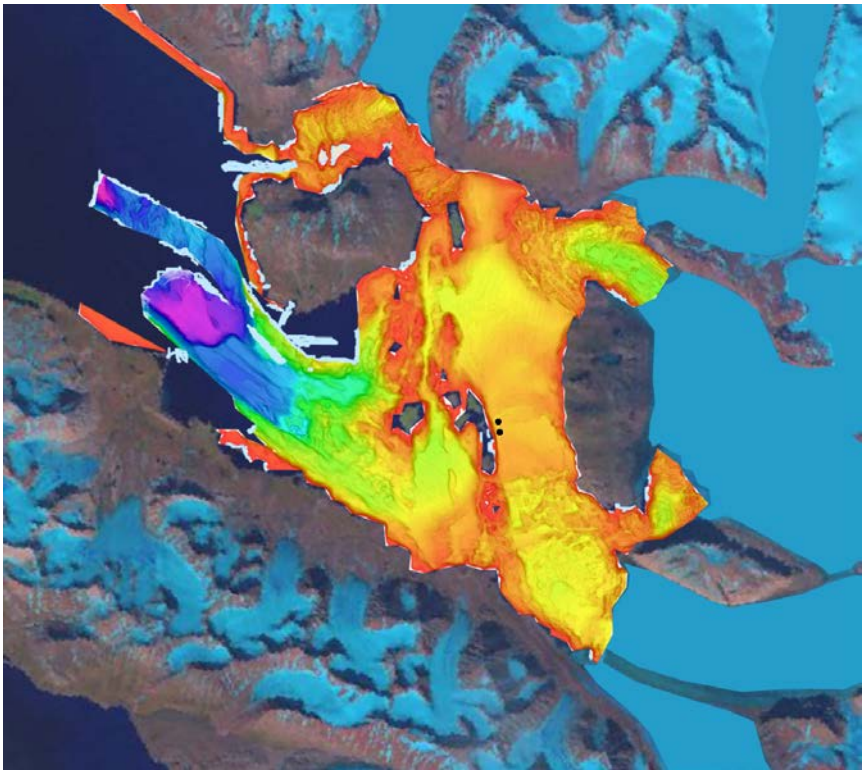

Katharina Streuff

GEO-3900 Master's Thesis in Geology

May 2013

GEO-3900

MASTER'S THESIS IN GEOLOGY

Landform Assemblages in Inner Kongsfjorden, Svalbard: Evidence of Recent Glacial (Surge) Activity

Katharina Teresa Streuff

May, 2013

FACULTY OF SCIENCE AND TECHNOLOGY

Department of Geology

University of Tromsø

Abstract

Swath bathymetry and chirp data have been used to investigate the submarine landform assemblages in inner Kongsfjorden, Svalbard, to reconstruct glacial dynamics during the Late Holocene. Multiple sets of landforms include two types of glacial lineations (groove-ridge features and small, drumlinoid ridges), terminal moraines and associated debris lobes, as well as small push moraines, and indicate repeated surge activity during the last 150 years for four of the five tidewater glaciers terminating in inner Kongsfjorden. Aside from confirming previously documented surges of Kronebreen in 1869, of Kongsvegen, in 1948, and of Blomstrandbreen in 1960, the local bathymetry also indicates a surge of Kongsbreen in 1897, a glacier that has so far been regarded as a non-surge type glacier.

A conceptual model was developed to summarize the surge-induced landform assemblages in Kongsfjorden, and to compare them with other models from terrestrial and marine settings. Striking similarities exist between the Kongsfjorden model and landform assemblages documented for other Spitsbergen fjords. However, eskers and crevasse-fill ridges, the latter thought to be the only landform certainly indicative of glacier surges, lack in Kongsfjorden. Furthermore, the small, drumlinoid ridges inferred to be suggestive of the past ice flow direction in the study area seem to have more in common with glacial lineations generated by surging glaciers on land.

The acoustic data was supplemented with two sediment cores from Kongsfjorden's innermost basin. The reworked glacimarine deposits at the base of the more proximal core reflect proximal conditions, as they are part of a debris lobe that formed on the distal flank of the terminal moraine deposited during the 1948 surge of Kongsvegen. The stratified muds from the second core contain varying amounts of clasts and also occur on top of the debris lobe. They reveal a relatively distal glacimarine environment mainly influenced by suspension settling from turbid meltwater emanating from Kronebreen or Kongsvegen. Geochemical fluctuations indicate temporal variations in the sediment supply from the two glaciers after 1948.

The few landforms in the outer parts of the study area suggest glacial activity unrelated to the glacier surges. Together with the landforms previously documented from outer Kongsfjorden and its adjacent trough (Kongsfjordrenna), the mega-scale glacial lineations in the outer part of the study area indicate part of a landform assemblage deposited from a fast-flowing ice stream during the Last Glacial Maximum.

Acknowledgements

As this thesis was an important part of my life for the past two years, I am grateful to everybody who supported me throughout this project.

My special thanks first and foremost, go to my two supervisors, Prof. Dr. Karin Andreassen and Dr. Matthias Forwick. Karin, I am very grateful for the opportunity to work with you on such a fascinating dataset and for the input you gave me throughout this time. You pushed or praised me at exactly the right moments and I sincerely thank you for your guidance throughout the past year. Matthias, this thesis would not have been half of what it is without you. Your endless patience, your dedication, your detailed and very constructive comments as well as your ability to calm me down in times of stress were extremely helpful and I am glad you were there for me throughout all of it. Thank you!!

Trine Dahl and Ingvild Hald were willing to help out throughout my lab work in Tromsø by answering all my questions and assisting me as much as they could. My thanks go to them especially for taking care of my grain size analysis when I was away.
Winfried Dallmann provided me with useful tips and helped me out a lot concerning the geological map.

My best friend in Tromsø, Livia Nardini, deserves special thanks for sticking around during some of my worst times ☺. You were a huge help, both, in giving constructive advice, hugs when I needed them, or just trying to help out when, once again, Word was against me. The lunch breaks in the sun, tea breaks in the kitchen and the occasional relaxed movie nights were not only fun, but necessary and I am grateful that you were there for me.
I am thankful to my other friends as well, who did not give up on me and were patient when times were stressful. Astrid, a big thanks to you for reading through my thesis and making sure I got out of the house every once in a while for a lovely dinner :). Pete, thank you for an amazing (!!) extended study break and your last-minute input!

And finally: having parents who support me in whatever I do and have faith in me even when I am frustrated to no end and start doubting everything, is one of the best and most important things in my life. I wouldn't be able to do half of what I do without you.

I am extremely grateful!

Katharina Streuff
Tromsø, May 2013

Table of Contents

1. Introduction

1.1 Objectives

This master thesis aims to reveal the past glacial processes and sedimentary environments of inner Kongsfjorden by addressing

1) The geomorphological features in inner Kongsfjorden,
2) The relationship between these landforms and the activity of the local glaciers,

and as supplementary information:

3) The sedimentological information from two gravity cores, its reflection of the glacial activity, and the extent to which this information mirrors the results of the acoustic data.

1.2 Background

The data used for this thesis was acquired by the GlaciBar project led by the University of Tromsø with the aim of improving the knowledge about the Barents Sea geological evolution during the Late Cenozoic.

The thesis is part of a collaboration between the department of Geology at the University of Tromsø, the Framsenteret (Norsk Polarinstitutt) in Tromsø and the University of Hamburg, Germany.

As the polar areas and their ice dynamics have become a major focus of climatic research in the past decades, interest in Arctic fjords, especially around Svalbard, has grown. This is partly due to the fact that glaciers in the higher latitudes are initially more likely to withstand small changes in climate, since the low sun angle in the polar areas allows for lower temperatures and less available energy to melt the ice (Benn & Evans, 2010). Nevertheless, the current warming of the global climate begins to show its effects, even in the polar areas (e.g. Dowdeswell et al., 1997; Kohler et al., 2007). Investigating glaciers and their behaviour at these latitudes may therefore allow for the reconstruction of the past and a better understanding of Earth's future.

Fjords play a key role in the reconstruction of glacial history. A fjord is a valley that was carved out by glacial activity and marks a contact zone between marine and terrestrial environments (Howe et al., 2010). Due to their half-enclosed nature fjords provide an archive for records of glacial activity and

related sedimentary processes. The sediments deposited in the fjords and the landforms generated by the glaciers around them are generally unmodified and well-preserved and are therefore invaluable for climatic research.

The sub-polar fjords in the Spitsbergen area are known to have undergone a complex history of glaciation and deglaciation (Elverhøi et al., 1995; Landvik et al., 1998; Jessen et al., 2010). Even today the numerous glaciers and their different characteristics influence the geology of terrestrial as well as submarine settings. Recently, the behaviour of surging glaciers has been of particular interest, as these glaciers can exhibit rapid ice advances (surges) independent of today's climate change (e.g. Meier & Post, 1969; Raymond, 1987; Dowdeswell et al., 1995; Gilbert et al., 2002). The geomorphic landforms left by these glaciers yield valuable information, eventually leading to a more qualified interpretation of the Pleistocene record (e.g. Bennett et al., 1999) and a better understanding of the glaciers' behaviour when subjected to an increasingly warmer environment. Due to its location in a high-latitude area and the prevailing oceanographic conditions the study area of Kongsfjorden, western Svalbard, is particularly sensitive to climate change and is especially interesting for scientific research (e.g. Lamb, 1977; Svendsen et al., 2002; Howe et al., 2003; Hald et al., 2004; Trusel et al., 2010).

1.3 Previous Work

1.3.1 Glacial History of the Western Svalbard Margin

The reconstruction of the glacial history of the Svalbard archipelago and its surroundings has been attempted by numerous authors (e.g. Birks et al., 1994; Elverhøi et al., 1995; Hald et al., 2004; Baeten et al., 2010; Dowdeswell et al., 2010; Jessen et al., 2010; Forwick & Vorren, 2011a) but a generalization remains difficult due to the manifold methods and locations used for the studies. Landvik,et al. (1998) presented a good overview of the results up until 1998.

Even though different ages have been reconstructed for the three main events (a) ice advance, (b) full glaciation, and (c) ice retreat, the majority of sources indicate a five thousand-year long ice advance. Elverhøi et al. (1995), for example, suggest the ice advance to have happened in two phases about 22 000 ^{14}C years BP and again at 18 000 ^{14}C years BP, where ice spread beyond the coastline and extended to the shallow western continental shelf (Landvik et al., 1998). Jessen et al. (2010) suggest that advance began about 5 000 years earlier at 32 000 calendar years before present (cal yrs BP, 27 000 ^{14}C yrs BP) and to last until 27 000 cal yrs BP (22 500 ^{14}C yrs). Full glaciation is assumed to have lasted for 3000 to 5 000 ^{14}C yrs, between 19 000 and 15 000 ^{14}C yrs BP, when the ice reached

the shelf break (Landvik et al., 1998). During this time fast-flowing ice streams drained the Svalbard-Barents Sea ice-sheet via the main fjord systems on Svalbard (Figure 1.1). The active ice streams were separated by areas characterized by slower and less dynamic ice flow (inter-ice-stream areas; e.g. Landvik et al., 2005; Ottesen et al., 2005; Ingólfsson & Landvik, 2013). Kongsfjorden, Bellsund and Isfjorden were the main channels for the fast-flowing ice streams along the western coast of Svalbard, whereas Woodfjorden, Wijdefjorden, and the Hinlopen Strait represented the main pathways in the north Ottesen et al., 2007).

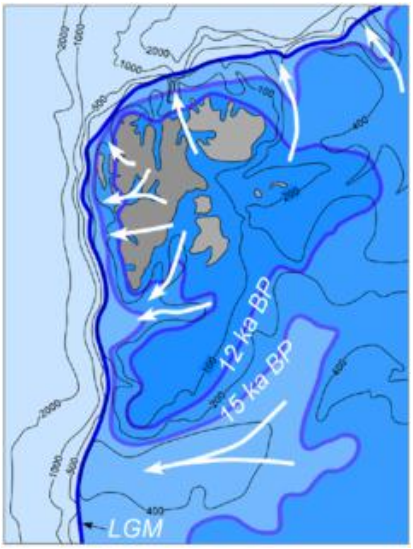

Figure 1.1: Reconstructed margins of the Svalbard-Barents Sea ice-sheet at the Last Glacial Maximum and during two stages of deglaciation: 15 000 ^{14}C yrs BP and 12 000 ^{14}C yrs BP (Ingólfsson & Landvik, 2013).

Deglaciation and accompanied retreat began around 17 700 cal years BP. Again, Elverhøi et al. (1995) suggest a second phase of ice recession from 13 000 to 12 000 ^{14}C yrs, when the ice reached the fjord mouths along the western coast of Spitsbergen (Elverhøi et al., 1995; Landvik et al., 1998). Generally, the deglaciation period is suggested to have lasted until approximately 11 300 cal years BP, its final stage being characterized by repeated still-stands and re-advances (e.g. Elverhøi et al., 1995; Baeten et al., 2010; Forwick & Vorren, 2011a). The Svalbard coasts and fjords are believed to have been ice-free by around 10 ^{14}C yrs BP (Landvik et al., 1998; Ingólfsson & Landvik, 2013). An interruption in general retreat is assumed to have been caused by a minor re-advance at 14 500 cal years BP (Elverhøi et al., 1995; Landvik et al., 1998; Ottesen et al., 2005; Jessen et al., 2010), though the magnitude of its extent in the western Svalbard areas is still debated. Another re-advance during the Younger Dryas cooling was suggested by Boulton (1979) and Svendsen et al. (1996) for the central Spitsbergen area, but remains uncertain due to the lack of geomorphological evidence. A core retrieved from the Kongsfjorden trough revealed ice-proximal settings during the Younger Dryas, which supports the theory of a small advance during that time (Skirbekk et al., 2010).

During the Holocene retreat is suggested to have occurred stepwise, as reconstructed from geomorphic landforms and sediment cores (e.g. Ottesen & Dowdeswell, 2009; Forwick & Vorren, 2009; Baeten et al., 2010; MacLachlan et al., 2010; Forwick & Vorren, 2011a). The reduced glacial activity in the early Holocene is related to a warming trend, which is expected to have lasted for half the Holocene. It was interrupted by shorter intervals of cooler climate (e.g. Hald & Hagen, 1998; Nesje et al., 2005; Forwick & Vorren, 2009). The significant warming is suggested to have reached its maximum between 10 000 and 9 000/8 800 cal yrs BP (e.g Hald et al., 2004; Rasmussen et al., 2007; Forwick & Vorren, 2009) and was probably accompanied by a large temperature gradient between

east and west Spitsbergen (Forwick & Vorren, 2009). This is inferred from the absence of glaciers along the western Spitsbergen coast at that time (Svendsen & Mangerud, 1997). The subsequent cooling around 9 000/8 800 cal yrs BP is suggested to have lasted approximately 5 000 yrs and was responsible for a general increase in glacial activity (e.g. Hald et al., 2004; Rasmussen et al., 2007; Forwick & Vorren, 2009). Depositional evidence from a few sites indicates another significant re-advance during the Little Ice Age (LIA), when glaciers were larger and ice advance stronger than during the Younger Dryas (Mangerud & Landvik, 2007). However, in most cases, this depositional evidence may be buried or overridden by surge-related ice advance, making it difficult to map the LIA extent of Svalbard glaciers. In fact, some glaciers on Spitsbergen have been found to have their maximum Holocene ice extent as a consequence of a surge event, rather than the LIA (e.g. Boulton et al., 1996; Plassen et al., 2004; Ottesen & Dowdeswell, 2006; Forwick et al., 2010).

1.3.2 Previous Investigations in the Study Area

Today about 60% of the Svalbard archipelago is still covered by ice (Figure 1.2; Kohler et al., 2007). Different glacier types exist in the area, most of which are tidewater glaciers terminating in water, but also smaller cirque glaciers and ice fields of polar and subpolar type (e.g. Mangerud & Landvik, 2007). All these glaciers are known to be retreating at different rates (Liestøl, 1975), either by melting or by iceberg calving in the case of tidewater glaciers (e.g. Ottesen & Dowdeswell, 2006; Benn et al., 2007); however, there are a number of them which readvance periodically as a result of a so-called surge. During the active phase of a surge cycle the ice that accumulated in the upper parts of the glacier during the quiescent phase (phase of slow retreat) is rapidly transferred to the lower parts of the glacier, often leading to the glacier's advance (e.g. Meier & Post, 1969).

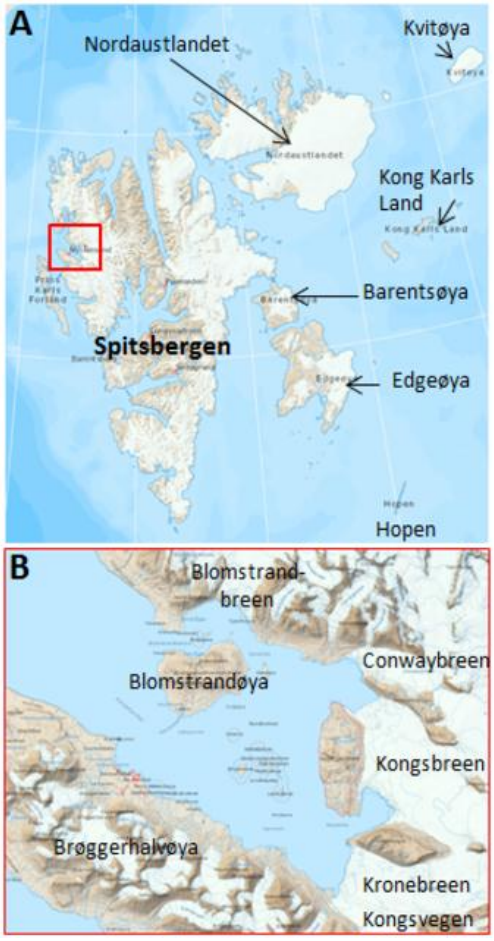

Figure 1.2: Overview map of the Svalbard archipelago and current ice cover with the study area indicated by the red rectangle.

The study area is located on the western coast of Spitsbergen, the largest island of the Svalbard archipelago (Figure 1.2). Kongsfjorden and surroundings are largely influenced by surge-type tidewater glaciers and therefore show a complex interaction between climate, glacier activity,

oceanography and sedimentation. All of these parameters have been investigated and documented up to a certain extent (e.g. Elverhøi et al., 1983; Boulton, 1990; Dowdeswell & Forsberg, 1992; Bennett et al., 1996; 1999; Glasser et al., 2001; Howe et al., 2003; MacLachlan et al., 2010; Trusel et al., 2010; Kehrl et al., 2011), although most investigations focussed only on parts of the fjord, such as the surrounding glaciers, the inner fjord basin, the central and outer parts, or the trough Kongsfjordrenna, which connects Kongsfjorden with its northern neighbour Krossfjorden to a fjord system. Svendsen et al. (2002) composed an overview over all data on Kongsfjorden, which was available up to that time.

Some of the first studies with the focus of Kongsfjorden were conducted in the late 1980s, when Elverhøi et al. (1980 and 1983) investigated the glacial erosion and sedimentation within inner Kongsfjorden in the basin adjacent to the ice front of Kronebreen and Kongsvegen at the head of the fjord (Figure 1.2). The occurrence of meltwater streams carrying large amounts of sediments was recorded and a decreasing rate of deposition of two orders of magnitude was inferred with increasing distance from the glacier front. Similar observations were later made by Trusel et al. (2010) and Kehrl et al. (2011). The former ascribed 20 to 25 % of the total sediment volume within the inner fjord to glacifluvial deltaic runoff from Kongsvegen, whereas the remaining 75 to 80 % were inferred to be provided by a subglacial meltwater stream beneath Kronebreen. The intact structure of heavily bioturbated but nevertheless finely laminated sediments was used as an indicator for the absence of turbidites and related gravity flows; however, signs of sediment creep and chute and slump activity were observed near the ice front (Elverhøi et al., 1983). The transformation of the meltwater streams described by Elverhøi et al.

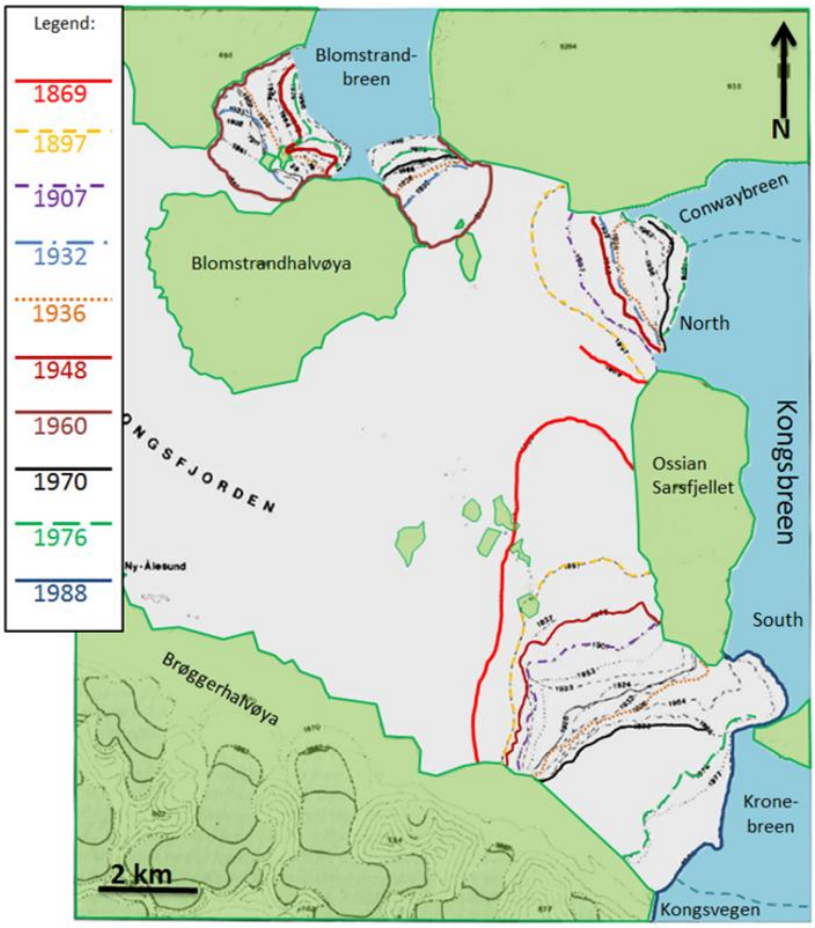

Figure 1.3: Ice front positions in Kongsfjorden during the past 150 years (modified after Liestøl, 1988).

(1983) into turbid brackish meltwater plumes at the sea surface was proposed by Boulton (1990), who furthermore hinted at the deposition of coarse-grained submarine fan bodies in close proximity to the ice margin as a result of suspension settling from these meltwater plumes.

Liestøl (1988) provided an overview over the glaciers in the area around Kongsfjorden. He detailed flow velocities as well as past ice front positions (Figure 1.3) of the most important glaciers in the area: Blomstrandbreen, Conwaybreen, Kongsbreen, Kronebreen, and Kongsvegen (section 2.3.4, below). Surge activity was inferred and documented for Blomstrandbreen, Kronebreen, and Kongsvegen and was again protocolled by Hagen et al. (1993). Kongsbreen enters into the marine milieu at two different locations, which will be referred to as Kongsbreen North and Kongsbreen South (see Figure 1.3) from this point onwards.

The repeated advance of the ice fronts during the respective surges has left a peculiar but characteristic pattern on the floor of the inner fjord basin, which will be the main focus of this thesis. A few landforms have been documented for the area directly in front of the ice margin of Kronebreen and Kongsvegen and are assumed to be the consequence of the glaciers' seasonal ice front oscillations (e.g. Elverhøi et al., 1983; Boulton, 1990; Trusel et al., 2010). The features in the central and outer parts of Kongsfjorden in contrast, including glacial lineations, recessional and lateral moraines, are believed to be mainly of Late Weichselian origin, created when Kongsfjorden served as a major pathway draining the Svalbard-Barents Sea Ice-sheet (Howe et al., 2003; MacLachlan et al., 2010). The mega-scale glacial lineations occurring in Kongsfjordrenna, the trough connecting Kongsfjorden to the open sea, are considered to be indicative of fast ice flow and are therefore associated with the glaciation period (Figure 1.4; Ottesen et al., 2007). This is supported by the occurrence of a lateral ice-stream moraine, a grounding zone wedge, and a terminal moraine inferred to be marking the maximum ice extent during the Late Weichselian.

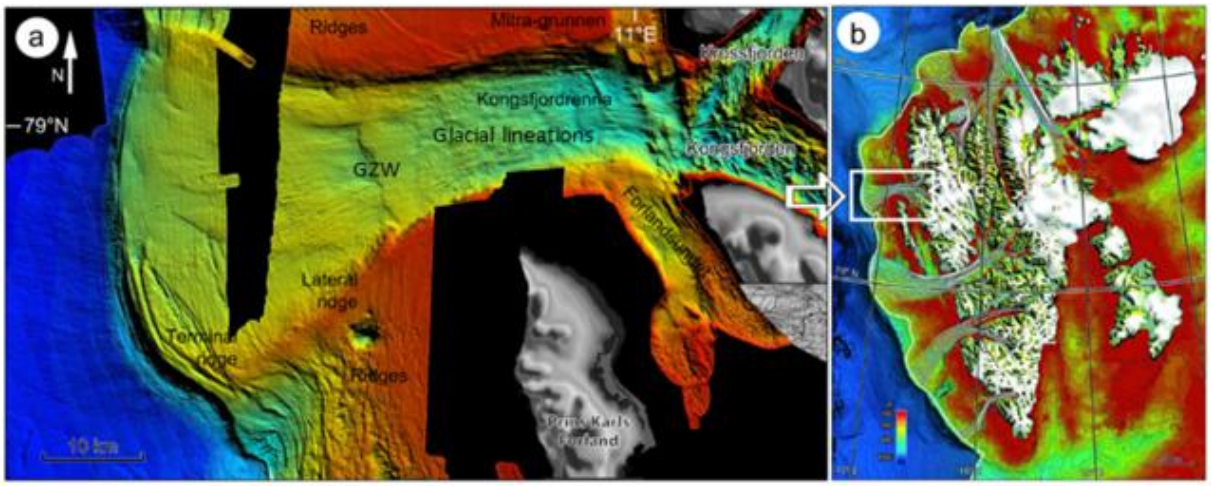

Figure 1.4: Swath Bathymetry of the Kongsfjorden trough with mega-scale glacial lineations, lateral ice-stream ridges, a grounding zone wedge and the terminal moraine marking maximum Late Weichselian ice extent (modified after Ingólfsson & Landvik, 2013).

Based on the geomorphic features occurring in the proximity of many glaciers, conceptual models have been developed to generalize the processes of deposition (e.g. Sharp, 1985; Evans et al., 1999; Evans & Twigg, 2002, Ottesen & Dowdeswell, 2009). Ottesen & Dowdeswell (2006) and Ottesen et al. (2008) have developed a model (Figure 1.5) describing a seafloor characteristic for the advance of Svalbard surge-type glaciers. This model focusses on the recurring geomorphological landform assemblages found in fjords around Spitsbergen, specifically adjacent to tidewater glaciers and will be compared to Kongsfjorden in section 7.4, below.

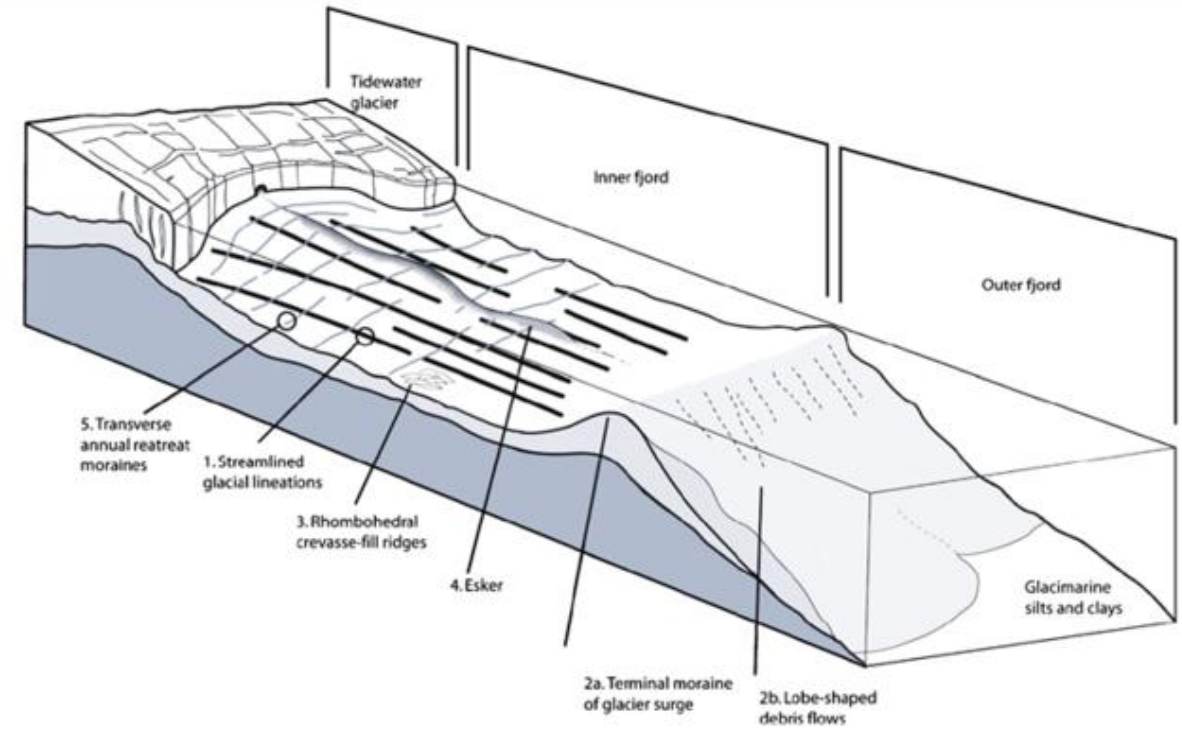

Figure 1.5: Landform assemblage model for surging tidewater glaciers in Svalbard. Numbering is according to inferred relative age of the features with 1 being the oldest (Ottesen et al., 2008).

2. Study area

2.1 Physiographic Setting

The study area is shown in Figure 2.1. Kongsfjorden is located along the western coast of Spitsbergen, the largest island of the Svalbard archipelago. It is the southern arm of a fjordic system which is comprised of Kongsfjorden and Krossfjorden, located between 78°58' N, 11°23' E, and 79°4' N, 11°38' E. The two fjords combine and open into a submarine glacial trough (Kongsfjordrenna) towards the coast (Figure 2.1c; MacLachlan et al., 2010). Kongsfjorden is orientated in a SE-NW direction, while Krossfjorden follows a general N-S trend.

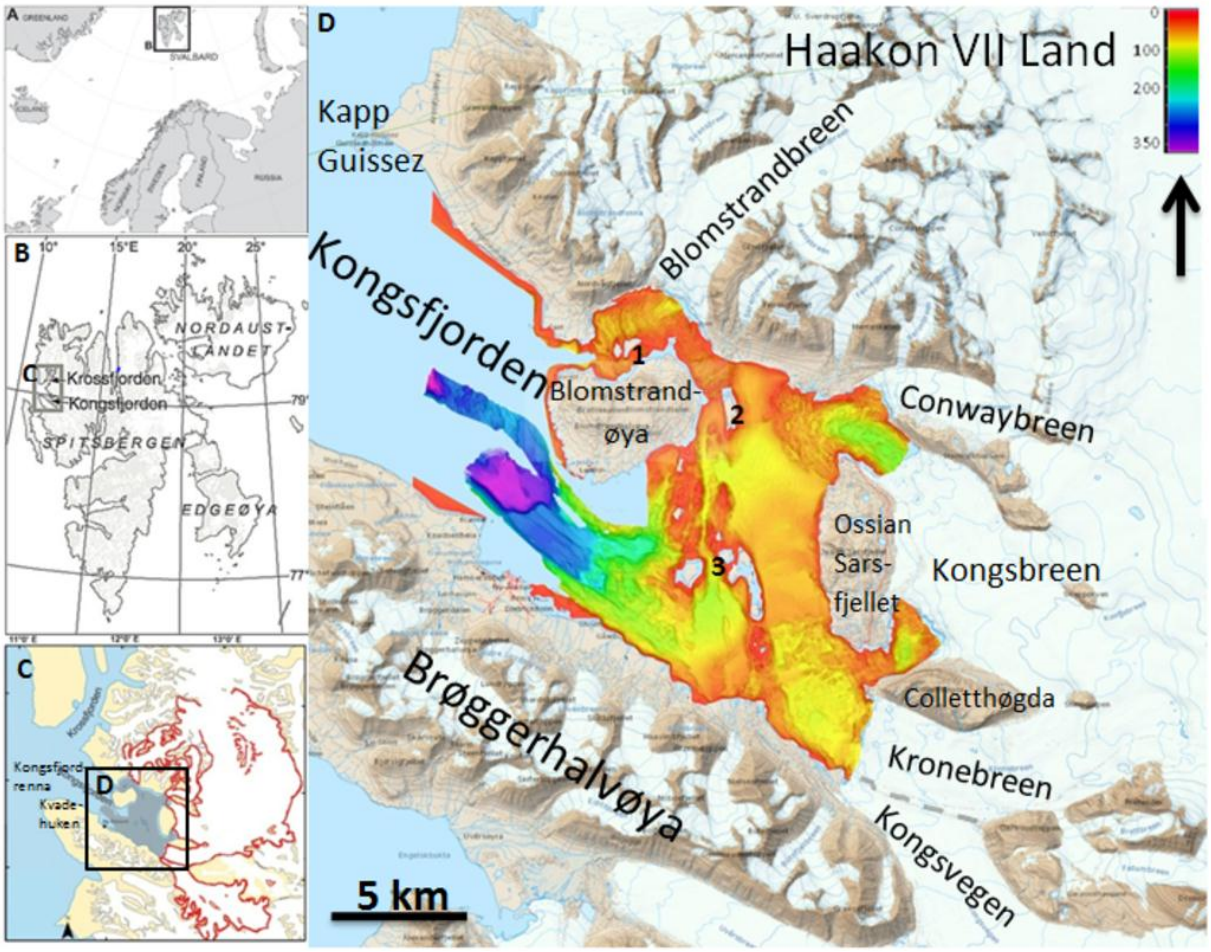

Figure 2.1: A) Overview Map of the Nordic Seas; B) Overview Map showing Svalbard with indication of the fjord system Kongsfjorden – Krossfjorden (Howe et al., 2003); C) Study area with the grey polygon showing outline of swath bathymetry used for this thesis; D) Study area and surroundings, with 1=Breøyane, 2=Gerdøya, and 3=Løvenøyane.

The mouth of Kongsfjorden is defined by the inlet between two spits: Kvadehuken on the southern coast (Figure 2.1c) and Kapp Guissez on the northern coast (Figure 2.1c, d), the latter of which also serves as the southern border to Krossfjorden's entrance. The inner part of Kongsfjorden is surrounded by a glacier-dominated coast with several terrestrial and five tidewater glaciers. A

number of islands occur in and around the fjord, specifically the islands Blomstrandøya and Gerdøya, and the island groups Breøyane and Løvenøyane (Figure 2.1d). Blomstrandøya used to be a peninsula (Blomstrandhalvøya) when Blomstrandbreen extended further into the fjord (e.g. Liestøl, 1988). In addition to the glaciers the coast is defined by Haakon VII Land in the north, Ossian Sarsfjellet and Colletthøgda in the east (at the head of the fjord) and Brøggerhalvøya towards the south.

Kongsfjorden is approximately 20 km long, between 4 and 10 km wide (MacLachlan et al., 2010) and covers an overall area of roughly 208.8 km², with a volume of 29.4 km^3 (Ito & Kudoh, 1997). It has a maximum water depth of 394 m in its deeper outer and central parts, whereas the inner part is shallower with water depths < 100 m (Howe et al., 2003).

2.2 Bedrock Geology

The geology of Svalbard is complex and not always clearly described. This is why the stratigraphic column of sediments found in the archipelago consists of Groups, Formations and Members with specific names, to be able to distinguish between rock material of the same kind but of different time periods in a reliable manner. Only a certain selection of these groups and formations can be found in the catchment area of Kongsfjorden, as will be described later. The geology of the study area is shown in Figure 2.2.

The fjord system of Kongsfjorden and Krossfjorden is located close to a major tectonic boundary separating the Northwestern Basement Province to the northeast and the Cenozoic fold- and thrust belt of western Spitsbergen to its southwest (Bergh et al., 2000), leading to a manifold petrology in the area. While pre-Devonian metasediments and related igneous rocks occur north of the fault zone, Brøggerhalvøya to the South shows Late Paleozoic sedimentary strata, such as carbonates, conglomerates and calcareous sandstones. The island Blomstrandøya within Kongsfjorden is made up of Devonian red conglomerates and sandstones interlayered with marbles from the Mesoproterozoic (MacLachlan et al., 2010).

In a little more detail, the catchment area of Kongsfjorden is characterized by the following Groups, Formations and Members (compare also legend of Figure 2.2):

The sedimentary cover is the youngest material found in the area and consists of unconsolidated deposits of quaternary age. They include moraines, marine shore deposits, and fluvial deposits. It furthermore includes the Tempelfjorden Group (Gp) with its Kapp Starostin Formation (Fm), which is made up of siliceous shales, cherts, limestones and sandstones from the Late Permian, and parts of the Gipsdalen Group, namely the Gipshuken Fm with dolomite breccia, dolomites, sandstones and.

Figure 2.2: Geological Map of Kongsfjorden, see next page for legend and Figure caption.

Figure 2.2: Geological Map of the Kongsfjorden area with original glacier front positions from 1990. Red dashed lines indicate glacierpositions in 2000 (modified after and printed with permission from W.K. Dallmann, Norwegian Polar Institute).

marl, and the Wordiekammen Fm. The latter contains limestones and dolomite, which are rich in Calcium. The Gipshuken and the Wordiekammen Formations are part of the Dickson Land Subgroup and are from the Middle Carboniferous/Early Permian. Sedimentary cover rocks of Devonian age include the greenish-grey sandstones, red siltstones and shales from the Dicksonfjorden Mb in the Andrée Land Group and undifferentiated sandstones and conglomerates, which do not belong to a group or subgroup. Parts of the Red Bay Group from Lower Devonian times can be found, mainly the Wulffberget Fm, which is made up of limestone conglomerates, quartz and polymict conglomerates.

The basement around Kongsfjorden includes rocks from the Kongsvegen Group, which is assumed to be of Middle to Late Proterozoic age and contains phyllites with interlayered quartzite of the Nielsenfjellet Fm, the marble of the Steenfjellet Fm, and mica schists, garnet-mica schists, and quartz-carbonate schists with interlayered marble in the Bogegga Fm. The Kongsvegen Gp mainly occurs south of the fjord on Brøggerhalvøya. North of the fjord the Generalfjella Fm crops out, which is expected to be of Middle Proterozoic age and is composed of quartzites, graphitic quartz-carbonate schists and marble. The Signehamna Fm is another abundant part of the metamorphic basement and provides mica schist with interlayered carbonate rocks and quartzites, also from the Mid-Proterozoic. The marble from the Generalfjella Fm is abundant in the north of Kongsfjorden and is, like the Siktefjellet Fm and the Smeerenburgfjorden Complex of Mesoproterozoic age. The Siktefjellet Fm is more typically referred to as the Signehamna Fm and is made up of quartzites, sericite-chlorite schists with aplites, various gneisses, schists, and metasedimentary rocks, and mica-schists. It may also include quartzites and marble in some cases. The Smeerenburgfjorden Complex includes migmatites and granitic orthogneiss.

The only intrusive rocks in the area stem from the dolerite dikes and sills from the Diabasodden Suite, which are believed to have originated in the Lower Cretaceous.

2.3 Glaciology

During the glaciation of Svalbard in the Late Weichselian the larger fjords along the western margin served as “gateways” for the fast-flowing ice streams that brought vast amounts of ice and material to the former ice margin and up to the continental shelf edge (see Figure 1.1; Landvik et al., 1998; Ottesen et al., 2005; MacLachlan et al., 2010; Ingólffson& Landvik, 2013). Kongsfjorden is considered to be one of the largest outlets of these paleo-ice streams in western Svalbard. Together with Krossfjorden, it is expected to have drained a large portion of the ice accumulated over the whole of NW-Spitsbergen. Its total drainage area is calculated to be roughly 3074 km² (Svendsen et al., 2002). The fast-flowing ice stream channelled in Kongsfjorden is assumed to have been separated from the slower and dynamically less active ice around it by sharp boundaries, causing a contradictory geological and morphological record (Mangerud et al., 1992; Svendsen et al., 1996; Landvik et al., 1998). Sediments along raised beaches adjacent to Kongsfjorden were inferred to be ice-free during the Late Weichselian (Miller, 1982; Forman & Miller, 1984; Lehman & Forman, 1992), opposing the marine record. The latter proposed the advance of grounded glacial ice at least up until the shelf break (see Figure 1.1; Landvik et al., 1998; Ottesen et al., 2005; Ottesen & Dowdeswell, 2007). Based on the seafloor morphology in Kongsfjordrenna, Landvik et al. (2005) proposed that the trough was filled with fast-flowing ice during the Late Weichselian, with repeated ice advances to the shelf break

during the Quaternary. The supposedly ice-free beaches were interpreted to be the result of ice cover with a low basal movement (Figure 1.1).

It is debated to what extent Kongsfjorden was glaciated during the peak glaciation. However, a consensus seems to be reached, for Lehman & Forman (1992) suggested that the minimal ice extent was the mouth of Kongsfjorden and Landvik et al. (1998) assumed Kongsfjordrenna to be filled with Late Weichselian ice during repeated glacier re-advances. This hypothesis was supported by Ottesen et al.'s (2005) proposition that the entire western Svalbard continental margin was glaciated at one point. This was derived from the characteristic landform assemblage found in according areas. That Kongsfjorden was once glaciated until the shelf break is suggested by Ingolfsson & Landvik (2013) and a terminal moraine at the shelf break in the south of Kongsfjordrenna is inferred to mark the maximum ice extent during the Late Weichselian (Ottesen et al., 2007; Figure 1.1, Figure 1.4).

During the deglaciation, Kongsfjorden is considered to be among the fjords that experienced comparably fast retreat of the ice. The deglaciation of the fjord is considered to have begun 13 000 cal years ago, as is common for most of the fjords along the western coast of Svalbard, and to have occurred in a two-step recession. The fjord is believed to have been free of ice 9 000 cal yrs BP (Lehman & Forman, 1992; MacLachlan et al., 2010). A glacial re-advance during the Younger Dryas has not been confirmed for the area, but the inner fjord is believed to have been glaciated at that time (Figure 2.3; Mangerud & Landvik, 2007; Skirbekk et al., 2010).

Figure 2.3: Inferred maximum ice sheet extent during the Younger Dryas (modified from Mangerud & Landvik, 2007).

Today, Kongsfjorden is largely influenced by the polythermal tidewater glaciers Blomstrandbreen and Conwaybreen, as well as Kongsbreen (North and South), Kronebreen and Kongsvegen (compare Figure 2.1; Liestøl, 1988; Dowdeswell & Forsberg, 1992; Hagen et al., 1993; Svendsen et al., 2002; Howe et al., 2003; Blaszczyk et al., 2009; MacLachlan et al., 2010). All glaciers are presented in detail in section 2.3.4, below.

2.3.1 Polythermal Glaciers

Polythermal glaciers are glaciers which consist of both, cold and warm ice and are widely spread in arctic and subarctic environments (Figure 2.4; Petterson, 2004). These glaciers show a large variety of thermal structures (Blatter & Hutter, 1991; Petterson, 2004), and are subdivided into predominantly cold and predominantly warm glaciers, the latter of which are the majority around Svalbard (Dowdeswell et al., 1984). The thermal behaviour of predominantly warm glaciers varies (Figure 2.4), but in Svalbard glaciers warm ice is created during spring when meltwater refreezes in the accumulation area. In winter the ablation area at the base of the glacier is subjected to the colder air temperatures, creating a layer of cold ice at the surface (Benn & Evans, 2010). Glacier surges may be related to changes between the transition of temperate and cold ice at the glacier bed (Hamilton & Dowdeswell, 1996; Murray et al., 2000).

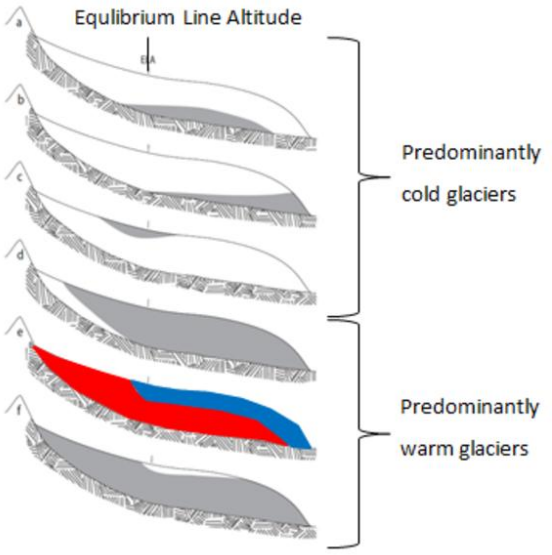

Figure 2.4: Types of polythermal glaciers and their thermal structure. White=cold ice, grey=warm ice. Svalbard glaciers are mostly type e (red=warm ice, blue=cold ice; modified after Petterson, 2004).

2.3.2 Tidewater Glaciers

Tidewater glaciers are glaciers terminating in a marine setting with grounded ice margins below sea level (e.g. Meier & Post, 1987; Ottesen & Dowdeswell, 2006). Tidewater glaciers make up about 20 % of the glaciers on the Svalbard coast (e.g. Dowdeswell, 1989; Benn & Evans, 2010). They often terminate in cliffs at the grounding lines and occur in fjords as well as at the open coast. Tidewater glaciers in the southern Arctic have been found to show the necessary characteristic for sustaining fast glacier flow (e.g. Meier & Post, 1987). In addition to this, sub- and englacial drainage is expected to be common, leading to rapid sliding as a consequence of high water pressures at the glacier sole (Benn & Evans, 2010). One of the main mechanisms of retreat for tidewater glaciers is the calving of icebergs from the glacier terminus, a process which is largely dependent on water depth and glacier stability (compare e.g. Ottesen & Dowdeswell, 2006; Kehrl, et al., 2011)

2.3.3 Surging Glaciers

Surging glaciers are glaciers that show cyclic switches from fast to slow ice flow, resulting from internally driven oscillations in the conditions at the glacier bed (Meier & Post, 1969; Raymond, 1987; Sharp, 1988). The passive, or quiescent, phase is characterized by ice movement slower than the balance velocity, where ice accumulates in the upper part of the glacier (reservoir area; Meier &

Post, 1969; Raymond, 1987). When a too high surface gradient is reached, with too much accumulation in the upper, and too little loss in the lower glacier, the active phase is initiated (Benn & Evans, 2010). Triggering of the active phase is thought to be climatically independent (Ottesen & Dowdeswell, 2006). The surge phase is characterized by fast ice flow (1 – 2 orders of magnitude higher than quiescent-phase flow) and results in the fast transportation of ice from the upper reservoir area to the lower accumulation area. This can result in an advance of the ice front (Benn & Evans, 2010). Both phases generally have more or less constant durations and changes between the two are therefore considered to be following a quasi-periodic cycle (Raymond, 1987; Benn & Evans, 2010). The durations of passive and active phase vary depending on the glacier characteristics and geographical location but are generally between several years and several hundred years (Meier & Post, 1969; Raymond, 1987; Dowdeswell et al., 1991; Björnsson et al., 2003). Surging glaciers on Svalbard often have active phases lasting for 4-10 years, and passive phases of 50 - 500 years, with velocities between 1.3 and 16 m/day (Benn & Evans, 2010).

The distinction between a surge-type and a non-surge-type glacier is not always clear (Meier & Post, 1969; Murray et al., 2003) and a glacier may evolve over time, changing from surging to non-surging conditions or vice versa.

2.3.4 Glaciers in the Area

Several polythermal glaciers can be found in the study area (Table 2.1). The five most important (tidewater) glaciers with immediate contact to Kongsfjorden (Figure 2.5) are most likely to have influenced the fjord bathymetry and will be presented in the following sections.

Infantfonna is a glacier of an area of about 85 km² and its main ice field is situated to the northeast and east of Kongsvegen and Kronebreen. The glacier was neglected in the older literature about Kongsvegen and Kronebreen, as it terminated on land behind the two glaciers. However, Trusel et al. (2010) and information from the Norsk Polarinstitutt (2013) indicate that Infantfonna nowadays separates Kongsvegen and Kronebreen by a 350 m wide outlet. The latter begins about 11.5 km inland and its contribution to the paleo-processes in Kongsfjorden is considered negligible. Infantfonna will therefore be included in the term Kongsvegen / Kronebreen throughout this thesis.

The glacier terminology is ambiguous in the area, particularly regarding the extent of Kronebreen. Some suggest that Kongsbreen and Kronebreen are in fact one glacier, Kronebreen, with three different ice fronts, where Kronebreen North and Central represent Kongsbreen North and South, respectively (Hagen et al., 1993; Lefauconnier et al., 1994; Bennett et al., 1996; 1999; Glasser et al., 2001; Kehrl et al., 2011). Others suggest the division into Kongsbreen (North and South) and Kronebreen (Figure 2.5; Liestøl, 1988; Boulton, 1990; Dowdeswell & Forsberg, 1992; Svendsen et al.,

2002; Howe et al., 2003; MacLachlan et al., 2010; Trusel et al., 2010; Geological Maps and TopoSvalbard from the Norsk Polarinstitutt, 2013), which will be the terminology used throughout this thesis.

Table 2.1: Glaciers > 1 km² around Kongsfjorden and their characteristics (Hagen et al., 1993; Blaszczyk et al., 2009)

Glacier Name	Tidewater / Land (T/L)	Surge / Non-surge (S/N)	Area [km²]	Volume [km³]	Location
Mørebreen	L	N	1.3	0.04	Brøggerhalvøya
Brøggerbreane (Vestre & Austre)	L	Austre S (ca. 1890), Vestre N	17	0.88	Brøggerhalvøya
Løvenbreane (Vestre, Midtre, Austre)	L	Midtre S (ca. 1890), Austre, Vestre N	14.6	1.11	Brøggerhalvøya
Pedersenbreen	L	N	5.6	0.46	Brøggerhalvøya
Botnfjellbreen	T/L	N	6.2	0.53	Brøggerhalvøya
Kongsvegen	**T**	**S (1948)**	**153.9**	**37.00**	**East-Kongsfjorden**
Infantfonna	**T**	**N**	**85**		**East-Kongsfjorden**
Kronebreen	**T**	**S (1869)**	**709.8**	**140.00**	**East-Kongsfjorden**
Kongsbreen	**T**	**N?**			**East-Kongsfjorden**
Conwaybreen	**T**	**N**	**34.5**	**8.9**	**East-Kongsfjorden**
Feiringbreen	L	N	7.6	0.7	Haakon VII Land
Skreifjellbreen	L	N	2.6	0.15	Haakon VII Land
Blomstrandbreen	**T**	**S (1960)**	**65.7**	**18.00**	**Haakon VII Land**
Olssønbreen	L	N	1.9	0.09	Haakon VII Land

Kongsvegen is believed to be the main glacier surging into Kongsfjorden (Elverhøi et al., 1983). It is located in the southeastern corner of Kongsfjorden, and, together with Infantfonna and Kronebreen, forms a tidewater margin. Kongsvegen is currently retreating with a velocity between 1.4 and 3.6 m a^{-1} (Blaszczyk et al., 2009). Ice flow of Kongsvegen is generally orientated towards the north-northwest but changes to a more easterly component when meeting Kronebreen just west of Garwoodtoppen (Figure 2.5). The glacier has been observed to undergo the active and passive phases typical for surge-type glaciers and has been recorded to have surged in 1948 (Hagen et al., 1993).

Kronebreen is a large tidewater glacier located at the east of Kongsfjorden. It is located directly to the north of Kongsvegen and the two glaciers are confluent about 5 km from the tidewater terminus. Kronebreen is the fastest-flowing glacier in Svalbard and currently recedes with velocities of 750 to 785 m a^{-1} (Lefauconnier et al., 1994; Melvold & Hagen, 1998; Bennett et al., 1999; Blaszczyk et al., 2009). The glacier drains the three ice sheets Holtedahlfonna and Infantfonna (Lefauconnier et al.,

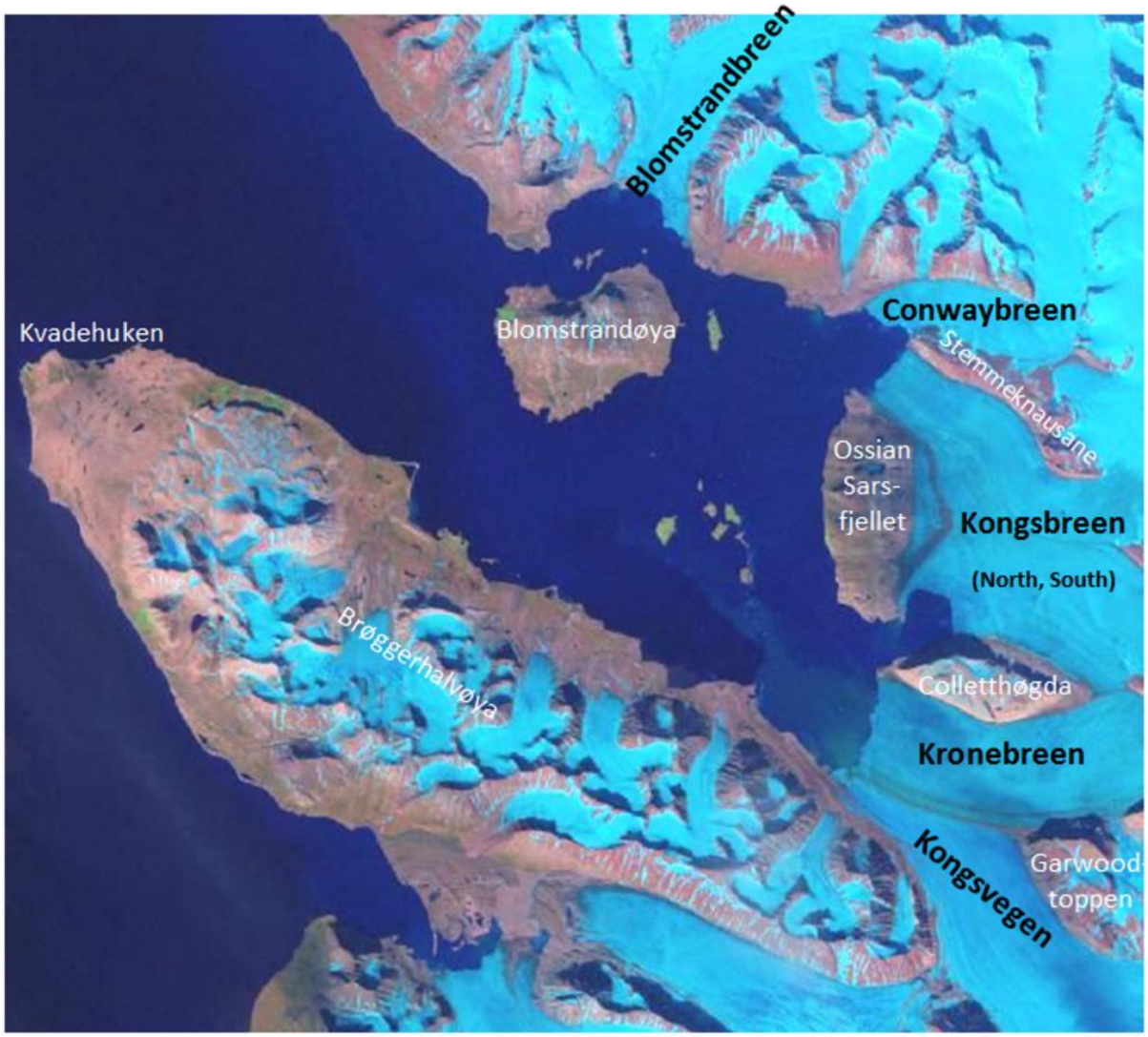

Figure 2.5: Aerial photograph from July 7th, 2002, showing glacier positions in the study area as well as their respective ice fronts in the fjord (USGS, GloVis).

1994) and represents the dominant part of the confluent tidewater front (Figure 2.5). A surge is registered for Kronebreen in the year of 1869 (Liestøl, 1988; Hagen et al., 1993); however, due to a lack of typical characteristics (such as looped medial moraines, quiescent flow velocities, etc.) it is debated whether Kronebreen is of surge-type (Bennett et al., 1999).

Kongsbreen is the tidewater glacier north of Kronebreen. It has a northern and a southern ice front located north and south of Ossian Sarsfjellet (Figure 2.5). Resulting from the varying terminology of the glaciers, it is impossible to find definite information on Kongsbreen concerning flow velocities, area, and surges. So far, no surge has been registered for Kongsbreen, although, if part of Kronebreen, it could have surged in 1869 (Hagen et al., 1993, Blaszczyk et al., 2009).

Conwaybreen is located north of Kongsbreen. The tidewater glacier's general southward flow direction is restricted and redirected to westward flow by the mountain complex Stemmeknausane

(Figure 2.5). Conwaybreen does not have any registered surges and is assumed to be a non-surging tidewater glacier.

The ice front of Blomstrandbreen is located exactly north of Blomstrandøya (Figure 2.5). Blomstrandbreen is considered to be or to have been of surge-type, as a surge is registered for the year 1960 (Hagen et al., 1993).

Table 2.2: Bedrock geology of the catchment area of each of the five tidewater glaciers terminating in Kongsfjorden

Catchment Area	**Metamorphic Basement**	**Sedimentary Cover**	**Age**
Blomstrandbreen	**Generalfjella Fm** (upper marble) **Signehamna Fm** (mica schists, garnet-mica schists)	Moraines Marine shore deposits	Mesoproterozoic Quaternary
Conwaybreen	**Signehamna Fm** (clastic sedimentary rocks, sericite-chlorite schists, quartzites and mica schists/garnet-mica schists with aplites) **Smeerenburgfjorden Complex** (migmatites, granitic orthogneiss)	Moraines	Mesoproterozoic Quaternary
Kongsbreen/Kronebreen	**Generalfjella Fm** (marbles, sericite-chlorite schists, mica schists) **Grey-Hoek Fm** *Dicksonfjorden Mb* (greenish-grey sandstones, red siltstone, shale) **Signehamna Fm** (sericite-chlorite schists with aplites, various gneisses, schists and metasedimentary rocks, quartzite) **Smeerenburgfjorden Complex** (migmatites)	Moraines **Wulffberget Fm** (limestone conglomerates, quartz and polymict conglomerates) **Wordiekammen Fm** (limestones, dolomites) **Gipshuken Fm** (dolomites, limestone, marl, gypsum and anhydrite, carbonate breccia)	Mesoproterozoic Late Devonian Middle Carboniferous – Early Permian Quaternary
Kongsvegen	**Diabasodden Suite** (intrusive dolerite) **Signehamna Fm** (mica schists)	Moraines **Kapp Starostin Fm** (siliceous shales, cherts, limestones, sandstones)	Lower Cretaceous Mesoproterozoic Late Permian Quaternary
Botnfjellbreen	**Nielsenfjellet Fm** (phyllites with interlayered quartzites) **Steenfjellet Fm** (marble) **Bogegga Fm** (mica schist, garnet-mica schists, quartz-carbonate schist with interlayered marble)	Moraines Fluvial deposits	Middle to Late Proterozoic? Quaternary

The geology of the catchment area of the different glaciers draining into Kongsfjorden is important to distinguish the different sources of sediments deposited within the fjord. This relationship is summarized in Table 2.2.

2.4 Geomorphology

A fjord is the result of glacial processes, when ice carves out a U- or V-shaped valley (Howe et al., 2010). Kongsfjorden is assumed to have formed in a depression that was carved from bedrock fracturing parallel to the Cenozoic thrust front (Howe et al., 2003) and shows the typical U-shape. Its walls are considered to be relatively shallow compared to other Spitsbergen fjords with slopes of 5-20°, although slope failure may occur due to oversteepening in the deeper parts of the fjord (Howe et al., 2003). A 300 m-high sill is separating Kongsfjorden from the shelf trough (Kongsfjordrenna; Howe et al., 2003). The fjord can be divided into a deeper central and outer basin with water depths between 200 and 400 m (Elverhøi et al., 1983, Howe et al., 2003) and an inner fjord with water depths below 100 m (Howe et al., 2003).

The influence of glaciation and deglaciation and especially the subjection of Kongsfjorden to the fast-flowing ice left its imprints on the fjord basin. Even though, according to Howe et al. (2003), the central and outer parts of Kongsfjorden are mainly comprised of bedrock which is covered by a less than 10 m thin sedimentary cover, some (relict) features of glacial processes are visible nevertheless (Figure 2.6): Ottesen et al. (2007) inferred a large transverse ridge which was located at the shelf break towards the southern end of Kongsfjordrenna to be the terminal moraine deposited from the Late Weichselian ice stream channelled in Kongsfjorden (Figure 1.4, Figure 2.6). The ridge represents the maximum ice extent during peak glaciation. Landvik et al. (2005) and MacLachlan et al. (2010) found similar ridges at the mouth of Kongsfjorden, and deduced these to be recessional moraines deposited during stagnation of ice movement or minor re-advances throughout the deglaciation (Figure 2.6). Furthermore, streamlined bedforms have been interpreted to be drumlins (Howe et al., 2003) and crag-and-tail ridges, generated in a parallel orientation to the ice flow direction (MacLachlan et al., 2010). Submarine linear groove-ridge features have been observed by the same authors and were interpreted to be glacial lineations indicating paleo-ice flow direction from east to west (Figure 2.6). Such lineations are common around the areas of Svalbard and are considered to be evidential for fast-flowing ice streams (e.g. Clark, 1993; Ó Cofaigh et al., 2005; Ottesen & Dowdeswell, 2006). Based on their distribution in central and outer Kongsfjorden as well as in the inner parts, it is considered possible that the outermost lineations were created during the progression of the ice, whereas the ones further in-fjord were generated during retreat (Landvik et al., 2005; MacLachlan et al., 2010). A glacial channel in inner and central Kongsfjorden is believed to

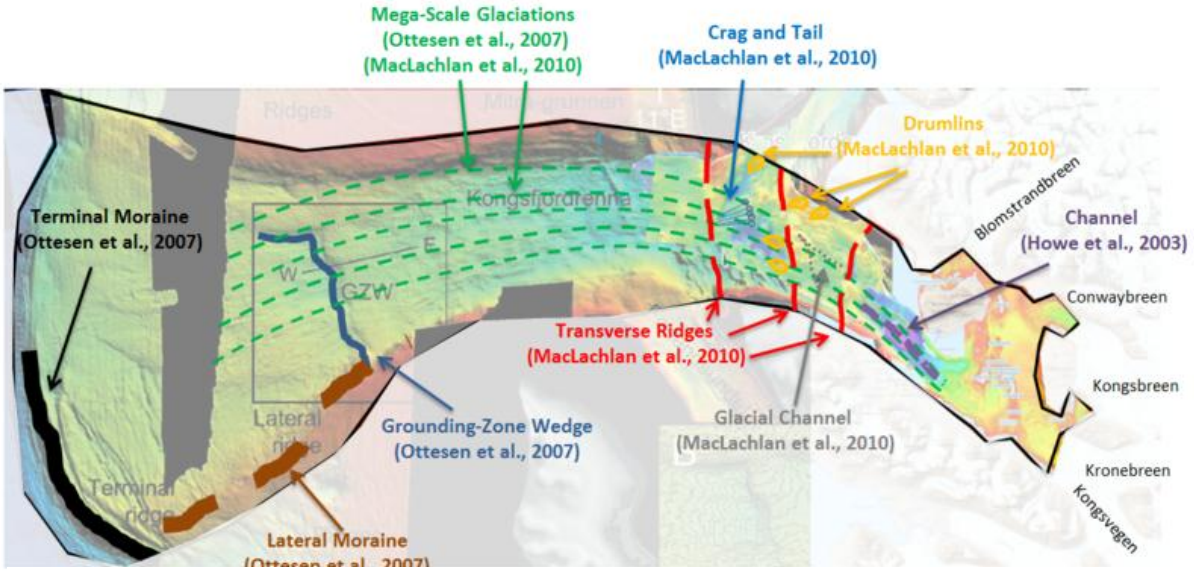

Figure 2.6: Compilation of the geomorphic features documented by Howe et al. (2003), Ottesen et al. (2007), and MacLachlan et al. (2010).

have formed either as a result of wash-out by meltwater or as a consequence of subglacial erosion (Figure 2.6; Howe et al., 2003; MacLachlan et al., 2010).

Boulton (1990) found some large fan bodies comprising coarse-grained sediments in the "ice-proximal zone" in front of Kongsvegen (compare with Kristensen et al., 2009). The fans were suggested to be a result of the settling of a high sediment load transported subglacially by meltwater until suddenly being halted when leaving the confined space of a meltwater channel and entering the sea. In the same area Elverhøi et al. (1983) found some terminal moraines indicating the ice extent of the two surges in 1869 and 1948 (see Figure 1.3) and some thick meltwater deposits associated with these. A sill was documented on the southern side of the Løven Islands and some evidence of chute and slump features were observed near the Kongsvegen ice front (Elverhøi et al., 1983). The inner basin of Kongsfjorden in front of the Kongsvegen / Kronebreen ice margin is furthermore characterized by a hummocky relief, which is thought to have developed through annual ice front oscillations of the non-surging northern ice front (Kronebreen, Elverhøi et al., 1983).

2.5 Climate

Spitsbergen is located in a climatically dynamic zone, which is subjected not only to the meandering polar front but also to the varying strength of the West Spitsbergen Current (Svendsen et al., 2002; Førland et al., 2009). This ensures a variable climate and makes Kongsfjorden especially susceptible to climate change (Svendsen et al., 2002).

Warm and cold air masses meet at the polar front. These air masses have different characteristics depending on their region of origin and can cause very cold or very mild temperatures on Spitsbergen. This makes differences between summer and winter temperatures especially high, but also makes seasonal average temperatures highly variable. Mean temperatures have been measured

in Ny Ålesund on the southern coast of Kongsfjorden from 1961 to 1990 and varied between -14.5°C in February and 5°C in July (Førland et al., 2009).

Precipitation is as variable as temperature and changes seasonally. Exact values are not known for Kongsfjorden, but mean precipitations are below 100 mm in summer and between 150 and 200 in autumn (Førland et al., 2009).

Winds are mainly influenced by the Icelandic Low between Iceland and Greenland, which extends into the Barents Sea in winter and is a main centre for the generation of cyclones. As cyclones move in an anti-clockwise direction in the northern hemisphere, mainly easterly or north-easterly winds prevail on Spitsbergen (Strahler & Strahler, 2005; Førland et al., 2009). The presence of sea ice in winter and spring is the reason for the climate around Svalbard to vary between maritime and continental conditions. The polar maritime climate prevails in ice-free conditions, when the weather is more temperate and the air more humid (summer and autumn). The cold and dry weather of winter and spring reflects the continental conditions, when sea ice prevents the storage of solar heat in the isolated ocean (Førland et al., 2009). As Kongsfjorden is largely subjected to the highly variable inflow of warm Atlantic Water (e.g. Jernas et al., in prep.) and its coastal climate varies accordingly. Especially in recent years the Atlantic Water masses have registered higher temperatures than usual (Cottier et al., 2007). As a consequence, Kongsfjorden has been recorded to show increased summer and winter temperatures, leading to a decrease of sea ice formation during winter (Hop et al., 2006; Skirbekk et al., 2010) and a more maritime climate throughout the year.

2.6 Oceanography

Due to a complicated fjord topography and coastline, the processes governing the oceanography in Kongsfjorden are complex with frequent changes. Annual, seasonal and diurnal variations play a major role, as they affect heat transfer in the ocean and in the atmosphere, which in turn influences the local climate (Svendsen et al., 2002). The oceanography is largely governed by the inflow of Transformed Atlantic Water, which is a mixture between the West Spitsbergen Current and the Coastal Current (Figure 2.7) and is formed outside the fjord. The former transports warm and saline waters from the North Atlantic along the western Spitsbergen coast, whereas the latter brings cold, less saline Arctic Water

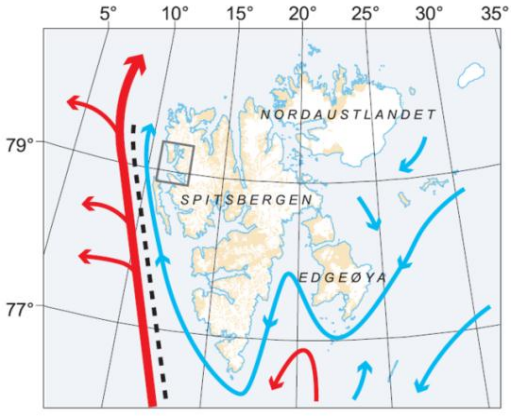

Figure 2.7: Oceanic currents in Svalbard. Red=West Spitsbergen Current, blue=Coastal Current (Svendsen et al., 2002).

from the eastern Svalbard area (Svendsen et al., 2002; Skirbekk et al., 2010). Transformed Atlantic Water is therefore slightly colder (1 instead of > 3°C) and less saline (34.7 instead of > 34.9 psu) than regular Atlantic Water (Svendsen et al., 2002; Howe et al., 2003). As the inflow and characteristics of the water masses are known to fluctuate over time, the coastal climate in Kongsfjorden is particularly susceptible to changes. The oceanography in Kongsfjorden has been reviewed in detail by Svendsen et al. (2002), Howe et al. (2003), Cottier et al. (2005), and Skirbekk et al. (2010).

In summer and early autumn the water column is controlled by the increased freshwater input from meltwater and rivers, which causes major differences between the upper and the lower layers (Figure 2.8). These result in strong temperature and salinity gradients and lead to a well-pronounced stratification of the water masses within the fjord (Figure 2.8; Svendsen et al., 2002). The density gradient between the layers is further enhanced by the seasonally prevailing air temperatures (Elverhøi et al., 1983; Svendsen et al., 2002).

In winter and early spring, on the other hand, stratification is weak and water masses are almost homogeneous (Elverhøi et al., 1983; Cottier et al., 2010). As freshwater input is significantly reduced, and the expulsion from brine solutions as an effect of sea ice formation further increases the salinity (Howe et al., 2003), the waters in the fjord are mostly saline with small-scale temperature variations between top and bottom (Elverhøi et al., 1983).

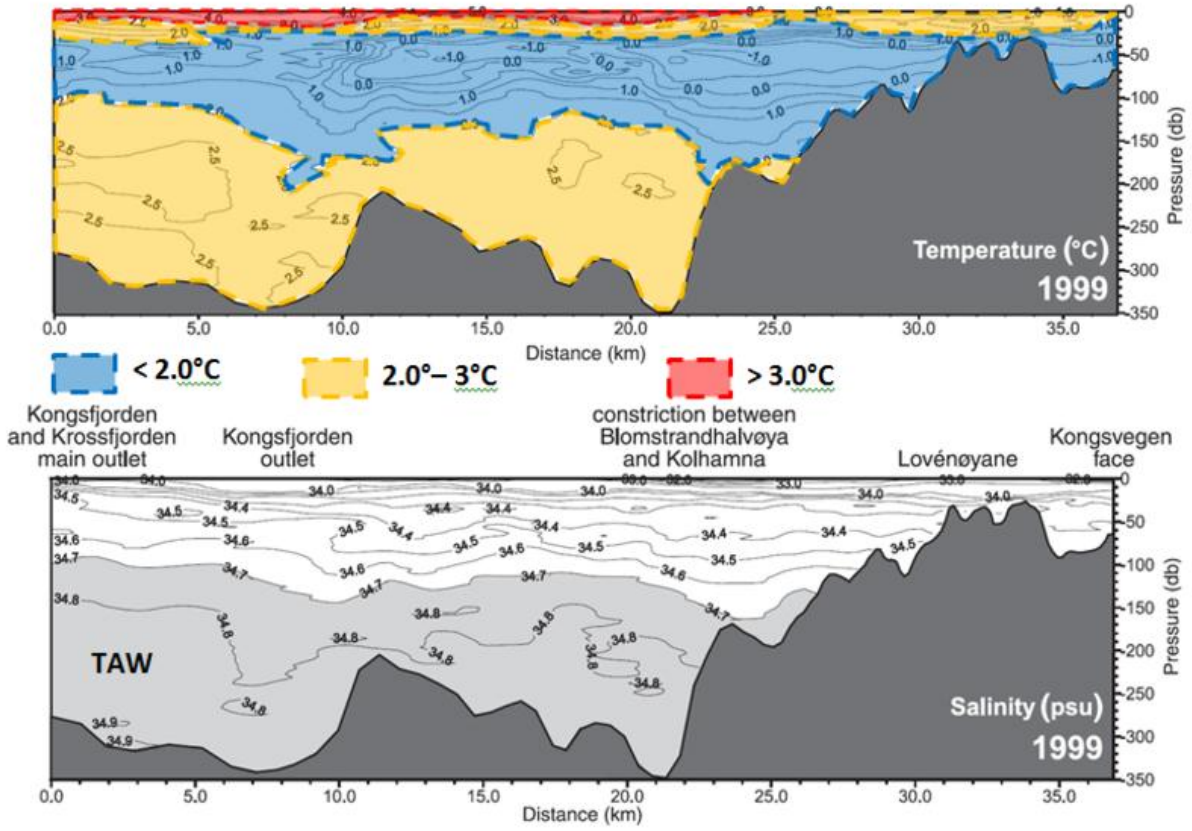

Figure 2.8: Temperature and salinity distributions along the main axis of Kongsfjorden in July 1999. Note the clear distinction in slainity between TAW (Transformed Atlantic Water) and surface waters (modified after Svendsen et al., 2002).

Winds in Kongsfjorden are mostly down-fjord, causing water masses to move in the same direction (Svendsen et al., 2002). However, because of the stratification in the water column winds only affect the uppermost layers during the summer months (e.g. Howe et al., 2003). They can penetrate deeper in winter, when stratification is weak. Winds have a more important effect when they influence the Ekman motion, which in turn, affects large-scale movement of the bottom water. Ekman motion leads to the piling up or removal of surface waters from the coast (Svendsen et al., 2002). This, in turn causes strong pressure gradients between the water masses inside and outside the fjord, forcing water exchange in both directions. This effect is further enhanced by the tide and density gradients. The former has an amplitude of 0.5 m in the ocean outside Kongsfjorden (Svendsen et al., 2002) and also favours water exchange between inner and outer fjord. The density differences are caused by the glacier-proximal setting of the inner fjord, which, especially in the summer months, leads to increased freshwater input and less dense waters in the inner part of Kongsfjorden, whereas water masses in the outer fjord remain unaffected by the density increase. Due to its location close to the North Pole currents in the fjord are further controlled by the Coriolis Effect, which deflects movement to the right in the northern hemisphere. It therefore steers inflow into the fjord along the southern flank and outflow along the northern side (Svendsen et al., 2002; Howe et al., 2003).

The oceanographic patterns close to the ice margins of the surrounding glaciers may be locally dominated by the input of suspended sediment. Elverhøi et al. (1983) and Boulton (1990) observed surface sediment plumes arising from sediment-laden meltwater close to Kongsvegen. The latter enters the fjord from englacial or subglacial channels and the plumes rise up to sea level as a result of their lower density. Here they tend to form turbid brackish-water plumes, which can influence the surface waters due to their high currents (velocities > 50 cm/s; Elverhøi et al., 1983; Boulton, 1990).

2.7 Sedimentology

Based on the proximity to the five tidewater glaciers the sedimentology in Kongsfjorden is mainly influenced by the sediment input from the glaciers (Howe et al., 2003). This is why sedimentation rates are very high near the termini (rates of 100 mm a^{-1}, > 0.6 m a^{-1}, and > 1 m a^{-1} were suggested for the Kongsvegen / Kronebreen margin by Elverhøi et al., 1983; Trusel et al., 2010; and Kehrl et al., 2011, respectively) but decrease away from the glaciers. At 10 km away from the Kongsvegen / Kronebreen ice margin a rate of 50 mm a^{-1} has been proposed by Elverhøi et al. (1983), which decreases to 0.4 mm a^{-1} in the outer fjord. The high sedimentation rates at the termini are mostly related to the influence of supraglacial, englacial and subglacial meltwater streams. These and the sediment plumes described by Elverhøi et al. (1983) and Boulton (1990) contribute to an estimated annual deposition of 2 million tons of sediment in the inner basin of the fjord (Elverhøi et al.,1983).

This was based on a sediment concentration of 300 to 500 mg l^{-1} of sediment near the ice margin. However, with the much higher sedimentation rates proposed by Trusel et al. (2010) and Kehrl et al. (2011) the deposited volume is inferred to be much greater today. As meltwater streams can reach high velocities, they can carry a range of grain sizes, leading to the deposition of coarse-grained submarine outwash fans (Boulton, 1990). A grounding-line fan is currently building in front of Kongsvegen / Kronebreen at a rate of > 1 m a^{-1}, whereas another, earlier fan is eroded. Sediment is supplied by a subglacial and an ice-marginal meltwater stream along Kongsvegen, whereas erosion is inferred to happen by mass-transport events depositing the material further downslope. The two different grounding-line fans are representative of the changing location of a meltwater channel, commonly due to wind or the Coriolis Effect (Forwick et al., 2010).

Turbid surface flows are considered to be the primary source for finer sediments (specifically glaciomarine mud) to glacial fjords (Hoskin et al., 1972; Elverhøi et al., 1980). However, about 90 % of their carried material is already deposited within the most proximal 400 m (Kehrl et al., 2011). This means that sediment concentrations within meltwater streams decrease significantly away from the glacier front (down to 1 to 5 mg l^{-1} in outer Kongsfjorden; Elverhøi et al., 1983). Furthermore, the meltwater streams lose momentum and hence lack the capability to carry coarser sediments. Suspension settling of glacimarine mud becomes the dominant process, which is accompanied by a decrease in grain size and sedimentation rate (Elverhøi et al., 1983; Boulton, 1990). Iceberg rafting is the main process of sedimentation in the outer fjord, as suspension settling loses significance (Boulton, 1990). In inner Kongsfjorden, icebergs deposit rafted material at a rate of 5 to 8 mm a^{-1} (Dowdeswell & Forsberg, 1992). Also sea ice may provide sediment to the fjord, and is considered the second main mechanism influencing the sedimentation in Kongsfjorden (Howe et al., 2003).

Most of the sediments in Kongsfjorden have been described as laminated and are therefore considered to be undisturbed by turbidites and associated gravity flow (Elverhøi et al., 1983). Nevertheless, mass-wasting may occur, which is mostly ascribed to the large sediment supply and fairly high deposition rates, which may lead to the entrapment of water within the sediments, thereby decreasing the angle of slope stability. Such mechanisms are particularly strong close to the ice margins of the tidewater glaciers (see Kehrl et al., 2011). Furthermore, sediment re-deposition may be related to iceberg scouring, where the keels erode the surface of the seafloor and transport the sediment until the keels lose contact. However, the majority of icebergs in Kongsfjorden have been found to be too small to cause any sediment reworking in water depths below 40 m (Dowdeswell & Forsberg, 1992).

3. Material and Methods

3.1 Geophysical Data

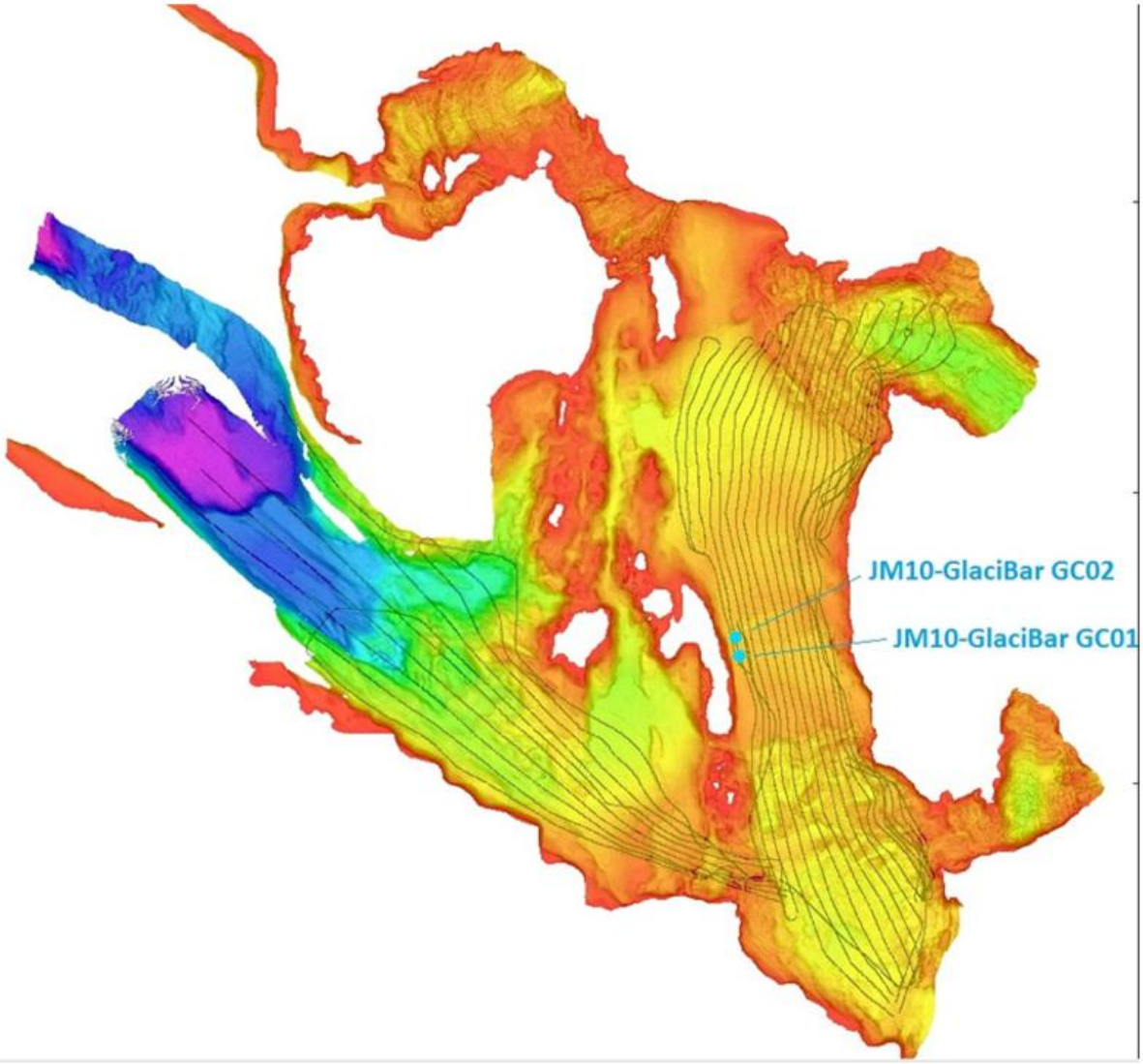

Figure 3.1: Overview of the obtained swath bathymetry. Black lines indicate the location of the chirp profiles, and blue circles reflect the respective core locations.

Swath bathymetry data and chirp profiles were collected with the research vessel R/V Jan Mayen (now Helmer Hanssen) from the University of Tromsø in October 2010. The swath bathymetry obtained throughout the cruise was later complemented with data from the Norwegian Hydrographic Survey (Figure 3.1).

3.2 Swath Bathymetry / Multibeam

Multibeam echo sounders, unlike single beam echo sounders, consist of a fan of multiple sound beams, which allow for high resolution and a wide coverage. As the width of the fan increases with water depth, multibeam echo sounders are very useful to map the seafloor in high detail.

The swath bathymetry data for this thesis was acquired using a Kongsberg Maritime Simrad EM 300 multibeam echo sounder operating at a frequency of approximately 30 kHz. It is a hull-mounted system with 135 beams spaced in equidistant 1-degree intervals, which allow a depth range between 10 and 5000 m and an angular coverage of up to 150°. Both of these factors are variable according to water depth to allow for optimum results.

The available swath bathymetry data was imaged using the Fledermaus v7 3D Visualization and Analyzing Software.

3.2.1 Chirp Sonar

All chirp profiles were acquired aboard the Jan Mayen in October 2010 using a frequency modulated (FM) full spectrum sub-bottom profiler operating at frequencies between 1.5 and 9 kHz. The pulse rate was set to 3 ms, while a ping rate of 1.9 Hz was used.

The chirp data was processed and later interpreted using SMT The Kingdom Suite Software (32-bit). The locations of the acquired chirp profiles are visualized in Figure 3.1.

Unlike the multibeam echo sounder which only maps the surface of the seafloor, the chirp sonar can map the upper 30 m of unconsolidated sediments with high resolution (Quinn et al., 1998). Depending on the resistance of the seafloor, the chirp sonar can penetrate even deeper and is particularly useful to gain information about the kind of deposited material. The chirp profiles used for this thesis were collected to help the classification of local marine bottom sediments as well as to gain a general idea of the solidity of the seafloor. This is particularly useful for distinguishing between ridges and sedimentary wedges, as it allows for previous estimation of core outcome during the cruise, as well as interpretation of sedimentary processes after the cruise.

In contrast to normal boomers and pingers the chirp sonar is frequency-modulated, which means that it operates over a range of frequencies per acoustic signal or pulse rather than just one frequency. The advantages of frequency-modulated chirp techniques opposed to those operating with a single frequency are the better vertical resolution, a higher signal-to-noise ratio and the precision of acquired data (Quinn et al., 1998).

3.3 Sediment Cores

Two gravity cores, 10JM-GlaciBar-GC01 and 10JM-GlaciBar-GC02 (Figure 3.1), were recovered with RV Jan Mayen from the inner part of Kongsfjorden in October 2010. GC01 was retrieved from the top of a surge-induced mass-transport deposit (see also sections 4.4, 5, 6) located at N 78°55'82", E 12°20'80. The core was recovered from a water depth of 50 m, is 286 cm long and was subdivided into three sections of roughly 100 cm length to facilitate measurements. GC02 was taken from the front of the same deposit (N 78°55'98", E 12°20'57", 53 m water depth) and is 339 cm long. This core was cut into four sections, where the upper three are about 100 cm and the fourth section is roughly 40 cm long.

The core sections were analysed in the laboratory to find out more details about the sediments within the cores. Measurements were taken to gain information about the physical properties, element geochemistry, grain size and sediment texture. The multiple analysing techniques are described in the following sections, while results are presented in section 5.

3.3.1 Multi-Sensor Core Logger (MSCL)

Both cores were measured with a Geotek LTD multi-sensor core logger (Figure 3.2) before opening. A MSCL measures various physical properties of soft sediment cores, including the core thickness, magnetic susceptibility, p-wave amplitude and velocity, gamma-ray attenuation, and temperature. The obtained results are then used to calculate wet-bulk density, fractional porosity and acoustic impedance. As some parameters (e.g. p-wave velocity) are temperature-dependent (e.g. Weber et al., 1997), the cores were stored at room temperature for a day prior to measurements. The core pusher and belt integrated into the MSCL enable the automatic logging in regular intervals (settings for this study were 1 cm intervals and a measuring time of 10 s). The measured parameters are explained in the following paragraphs. All explanations are based on the MSCL User Manual provided by Geotek Ltd. (GEOTEK, 2000).

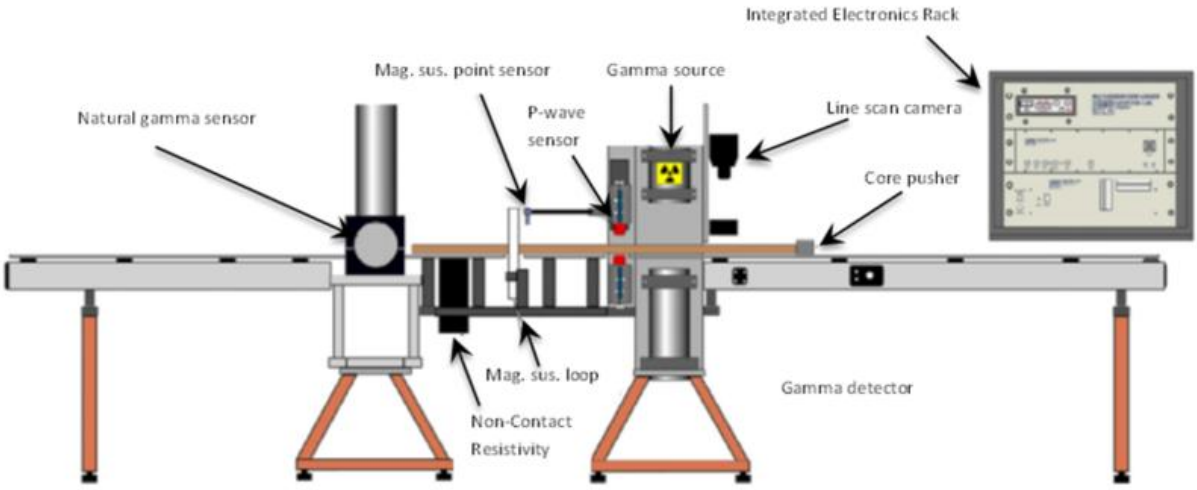

Figure 3.2: Setup of the different sensors in the Multi-Sensor Core Logger (GEOTEK, 2000).

Core Thickness

The thickness of the sediments within the core liner is measured by determining the deviation from a standard thickness. In this case the standard thickness was set to 110 mm.

Magnetic Susceptibility

The magnetic susceptibility is determined in a loop sensor (Figure 3.2), inside which a coil generates a magnetic field. When the core liner passes through the loop and is exposed to the magnetic field, the sensor determines how easily the sediments can be magnetized. A magnetic material approaching the sensor will hence disturb this magnetic field by sending out different frequencies. The resulting changes in frequency are integrated over an area of 10 cm with a Gaussian distribution and later converted to mass-specific or volume-specific magnetic susceptibility.

P-Wave Amplitude

At the p-wave sensor (Figure 3.2) the velocity and amplitude of the primary waves are measured. Two p-wave transducers, one transmitter and one receiver are mounted on opposite sides of the MSCL rail. The transmitter sends out a short pulse, which is recorded in the receiver. The value of the amplitude is directly dependent on the intensity recorded at the receiver. High amplitudes are indicative for (a) a low porosity and (b) for a good contact between core liner and the sediments.

P-Wave Velocity

The p-wave velocity is an important measure in relation with the acoustic data. It shows the travelling velocity of the acoustic signal in the sediments, which is in accordance with the propagation velocity of the compressional waves created by the acoustic signal. The p-wave velocity changes with the material and its characteristics (e.g. density, porosity etc.).

The p-wave velocity is determined from the travel time and distance of the pulse between transmitter and receiver. As this parameter is fairly sensitive to external influence, it is important to always ensure an excellent connection between the core liner and the p-wave sensor (high quality of the p-wave amplitude results). This is achieved by regularly wetting the core liner with a few drops of water. The p-wave velocity allows for the calculation of the acoustic impedance.

Gamma-Ray Attenuation

At the gamma (Caesium-) source gamma rays are emitted as photons and travel through the core towards the receiver on the other side of the MSCL rail. As the photons pass through the core, they are scattered by electrons within the sediments. The amount of resulting energy loss depends on the electron density within the sediments as well as on the thickness of the core. The density of the electrons within the sediments is furthermore directly related to the bulk density, allowing the latter to be calculated from the gamma-ray attenuation.

Acoustic Impedance

The acoustic impedance is the product of the p-wave velocity and the density. If either the density or the p-wave velocity varies strongly between two adjoining layers, the acoustic impedance will be high, resulting in strong, opaque chirp reflections. This means, that changes in the reflections are caused by changes in the sediment properties, leading to a stratified reflection for layered sediments. As gamma-ray attenuation allows for the calculation of bulk density and the p-wave velocity is measured at the p-wave sensor, the acoustic impedance can be calculated from the results of the MSCL analysis. Acoustic impedance gives information about the rigidity of the sediments, as a high impedance is caused by high density and high p-wave velocities. The acoustic impedance is useful to detect changes in sediment properties (e.g. density, porosity).

3.3.2 Opening of the cores

The cores were opened with a circular saw and an osmotic knife cutting the core liner and the sediments into two halves from top to bottom. This prevents older layers to be dragged into younger sediments, leading to a possibly falsified chronology when dating the sediments. The archive half was stored for future reference and the working half was subjected to subsequent laboratory investigations.

3.3.3 X-Ray-Fluorescence (XRF) Core Scanner

XRF Core Scanning is a non-destructive method for acquiring a near-continuous down-core element-geochemical profile. Primary x-rays are shot at the core surface where the electrons contained in the sediment are expelled from their atomic shell. The generated vacancies are subsequently filled by electrons from a lower configuration, resulting in the emission of fluorescence energy. This energy is element-specific and creates an intensity spectrum related to the element concentrations. These spectra are then processed to obtain the element concentrations in counts per a 10-second interval. A XRF core scanner therefore records the major element compositions along the surface of a core's working half (e.g. Potts, 2003).

The measuring device is a He-flushed chamber, which is located directly on top of the sediment surface. To avoid contamination and falsified measurements the core was covered with 4 µm thick ultralene foil prior to core scanning. Measurements for this thesis were acquired using an Avaatech XRF Core Scanner located at the University of Tromsø. Two measurements were carried out on an area of 10 x 12 mm (down-core slit size x cross-core slit size) in 10mm intervals. For the elements Al, Si, S, Cl, K, Ca, Ti, Mn, Fe and Rh measurements were conducted using 10 kV, 1000 µA, 10 seconds counting time, and no filter. To measure Rb, Zr and Sr the settings were changed to 30 kV, 2000 µA, 10 seconds counting time, and Pd-thick filter.

Possible errors can occur as a result of the contact between two core sections. As each section of a core is sealed with a plastic lid, the borders between the two are not ensuring continuous sediment contact. This results in missing values at certain depths or unreliable element concentrations close to the transitions, which were not taken into account for data interpretation. Another possibly factor falsifying results is, for example, the occurrence of air or water between the sediment surface and the foil. Furthermore, some specific elements are more easily disturbed by external parameters and therefore record false concentrations. These elements are mainly light metals with low atomic numbers, such as Al, Ca, K, but also elements like Si, Ti and Mn (Tjallingii et al., 2007). To minimize these errors, element ratios are used rather than single element intensities, as the former are less sensitive to small disturbances (Weltje & Tjallingii, 2008). Ratios for this thesis were based on the sum of the ten most important elements (Al, Si, S, K, Ca, Ti, Fe, Rb, Sr, and Zr), and the counts per each element were divided by this sum. Results are therefore in [x/sum], with x = the element of interest and sum = the sum of the ten elements. As Ca and Fe are the most abundant elements and ratios for the eight remaining elements were too small to yield considerable information, the presentation of the XRF-results focusses only on Ca and Fe. Results are presented in chapter 5.

3.3.4 Colour Imaging

Colour images were taken with a Jai L-107CC 3 CCD RGB Line Scan Camera which has a resolution of 70 µm and is integrated into the XRF core scanner. To avoid reflections and contaminations, the core half was cleaned and smoothed with a plastic card, before being exposed to air to allow any superficial water to evaporate.

3.3.5 X-Ray Photography

The logging of the core lithology was mainly based on visual impressions. As these are strongly restricted to superficial structures, taking x-ray pictures of the core sections is a common method to also gain information about sub-surface sediments. X-rays were generated using a Beryllium source and pictures were projected onto an AGFA D7 film. The attenuation of the x-rays passing through the core half is related to the material density, which is thereby reflected on the radiographs. Darker areas are indicative of less dense material, whereas rocks, shells or pebbles appear very light. Layering between denser and softer sediments can hence be easily recognized on radiographs and a rock encased in soft mud can be detected even if it is not visible at the sediment surface. The same is ture for bioturbation and fossils hidden within the core sections.

A preliminary log was drawn from the radiographs reflecting such internal structures in both cores. The preliminary log was later combined with the real core log to receive a composite log, which

yields information about the sediments and their depositional environment by identifying e.g. sediment structures, shells, clasts, and organic material.

The x-ray photographs were taken with a Philips Macrotank with a current of 5 mA. The acceleration voltage was 80 kV. Density values obtained from the MSCL were used to estimate appropriate exposure times, which varied from one minute and forty seconds to four minutes.

3.3.6 Core logging

A second log was created by describing the sediment surface of the working halves of both cores. This second core log is important for a full core description, as it yields important information invisible on the radiographs. Colours and their changes, for example, can reflect changes in sediment source or in a varying depositional environment as a consequence of e.g. oscillations in climate, sediment source, energy availability etc. They serve as an important tool for the analysis of sediments. Colours were determined using Munsell's Soil Colour Chart.

The detailed and highly resolved colour images provided by the XRF core scanner yield more detailed information about colour changes and were used as a supportive tool throughout the logging process.

3.3.7 Grain Size Analysis

The grain size distribution within the two sediment cores was measured with a Beckman Coulter LS13320 Laser Diffraction Particle Size Analyser at the geological department of the University of Tromsø. The counter resolves grain sizes between 0.4 and 2000 µm. For sample preparation, about half a cubic centimetre of sediment was taken from the core halves in 10-cm intervals, added with distilled water and stored in a cooling room. Prior to measuring about 1 g of bulk material was dissolved in 50 ml water, and set into a shaker for homogenization. Part of the bulk material was then transferred to a tube to be used in the machine's autosampler.

4. Acoustic Data - Results

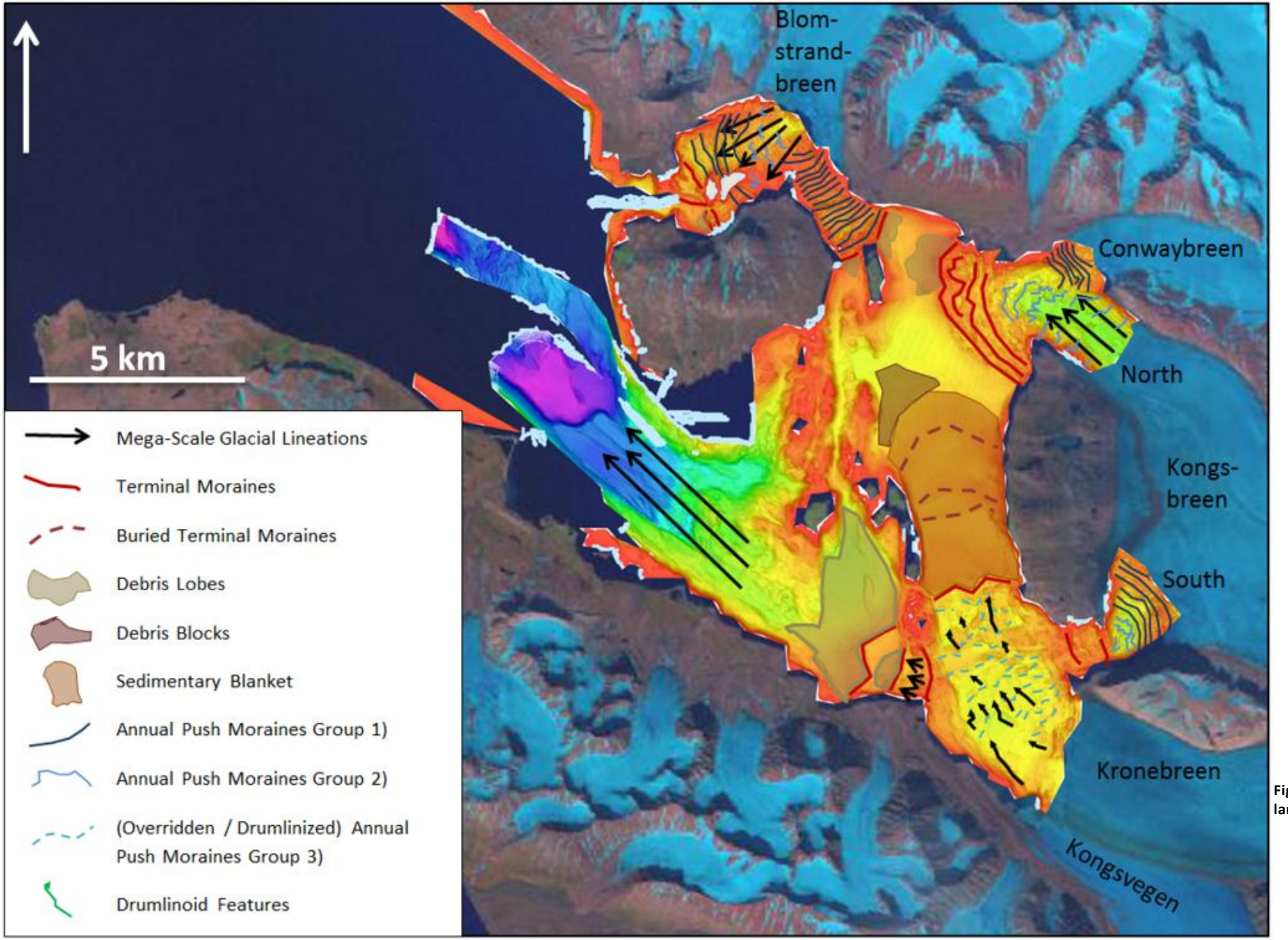

Figure 4.1: Distribution of the landforms found in Kongsfjorden.

The acoustic data available from Kongsfjorden reveals a variety of submarine geomorphological landforms, all of which are presented in **Error! Reference source not found.** and will be described in detail in the following paragraphs.

4.1 Streamlined Groove-Ridge Features – Glacial Lineations

4.1.1 Description

Across parts of the Kongsfjorden seafloor streamlined features are aligned parallel to the main local fjord axis. Two types of lineations occur: Type-I lineations consist of linear parallel grooves and ridges giving the seafloor a wavy morphology (Figure 4.2A). Type-II lineations consist of drumlinoid features: small, narrow ridges aligned parallel to the direction of past ice flow (Figure 4.2B).

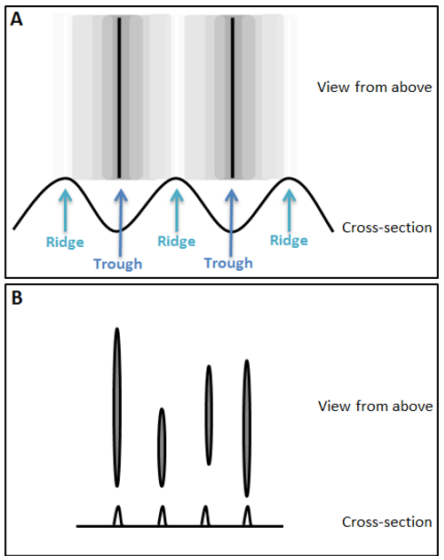

Figure 4.2: Sketch showing Type-I lineations with grooves and ridges from above and in cross-section, and Type-II Lineations as small, drumlinoid ridges from above and in cross-section.

Type-I lineations can be between 500 m and between 2 and 5 km long. The lineations appear over the local width of the fjord basin in sets. Individual features are between 50 and 100 m wide (Figure 4.4-Figure 4.7). This leads to varying elongation ratios (length:width) between 10:1 up to almost 50:1. The elongated depressions are generally no deeper than 3 to 4 m but may locally reach up to a negative relief of 10 m. The ridges mirror these values with average heights of 4 m. This leads to an overall relief of 8 m on average (e.g. Fig. 4.5).

The drumlinoid features of Type-II lineations on the other hand are generally short (up to 600 m) and narrow (around 30 m). The small ridges are 2 m high and occur in sets. The two types of lineations usually do not appear in the same place.

4.1.2 Interpretation

Streamlined, elongate bedforms orientated parallel to former ice flow are very abundant in previously glaciated areas (e.g. Boulton, 1976; Menzies, 1979; Menzies & Rose, 1989; Clark, 1993; Benn & Clapperton, 2000; Ottesen & Dowdeswell, 2006; Ottesen et al., 2008). Such features have been found in the Arctic as well as in Antarctica and are often documented to be either ridges, or grooves, or a combination of the two (e.g. Prest et al., 1968; Boulton et al., 1985; Wellner et al., 2001; Howe et al., 2003; Dowdeswell et al., 2004; 2008; 2010; Ottesen et al., 2005; 2008; Ottesen & Dowdeswell, 2006; King et al., 2009; MacLachlan et al., 2010). As their characteristics vary greatly, a number of different names and an even larger number of formation mechanisms have been

suggested for these geomorphic features. The term lineation was originally used to circumvent the decision whether the geomorphic features were ridges or troughs (Benn & Evans, 2010), and whether they had been formed as a result of erosion or deposition. In recent years the literature has often referred to sets of grooves and ridges, rather than just one of the two (e.g. Clark et al., 2003; Dowdeswell et al., 2004; Ottesen & Dowdeswell, 2006; Andreassen et al., 2007; King et al., 2009). The different names describing the elongated landforms are trying to accommodate characteristics like length, shape and, in some cases, formation mechanisms. Drumlins, crag-and-tail ridges, flutes, mega-flutes and mega-scale glacial lineations are only some of the landforms reported in the vicinity of glaciers and ice sheets (e.g. Menzies & Rose, 1989; Clark, 1993; Benn & Clapperton, 2000; Clark et al., 2003; Ottesen et al., 2005; Dowdeswell et al., 2010). Ice flow velocity is suggested to govern the elongation ratio, with fast velocities representing high length:width ratios (Clark, 1993; Stokes & Clark, 2002; King et al., 2009). Since it is not always easy to identify a landform unambiguously, and many different processes may generate it, the geomorphic features described for Kongsfjorden will be interpreted as mere glacial lineations at this point. These are assumed to be generated as a result of ice flowing over a deformable glacier bed. The Type-II lineations have not been documented for Svalbard surge-type glaciers. Although drumlins and crag-and-tail ridges may be similar to the Type-II lineations, it is believed that the drumlinoid features in Kongsfjorden were generated as a result of two subsequent ice advances. The second one would cause the features created during the first advance to be drumlinized, thereby forming the small parallel ridges. A more specific interpretation will be discussed in section 957.2.1.

4.1.3 Distribution and Geomorphic Characteristics

The glacial lineations occur in front of most of the glaciers terminating into the fjord (Figure 4.3). They are very well preserved in some areas and very faint in others. However, this may be an impression due to the resolution of the dataset or the visualization possibilities of the software, which do not always allow for perfect mapping of the structures. Glacial lineations of Type-I occur north of Blomstrandøya (Figure 4.4), in front of Conwaybreen (Figure 4.5), in front of Kongsbreen South (Figure 4.6) and towards the outer fjord (Figure 4.7). Glacial lineations of Type-II occur in front of Kongsbreen North

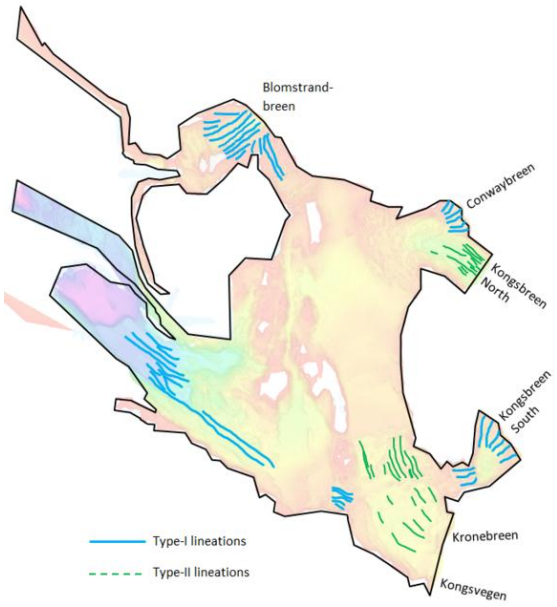

Figure 4.3: Distribution of glacial lineations in Kongsfjorden. Blue lines: Type-I lineations, green lines: Type-II lineations.

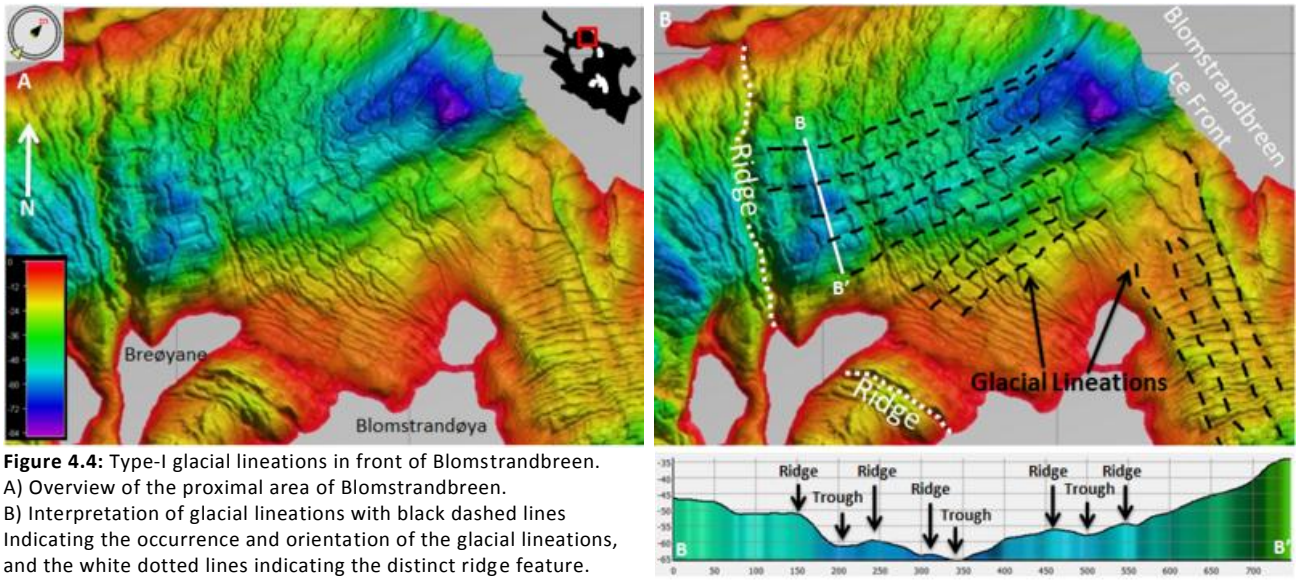

Figure 4.4: Type-I glacial lineations in front of Blomstrandbreen.
A) Overview of the proximal area of Blomstrandbreen.
B) Interpretation of glacial lineations with black dashed lines Indicating the occurrence and orientation of the glacial lineations, and the white dotted lines indicating the distinct ridge feature.

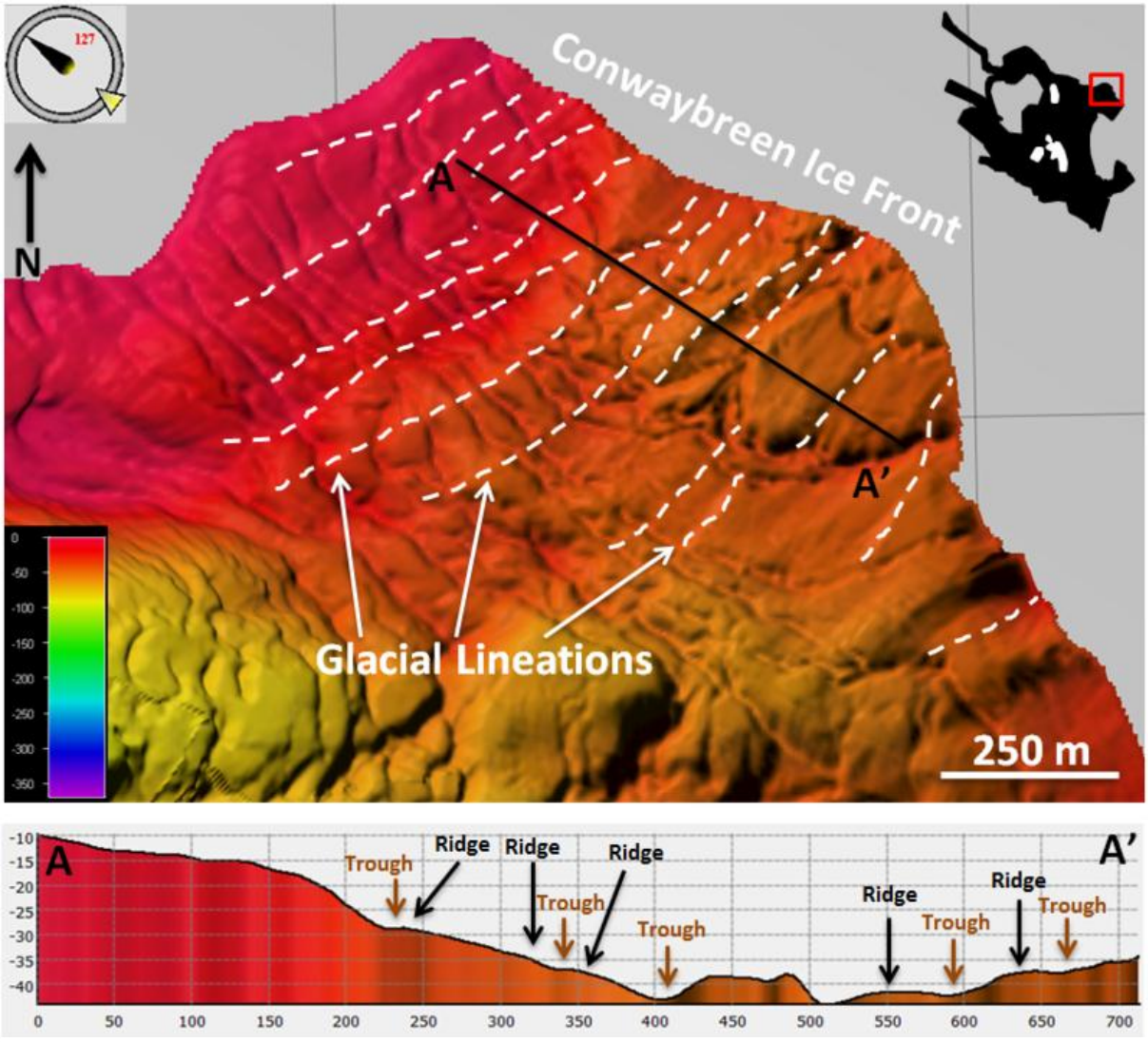

Figure 4.5: Type-I glacial lineations in front of Conwaybreen. White dashed lines indicate occurrence and orientation of the lineations, black line indicates location of the cross-sectional profile A-A'. Grooves (troughs) and ridges of the glacial lineations are indicated on the cross-sectional profile. The colour scale shows water depths between 0 (red) and 350 m (purple). The image was generated using a sun angle of 17.6618; a vertical scale of 0.907, and an azimuth of 127.

(Figure 4.8) and in the vicinity of the Kongsvegen / Kronebreen ice margin (Figure 4.9).

The Type-I lineations north of Blomstrandøya cover a large area of 3.3 km². They occur between the modern ice front of Blomstrandbreen and a distinct transverse ridge feature, and spread radially along both fjord arms (Figure 4.4). The lineations are up to 2.2 km long, around 50 m wide, and have a relief of roughly 5 m (Figure 4.4B).

Based on their short lengths (maximally 700 m), the Type-I lineations in front of Conwaybreen (Figure 4.5) only cover an area of roughly 800 m². The lineations are very faint and hard to see. Their relief is between 1 and 5 m and they are between 20 and 50 m wide.

Type-I lineations also occur sparsely in front of Kongsbreen South (Figure 4.6). The lineations are up to 800 m long directly at the ice margin, but appear to be cut off by the deep central fjord basin (Figure 4.6). They reappear in the shallow parts just north of Colletthøgda's westernmost tip (Figure 4.6), where they extend over short distances (ca. 400 m) up to a larger ridge feature (Figure 4.6). The glacial lineations in this part of the fjord have a relief of 5 m and are around 60 – 80 m wide.

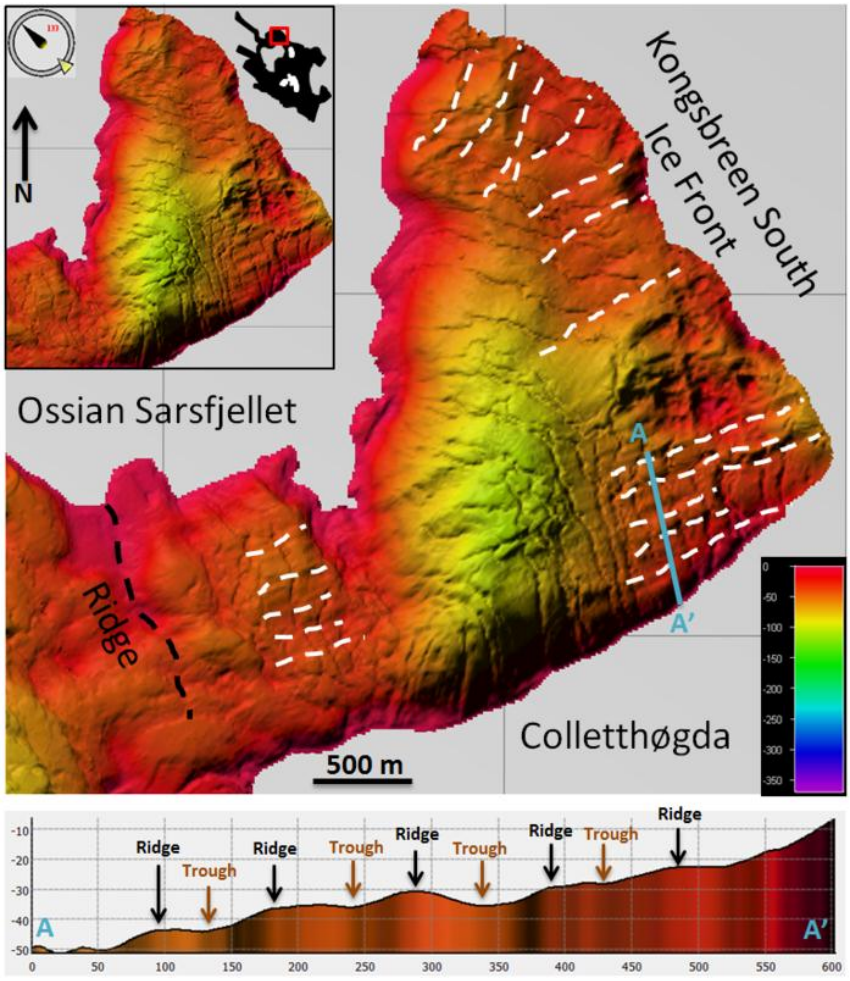

Figure 4.6: Type-I glacial lineations in front of Kongsbreen South. A) Overview over the proximal area of Kongsbreen South. B) Interpretation of the glacial lineations. White dashed lines indicate the occurrence and orientation of the lineations, black dashed line indicates a large transverse ridge. The blue line shows the location of the cross-sectional profile A-A'. Ridges and grooves of the lineations are indicated on the profile. The images were created using a sun angle of 17.6618, an azimuth of 133, and a vertical scale of 0.907. The colour scale shows water depths from 0 (red) to 350 m (purple).

West of the Kongsvegen / Kronebreen margin, further towards the outer fjord, glacial lineations become much more pronounced than elsewhere in the fjord. Here, the linear features occur both in a larger area along the southwestern side of Blomstrandøya, which covers about 5.4 km² (Figure 4.7a, b) and a very small area of roughly half a square kilometer (Figure 4.7a, c). These lineations,

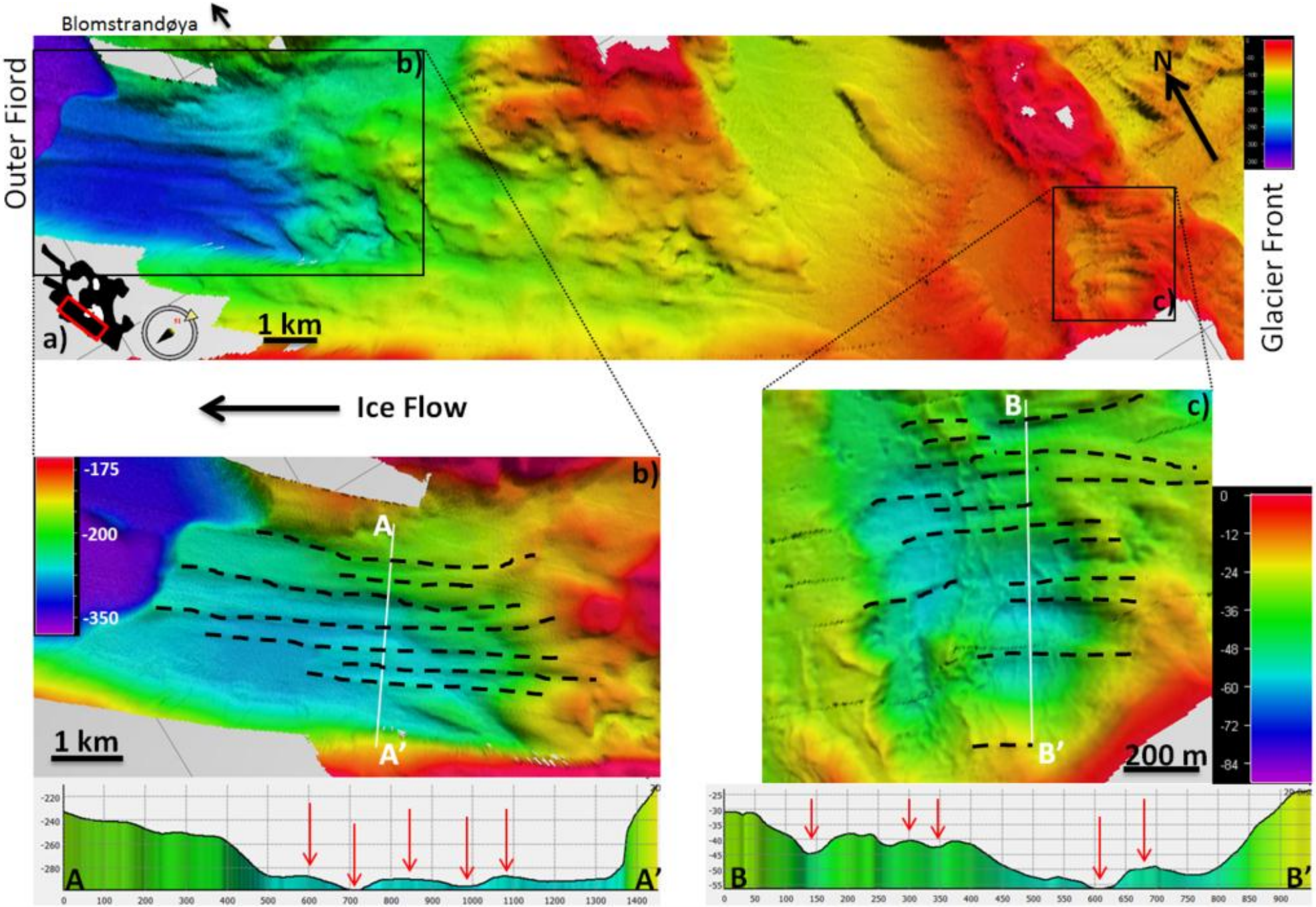

Figure 4.7: a) Overview of the Type-I glacial lineations in the southwestern parts of the study area with the black rectangles indicating the base for zoomed-in pictures b) and c). The colour scale in a) represents water depths between 0 (red) and 350 m (purple). White lines in b) and c) represent orientation of cross-sectional profiles A and B. Black dashed lines indicate the occurrence and orientation of the glacial lineations. All images were generated using a sun angle of 23.8115, a vertical scale of 0.861, and an azimuth of 51.

located in the more proximal region of the glacier termini, only range between 2 and 5 m in height (Figure 4.7c, profile B), and stretch along a maximum length of 600 m. Those in the outer fjord are around 3.5 km long and have a relief close to 10 m (Figure 4.7b, profile A).

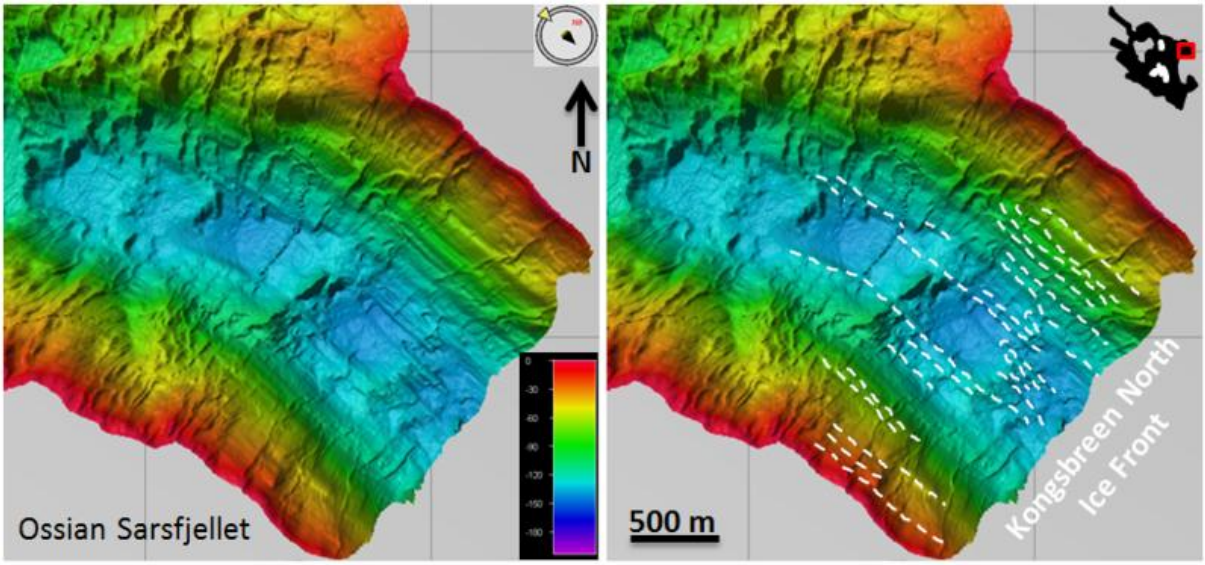

Figure 4.8: Type-II glacial lineations in front of Kongsbreen North. A) Overview over the proximal area of Kongsbreen North. The colour scale shows water depths between 0 (red) and 350 m (purple). B) White dashed lines show the interpretation of the occurrence and orientation of the glacial lineations. The images were created using a sun angle of 17.6618 and a vertical scale of 0.907.

In front of Kongsbreen North the geomorphic features are much clearer along the fjord walls and close to the ice front compared to their more hidden character within the central and deeper part of the fjord basin (Figure 4.8). These lineations are again restricted to the immediate fore-field of the modern ice front and reach lengths of maximally 3 km, widths of maximally 60 m and a faint relief of up to 5 m. As the seafloor in this area is rough and small ridge features are ubiquitous, the glacial lineations do not stop abruptly but rather gradually, indicating their possible burial by the ridges.

The fjord basin in front of Kongsvegen / Kronebreen shows some weak signs of glacial lineations (Figure 4.9). Small ridges of about 1 to 5 m relief are between 50 and 150 m wide and 200 m to 1.7 km long. They are aligned parallel to the fjord axis. Due to their orientation and their character in a cross-sectional profile, these small, elongated ridges are interpreted to be glacial lineations as well. If looked at carefully the entire area shows a certain dynamic character, indicating movement from the glacier front deeper into the fjord. This is especially pronounced in the small elongated ridges, which align with these dynamics and appear to be indicative of past ice flow. The differences between the two types of glacial lineations and their possible formation mechanisms will be further addressed in section 7.2.1.

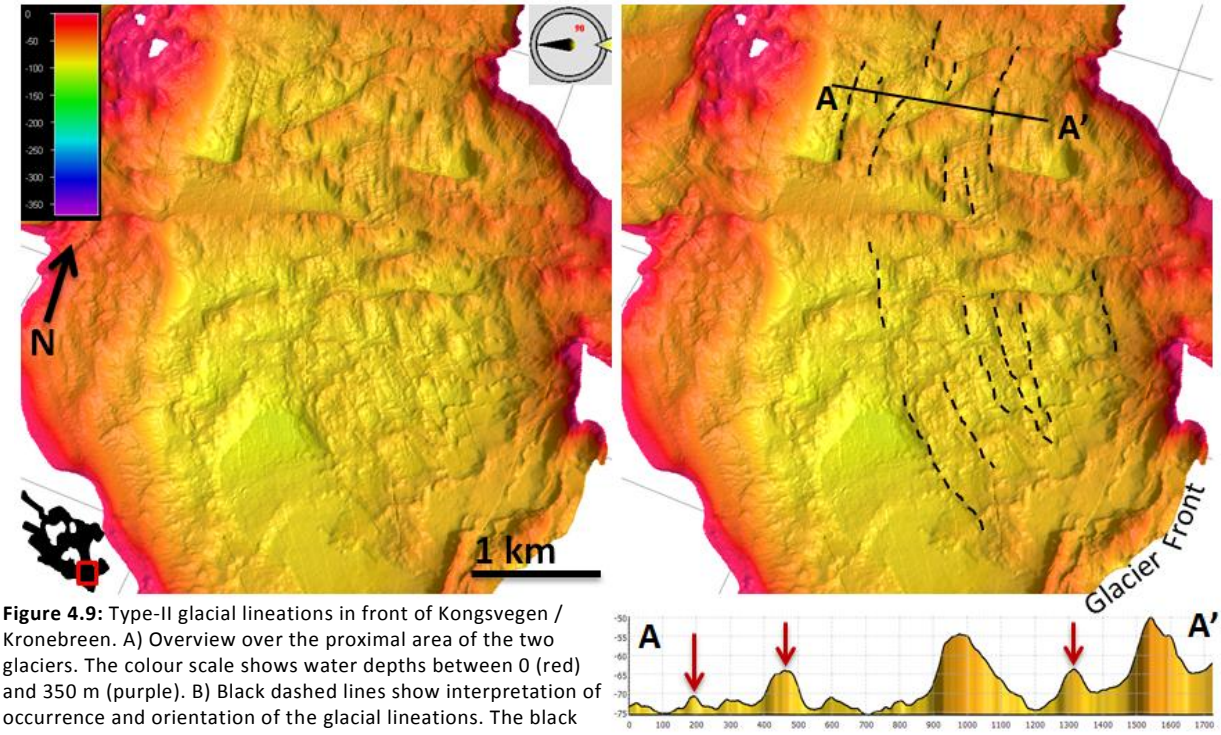

Figure 4.9: Type-II glacial lineations in front of Kongsvegen / Kronebreen. A) Overview over the proximal area of the two glaciers. The colour scale shows water depths between 0 (red) and 350 m (purple). B) Black dashed lines show interpretation of occurrence and orientation of the glacial lineations. The black solid line indicates the location of the cross-sectional profile A-A'. The small ridges (glacial lineations) are highlighted by the red arrows in the profile. The image was generated using an azimuth of 90, a sun angle of 15.5349 and a vertical scale set to 1.04. The colour scale ranges from 350 m (purple) to 0 m (red) water depth.

4.2 Large Ridges – Terminal Moraines

4.2.1 Description

A number of large ridges occur within Kongsfjorden, often in association with some smaller ones. An example is shown in Figure 4.10. The large ridges act as a kind of border between the landforms found in the proximal areas of the glaciers and the smooth sea floor in the distal parts. The large ridges are normally orientated perpendicular or sub-perpendicular to the direction of past ice flow and transverse to the main fjord axis. The only landforms appearing beyond these ridges are lobe-like features, which will be described in section 4.3. The transverse ridges occur as single features as well as in sets of two or four. They are typically 15 to 20 m high, but can reach 27 m, are generally around 2 km long, and between 500 and 800 m wide. Cross-sections of these ridges (e.g. Figure 4.10) reveal their asymmetrical character, with a steeper proximal and a smoother, more gradual distal flank. The crests are defined and slightly curved.

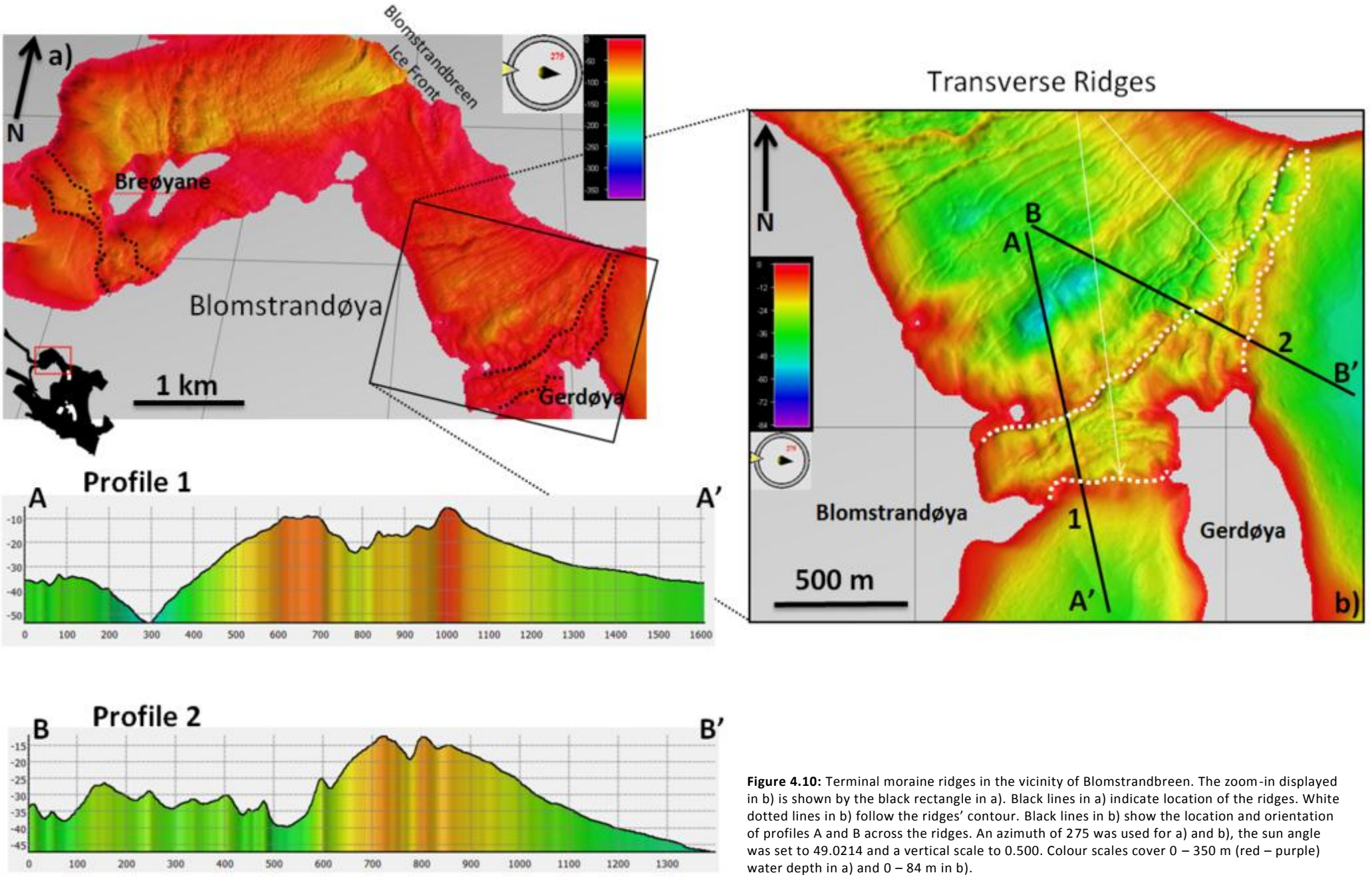

Figure 4.10: Terminal moraine ridges in the vicinity of Blomstrandbreen. The zoom-in displayed in b) is shown by the black rectangle in a). Black lines in a) indicate location of the ridges. White dotted lines in b) follow the ridges' contour. Black lines in b) show the location and orientation of profiles A and B across the ridges. An azimuth of 275 was used for a) and b), the sun angle was set to 49.0214 and a vertical scale to 0.500. Colour scales cover 0 – 350 m (red – purple) water depth in a) and 0 – 84 m in b).

4.2.1 Interpretation

Large ridges with a generally parallel orientation to the modern ice front are commonly found in the vicinity of tidewater glaciers around Svalbard (e.g. Ottesen & Dowdeswell, 2006; Ottesen et al., 2008; MacLachlan et al., 2010). Their formation is ascribed to several mechanisms, for instance the pushing up of glacier-transported debris in front of the terminus during stagnation, but is generally assumed to be indicative of past ice positions (e.g. Solheim & Pfirman, 1985; Boulton, 1986; Boulton et al., 1999; Bennett, 2001; Ottesen et al., 2005). As the ridges in Kongsfjorden have been described to be large, extensive in width and length, with moderately arcuate crests and an asymmetrical shape, where the ice-proximal flank is considered to be steeper than the smooth distal flank, they all show the characteristics described by Solheim & Pfirman (1985), Solheim (1991), Ottesen et al. (2005, 2009), Ottesen & Dowdeswell (2006) and MacLachlan et al. (2010). The ridges are hence inferred to be recessional moraines, with the most distal feature marking the outermost extent of the glacier front at a certain time. As the study area is largely influenced by modern glacial activity there are two possibilities for the terminal ridges: (1) terminal (surge) moraines or (2) terminal moraines indicating the maximum ice extent during the glaciated periods, i.e. the Late Weichselian or the Little Ice Age. The ridges are inferred to be the result of surge activity, an issue which is further addressed in section 7.2.2.

4.2.2 Distribution and Geomorphic Characteristics

The large ridges are common in Kongsfjorden and appear in the north in front of Blomstrandbreen and along the eastern side of the dataset in front of Kongsbreen North and Conwaybreen, close to Kongsbreen South, and in front of Kongsvegen / Kronebreen (Figure 4.11).

Both fjord arms close to Blomstrandbreen (east and west of Blomstrandøya) host two of these larger transverse ridges each (Figure 4.10, Figure 4.12). A large transverse ridge can be found on the eastern side of Blomstrandøya (Figure 4.10). It is located at a distance of about 3.5 km from today's ice margin. The height is determined to be between 30 and ~ 42 m (compare Figure 4.10,

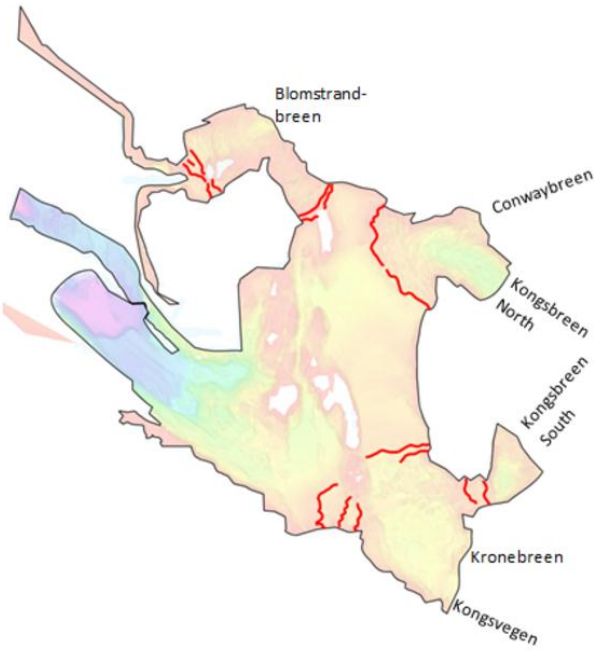

Figure 4.11: Distribution of terminal moraines in the study area.

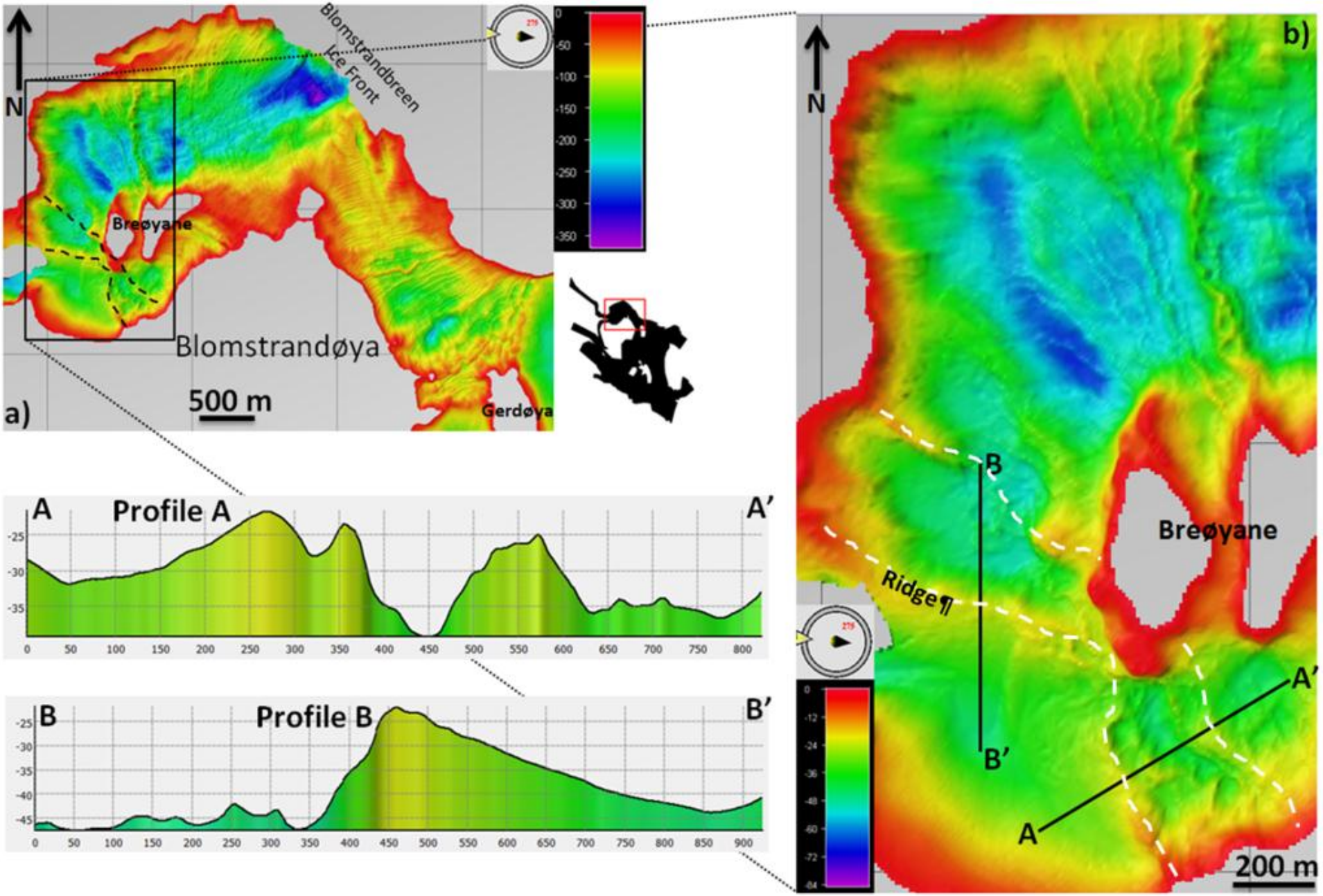

Figure 4.12: Large transverse ridges / terminal moraines in the surroundings of Blomstrandbreen, particularly to the west of Blomstrandøya and to the west and south of the two Breøyane. Black rectangle in a) indicates location of b) and profiles A and B are indicated by black lines. Black and white dashed lines follow the contours of the transverse ridges. All images were generated using a sun angle of 49.1324, a vertical scale of 0.500 and an azimuth of 275.

profiles A and B).

It is located directly northwest of the small island Gerdøya, where Kongsfjorden is represented by one fjord arm with a width of approximately 1.7 km. Here, the ridge is observed to extend across the entire basin. Approximately 400 m further to the southeast two more ridges can be found next to each other, which, together, are assumed to reflect a second moraine. Gerdøya separates the fjord into two separate arms here (Figure 4.10) and therefore also divides the ridge into two ridge forms with lengths of 750 m for the ridge more to the west and a little over 1 km for the more eastern feature. The ridge here is well-defined, especially when looking at the ridges from the bird's eye perspective (Figure 4.10, profile A). The cross-sectional profiles (Figure 4.10, profiles A and B) show a defined crest and a steeper proximal and more gradual, flatter distal flank of the ridge. The crest is located in extremely shallow water: In some parts, the ridge's peak is only barely covered by water in a depth of 7 - 8 m.

The seafloor of Kongsfjorden just west of Blomstrandøya's northern part hosts two ridges with similar characteristics as those just described. The ridges are located directly to the south of Breøyane (Bre Islands, Figure 4.12, profile A) and at the western flank of the two islands (Figure 4.12, profile B). The ridge south of the islands has a north-south orientation (Figure 4.12b) and is divided into several peak crests (Figure 4.12, profile A). The most distal crest is located about 4.5 km from the present glacier terminus, is almost 20 m high and is in a water depth of roughly 23 m. It is closely followed by a much smaller peak occurring on its proximal flank, about 80 m from the distal peak. A third crest is located about 300 m further towards the present ice margin of Blomstrandbreen, which has a height of 15 m and is pointier than the other two peaks. This appearance of several peaks suggests the presence of two terminal moraines in this area.

The ridge in the west of Breøyane has a NE-SW orientation across the fjord arm and is roughly 3 km away from the ice margin of Blomstrandbreen (Figure 4.12, profile B). This ridge is roughly 25 m high and approximately 700 m long. The northern flank of the ridge is very steep with slope values between 10 and 21, while its southern and ice-distal flank very gradually slopes down with an angle of roughly 3 degrees. Generally the two features in the west of Blomstrandøya are very similar. Both ridges have comparable slope angles with flatter angles for the distal and steeper values for the proximal flanks. The water depth of both features is just above 20 m for the peaks and the ridges seem to be connected to each other at the southwestern tip of the western Breøyane (Figure 4.12). This indicates that the situation is similar to the ridges found in the east of Blomstrandøya and that again the fjord basin is separated into two arms by small islands (Breøyane). Consequentially the

ridge feature is also divided into two parts which, most likely, reflect one single terminal moraine deposited partly up against the western of the two Bre Islands (Figure 4.12).

In the rough area that defines the region in front of Conwaybreen and Kongsbreen North (Figure 4.13), it is not easy to distinguish single ridges. The relief is so variable that larger ridges seem to stretch over an entire area of over 6 km². A cross-sectional profile across the most defined crests, which are located along the northern fjord wall (Figure 4.13, A) shows the occurrence of at least three ridges over a distance of about 2 km. The ridge furthest from the ice margin is very similar to the previously described ridges: it is large with heights of almost 40 m, a length of 3650 m and a width exceeding 600 m. As "beginning and end" of the ridge are not clearly visible, however, it is not possible to determine the width accurately. The ridge crest is very well-defined near the northern fjord wall, where it is located in a water depth of roughly 15 m, but is gradually less distinguishable further southeast. This is also due to the separation of the one pronounced crest into two less defined ridge tops.

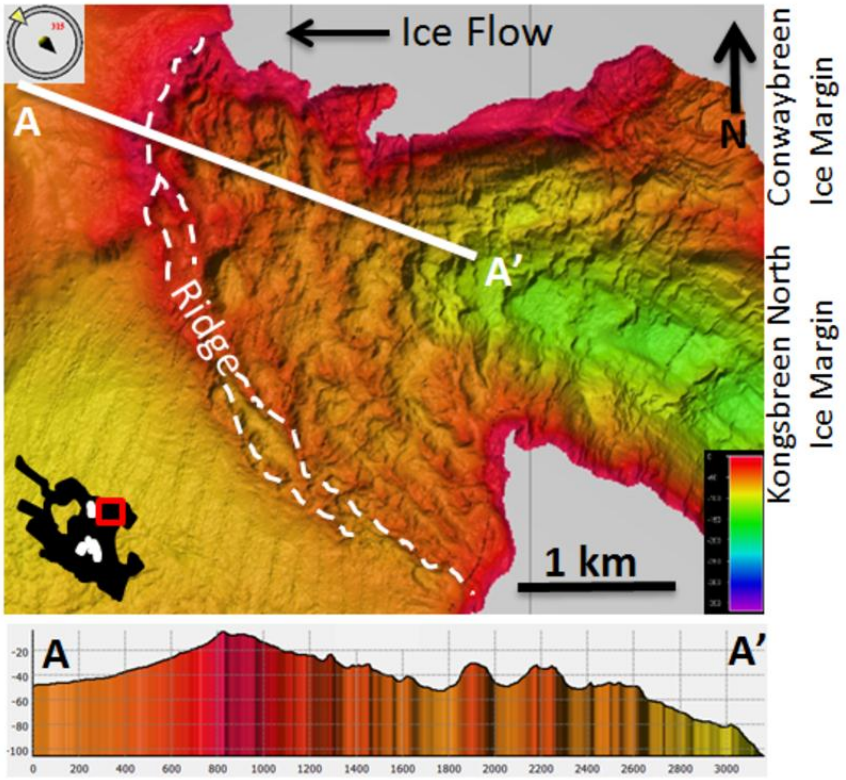

Figure 4.13: Large transverse ridges in front of Conwaybreen and Kongsbreen North are shown by white dashed lines. The white solid line shows the location of the cross-sectional profile A-A'. The sun angle for the generation of the image was 16.116 with an azimuth of 315. A vertical scale of 2.0 was used. The colour scale reflects water depths between 350 (purple) and 0 m (red).

A general trend for the ridges to become more defined with increasing distance to the glacier front can be observed in the chirp profiles for this area (Figure 4.14). This is particularly noticeable west of the Kongsbreen North terminus. Two large ridges with multiple crests each are well pronounced and have a height of about 40 m (Figure 4.14, A). The crests are 1 km apart. The basin in between the crests shows thick, stratified semi-transparent reflections, indicating a sink for sediment accumulation (Figure 4.14). The ridges' reflections are thin on the slopes, suggesting hard, impenetrable material. The reflections are transparent, but take on a more semi-transparent character on the flatter ridge tops and the more gradual slopes at their bases. Areas located south or

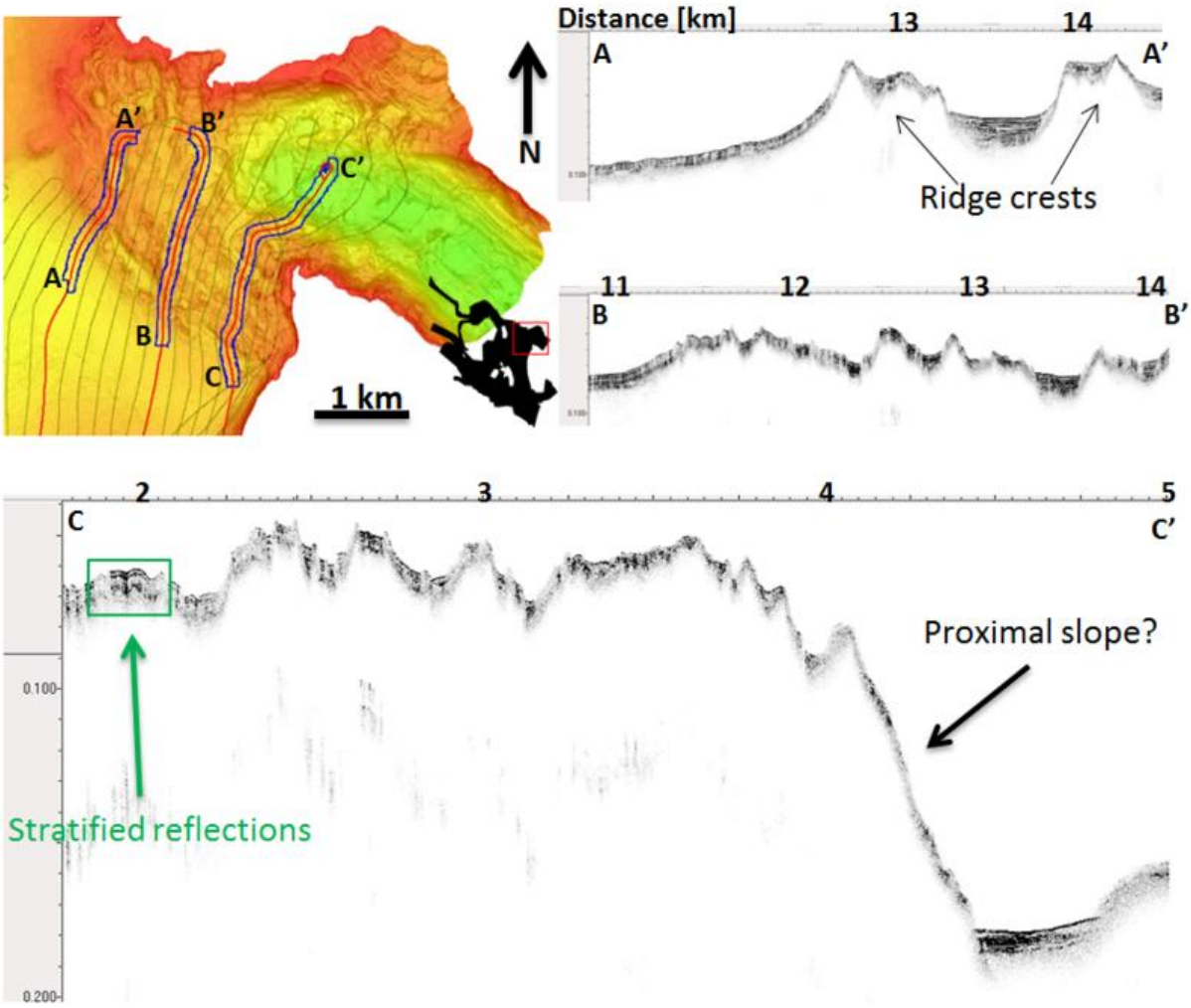

Figure 4.14: Selected chirp lines across the distal regions of Conwaybreen and Kongsbreen North. Reflections indicate a rugged terrain and the occurrence of several ridge features. Two ridges are particularly pronounced (profile A) whereas other features are shallower and less defined. Chirp lines are displayed with distance in km on the x-axis and two-way-travel time on the y-axis.

southwest of the Conwaybreen / Kongsbreen North glacier fronts are characterized by a rougher seafloor with less defined features (Figure 4.14, B and C). The most pronounced ridges here reach heights around 18 m. The features are located closer together with distances between 0.25 and 0.5 km (Figure 4.14, B and C). The reflection character has a more semi-transparent appearance and reflections are generally thicker than for the two well-defined distal ridges from profile A (Figure 4.14). Stratification is visible but very discontinuous and not well-defined. The transition between the basin directly in front of the two glaciers and this rougher terrain is defined by a steep decrease in water depth (Figure 4.14, C). It is possible that this slope indicates the steep proximal slope of a terminal moraine; however, there is no distal flank to support this theory. Instead of the distal flank the previously discussed ridges occur and water depth stays more or less the same after this sudden increase (Figure 4.14, C). The rougher terrain and the two well-defined distal ridges are inferred to be recessional moraines generated during retreat: the most distal ridge (Figure 4.14, A) is inferred to represent the maximum ice extent. It is interesting that Conwaybreen and the northern front of Kongsbreen have produced a distinct terminal moraine with debris lobes on the distal flank (see

section 4.3, below), when both glaciers are supposed to be of non-surge type (Hagen et al., 1993). The large moraine must be marking the maximum ice extent of the two glaciers as there are no features beyond this ridge. The only features that occur in even more distal terrain are features that

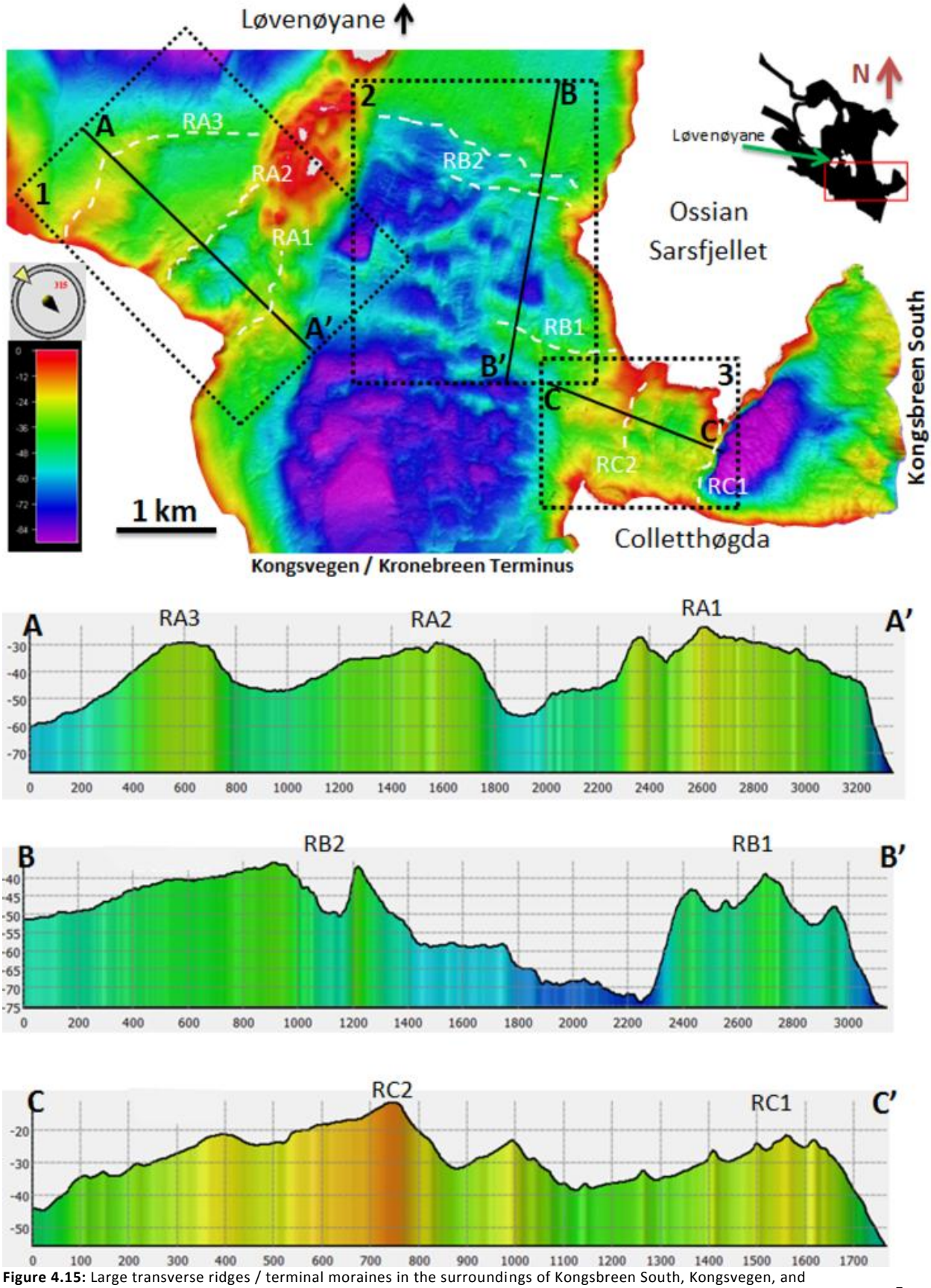

Figure 4.15: Large transverse ridges / terminal moraines in the surroundings of Kongsbreen South, Kongsvegen, and Kronebreen. White dashed lines follow the contours of the large ridges. All images were created using a sun angle of 49.1324, a vertical scale of 0.500 and an azimuth of 275.

are clearly originating from one of the other glaciers. This phenomenon leaves room for discussion and will be evaluated further in section 7.2.2.

Similar ridges to the ones described in the previous paragraphs appear in the south and east of the study area in the vicinity of the southern ice front of Kongsbreen and close to the shared ice margin of Kronebreen and Kongsvegen (Figure 4.15). The ridges in this area are not as well defined as in the proximity of Blomstrandbreen, but cross-sectional profiles reveal clearly defined ridge tops (Figure 4.15A, B, C). Due to a rougher general relief it is not easy to describe one single ridge; the features around Kongsvegen and Kronebreen seem to occur mostly in sets of two or three (Figure 4.15). On the profiles a certain asymmetry is visible, just as for the structures near Blomstrandbreen, and the typical trend of a steeper proximal and a more gradual distal flank can be observed (e.g. Figure 4.15, profile C).

A rugged relief characterizes the southwestern fjord arm just beneath the Løvenøyane Island Group. At the entrance to this fjord arm, which is in close proximity to the Kongsvegen / Kronebreen terminus, a number of three ridge-like features can be identified (Figure 4.15, (1), profile A). It is not easy to distinguish a definite asymmetry, but on the profile at least the two more distal features seem to have the typical steep proximal and flat distal slopes. The three ridges are all around 30 to 40 m high and their crests 30 m deep (water depth). The three different ridge peaks are located about one kilometer apart from each other, with a total distance to the present glacier terminus of between 3.7 km (most proximal ridge) and 5.7 km (most distal ridge).

The area indicated by Figure Figure 4.15 (2) is located directly to the northwest of the present glacier terminus. It is characterized by a fairly chaotic morphology with numerous smaller ridges. A profile across the seafloor suggests the presence of two larger ridges. The more distal of the two is inferred to be a possible terminal moraine, as it reveals the typical asymmetry. Furthermore, this distal feature has a height of about 40 m and its highest point is located in a water depth of roughly 35 m. It is divided into two small peaks, with the more proximal one being slightly smaller and deeper than the “main” more distal crest. Both features extend across the entire fjord basin and are approximately 2.2 km long.

The third main feature in the area is a ridge located in front of the southern ice margin of Kongsbreen (Figure 4.15, (3), profile C). It is noticeable that this feature does not extend across the entire width of the fjord, but is constricted to a fairly short length of roughly 500 m. Its asymmetry is rather clear; however, again, the seafloor is characterized by a rugged and fairly chaotic nature. The ridge has a height of around 40 m and reaches into shallower areas with a water depth of ~ 10 m. The profile across the main ridge indicates the presence of another elevated area, which may also represent a

certain asymmetrical nature. This feature could hence be interpreted to be a second terminal moraine, located in a more proximal setting than the other, second feature. Both structures are defined by their steep proximal flanks and flatter distal slopes although both distal slopes are characterized by additional features (such as small, sharply defined ridges with a relief of about 1 m, or less defined bumps on the seafloor, compare Figure 4.15, profile C). The more proximal ridge is approximately 35 m high and is located at a water depth of 20 m. Its length of 800 m represents the width of the local fjord basin.

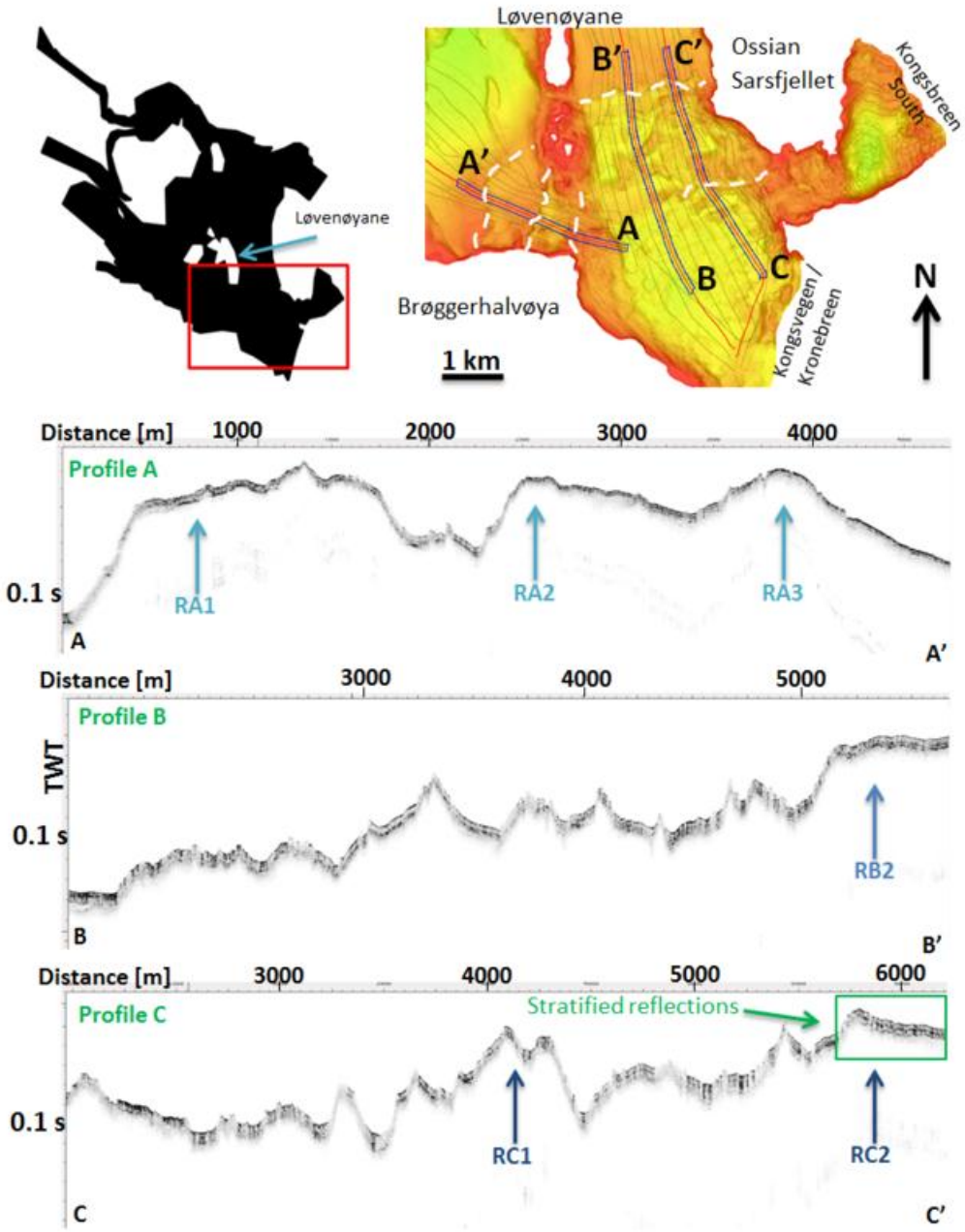

Figure 4.16: Selection of chirp profiles indicating large transverse ridges in front of the Kongsvegen / Kronebreen ice margin. Respective location of profiles is indicated on the left. The Y-axis shows the travel time of the acoustic signal to the seafloor and is commonly between 0 and 0.1 ms.

Chirp data (Figure 4.16A) confirms the occurrence of three ridges west of the Kronebreen / Kongsvegen ice margin. Profiles B and C (Figure 4.16) indicate the occurrence of at least one large transverse ridge in the area north of the present glacier termini: in profile B the transition from the rough relief to a bulging ridge is obvious, showing the presence of one terminal moraine in that position. The ridge exhibits the previously mentioned asymmetry of proximal and distal slope. Profile C shows two locations with significantly higher elevations: one at 4 km away from the start of the chirp line and the other one at about 5.5 km away. The ridges are not as clearly defined as in previous profiles and no trend in symmetry is definable. The even rougher sea floor on the east side of the fjord becomes apparent, which is why the large ridges do not stand out as clearly defined features.

4.3 Lobe-Shaped Features – Mass Transport Deposits

4.3.1 Description

Several sets of lobe-shaped features appear in Kongsfjorden (Figure 4.17). They are in every case closely associated with the terminal moraines described in section 4.2. The features occur on the distal flank of the latter and often appear in sets of several lobes (Figure 4.17), but single lobes also occur, especially when the terminal moraine is short (see Figure 4.19, below). The lobes extend over areas between roughly 0.06 km² (single lobes) and about 1.1 km² (lobe sets) and reach lengths of up to 1.2 km. The width of single lobes may reach up to 360 m, but this is not always clearly visible as especially the lobe sets seem to be made up of several single events that partly superimpose each other (Figure 4.17). As they are located down-stream of the terminal moraines, the lobes follow the ridges' outlines: they often extend from a water depth of roughly 15 m down to around 50 m. In one case water depth exceeds 100 m (see Figure 4.21). Sometimes it is possible to see distinct surface reliefs of the lobes, such as grooves and craters in the sediment surface, indicating activity related to different processes.

4.3.2 Interpretation

Sedimentary lobes have been observed multiple times on Svalbard, also intimately linked to transverse ridges (e.g. Ottesen & Dowdeswell, 2006; Kristensen et al., 2009). They are always positioned on or at the foot of the distal flanks of the latter and cover areas of varying sizes (see also Plassen et al., 2004). The lobes have been described to be large subaquatic outwash fans (Boulton, 1986) or mud aprons (Kristensen et al., 2009), and are interpreted to be glacigenic debris flows originating at the glacier terminus during the last advance of a glacier (e.g. Boulton et al., 1996; Plassen et al., 2004; Ottesen & Dowdeswell, 2006).

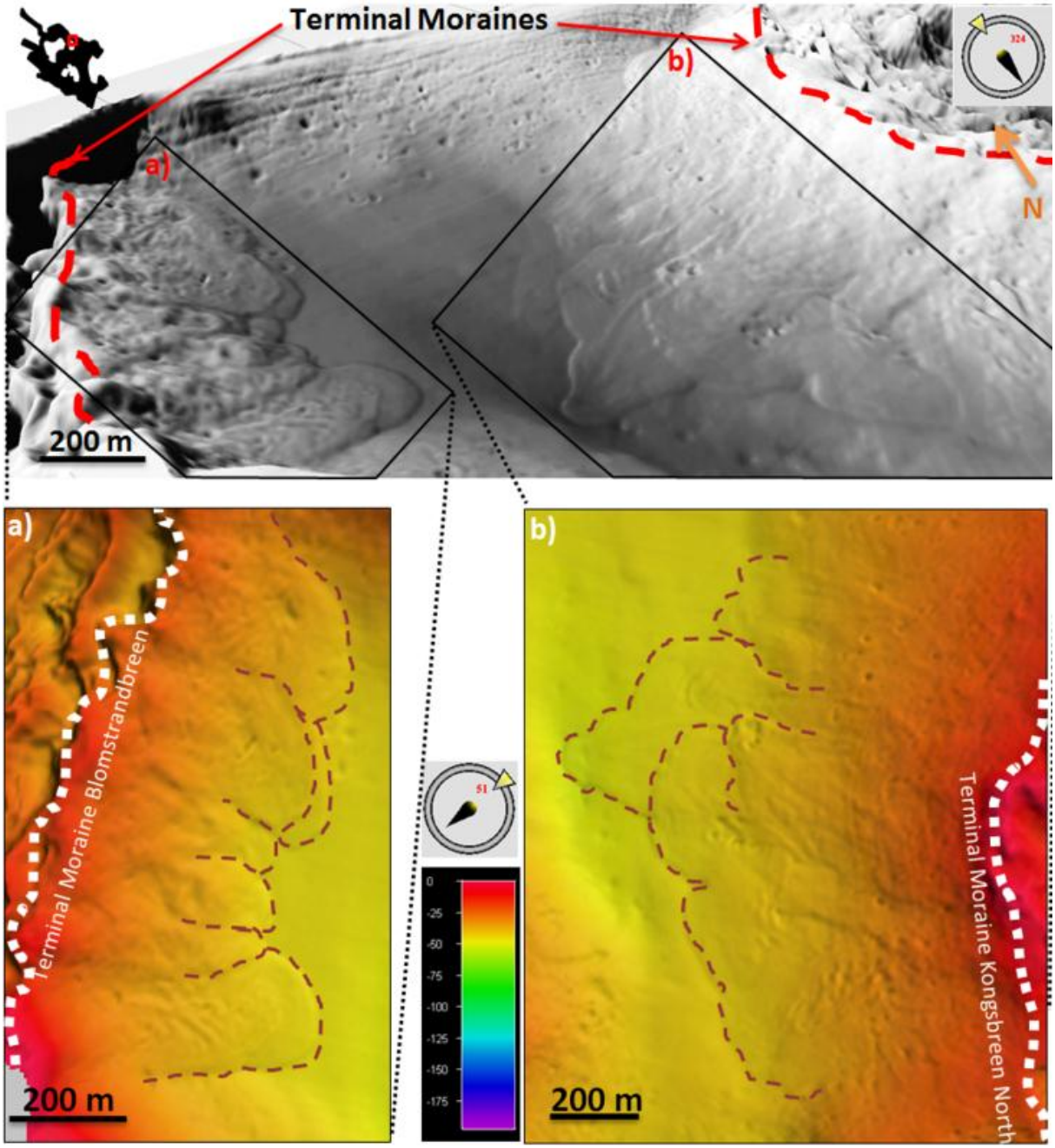

Figure 4.17: Lobe-shaped features observed along the north-eastern side of Gerdøya in the northern part of the study area. a) and b) are detail images of the corresponding selected areas in the overview image on top. Red dashed and white dotted lines indicate transverse ridges, whereas brown dashed lines mark the tentative extent of the lobes. Colour changes were conducted for enhanced visualization. The images were generated using a sun angle of 0.5195 and a vertical scale of 1.071.

Ottesen et al. (2008) suggest two possible origins of the mass flows: (1) the failure of the distal slope of the terminal moraine or (2) the extrusion of subglacial sediments that were transported to the glacier terminus during its surging phase. The deposition of the sediment lobe would then take place during the stagnation of the ice margin before retreating again (e.g. Boulton et al., 1996). Based on observations and the frequent occurrence of such glacier-related sediment lobes Ottesen et al. (2008) assume this second possibility to be the more likely triggering mechanism.

4.3.3 Distribution and Geomorphic Characteristics

In Kongsfjorden, sedimentary lobes can be found almost everywhere where there is a terminal moraine. Figure 4.18 shows their distribution. Their lower extent is almost always well-defined, clearly visible and indicated by dashed lines in the figures (e.g. Figure 4.17, Figure 4.19,Figure 4.20), whereas it is not entirely certain whether they originate on top of the moraine or further down-slope. Two lobe sets appear in a small basin between two terminal moraines (one of Kongsbreen North and one of Blomstrandbreen, north-northeast of the bathymetric data set (Figure 4.17). These sets are particularly well-defined and suggest the presence of several lobes that partly superimpose each other (Figure 4.17). These tongue-shaped lobes may have been generated as a result of different flow behavior during one mass transport, or they may reflect single, timely independent events. The sets face each other as they occur on opposite sides of the basin, and thereby indicate two different source regions, which are believed to be Kongsbreen North for the more easterly lobe set and Blomstrandbreen for the westerly (Figure 4.17). Each set is made up of up to four lobes, with maximum lengths of 420 m for the northwestern set (minimum 255 m) and 800 m for the set on the southeastern flank of the basin (minimum 555 m). The widths of the entire sets are minima of 840 and 1150 m, respectively. The width however, cannot be identified unambiguously, as the marginal areas of both sets are blurred by the appearance of circular depressions (see section 4.6, below) on their surfaces. Both lobe sets originate on the top of a terminal moraine in shallow water with depths of 15 m and may extend down to 45 m in the northwest and 52 m in the southeast.

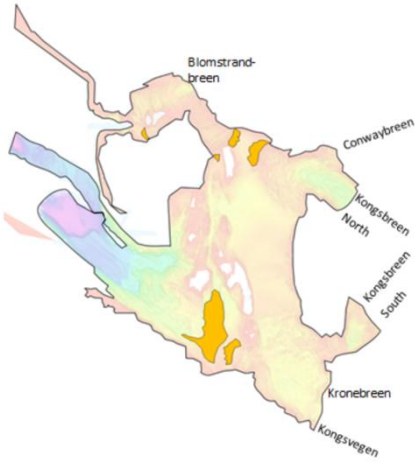

Figure 4.18: Distribution of sedimentary lobes in Kongsfjorden.

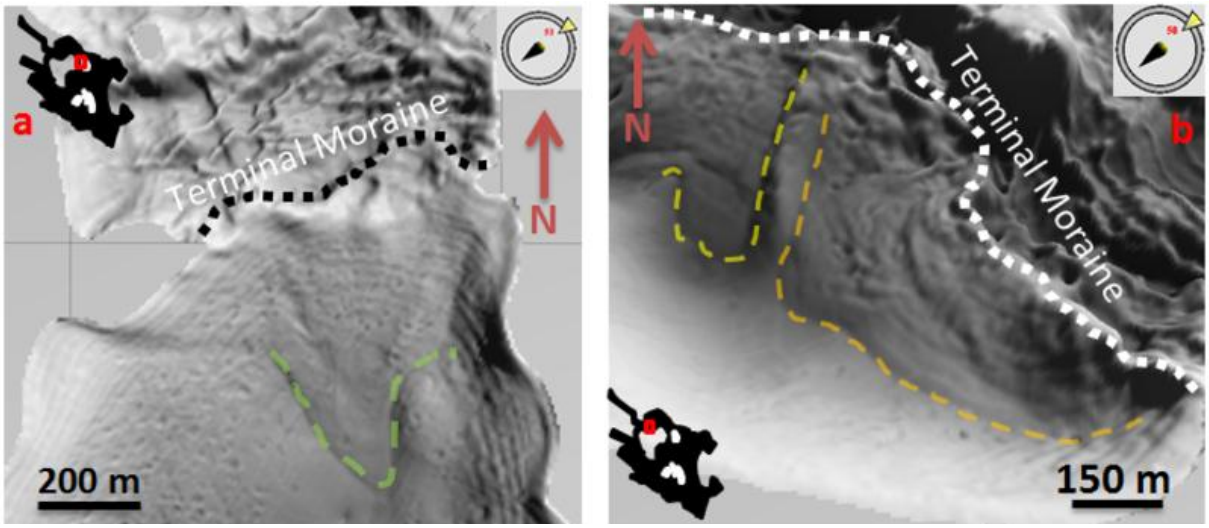

Figure 4.19: Single sedimentary lobes located to the east of Gerdøya (a) and to the north of Blomstrandøya (b). The lobes are located on the distal flank of a terminal moraine created by Blomstrandbreen. Tentative extents are indicated by dashed lines. Both images were created using a sun angle of 12.6247 and a vertical scale of 1.696.

The terminal moraine located on the western flank of Gerdøya was also created by Blomstrandbreen and has a sedimentary lobe on its distal side as well (Figure 4.19a). This lobe differs from the lobe sets, as it is one single feature with clear outlines and has a pointier end, reminding of the shape of a tongue. Its width is restricted due to the local fjord topography and the small lateral extent of the terminal moraine: the lobe is only approximately 340 m wide and maximally 600 m long. A fourth and fifth lobe just north of Blomstrandøya have an extent of 130 x 250 m and 520 x 210 m (width x length), respectively (Figure 4.19b). Again, the terminal moraine they are associated with is inferred to have been produced by the surge of Blomstrandbreen in 1960. As discussed previously, it is possible that the lobe set in the northeast of Blomstrandbreen (Figure 4.17a), the lobe west of Gerdøya (Figure 4.19a) and the two north of Blomstrandøya (Figure 4.19b) all originate at the top of the same terminal moraine, if a connection of the ridges in this area is actually given (Figure 4.20).

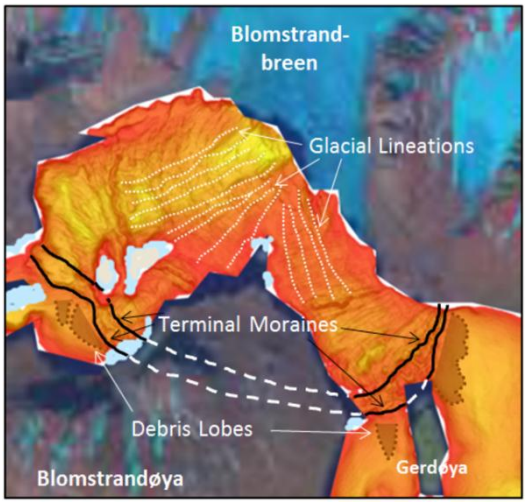

Figure 4.20: Glacial lineations (white dotted lines), terminal moraines (black solid lines) and their possible continuity across Blomstrandøya (white dashed lines) and debris lobes (brown shaded areas) in front of Blomstrandbreen.

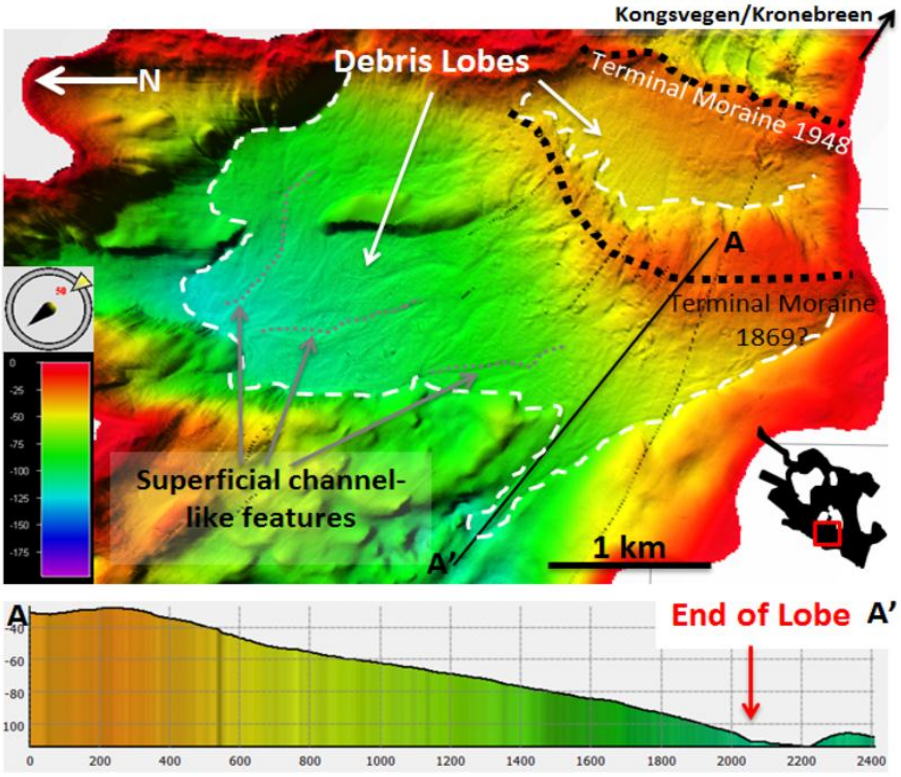

Figure 4.21: Large sedimentary lobes associated with the terminal moraines close to the present margin of Kongsvegen / Kronebreen. The terminal moraines of 1948 and 1869 are outlined by the black dotted lines. Lower boundaries of the debris lobes are indicated by white dashed lines. Superficial channel-like features are marked by grey dotted lines on the larger of the two lobes. Cross-sectional profile A shows the local topography. The image settings were a sun angle of 19.5195 and a vertical scale of 1.071.

A large area south of Løvenøyane contains two terminal moraines (probably from the surges of 1869 and 1948 of Kongsvegen / Kronebreen) and associated lobes (Figure 4.21). Due to a fairly uneven relief it has not been easy to map out the exact extent of the lobes, but a tentative lower boundary is outlined in Figure 4.21 (white,

dashed lines).

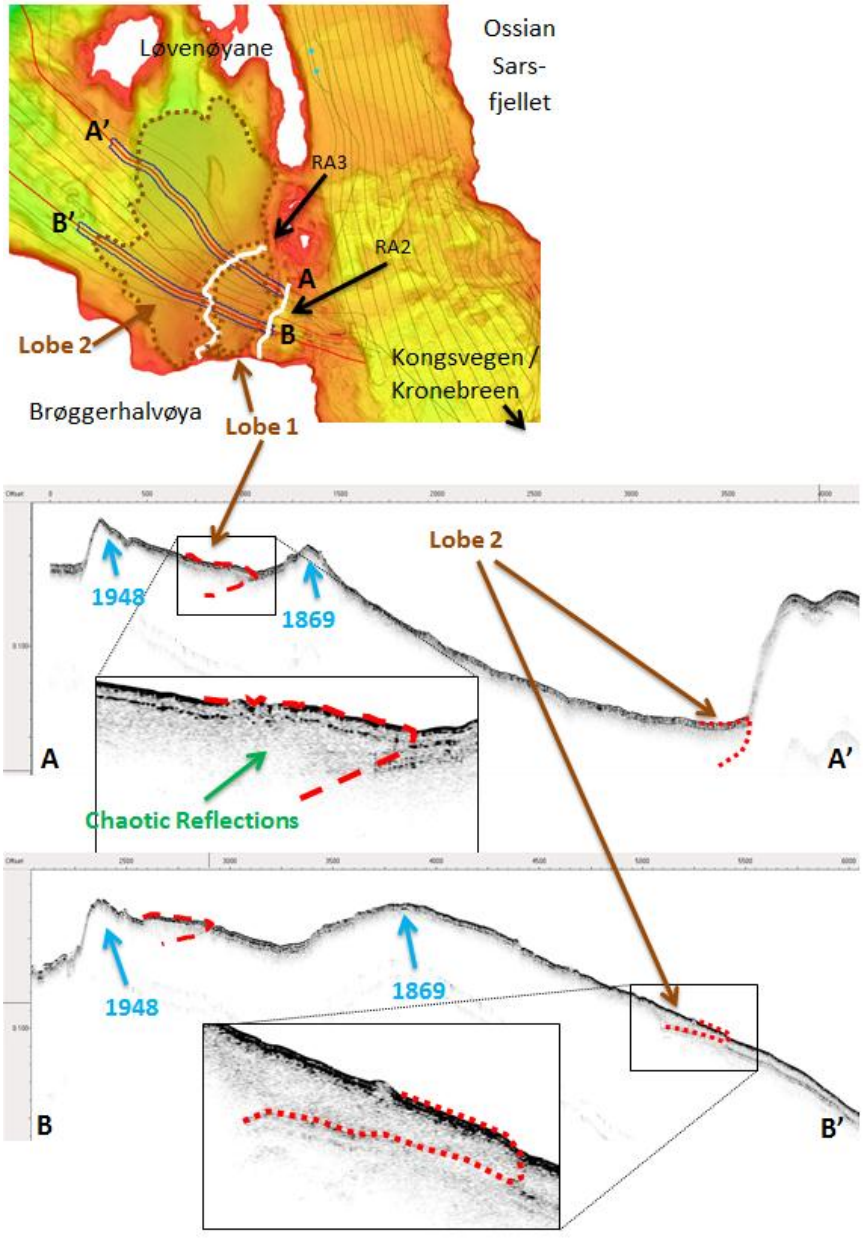

Figure 4.22: Two chirp lines across the two lobate areas west of the Kongsvegen / Kronebreen ice margin. White solid lines indicate terminal moraines inferred to be from 1869 and 1948. The sedimentary lobes are deposited on the distal flanks of these moraines. Their tentative extent is outlined by the brown polygons. In the chirp profile red dashed and dotted lines indicate the wedge-shaped, mostly chaotic reflections common for the debris lobes.

One large lobe of roughly 5.7 km² is located at the foot of the inferred 1869 surge moraine of Kongsvegen / Kronebreen (Figure 4.21). It has extensive flow structures on its surface (grey, dotted lines, Figure 4.21). The second lobe occurs on the flank of the more proximal moraine believed to be deposited in 1948. The lobe is maximally 750 m long and 1.3 km wide and covers an area of approximately 1 km². There are no significant channel features on its surface. Both lobes originate in a water depth of about 35 m. While the more proximal lobe only reaches as deep as almost 50 m at its end, the deepest point of the second lobe area is at a water depth of approximately 110 m (cross-sectional profile in Figure 4.21). Two chirp profiles across the area show two sedimentary wedges of transparent and chaotic reflections (Figure 4.22). The latter are often associated with mass-transport deposits (**Forwick et al., 2010**). Both wedges on the chirp profile clearly mark the lowest boundary of the mass-flow deposits (Figure 4.22) and confirm the tentative extent of the two lobes in Figure 4.21.

4.4 Large Lobe-Shaped Feature – Combined Landform Assemblage from Two Surges

4.4.1 Description and Distribution

A large lobe-shaped feature is located in the eastern part of the dataset (Figure 4.23), which differs from the sedimentary lobes described previously. It extends over an area of approximately 11 km², with a length of 5 km and an average width of 2.2 km. The surface of the seafloor is comparably smooth. Local changes in water depth do not exceed 20 m. The absence of the small ridges so abundant in other parts of the fjord is noticeable. A cross-sectional profile across this area reveals three large ridge-like structures with the tops clearly visible. Their respective crests are less pronounced than in any of the other ridges described from Kongsfjorden and lose clarity with increasing distance from the glacier margin. The ridges' orientation is transverse to the main fjord axis. A very weak asymmetry is visible from the profile, but due to some smaller bumps close to the ridge tops it is impossible to define a steeper proximal and a flatter distal slope for certain. In any case the asymmetry would be much less pronounced than in the previously described terminal moraines. The ridges have heights of roughly 20 m for the one closest to Kongsvegen / Kronebreen and around 10 to 15 m for the two ridges further away. The ridges are set at distances of almost 6 km, almost 8 and 9.5 km away from the present ice margin. Their lengths are 2.4 km for the two features closer to the glacier termini, and 3.1 km for the most distal feature, which is curved into a tongue-like shape. Widths vary from about 1 km (most proximal) to 600 m (middle) to 1.5 km (most distal feature). The end or most distal part of the lobe is characterized by a small area (roughly 1.87 km²) of rough seafloor with a patchy appearance (see Figure 4.24b). The local variability in relief is relatively pronounced, giving the seafloor a bumpy character. Some straight, parallel lines extend along the length of the fjord in this area, which are particularly defined on top of the smooth lobe. These are inferred to be geophysical artefacts, generated as footprints of the chirp or multibeam signal.

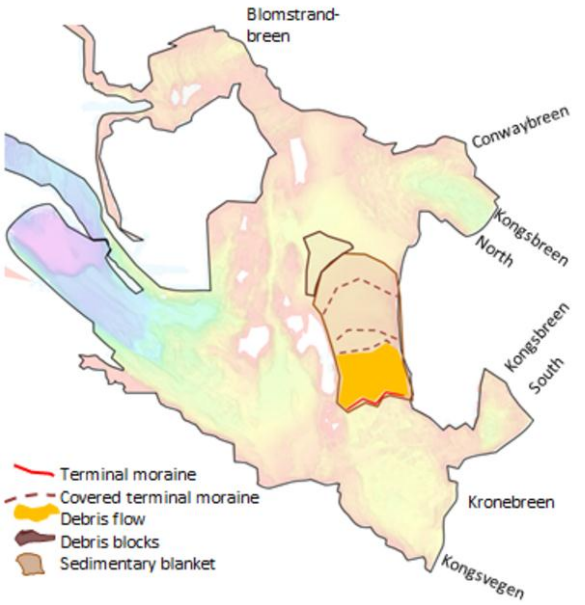

Figure 4.23: Distribution of large lobe-shaped feature and associated landforms terminal moraines, sedimentary blanket, debris blocks and debris flow).

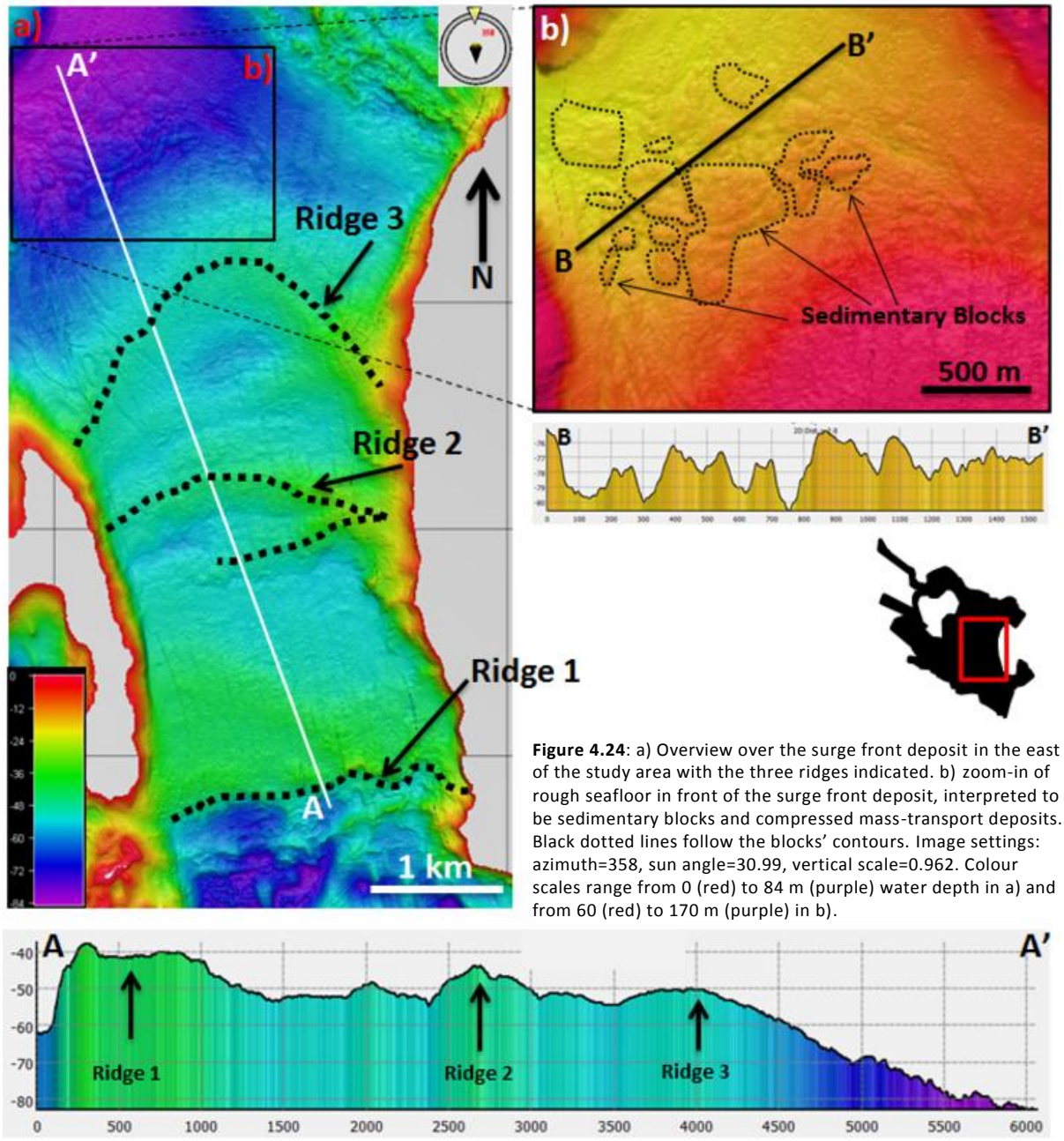

Figure 4.24: a) Overview over the surge front deposit in the east of the study area with the three ridges indicated. b) zoom-in of rough seafloor in front of the surge front deposit, interpreted to be sedimentary blocks and compressed mass-transport deposits. Black dotted lines follow the blocks' contours. Image settings: azimuth=358, sun angle=30.99, vertical scale=0.962. Colour scales range from 0 (red) to 84 m (purple) water depth in a) and from 60 (red) to 170 m (purple) in b).

Chirp profiles across the area reveal some interesting features (Figure 4.25). Next to the three ridges, whose crests are even less defined than on the multibeam data, the patchy and rough area next to the most distal feature appears as a number of bumpy reflections. Between the most proximal and the second ridge, at a distance of 7 km from the ice margin, a wedge-like reflection appears, giving the impression of interrupted reflections and hence a separation of features. The wedge is a consequence of a change in reflection thickness: Up to the wedge the seafloor is defined by semi-transparent, stratified reflections of 0.003 s (3 ms). In the wedge area itself reflections are semi-transparent for the same time interval but reach much farther down in a transparent wedge,

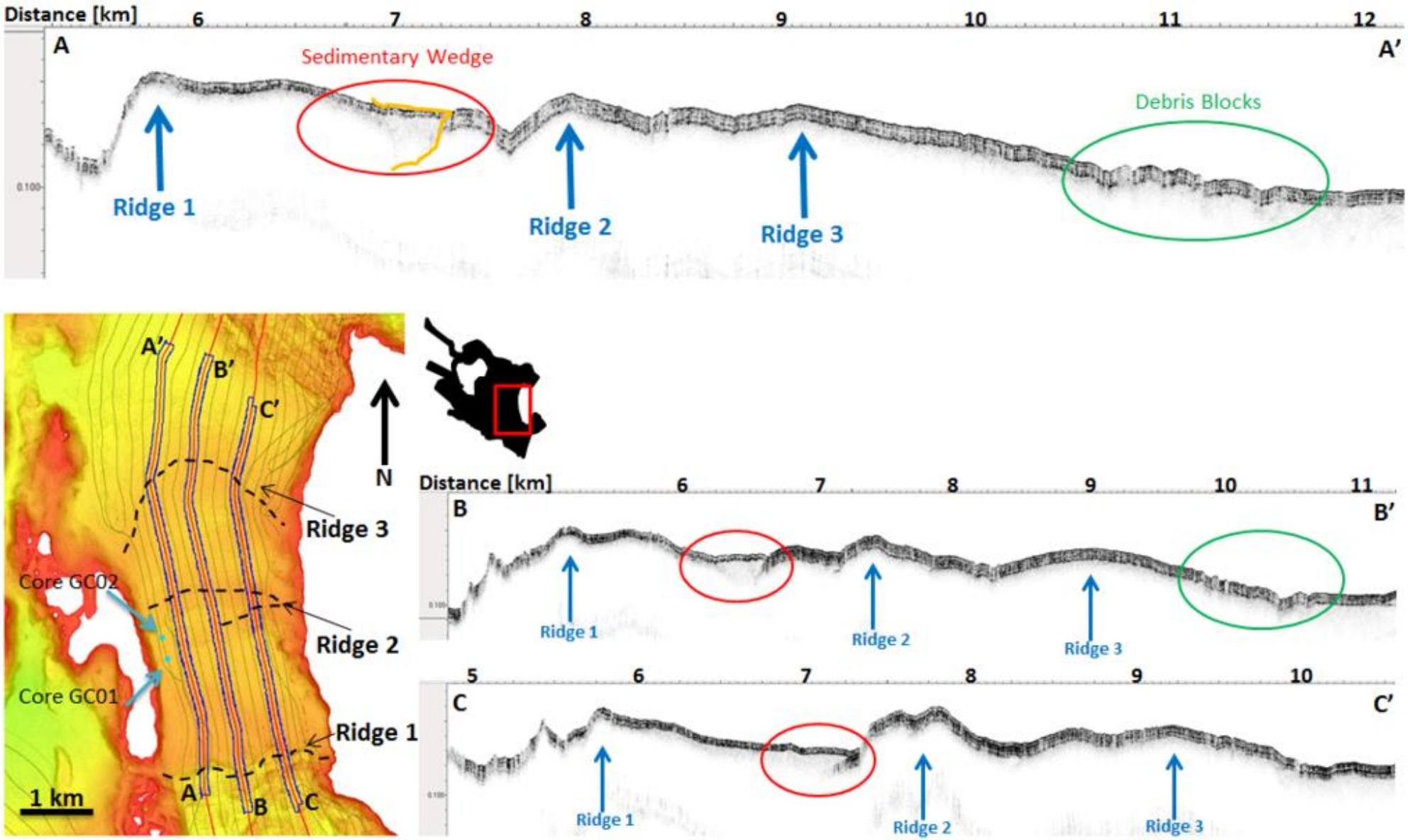

Figure 4.25: Three chirp profiles across the large lobe-shaped feature in front of Kongsvegen / Kronebreen. The three ridges are indicated with black dashed lines. Core locations of the two sediment cores 10JM-GlaciBar-GC01 and 10JM-GlaciBar-GC02 are indicated by two blue dots.

resulting in a total thickness of approximately 18 ms. On the distal side of the wedge the reflection of the seafloor is characterized by a thickness of about 9 ms and a very layered appearance. As thicknesses are based on the two-way-travel time of the acoustic signal, the real depth can be calculated when the speed of sound in the sediment is known. Assuming a p-wave velocity of 1600 m s^{-1} in the marine sediments (compare with Elverhøi et al., 1995; Forwick et al., 2010), the chirp reflections would reflect the upper 2.4 (=3ms), 14.4 (=18 ms), and 7.2 m (=9 ms) of the seafloor.

4.4.2 Interpretation

Based on the morphology and the different characteristics of the chirp reflections (semi-transparent, stratified, regular) the lobe-shaped feature is interpreted to be a sedimentary blanket with locally varying thicknesses. It probably partly covers the landform assemblage of a previous surge. The three ridges are interpreted to be recessional moraines: the most proximal one is expected to be marking the outermost extent of the 1948 surge of Kongsvegen / Kronebreen. The chirp reflections are thinner and more chaotic in this proximal region than in the distal areas. Thinner reflections represent a thinner sediment cover, and a chaotic character often implies reworked sediments.

The second and third ridges are inferred to be terminal moraines of the surge of 1896. This is based on the differences in reflection character. As it is not always clear on Svalbard whether a terminal moraine reflects the maximum position during a surge or during the Little Ice Age, it is possible that one of the two more distal moraines is, in fact, from an ice advance during the LIA. This will be further evaluated in section 7.2.2.
The sedimentary wedge adjacent to the 1948 moraine is inferred to be a debris flow deposited from a subglacial or englacial meltwater channel when the ice front stagnated after the surge.

As ridges 2 and 3 are assumed to be from 1896, the most distal feature (ridge 3) would hence mark the outermost extent of the surge (Figure 4.25). It has been shown that lobe-shaped debris flows are often draped across the distal flanks of such terminal moraines (see section 4.2). Due to the increase in reflection thickness (from 9 to a maximum of 20 ms) at the base of the most distal ridge, it is suggested that the surge of 1896 also produced a mass-transport event. The patchy part of seafloor at its base is assumed to reflect slide blocks originating from this flow event. The features described in this section and their formation mechanisms will be further discussed in section 7.2.3.

4.5 Small, Transverse Ridges – (Overridden / Drumlinized) Annual Push Moraines

4.5.1 Description

The entire dataset of the Kongsfjorden bathymetry is dominated by small ridges (between 1 and 5 m high; **Error! Reference source not found.**, Figure 4.26–Figure 4.28). Three groups of ridges with different characteristics are defined based on orientation, shape and continuity, and will be described separately in the following paragraphs.

Group 1 is defined by ridges that are continuous across the entire fjord basin and reach lengths of up to 2.5 km (Figure 4.26). All ridges within this group are perpendicular to the main fjord axis, slightly curvilinear, and the crests are smooth, arcuate and well-defined (Figure 4.26). The ridges have an average spacing of about 40 m, but, in rare cases, are as far apart as 250 m. The height of the ridges varies between 1 and 5 m while their average width is around 10 m.

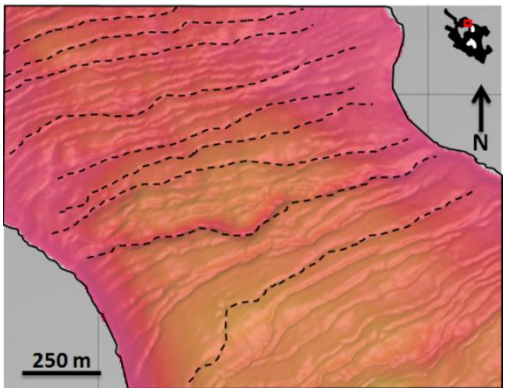

Figure 4.26: Example of Group 1 ridges. Dashed lines follow the contours of the ridges.

The second group is characterized by a more chaotic distribution of discontinuous and continuous ridges. They are generally much shorter than the Group 1 ridges. Due to the ridges' irregular pattern and their excessive branching it is difficult to define single ridges, but some apparently continuous features can be several hundred meters long. Discontinuous ridges are close to 100 m long. Short ridges are clustered in the center of the fjord basin (Figure 4.27), whereas the more continuous features are found more towards the sides (Figure 4.27). The latter are similar to Group 1 ridges with slightly curvy crests, but a generally linear character. The shorter ridges in Group 2 show variable, seemingly random orientations to one another and can have very wavy crests (Figure 4.27). Ridges may touch each other with effective distances of 0 m but may also be as far apart as 100 m. The majority of the Group 2 ridges are also orientated transversely with respect to the main fjord axis. Like the ridges from Group 1, the height of the ridges is between 1 and 5 m.

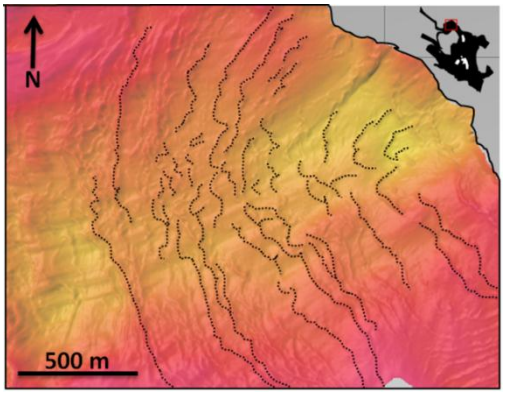

Figure 4.27: Example of Group 2 ridges. Dotted lines follow the ridges' contours.

Group 3 contains long ridges (partly up to 3 km) and ridges that are extremely short with low discontinuity (below 50 m length; Figure 4.28). The crests have numerous bends and change orientation frequently (Figure 4.28). The rough seafloor makes it especially hard to define beginning and end of the short Group 3 ridges, as they do not have a pronounced relief. Most of these are around 1 m high. The longer ridges are much easier to see as they are generally higher with up to 10 m.

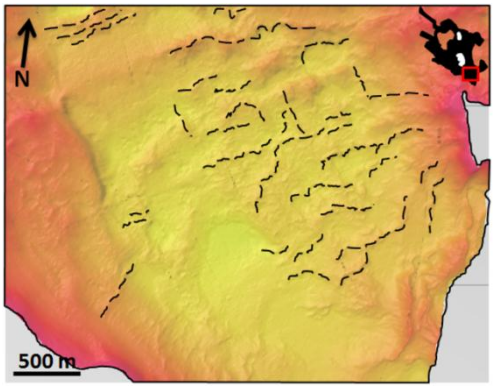

Figure 4.28: Example of Group 3 ridges. Dashed lines follow the ridges' contours.

4.5.2 Interpretation

Based on the high similarity in character to previously described ridge features (e.g. Solheim, 1991; Boulton, 1986; Ottesen& Dowdeswell, 2006), the small and continuous transverse ridges of Group 1 are interpreted to be annual push moraines, which are generated as a result of shore-fast sea ice. During winter, when calving and further glacier retreat is inhibited by the presence of sea ice, the glacier front stagnates or readvances, leading to the deposition of the small push moraines. When the sea ice melts during summer calving is no longer inhibited and the glacier retreats. In the ideal case the long, continuous, slightly curved ridges reflect the shape and extension of the glacier front each winter; however, as the generation of sea ice is sensitive to climate (e.g. Chapman & Walsh, 1993), depositional irregularities could occur in abnormally warm years.

Group 2 ridges are also interpreted to be annual push moraines representing past positions of a less regular and less even ice front. Based on their distribution in deeper water, it is believed that the discontinuous character stems from calving processes at the base of the glacier. This is further discussed in section 7.2.4.

The ridges of Group 3 could be a mixture of annual push moraines and drumlinoid features (glacial lineations). The latter could be generated as a result of a recent advance overriding the landforms deposited during a previous advance. The ridges could also represent crevasse-fill ridges, produced when soft basal sediments are squeezed into the abundant crevasses at the glacier front. This issue is further discussed in section 7.2.4.

4.5.3 Distribution and Geomorphic Characteristics

Group 1 ridges are particularly well-defined in front of Blomstrandbreen, in front of Conwaybreen and in the southeast close to the southern ice front of Kongsbreen (**Error! Reference source not found.**, Figure 4.29). A high frequency of closely spaced ridges characterizes the seafloor in front of Blomstrandbreen (Figure 4.30) with the ridges covering a total area of approximately 7.5 km^2. Two main directions can be identified: extension of the ridges from the ice margin in a west-southwesterly (WSW) direction and extension of the ridges from the ice margin towards the southeast (SE). The two different directions occur as a consequence of the division of the fjord into two arms by the island Blomstrandøya (Figure 4.29, Figure 4.30). As Blomstrandøya is above the current sea level, the bathymetric dataset does not include any geomorphic features located there. However, the arcuate character and the orientation of the ridges seem to suggest that they were deposited at the same time and may even continue across the island. The ridges are generally about 2 m high and up to 1.5 km long. Their spacing exceeds 100 m in some area, but is usually around 30 to 50 m. Their width is at an average of 10 m. Profiles across these landforms (Figure 4.30) reveal relatively symmetrical ridges with slopes of roughly 17 degrees. The ridges in the WSW of the glacier are located in water depths between 35 (crests) and 70 m, whereas the push moraines to the SE of the glacier only reach water depths of maximally 35 m. Most of the crests are in fairly shallow waters at approximately 15 m.

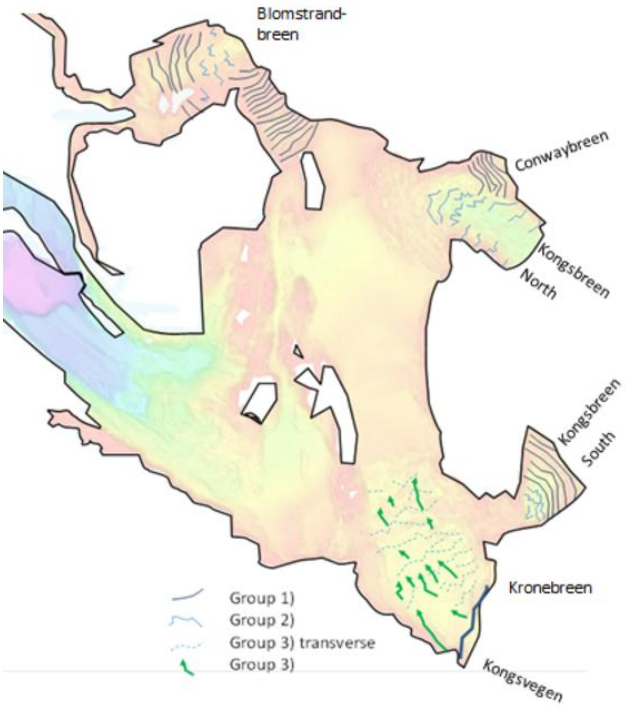

Figure 4.29: Distribution of Group 1), Group 2) and Group 3) ridges in Kongsfjorden.

Three of the small ridges found in the vicinity of Blomstrandbreen stand out as they are much more clearly defined than the others (Figure 4.30), mostly by being higher (18 m on average, but up to 27 m in the deeper fjord areas) and having slightly more pronounced crests. The distinct local relief caused by this ridge is shown in the cross-sectional profile in Figure 4.30, which shows a split-up of the ridge into two crests positioned close together. The crest located more to the east is ca. 5 m higher than the one to the west. The ridges extend across the entire fjord basin, which leads

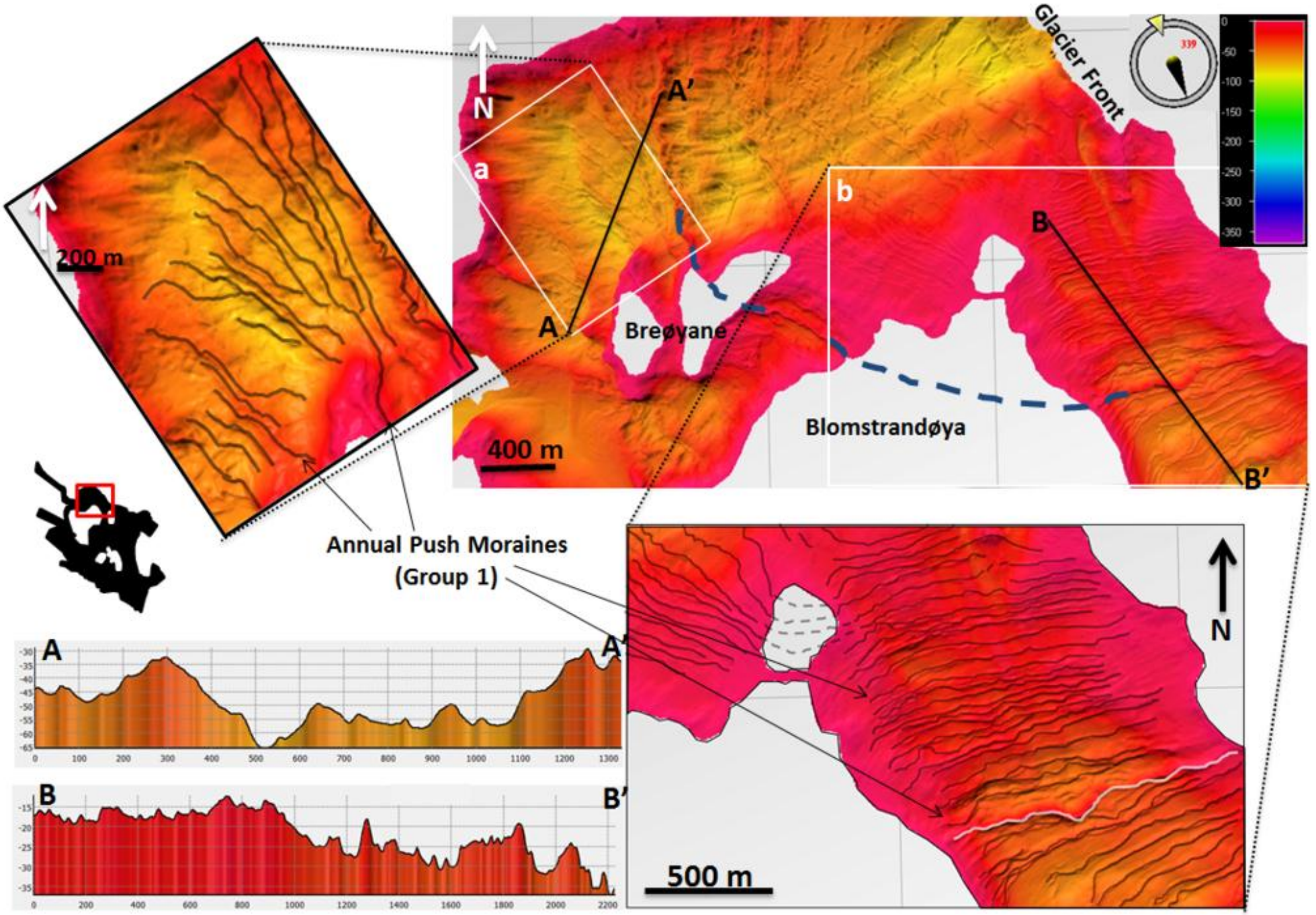

Figure 4.30: Example for Group 1) ridges in front of Blomstrandbreen. The curvilinear character becomes clear in the zoomed-in pictures where grey lines follow the ridges' outlines. Blue dashed lines may indicate extent of the ridges across Blomstrandøya. Two profiles across the ridges show the local relief and the height of individual ridges. The image was created with a sun angle of 29.1876 and a vertical scale of 0.517.

to lengths of approximately 1400 m for the ridge west of Breøyane, ~ 600 m for the ridge between Breøyane and Blomstrandøya, and approximately 1250 m for the ridge east of Blomstrandøya (see Figure 4.30). The features have a curved character as the distance to the glacier margin differs for the two opposite ends of each ridge. For the ridge located on the west of Breøyane, the more proximal part is roughly 1500 m away, while its southern end is approximately 2300 m away from the ice margin (compare Figure 4.30). In the fjord arm between Breøyane and Blomstrandøya, the ridge is between 2000 and 2200 m away from the present terminus. To the northeast of Blomstrandøya the ridge also has a minimum distance of 1950 and a maximum distance of about 2200 m from the glacier front. The similar distances from the present-day ice margin also suggest that the ridges in the three fjord arms in front of Blomstrandbreen have been generated simultaneously. This ridge is different than the other annual push moraines, but is also believed to reflect a short readvance or stagnation of the glacier front during general retreat. Its more defined character could be caused by a particularly cold summer, which did not allow for retreat during two winter seasons and led to the deposition of a "double" annual push moraine.

In front of Conwaybreen (Figure 4.31) the Group 1 ridges occur more scarcely, but are as well defined as in the vicinity of Blomstrandbreen. Heights are the same as for Blomstrandbreen, around 2 m. The spacing is very similar to that of the previous area with distances between 20 and 135 m. The ridges are again symmetrical with slopes of around 17 degrees (Figure 4.31, A-A'). Lengths are close to 1 km. Furthermore, the previously described curvilinear character and the sharp arcuate crests are also present in this ridge set. However, the ridges extend over a much smaller area of only roughly one square kilometer, resulting in much fewer ridges in comparison to Blomstrandbreen. Only twelve very continuous ridges can be found close to Conwaybreen and their occurrence is terminated rather abruptly by a sudden deepening of the fjord basin (Figure 4.31). A few of the ridges seem to be heavily bent on one of their sides, because they turn from a general southeastern direction to a north-south orientation. Water depths in front of Conwaybreen are again

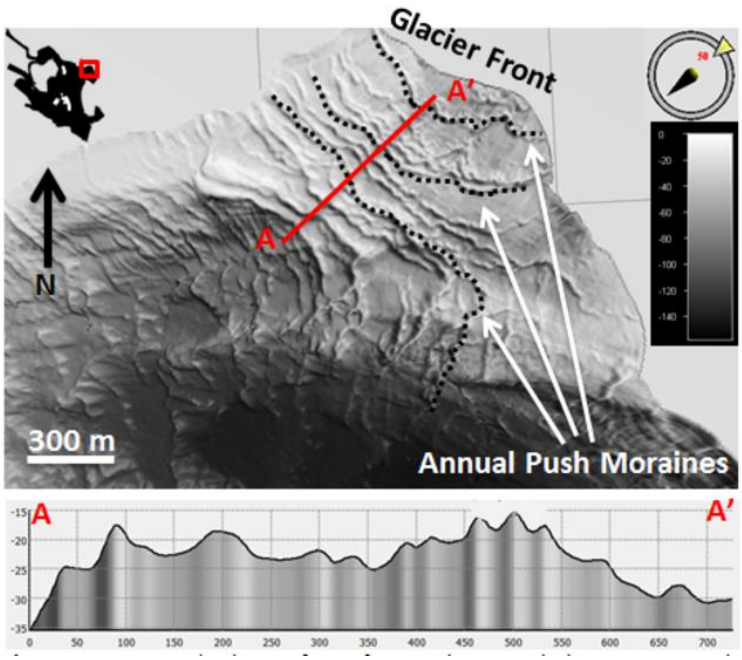

Figure 4.31: Group 1) ridges in front of Conwaybreen (black dotted lines), with the cross-sectional profile indicating the relief. Image settings were set to 0.517 for vertical scale and a sun angle of 29.1876.

between 13 and 30 m, whereas the more distal regime (further than 1 km from the ice front) is defined by a sudden increase to a depth of almost 100 m. Here, ridges tend to adapt a more chaotic character similar to Group 2 and might be associated with Kongsbreen North as well as Conwaybreen as both glaciers flow together in this point. For simplicity these features will be described together with the Group 2 ridges in front of Kongsbreen North, a little later.

The third area with ridges of Group 1 is in front of Kongsbreen South, immediately south of Ossian Sarsfjellet (Figure 4.32). The ridges in shallower water (20 – 50 m) along the fjord walls have the linear and continuous character of Group 1 ridges, whereas ridges towards the deeper part of the basin (~100 m) adapt a character similar to the Group 2 ridges. The occurrence of both, Group 1 and Group 2 ridges should be noted, as it will be discussed further in section 7.2.4. The ridge features in front of Kongsbreen South have a wider spacing as observed elsewhere, and are between 150 and 200 m apart. A few ridges occur more closely to each other, especially in the deeper parts of the fjord. They are also higher with heights of 5 m. The ridges are between 100 m and 2 km long with the shorter features clustered in the deeper fjord. The latter have a slightly more random orientation than the ones close to the fjord walls, which are perpendicular to the main fjord axis.

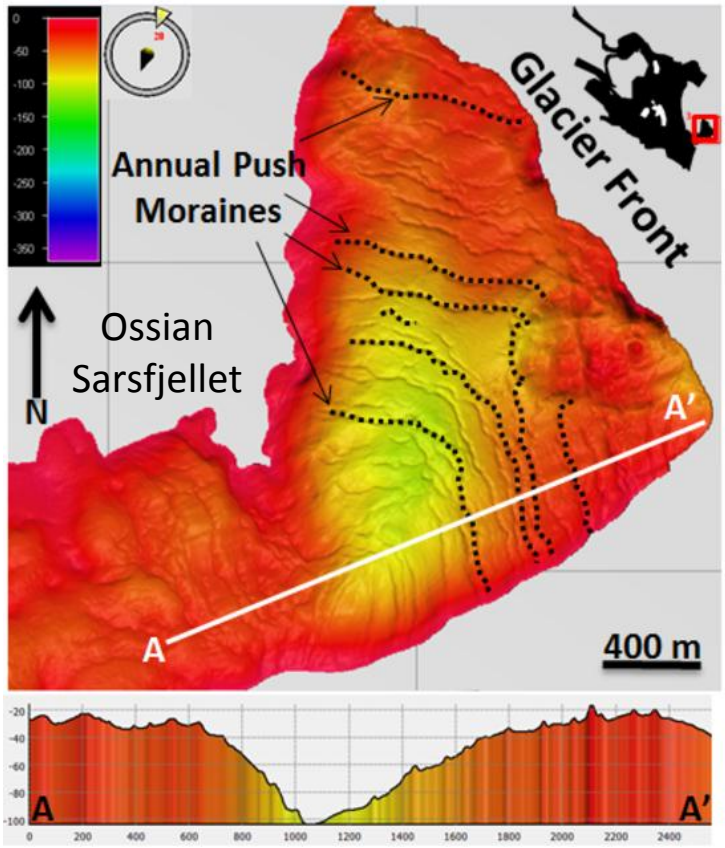

Figure 4.32: Group 1) ridges in front of Kongsbreen's southern ice margin (black dotted lines) with the cross-sectional profile indicating the local relief. The image was generated using a sun angle of 49.1324 and a vertical scale of 0.500.

Group 2 ridges are located in front of Kongsbreen North and South and in the central part of the proximal basin of Blomstrandbreen (see Figure 4.30). The distribution of these ridges in front of Kongsbreen South has been described in the previous paragraph.

The fjord in front of Kongsbreen North is much deeper than for most of the other glaciers with water depths of approximately 150 m in the deepest part. The ridges here are more frequent along the fjord walls, and can be absent in the deepest parts (Figure 4.33). The ridges can be fairly straight in shallow areas, but have more bends and curves towards the deeper fjord (Figure 4.33), where they

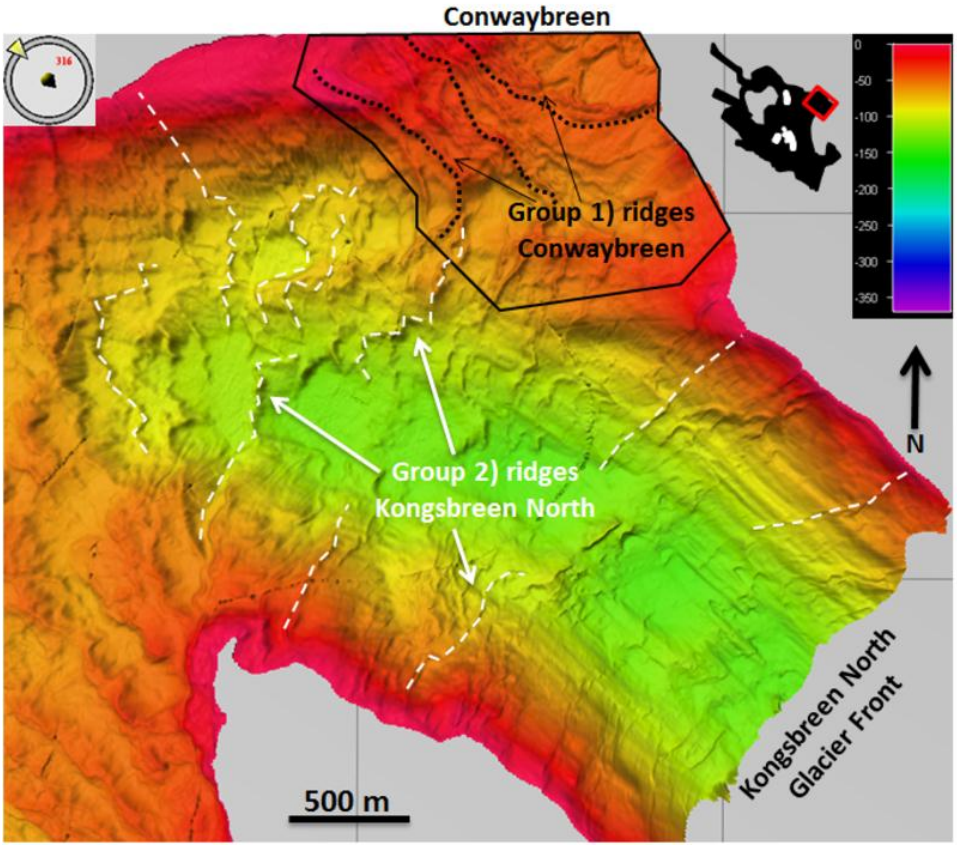

Figure 4.33: Group 2) ridges in front of Kongsbreen North and Conwaybreen. Black polygon indicates previously described Group 1) ridges in front of Conwaybreen. White dashed lines follow contours of selected Group 2) ridges in the area. Image settings were set to a sun angle of 45.219 and a vertical scale of 0.962.

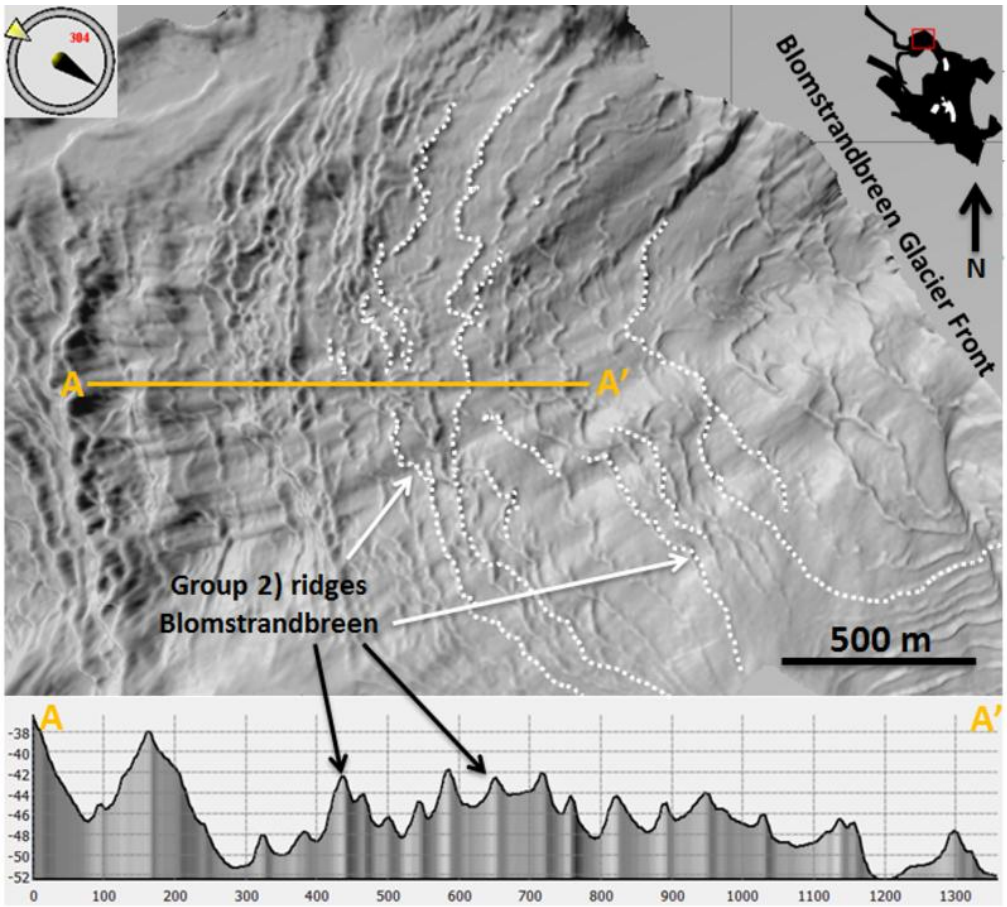

Figure 4.34: Example of the more randomly orientated ridges of Group 2), positioned in front of Blomstrandbreen in the north of the study area. White dotted lines follow the ridges' contours. The local topography is shown in cross-sectional profile A. Image settings were a sun angle of 29.941 and a vertical scale of 0.500.

are also shorter. The ridges in front of Kongsbreen North are generally between 200 and 800 m long, and between 1 and 5 m high. As mentioned above, it is not possible to unambiguously ascribe the ridge features to Kongsbreen North, as especially in more distal settings (about 2 km from the present ice margin) Kongsbreen is confluent with Conwaybreen.

In front of Blomstrandbreen the ridges of Group 2 are concentrated over a small area directly in front of the glacier (Figure 4.34). The area covers about 1 km² and is confined to the deepest part of the basin, with water depths between 50 and 100 m. The ridges here are short (around 30 m) and have much more irregular crests than Group 1 ridges. Due to excessive branching of longer and shorter ridges it is hard to define single continuous ridges. The spacing between the ridges is much more irregular than for the Group 1 features: ridges may be touching each other or be as far apart as 200 m, opposing the regular spacing often assigned to annual push moraines (e.g. Ottesen et al., 2008). The ridges are generally longer along the shallower sides of the fjord (around 1 km in water depths of 10 – 30 m; Figure 4.34). However, occasional ridges are continuous across the fjord and can be 2.5 km long

.

Ridges of Group 3 only occur in the south of the study area in the vicinity of Kongsvegen / Kronebreen (Figure 4.35). Group 3 contains shorter (around 50 m) and longer (partly up to 3 km) ridges, which is similar to the other two defined groups. Their height for the most part is between 1 and 5 m, but can be up to 10 m. The main difference to the other two groups is the features' orientation: whereas ridges of Groups 1 and 2 are generally transverse, ridges of Group 3 may also be aligned parallel to the main fjord axis. Due to the chaotic character and the very bendy crests, it is hard to define individual ridges, which makes it difficult to say whether one ridge changes orientation by about 90 degrees

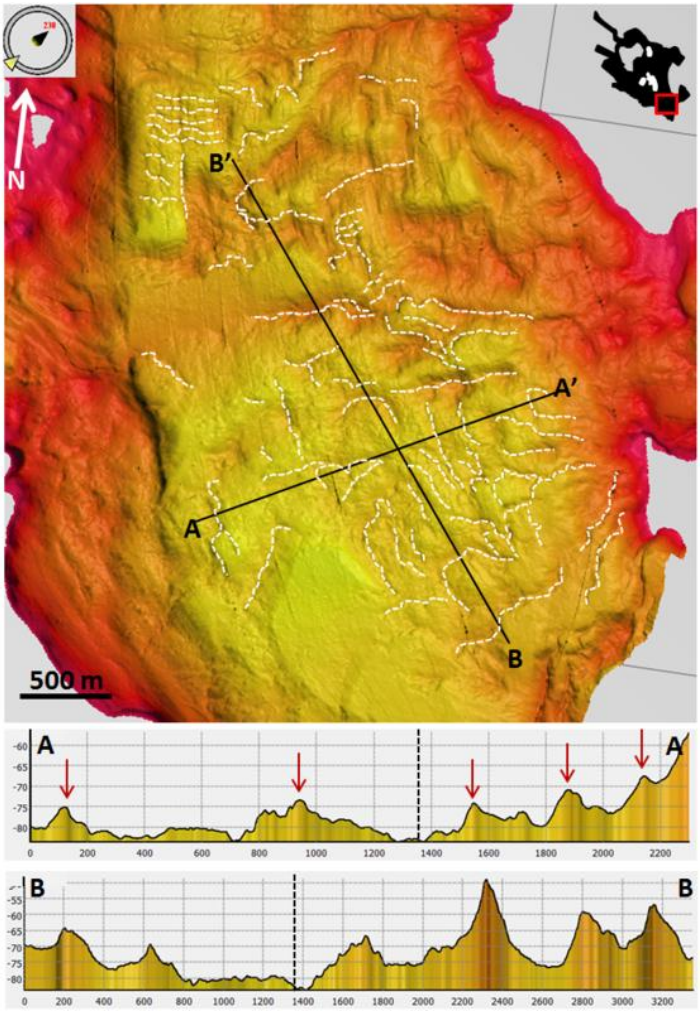

Figure 4.35: Example of Group 3) ridges (white dashed lines) with profile A showing a cross-section through the ridges orientated parallel to the main fjord axis and profile B showing a cross-section through the transverse ridges. Red arrows point at ridges parallel to the main fjord axis. Dashed black lines in the profiles indicate point of intersection between A and B. Images were generated using a vertical scale of 0.876 and a sun angle of 33.4048.

or whether two perpendicular ridges are touching each other. The fact that the ridges vary in width is notable. Whereas ridges from Groups 1) and 2) are fairly similar regarding their geometry, the area in front of Kongsvegen / Kronebreen hosts a lot of narrow features of about 40 m width (which is similar to the other groups), but some ridges are as wide as about 200 m. These features are also noticeably higher than the narrow ridges, reaching as high as 30 m above the seafloor. As the most ice-proximal of these ridges is located about 3.2 km away from the present ice margin, it is assumed that these ridges are drumlinized features as well, but were possibly generated by different processes than the annual push-moraines. This issue is further discussed in section 7.2.4.

4.6 Crater-like Features – Pockmarks

4.6.1 Description

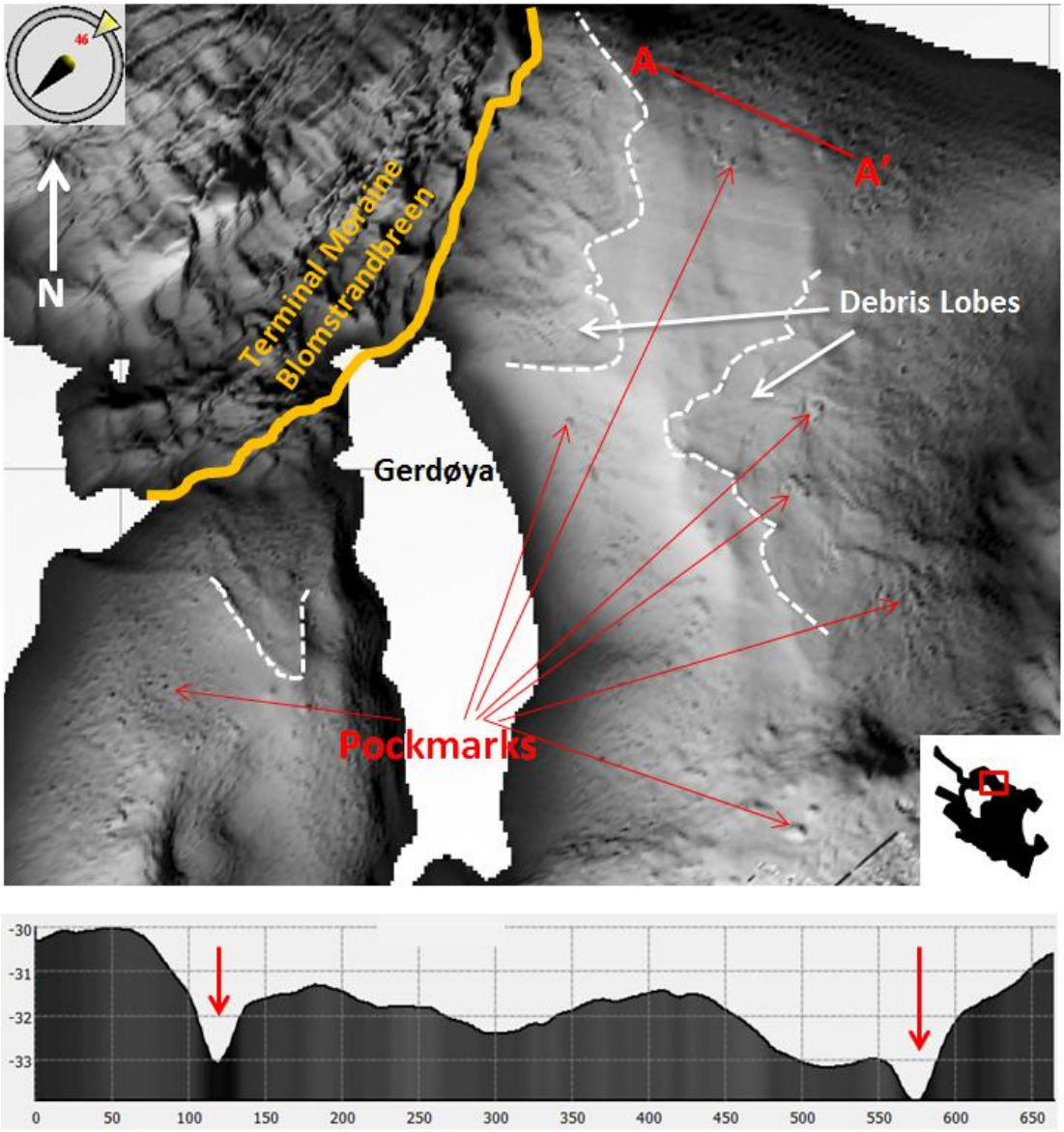

Figure 4.36: Crater-like features on the seafloor of Kongsfjorden. White dashed lines indicate debris lobes, orange solid line represents a terminal moraine. Red arrows are pointing at pockmarks. The image was created using an azimuth of 46, a sun angle of 9.13 and a vertical scale of 1.797.

Over the entire study area small circular depressions occur (e.g. Figure 4.36). They assume the shape of holes or craters with steep side walls, as they have a circular outline and are roughly 1 m deep. They only occur in groups which mostly include a high number of these features; however, there are also some places where there are just very few craters. The features are fairly small with average diameters of 10 m and maximum widths of approximately 30 m. The concentration of the depressions seems to be closely related to the presence of slopes, especially the ones covered by sedimentary lobes.

4.6.2 Interpretation

Similar craters to the features described above have been documented by several authors. Andreassen et al. (2007) described depressions of circular or semi-circular character in the SW Barents Sea, with widths ranging around 1000 m and depths between 10 and 16 m. Hovland et al. (2010) report circular depressions with diameters of less than 5 m, which occur as single features as well as in elongated strings or clusters. Forwick et al. (2009) found pockmark strings alongside random, elliptical, and composite pockmarks in four Spitsbergen fjords with depths around 10 and diameters between 100 and 250 m. All features have been interpreted to be pockmarks, which are inferred to have formed from the rapid upward migration of (gas-containing) pore fluids.

The crater-like features in Kongsfjorden are interpreted to be pockmarks. Next to their similar character with pockmarks described in the literature, their association with the sedimentary lobes is another typical quality. This is due to the fact that the chaotic deposition of mass-transport deposits has been found to be a very suitable host for large pore spaces in which gas or water can easily be enclosed (Forwick et al., 2009).

Pockmarks are ubiquitous on the floor of Kongsfjorden and can be found almost everywhere. In all cases the pockmarks are associated with a sloping bathymetry, either as a consequence of the terminal moraines and their sedimentary lobes or along the fjord walls. Especially the flanks of the islands show a rather high concentration of the circular depressions. Figure 4.37 shows another example of the distribution of pockmarks, and together Figure 4.36 andFigure 4.37 can be considered representative of all pockmarks in Kongsfjorden.

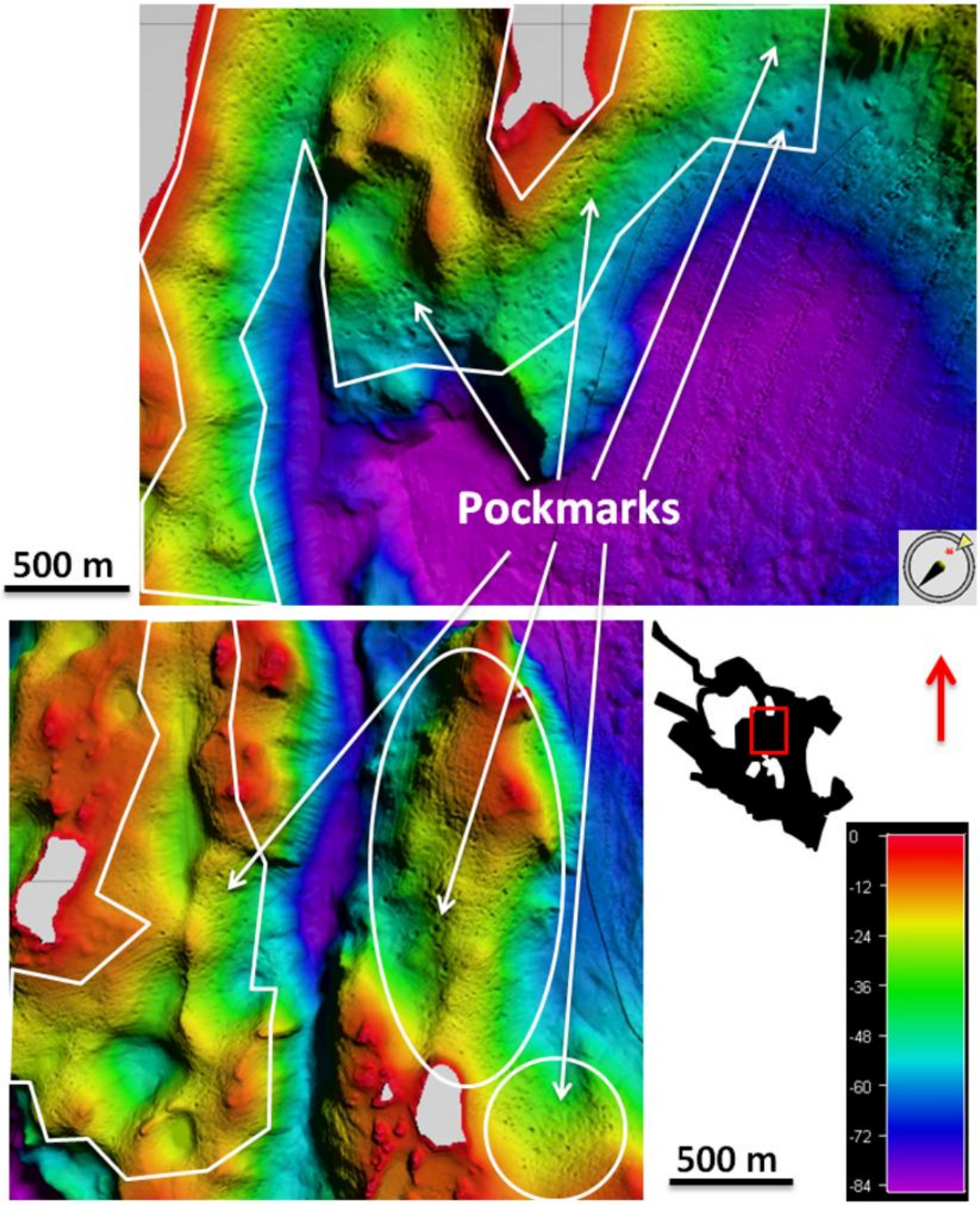

Figure 4.37: Pockmarks in Kongsfjorden. Image settings were an azimuth of 46, a sun angle of 9.13 and a vertical scale of 1.797

5. Lithostratigraphy - Results

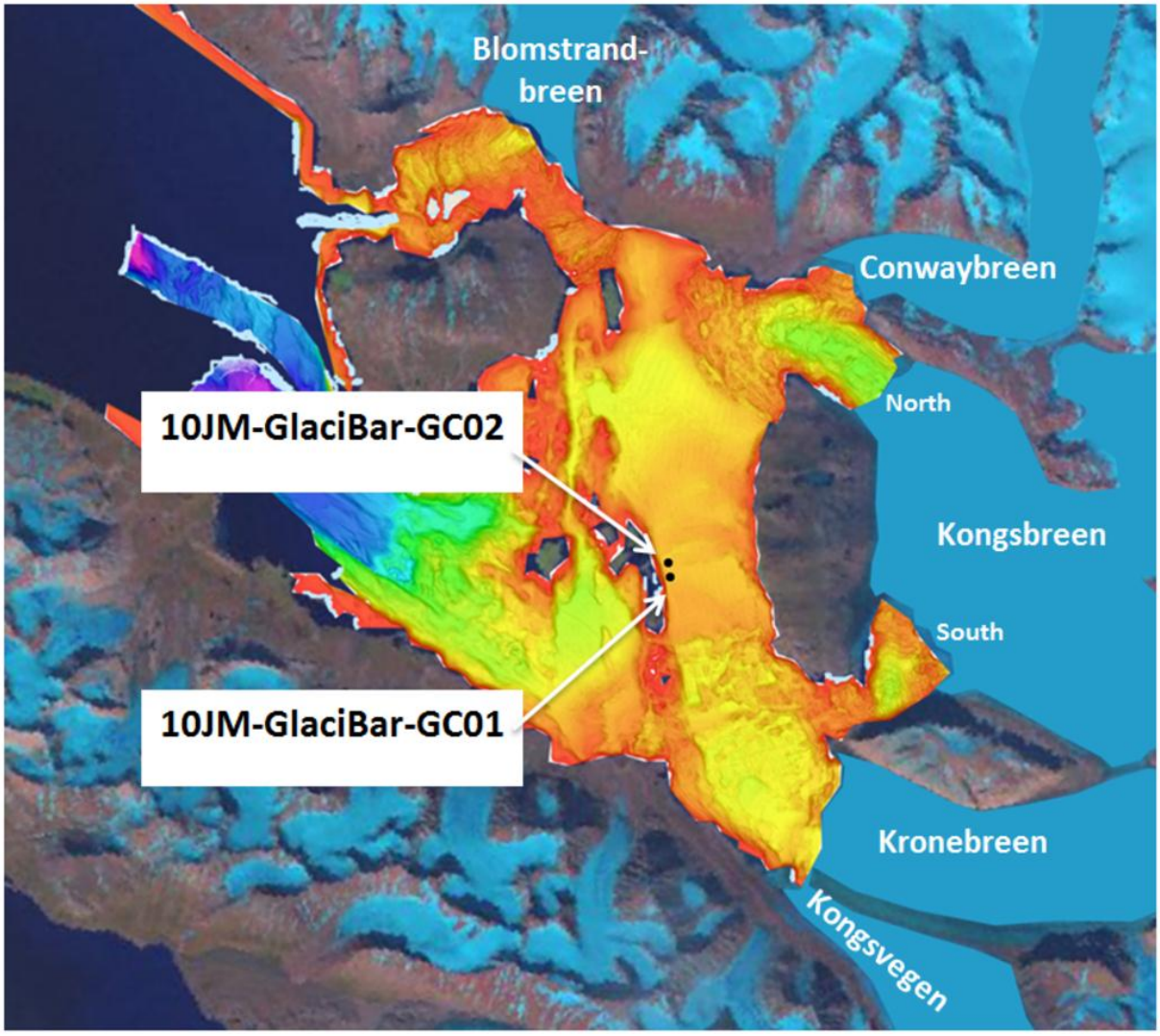

Figure 5.1: Locations of cores 10JM-GlaciBar-GC01 and 10JM-GlaciBar-GC02 with respect to the bathymetry and glacier positions.

Two sediment cores, 10JM-GlaciBar-GC01 and 10JM-GlaciBar-GC02, were taken from the study area for supplementary information to the acoustic data. The two cores originate from the area described in section 4.4, which is located in front of Kronebreen and Kongsvegen (Figure 5.1). GC01 is the more proximal core with a distance of approximately 7.2 km to the ice margin (in 2010). GC02 is the more distal core with a distance of approximately 7.5 km. The exact distance between the cores is 309 m and the exact coordinates are at 78º55.82 N and 12º20.81 E for GC01, and 78º55.98 N and 12º20.7 E for GC02.

10JM-GlaciBar-GC01 is 286 cm long and was taken from a water depth of 50 m. The purpose of taking this core was to penetrate into a sedimentary lobe that was believed to be deposited in

relation to the Kongsvegen surge of 1948. 10JM-GlaciBar-GC02 is from the front of this surge-induced deposit. GC02 is 339 cm long and was retrieved from a water depth of 53 m.

5.1 Lithology

Logs have been created for both sediment cores from Kongsfjorden. Based on characteristics like grain size, colour, internal structures etc. four different lithofacies (units) can be defined for the two cores: U1, U2, U3, and U4, which will be described in the following paragraphs.

Unit 1

The first lithological unit consists of a matrix of clayey silt and shows distinct fine stratification (Figure 5.2Figure 5.3). The latter occurs in regular intervals and is mostly visible by slight colour changes (although Munsell codes do not differ in some parts). Transitions between the brighter horizons and the slightly darker matrix are typically well-defined and sharp but can become more blurred down-core. Changes in material cannot be detected. The stratas' thicknesses vary between only a fraction of a millimetre or several centimetres; however, the majority of the horizons have an average thickness of roughly half a centimetre. Strata occur as single events or as a group of horizons. Despite the stratification, the unit is defined by its fine, sorted and apparently uniform texture. It contains relatively few clasts, which only appear in concentrated layers or small clusters (Figure 5.2Figure 5.3). Coarse horizons made up of small clasts (~ 1-2 mm in diameter) occur over short widths of ~ 2 to 5 cm or as continuous horizons across the core's diameter. Their thickness is commonly around 1 mm, but can be larger. Locally more consolidated patches of sediment may reflect bioturbation (Figure 5.3).

The water content is very high in the uppermost tens of centimetres, but is decreasing very gradually down-core.

Unit 2

U2 is built up of a similar matrix of clayey silt but no distinct stratification occurs (Figure 5.2). The matrix is massive. However, an orderly character (like in U1) is locally preserved in concentrated clast layers (Figure 5.2). The frequency of clasts is slightly higher than in U1, as coarser components appear throughout the entire unit. They occur in layers, clusters, and, unlike in U1, as single components with a random distribution (Figure 5.2). Layer thicknesses vary but are commonly between 1 and 10 mm. Clast size also varies but most of the coarse components in U2 are slightly larger than clasts from U1 with an average size of roughly 3 mm.

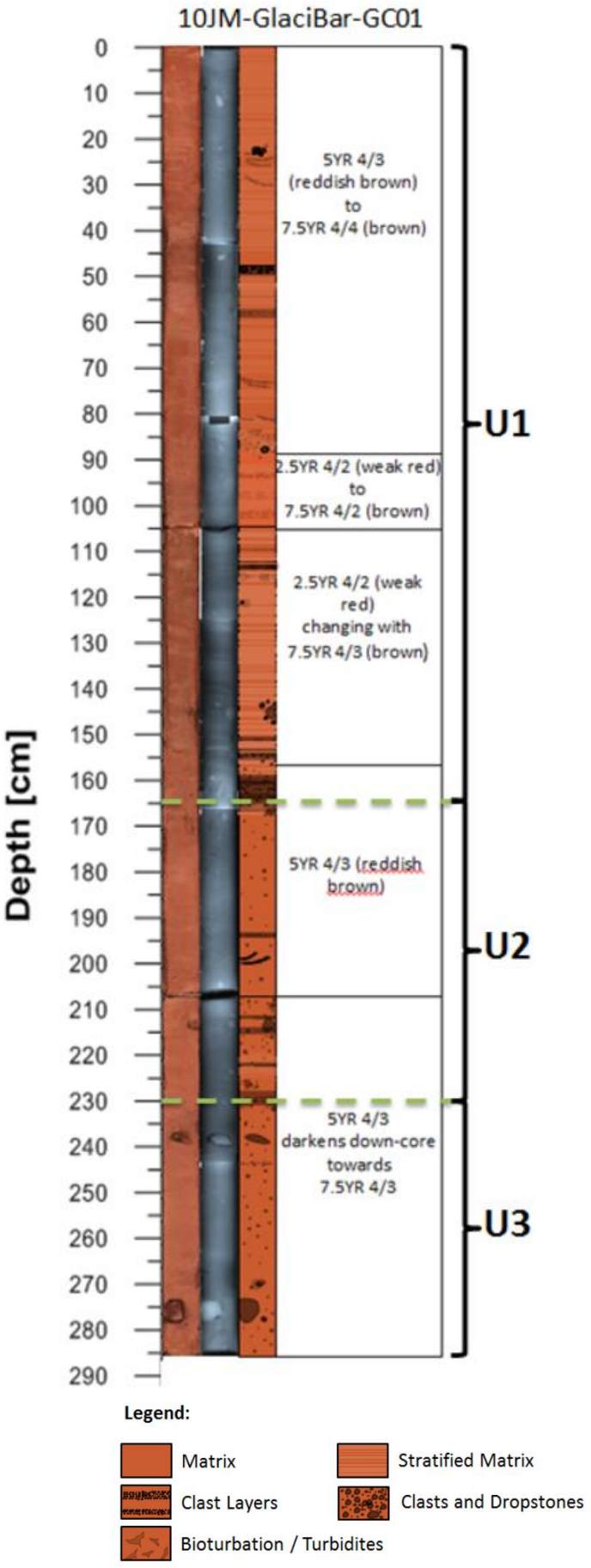

Figure 5.2: Lithological Log for 10JM-GlaciBar-GC01. Left: compilations of colour images, middle: compilation of radiographs, right: composed lithological log.

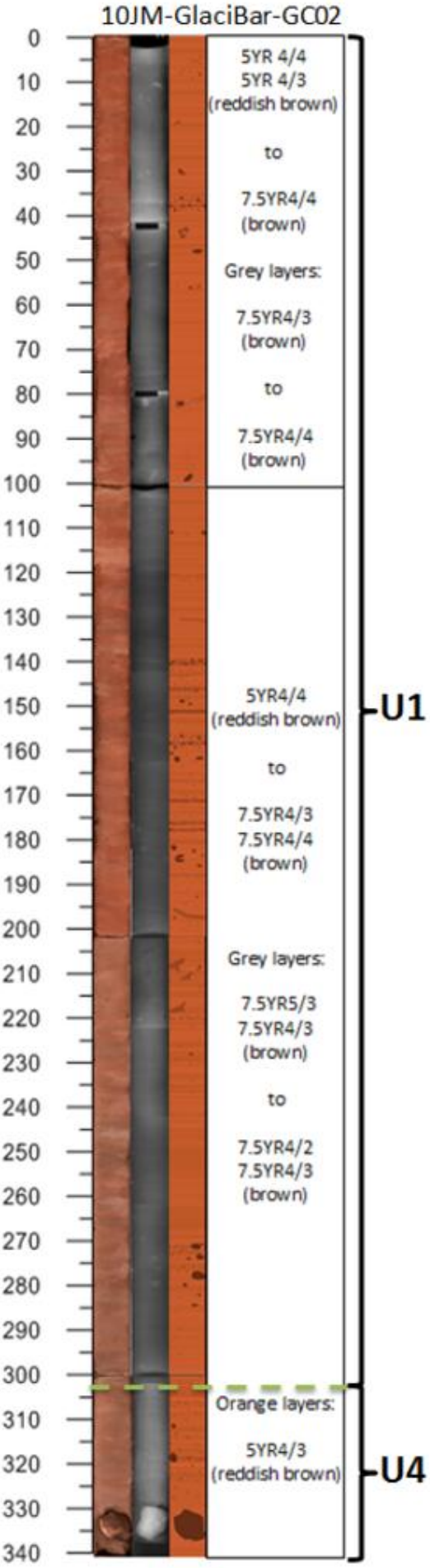

Figure 5.3: Lithological Log for 10JM-GlaciBar-GC02. Left: compilations of colour images, middle: compilation of radiographs, right: composed lithological log.

Unit 3

U3 is made up of massive clayey silt. Clast abundance is even higher than in U2 and coarse components are present throughout the entire unit. Their sizes vary from a few millimetres to up to 7 cm and their distribution is random (Figure 5.2). No concentrated strata or clusters occur but the clasts appear to be distributed almost equally throughout the unit (Figure 5.2). This lowest unit appears to be entirely unsorted.

Unit 4

In the laminated U4 the reddish matrix is intercalated with greyish laminae, as observed earlier, but also with some orange horizons (colour code 5YR 4/3, reddish brown, Figure 5.3). The matrix intervals predominate and become thicker towards the core bottom. Colour changes are not easily distinguishable but visible. Coarse clasts occur but are not as frequent as in any of the other three lithofacies. Occasional rocks can be up to 8 x 10 cm large (Figure 5.3).

Three of the four lithofacies occur in 10JM-GlaciBar-GC01: U1 (0 – 165 cm depth), U2 (165 – 230 cm depth), and U3 (230 – 284 cm depth). The log for GC01 is displayed in Figure 5.2.

The sediment colour is reddish brown or brown (Munsell codes 5YR 4/3, 5YR 4/4 and 7.5YR 4/3, and 7.5YR 4/4). It changes minimally throughout the core. Colour changes are most pronounced in the stratified intervals (although Munsell codes can stay the same) but can also occur gradually throughout the matrix. The strata in the core appear generally lighter than the surrounding matrix.

In U1 at 50 cm depth there is a small area of roughly 5 cm diameter, which shows an uncharacteristically high water content, similar to the lithofacies' uppermost centimetres. Coarse layers are frequent at the base of the unit, between 150 and 165 cm (Fig. 5.2).

The transition between U1 and U2 occurs at 165 cm and is marked by the abrupt change between stratified and massive sediments. The transition between U2 and U3 is more gradual and occurs at 235 cm. This is based entirely on the lithological observations. However, the physical parameters may indicate different depths for the transitions (see section 5.4). A large rock (7 cm diameter) is the most distinct feature of U3 in the first core, and is located at its base (275 cm).

Two of the four lithofacies occur in 10JM-GlaciBar-GC02: U1 (0 – 302 cm) and U4 (302 – 341 cm; Figure 5.3). Sediment colours are reddish brown and brown and very similar to GC01 (Munsell codes 5YR 4/3, 5YR 4/4, 7.5YR4/2, 7.5YR4/3, 7.5YR 4/4, and 7.5YR 5/3). Colour changes between the strata become more and more pronounced with increasing depth. Clusters and horizons of coarser clasts can be found throughout the entire core in varying thicknesses and abundance, and also single rocks are common. Stratification is more pronounced in this second core.

U1 in GC02 is characterized by a high clast concentration from 140 cm down-core leading to an increasing density (needle test). Clasts generally occur in random distributions and concentrated layers are much more seldom than in GC01. The sediment seems gradually more rigid and more resistant to external influence (e.g. sticking a metal pin into the sediment). From 200 cm down-core, the sediments are characterized by a very tough behaviour and a generally rougher surface than previously observed.

Between 205 and 220 cm depth some curved features are highly resistant, although the sediments seem more consolidated rather than coarser-grained (Figure 5.3). The bands are roughly half a centimetre thick and appear darker than any other components of the core. As no individual clasts can be identified, it is possible that the bands represent consolidated tracks of small animals (i.e. worms) caused by bioturbation, or that the sediments reflect turbidites.

5.2 Interpretation

Both cores 10JM-GlaciBar-GC01 and 10JM-GlaciBar-GC02 are interpreted to reflect a glacimarine environment with changing proximity to and activity of the glaciers. As the cores are taken about 7 km in front of the present-day termini of Kronebreen and Kongsvegen, the sediments are inferred to be deposited from glacial activity of these two glaciers.

Unit 1 is interpreted to be indicative of an increasingly distal (with respect to U2, U3, and U4) glacimarine environment with decreasing glacial activity (ice front retreat). The silt and clay fraction of the sediments are believed to be deposited from suspension. The stratification can either mark variations in the sediment source, or seasonal variations in sediment input. Based on the absence of the spring bloom varves documented for the area by Elverhøi et al. (1980), the latter is not considered very likely. However, considering the very small variations between the strata, it is not clear what could have caused the regular changes in sediment source or what these sources could have been. It is therefore impossible to clearly identify the reason for the stratification. The coarser layers and clast components, which are here defined as particles with a diameter exceeding 63 µm, are inferred to be debris transported and dumped by icebergs or ice floes.

The massive character of Unit 2 is believed to originate from a more proximal setting than U1. The grain size distribution records slightly higher silt and clay contents for this unit, but a decrease in influx of IRD. This could support a more proximal setting where icebergs and floes are still intact for the most part and only few melt fast enough to deposit any incorporated material. The lack of stratification could be explained by a more proximal setting as well: if the regime in which U2 was deposited is proximal enough, the sediments at the bottom of the fjord may be subjected to the

turbulent conditions triggered by the uprising meltwater plumes discussed by (Elverhøi et al., 1983; Boulton, 1990). Due to the fairly shallow water depths around the core location (around 50 m) any freshly deposited material could possibly be taken up by turbulent currents, mixing different sediments together and preventing a pronounced layering. The many similarities between U2 and U3 could indicate that the two units actually represent the same lithology. Their only difference is the occasional occurrence of clast layers in U2. However, as the sediment core only represents a tiny fraction of the real sedimentary environment and there is no way to know the constraints of such a "layer", the clast "layers" in U2 could really be random clusters of IRD and dropstones (see section 5.4).

U3 is interpreted to be a debris lobe deposited at the foot of the terminal moraine from the 1948 Kongsvegen surge. It is believed to originate from a mass-transport deposit triggered on top of the terminal moraine (see chapter 4.4). The massive and unsorted character of the matrix, the high frequency of randomly distributed clasts and larger rocks, as well as density, granulometry and geochemistry (see section 5.3) all indicate sediment deposition in a high-energy environment. The acoustic data clearly shows that GC01 was taken from the top of this surge deposit (chapter 6).

U4 is interpreted to represent a distal setting (compared to U2 and U3) with increasing glacial activity (ice front advance). The high similarities with U1 allow for this interpretation. Based on its location in front of the debris lobe, the lower parts of GC02 are believed to be older than 1948. Together with accumulation rates estimated from Elverhøi et al. (1983) and the acoustic data from this thesis, the thickness of U4 indicates a deposition time of 7 to 12 years. With the active phase of glacier surges lasting between 4 and 10 years on Svalbard (Benn & Evans, 2010) it is reasonable to assume that the Kongsvegen glacier front may have begun advancing as early as 1938, thereby subjecting the GC02 core site to more and more proximal conditions during the deposition of U4. The orange layers observed within U4 could be related to the input of perhaps supraglacial water influenced by a different catchment area with another chemical signature. Based on the geochemical data and the physical properties, this does not seem likely however, as there are no apparent changes between U1 and U4. Therefore it is not possible to clearly identify the source for the "orange" sediments.

5.3 Physical Properties, Granulometry, and Element Geochemistry

5.3.1 10JM-GlaciBar-GC01

The magnetic susceptibility in 10JM-GlaciBar-GC01 is low at the top and increases down-core (Figure 5.4, Table 5.1). It is lowest at the top and at the bottom. At 100 and 200 cm depths the magnetic

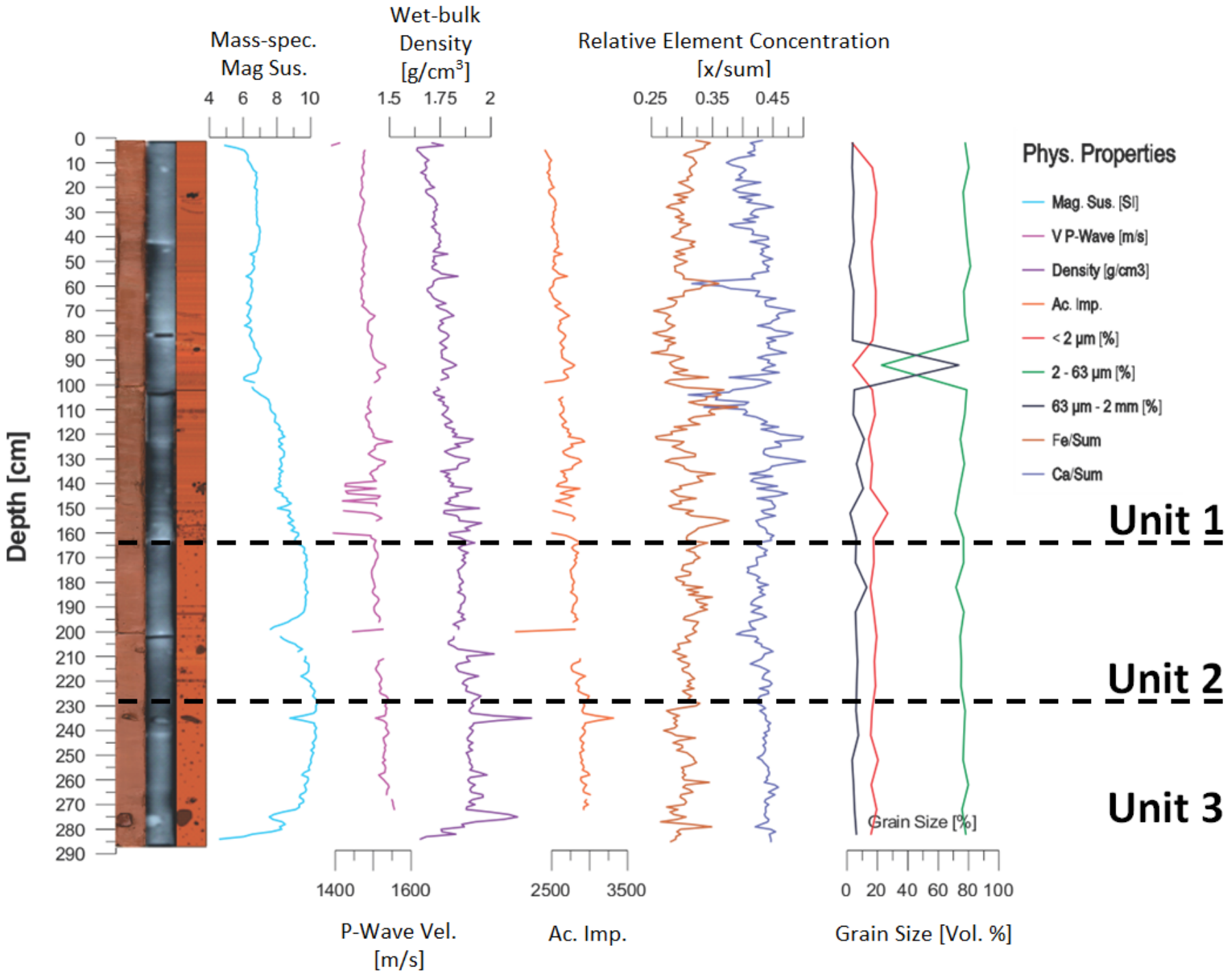

Figure 5.4: Results for core 10JM-GlaciBar-GC01. MSCL results are represented with magnetic susceptibility [10^{-8} m^3 kg], p-wave velocity in metres per second, density in g/cm^3, acoustic impedance (dimensionless). Chemical results include relative Ca and Fe concentrations in x/sum with x=Ca/Fe and sum=sum of the counts of the ten most important elements from XRF analyses (Al, Si, S, K, Ca, Ti, Fe, Rb, Sr, Zr). Results from Grain Size analysis are displayed as grain size distribution in Volume per cent.

susceptibility is comparably low, which is probably related to the transition of core sections. In this case measurements could be taken for the empty space between two sections or on the cap of the PV-liner, where the core diameter is larger, altering measurements accordingly. For the magnetic susceptibility two sections can be identified: The magnetic susceptibility gradually increases from the top until a depth of roughly 235 cm (throughout units U1 and U2). From 235 cm (U3) it slowly decreases (Figure 5.4).

Table 5.1: Maximum, minimum and average values for the physical properties and grain size distribution of GC01

Property	**Minimum**	**Depth [cm]**	**Maximum**	**Depth [cm]**	**Average**
Density [g/cm2]	1.63	5	2.20	235	1.82
P-Wave Velocity [m/s]	1390.74	3	1555.83	272	1497.86
Magnetic Susceptibility [10^{-8} m^3 kg]	4.61	284	10.40	229	8.17
Fractional Porosity	0.32	235	0.65	5	0.54
Grain Size < 2 µm [%]	3.34	2	26.75	152	16.71
Grain Size 2 µm - 63 µm [%]	22.70	92	81.20	52	74.96
Grain Size 63 µm - 2 mm [%]	1.58	52	73.52	92	7.80

P-wave velocities range from 1390 to 1555 m/s (Figure 5.4, Table 5.1). Between 140 and 160 cm the generally increasing trend is interrupted and velocities frequently change between very low and higher values. This may indicate a possible pronounced layering with very soft and more consolidated or coarser sediments interchanging at relatively regular intervals. A higher concentration of coarser clasts and layers with distinct horizons was in fact recorded in the core log (Figure 5.2).

The density of GC01 is relatively constant throughout the core. A very slight increasing trend can be observed from the top to the bottom (Figure 5.4, Table 5.1), which can be explained by the increasing sedimentary load and therefore increasing compression of the deeper materials. The wiggled appearance could reflect the interlayering of coarser or more consolidated layers with the soft matrix. The generally higher density in the lowermost 80 cm should reflect the increasing concentration of coarser components (see section 5.1) and coarser layers or rocks may be represented by the peak densities in this part of the core (Figure 5.4). Densities are slightly higher for U3 as for U1 and U2.

The acoustic impedance measured for GC01 generally increases down-core (Figure 5.4, Table 5.1). However, more pronounced fluctuations occur occasionally. High acoustic impedances are probably due to the transition between the soft matrix and a rock or a very coarse layer. The pronounced wiggly character nicely shows the layering of more resistant with softer layers throughout the first unit. The acoustic impedance is more constant in U2 with just a few local peaks. This pattern fits nicely with the massive matrix and the occasional coarser layers. For U3 the acoustic impedance is

almost constant, but higher than for units U1 and U2. The peak value at the transition between U2 and U3 may reflect the local occurrence of a thick clast layer (compare with Figure 5.4).

Table 5.2: Maximum, minimum and average values for the ten most important chemical elements for GC01, [x/sum]

Element	**Ca**	**Fe**	Si	K	Ti	Al	S	Zr	Sr	Rb
Minimum	**0.310**	**0.250**	0.049	0.076	0.029	0.004	0.003	0.005	0.003	0.003
Maximum	**0.503**	**0.392**	0.136	0.122	0.042	0.015	0.015	0.013	0.007	0.005
Average	**0.430**	**0.306**	0.103	0.099	0.033	0.010	0.005	0.007	0.004	0.003

The description of the element geochemistry focusses on Ca and Fe (Figure 5.4) as these are the most abundant elements (Table 5.2). Plots for the eight remaining elements can be found in the appendix.

Relative element concentrations of Fe and Ca are characterized by numerous oscillations. In general, Ca is more abundant than Fe (Figure 5.4, Table 5.2). Fe concentrations are particularly high where Ca concentrations are very low. The reversed relationship between Ca and Fe is pronounced in U1, but absent in U2 and U3, where fairly constant concentrations of both elements prevail (Figure 5.4). This should confirm the assumed change of lithology at the border between U1 and U2. The small peaks in the Fe/SUM and Ca/SUM ratios as well as the generally reversed relationship between Ca and Fe in U1 could be related to the stratification of the sediments in U1, indicating fairly regular changes in the sediment source. This issue will be further addressed in section 5.4.

As inferred from the core log, the results from the grain size analysis reveal a silt matrix with a small clay component (Figure 5.4). Between 75 and 80 % of the total sediment are between 2 and 63 µm (the silt fraction; Table 5.1). Coarser layers on the other hand are particularly concentrated between 82 and 102 cm depth, as a maximum of 73% is recorded for a depth of 92 cm (Figure 5.4, Table 5.1). This fits with the core log documenting a high concentration of coarse layers between 90 and 99.5 cm depth (Figure 5.2, Figure 5.4). In contrast, based on the grain size analysis, the coarser layers or components are very rare in other parts of the core. However, due to the sampling technique, it is likely that the results are not always representative as only a very small fraction of the sediment surface was sampled. Also the spacing of 10 cm between each sample does not allow for the recording of coarse layers occurring between sample points and is more useful to get a general overview of the material in the core.

5.3.2 10JM-GlaciBar-GC02

For the evaluation of the physical properties of 10JM-GlaciBar-GC02 the same properties as for GC01 were selected (Table 5.3).

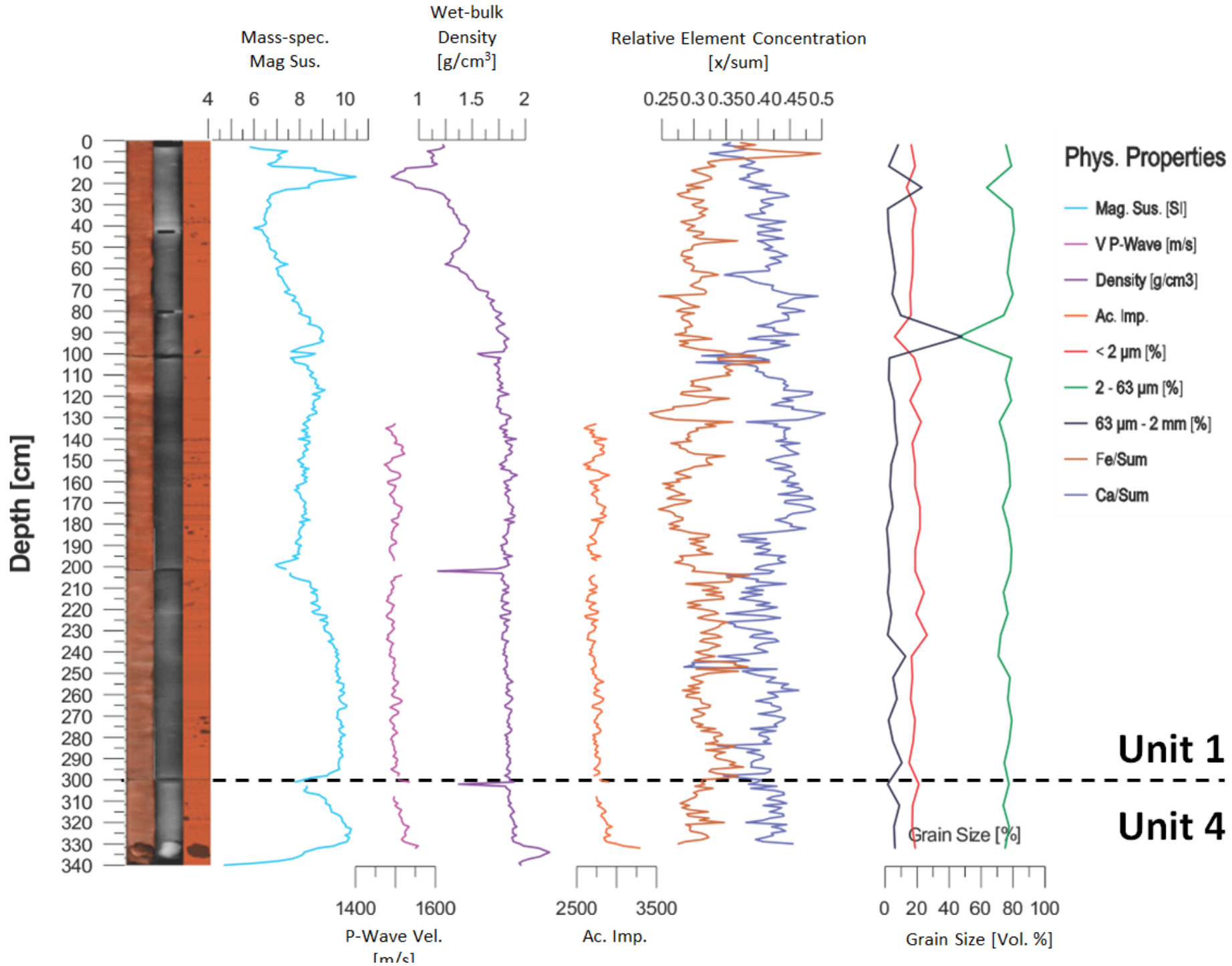

Figure 5.5: Results for core 10JM-GlaciBar-GC02. MSCL results are represented with magnetic susceptibility [10^{-8} m^3 kg], p-wave velocity in m/s, density in g/cm^3, acoustic impedance (dimensionless). Chemical results include relative Ca and Fe concentrations in x/sum with x=Ca/Fe and sum=sum of the counts of the ten most important elements from XRF analyses (Al, Si, S, K, Ca, Ti, Fe, Rb, Sr, Zr). Results from Grain Size analysis are displayed as grain size distribution in Volume per cent.

Table 5.3: Minimum, maximum and average values for the physical properties determined with the MSCL. And for the Grain size distribution within 10JM-GlaciBar-GC02

Property	Minimum	Depth [cm]	Maximum	Depth [cm]	Average
Density [g/cm2]	0.74	17	2.23	334	1.71
P-Wave Velocity [m/s]	1472.55	152	1556.95	331	1499.09
Magnetic Susceptibility [10^{-8} m^3 kg]	4.70	340	10.46	17	8.43
Fractional Porosity [%]	0.30	334	1.16	17	0.61
Grain Size < 2 µm [%]	5.96	92	26.16	232	18.10
Grain Size 2 µm - 63 µm [%]	45.99	92	80.66	42	75.31
Grain Size 63 µm - 2 mm [%]	1.07	182	48.05	92	6.59

The magnetic susceptibility in the second core (Figure 5.5) is generally slightly higher than in the first core with an average value of 8.44 (Table 5.3; 8.2 in GC01). GC02 has a low magnetic susceptibility at the top interrupted by a peak at about 15 cm depth. From about 50 cm the magnetic susceptibility gradually increases before decreasing very slightly throughout the entire second core section (100 – 200 cm). Between 200 and 330 cm the magnetic susceptibility is significantly higher than in the upper core parts, with an increasing trend between 200 and 255 cm. A small decrease occurs around the section transition (302 – 310 cm). These comparably low values probably stem from false measurements on the core liner or the empty space between the two sections, as the other transitions (at 100 and 200 cm depth) are also characterized by outlier values. However, it is not always possible to identify the accurate depth in which outliers begin and end, which is why only the most extreme values were discarded for the presentation of the results. Due to the shortness of the last core section (41 cm) it is difficult to ascribe a definite trend for the magnetic susceptibility to U4. After the small decrease around the top of the unit a strong increase can be observed, reaching its peak around 330 cm. From 330 cm depth the magnetic susceptibility decreases significantly, but this could also be related to inaccurate measurements rather than the actual trends (Figure 5.5).

The p-wave amplitude throughout the core could not be measured satisfactorily, which strongly influenced the quality of the p-wave velocity. Due to a poor contact between the core liner and the p-wave sensors, velocity results were inaccurate for the top 130 cm of the core. This is probably due to a deformation of the core liner. The p-wave velocity is characterized by numerous fluctuations. Nevertheless, the average velocity appears to be relatively constant as the local changes do not show a preferred trend (Figure 5.5). The p-wave velocity for GC02 is similar to the values measured for GC01 (Table 5.3). However, fluctuations are much more pronounced in the second core. This could be related to a more distinct stratification in GC02. It has been mentioned that the stratification in both cores cannot be explicitly linked to changes in lithology. Nevertheless, some change of material must occur, as there would be no explanation for a change in colour otherwise. It is possible that changes in lithology are so small that they are not perceptible to the cruder manual logging techniques. This theory would be supported by the wiggly character of the acoustic impedance plots

(Figure 5.4, Figure 5.5), as the latter should imply changes in acoustic impedance and hence either in density or p-wave velocities. If the material would stay the same throughout the entire layered sections, there should be no registration of changes in either of the physical properties. Stronger local changes in the p-wave velocity for the sediments of GC01 could therefore imply higher differences between the layers (e.g. porosity, density etc.), whereas the layering in GC02 might be characterized by the interchanging of more similar materials.

Density trends for GC02 are similar to GC01. For most parts of the core, the density appears to be more or less constant with frequent very small changes. Density is increasing very slightly down-core (Figure 5.5). Unlike GC01 local changes in GC02 can mostly be observed close to the section breaks and are probably related to false measurements. The average density is lower for GC02 than for GC01 (Table 5.3). It is noticeable that the density is very low and irregular at the top of GC02. Even though densities are increasing rapidly in this core part, two areas are defined by particularly low values (at approximately 15 and 60 cm depth). In these areas the magnetic susceptibility is high. It is possible that these density minima are related to empty spaces in the core liner. However, this has not been observed on the open core. Therefore, these changes could have been caused by very soft sediments.

Resulting from the poor p-wave amplitude measurements, the acoustic impedance for GC02 only yields values from 130 cm down-core. Nevertheless, the slight down-core increase in acoustic impedance is visible. This increase is much less defined than the trend observed for GC01 (compare with Figure 5.4). Similar to GC01, a wiggly appearance is visible (Figure 5.5), although fluctuations are much less defined than for the first core. This is the main difference for the acoustic impedance between the two cores: GC01 has a very irregular appearance with numerous peaks, whereas local changes are only small in GC02. Based on the concentration of coarse clast layers in GC01, the many peaks in the acoustic impedance could be ascribed to these coarser layers. This, in turn, would explain the lack of pronounced peaks in the acoustic impedance for GC02, as the latter has a very low occurrence of such coarse layers. Nevertheless, the regular small peaks and wiggles of the GC02 plot would indicate the stratification discussed earlier, which could be slightly more pronounced in GC02 than in GC01.

The grain size analysis shows similar results for the second core as for GC01 (Figure 5.5, Table 5.3).The matrix is predominantly silty with small amounts of clay and coarse components (larger than 63 µm). Clay contents are around 2 vol % higher in GC02 than in GC01 and the concentration of coarser clasts is slightly lower. This may indicate a very small change in depositional environment, which is further discussed in section 5.4.

Table 5.4: Maximum, minimum and average values for the ten most important chemical elements, [x/sum]

Element	**Ca**	**Fe**	Si	K	Ti	Al	S	Zr	Sr	Rb
Minimum	**0.284**	**0.231**	0.023	0.076	0.028	0.002	0.002	0.005	0.003	0.003
Maximum	**0.504**	**0.498**	0.140	0.123	0.044	0.015	0.016	0.012	0.007	0.007
Average	**0.417**	**0.310**	0.108	0.102	0.033	0.011	0.005	0.007	0.004	0.003

Ca and Fe again show several oscillations and a generally opposing trend with higher abundance of Ca (Figure 5.5, Table 5.4). Where Ca concentrations peak, Fe minima occur and vice versa. The trend is much more pronounced in GC02 than it was in GC01 and the reversed relationship prevails throughout the entire second core, independent of the unit (Figure 5.5). This is especially notable as U2 and U3 in GC01 did not show this anti-phase relationship. The calcium and iron concentrations in those units were relatively constant and did not show an apparent co-dependence. This issue is further discussed in section 5.4.

5.4 Correlation

This section is dedicated to the correlation of the two sediment cores presented throughout this chapter. As some changes in physical or chemical parameters are more pronounced between the cores than others, the reasons for such changes will receive specific attention. Correlations of the cores will be based on the most pronounced differences, which are given for the grain size analysis, density and the geochemical results.

It is believed that the lowermost 76 cm of GC01 reflect a debris lobe deposited in the course of a mass-transport event. The latter was probably triggered on the terminal moraine of the 1948 surge of Kongsvegen (see section 4.4). Aside from the different lithofacies present within the core (section 5.1) this is based on a correlation between the two cores regarding density, geochemistry, and grain size distribution, as shown in the following paragraphs.

The densities for the two cores vary strongly from one location to the other and do not correlate well. The density for GC01 strongly fluctuates, and increases throughout the core, with the most pronounced fluctuations and increase in the lowest 76 cm of the core (Figure 5.6). This fits well with the assumed upper boundary of the mass-transport deposit. The pronounced peaks in GC01 are probably related to density changes between coarse, dense layers and the soft, less dense matrix mud. The density of GC02, on the other hand, only increases at the top but stays relatively constant from 80 cm down-core (Figure 5.6). It is believed that the lowest part of GC01 reflects deposition in a high-energy environment (i.e. mass-transport event), whereas the rest of GC01 and all of GC02 were deposited in a low-energy environment. The latter is supported by the distinct stratification and the fine mud of U1 and U4, both of which are indicative of low energy.

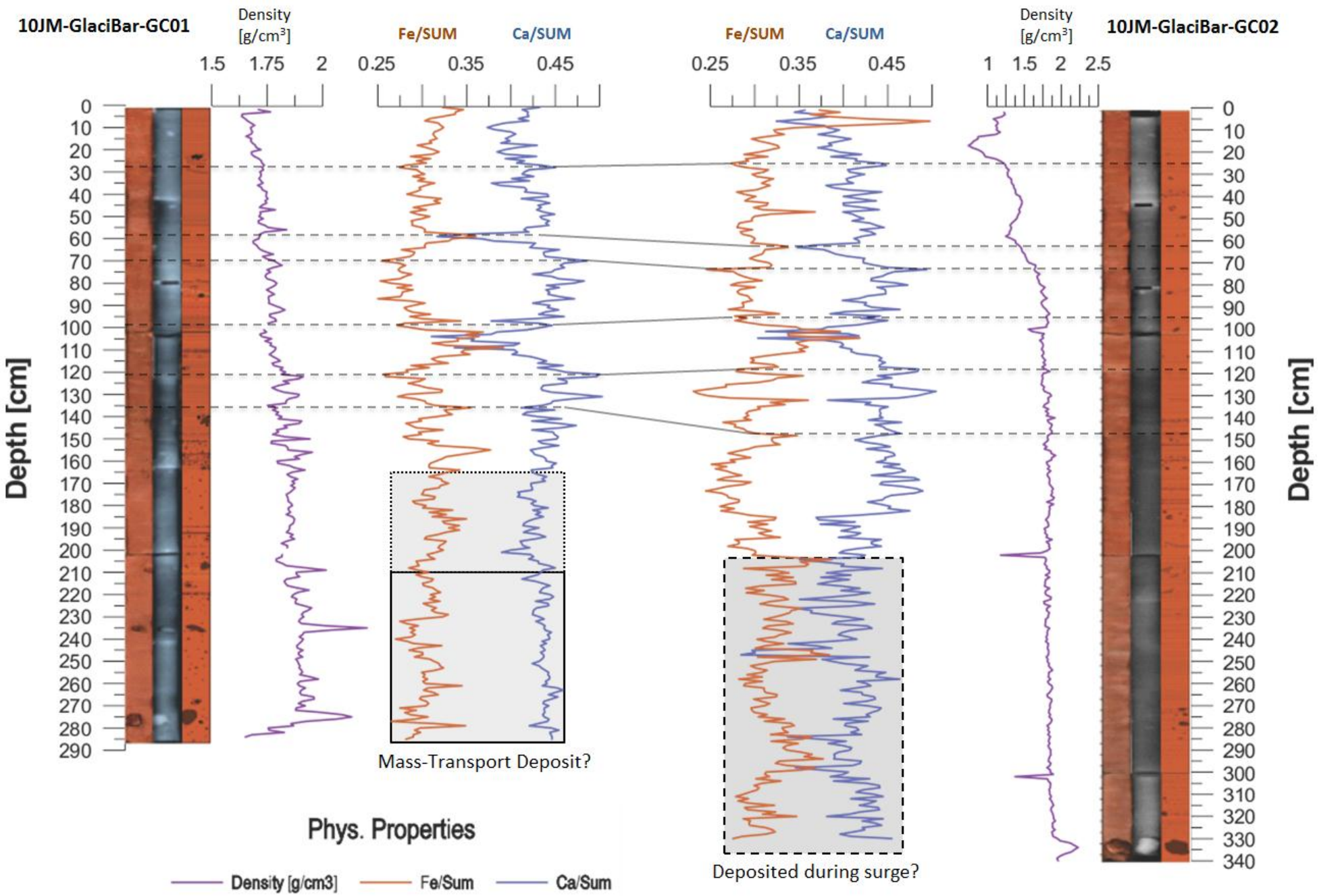

Figure 5.6: Correlation of GC01 and GC02 regarding lithology, density, and Ca- and Fe-content. Geochemical trends correlate well in the upper cores but change towards the lower parts. The grey rectangles indicate the occurrence of the mass-transport deposit within GC01, whereas the grey rectangle for GC02 could indicate extremely proximal conditions.

Regarding the geochemistry, the upper parts of the two cores correlate well (Figure 5.6). The high Ca concentrations in the upper 130 cm of the first core coincide with high Ca-concentrations in the upper 160 cm of the second core (Figure 5.6). The same is true for the Fe-concentrations, due to the intimate counter-relationship (Figure 5.6). In the deeper core parts the regularly changing intervals of high Ca / low Fe and vice versa are completely absent in core GC01 (grey rectangle in Figure 5.6). This is interpreted to reflect the mixture of the previously stratified sediments as a result of the mass-transport event. The second core on the other hand shows a more "compressed" plot than GC01 below 185 cm depth. The anti-phase oscillations between Fe and Ca are still given, but Ca-maxima and Fe-minima have lower and higher values, respectively, than in the upper core parts. This is possibly related to a high proximity to the glacier front, which should have stagnated about 500 m away from the second core location (as inferred from the position of the terminal moraine). This probably means that the lower 140 cm of GC02 were deposited during the surge, whereas the upper ca. 200 cm reflect increasingly distal conditions. The according changes in Ca- and Fe-abundance could be explained by changes in the sediment source. This will be further discussed at the end of this chapter.

The cores differ very slightly with respect to their grain size distribution. GC01 has a generally higher content in coarser components with an average of 7.8 vol % in comparison to 6.59 vol % for GC02 (compare also with Table 5.1Table 5.3). On the other hand the clay and silt contents are higher in GC02 by roughly 2.5 vol % and 0.5 vol %, respectively. Even though these changes are not very distinct they indicate that some differences in the physical environments occurred during the deposition at the two core sites. It is believed that the decrease in the abundance of coarser particles in GC02 can also be ascribed to a decrease in the available energy. According to Hjulström (1935) the efficiency with which water can transport particles is dependent on the grain size of the particles and the flow velocity of water (Figure 5.7). This means that the faster the water (and the higher the available transport energy) the coarser the particles that can be transported. In a glacimarine environment sediment supply into the fjord is mainly steered by turbid surface flows (e.g. meltwater) and meltout from icebergs and bergy bits

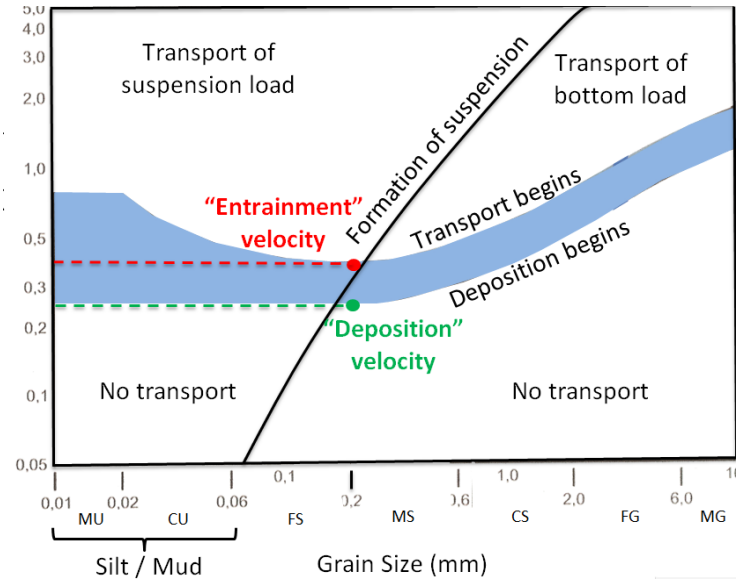

Figure 5.7: Hjulström-Sundborg-Diagram showing the relationship between flow velocity, grain size, sediment transport, and deposition. With F, M, C = Fine, Medium, Coarse, and U, S, G = Silt / Mud, Sand, Gravel (modified after Sundborg, 1967).

(Hoskin et al., 1972; Elverhøi et al., 1980; Boulton, 1990; Dowdeswell & Forsberg, 1992). The higher concentration of coarser particles in GC01 therefore suggests either higher energy available during deposition, or higher input from icebergs. The former could be achieved by a faster flowing meltwater channel (e.g. due to a confined channel diameter), but would not explain the difference between two cores located so close together. The same would apply if more coarse material was incorporated into ice floes. The difference in energy is therefore believed to originate from the mass-transport deposit, which was able to rip up coarser components from the seafloor, mix it with the silty clay and deposit it as a sedimentary lobe at the bottom of the terminal moraine's distal slope. Aside from the observations mentioned above (density, lithology, chemistry, grain size) this theory is supported by a particularly high magnetic susceptibility and a fairly constant acoustic impedance for the lowest part of GC01 (see Figure 5.4). Defining the exact transition between the "normal" glacimarine sediments deposited from suspension and the debris lobe is tricky. Based on the density, acoustic impedance and magnetic susceptibility, it seems likely that the transition is located at a depth of roughly 210 cm, with U3 and the lowermost 20 cm of U2 representing the mass-transport deposit. However, the lithology and geochemical signature suggest a transition at 165 cm, where the stratified character of U1 changes to the massive sediments of U2 (and later U3). It is therefore possible that U2 and U3 are actually the same. The distinction into two units was based on the occurrence of clast layers in U2, which could in fact be clast clusters dumped from an overturning iceberg (see Vorren et al., 1983).

The relationship of the two elements Ca and Fe is inferred to derive from fairly regular changes in the sediment source. Due to the location of the two cores it is assumed, that Kronebreen and Kongsvegen (with Infantfonna) are the two glaciers mainly dominating the sedimentary input. As shown in Figure 5.8, the catchment of Kronebreen is mostly influenced by two different kinds of rocks: sandstones and shales from the Dicksonfjorden Member in the Andrée-Land Group and marbles and dolomite marbles from the Generalfjella Formation (compare also with Figure 2.2). Although no exact classification is available for these rocks, it is assumed that the former are characterized by a high Fe-content, especially compared to the Ca-rich marbles and dolomites of the latter, which are also known as calcium carbonate ($CaCO_3$) and calcium magnesium carbonate ($CaMg(CO_3)_2$), respectively. The catchment of Kongsvegen on the other hand is largely influenced by the dolomites and limestones of the Gipshuken and Wordiekammen Formations (compare with Figure 2.2) with only occasional appearance of the sandstones and shales from the Dicksonfjorden Member (Figure 5.8).

Based on this it is considered likely that the changes in relative Ca- or Fe-concentrations are related to the variable input of one or the other glacier. As both glaciers provide Ca-rich sediments to the

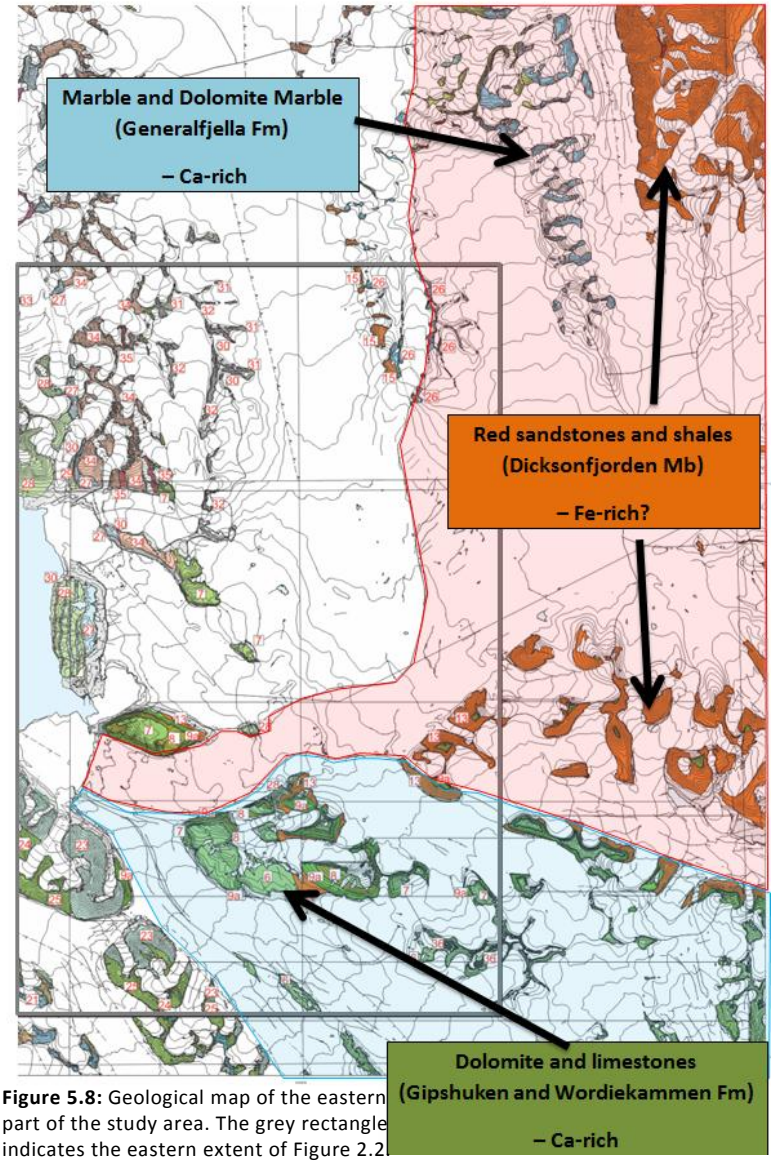

Figure 5.8: Geological map of the eastern part of the study area. The grey rectangle indicates the eastern extent of Figure 2.2. Red and blue polygons outline the catchment areas of Kronebreen and Kongsbreen, respectively. Modified after and printed with permission of W.K. Dallmann, Norsk Polarinstitutt.

fjord, it is a logical consequence that the general amount of Calcium in the cores is higher than Fe (Table 5.2, Table 5.4). Nevertheless, higher values for Fe are probably related to an enhanced input of Kronebreen, whereas higher Ca concentrations would suggest Kongsvegen as the dominating source (Figure 5.8). This is in accordance with Ottesen et al. (2010), who mapped a high abundance of Fe in the rocks northeast of the study area, whereas a higher Ca-concentration is found in the catchment areas southeast of Kongsfjorden.

Variations in sediment input between the two glaciers could be related to different processes. The most likely possibility is a change in the internal hydrology of the glaciers, resulting in enhanced (or inhibited) meltwater input from subglacial, englacial or even supraglacial channels. As glacier hydrology is a complex topic in itself, explaining the many different processes leading to changes in the meltwater output or delay would exceed the scope of this thesis; however, to name a few examples, an increase in meltwater supply could be related to an increase in temperature of the ice (climate- or friction-induced) or the confluence of two previously unconnected englacial channels (e.g. Benn & Evans, 2010).

Aside from a mass-transport event, the Ca- and Fe-signature of the lowermost 76 cm of GC01 could have been caused by 1) a constant sediment supply from Kronebreen and Kongsvegen with equal contributions, or 2) a homogenization of the sediments in the water column. However, as the occurrence of U1 in the upper core shows that changes in glacier contribution are typical and pronounced, and mixing in the water column is uncommon, it is still considered most likely, that GC01 partly contains a mass-transport deposit.

Such close proximity probably inhibits the deposition of sediments from meltwater streams, as the latter still have too high a velocity to allow for suspension settling (compare with Figure 5.6). As the surge in 1948 was initiated by Kongsvegen, which usually transports Ca-rich sediments in the meltwater (Figure 5.8), a lack of such sediments could hence account for a decrease in Ca-input. As the glacier began to retreat (represented by the upper 185 cm of GC02), the deposition of Ca-rich sediments from meltwater most probably increased, thus explaining the higher Ca-concentrations in the upper core parts.

Based on the discussion and interpretation of all results and the correlation of the two cores it becomes apparent that lithological units defined from the lithological log do not always coincide with such units proposed by the physical properties and the chemistry of the sediments. Taking these parameters into account, GC01 would incorporate U1 from 0 – 165 cm (as before), U2 from 165 to 210 cm (before 230 cm), and U3 from 210 to 286 cm. U1 in GC02 on the other hand would only represent the upper 185 cm instead of the previously assumed 300 cm. U4 on the other hand would extend from 185 cm down to the bottom of the core.

6. Correlation of Acoustic and Sedimentary Data

The chirp line in **Error! Reference source not found.** clearly indicates the occurrence of a wedge-

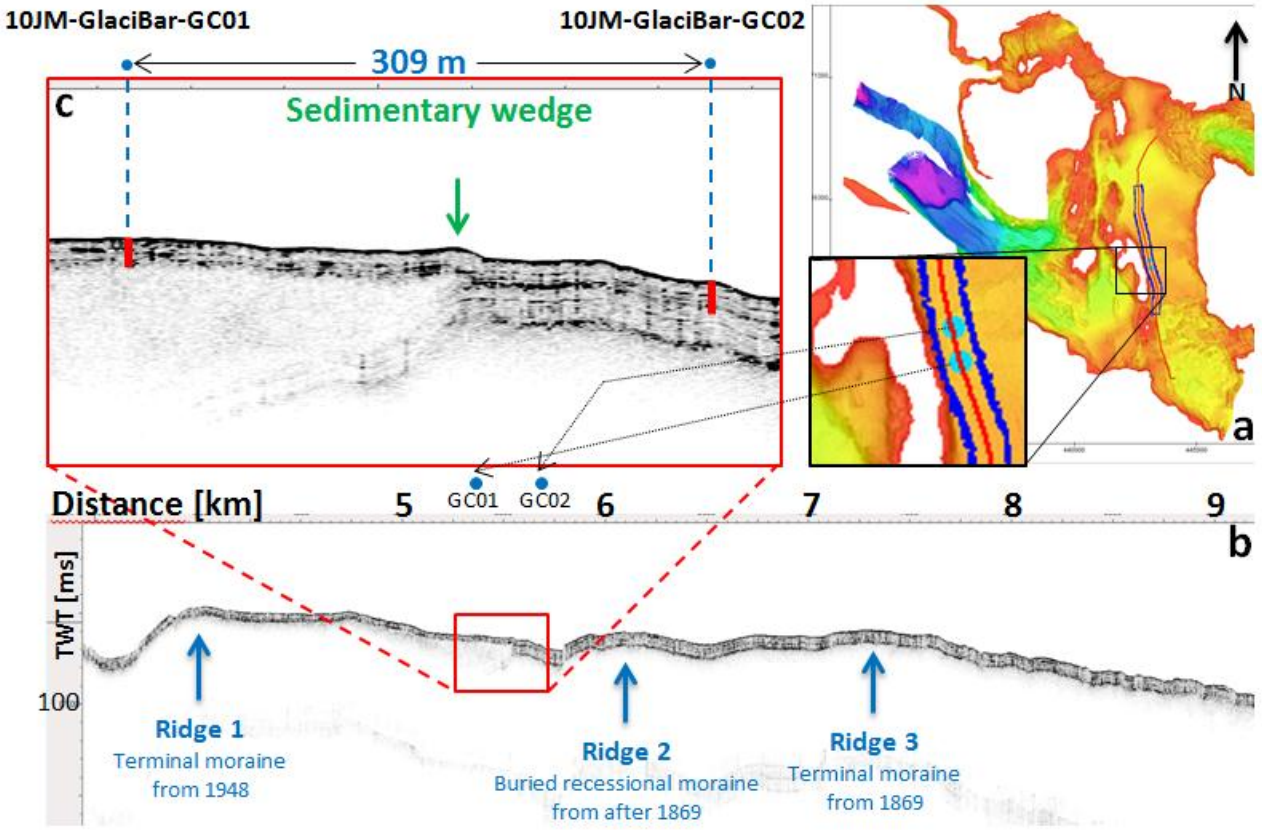

Figure 6.1: A) Overview over the location of the two cores and a chirp line across the core sites with respect to the bathymetry. The blue shape indicates the limit of b. B) Chirp line across the two core sites outlining the three ridges presented in section 4.4. The terminal moraines are from 1869 and 1948 and the red rectangle outlines the debris lobe found on the distal flank of the latter. C) Zoom-in of the red rectangle in B) with the sedimentary wedge representing the mass-transport deposit. Blue dots indicate core locations, whereas the bold, red lines indicate approximate penetration depths of the cores.

shaped, transparent to semi-transparent reflection (sedimentary wedge in Figure 6.1). This is interpreted to be the mass-transport deposit derived in section 4.4. It was said, that two terminal moraines were created at 8 and 9.5 km away from the ice margin (Figure 6.1, Ridge 2 and 3) during the Kronebreen surge of 1869. A third terminal moraine was generated during the Kongsvegen surge of 1948 at a distance of almost 6 km from the ice margin (Figure 6.1, Ridge 1). The mass-transport deposit is located on the distal flank of this, most recent, terminal moraine. For simplification the mass-transport deposit will be referred to as the "sedimentary wedge" throughout the next paragraphs to distinguish its wedge-like shape.

The chirp line across the two core sites clearly indicates the occurrence of a sedimentary wedge where GC01 is located (Figure 6.1). This is interpreted to be the mass-transport deposit from the 1948 Kongsvegen surge, as described in section 4.4.

Calculations from section 4.4 based on a p-wave velocity of 1600 m s^{-1} (Elverhøi et al., 1995) showed the mass-transport deposit to be 14.4 m thick, with a sedimentary cover of 2.4 m. The distal reflections on the acoustic data were found to correspond to a sediment thickness of 7.2 m. Given the average p-wave velocity of 1497.86 m s^{-1} determined in section 5.3 the sedimentary wedge is in fact 13.48 m thick and is covered by 2.25 m of sediments. The latter are inferred to be deposited after 1948. The distal sediments are 6.74 m thick, with the lower 4.49 m older than 1948.

The 2.25 m of stratified, semi-transparent reflections indicate layered or laminated sediments and therefore fit very well with U1 in both cores. Given the thickness of this sedimentary cover, it is very likely that at least the lowermost 61 cm of GC01 represent the debris lobe. This fits very well with the previous interpretation of the lowermost 76 cm being the mass-transport deposit, as the acoustic data only allow for an approximation of the two-way-travel times.

Furthermore the sedimentary cover indicates that the lower 116 cm of GC02 were deposited before and during 1948. Assuming that the sedimentation rates were very high during the maximum ice extent, it is well possible that only U4 (the lowermost 39 cm) is older than 1948, whereas the remaining 77 cm were deposited when the ice front stagnated (in 1948).

7. Discussion

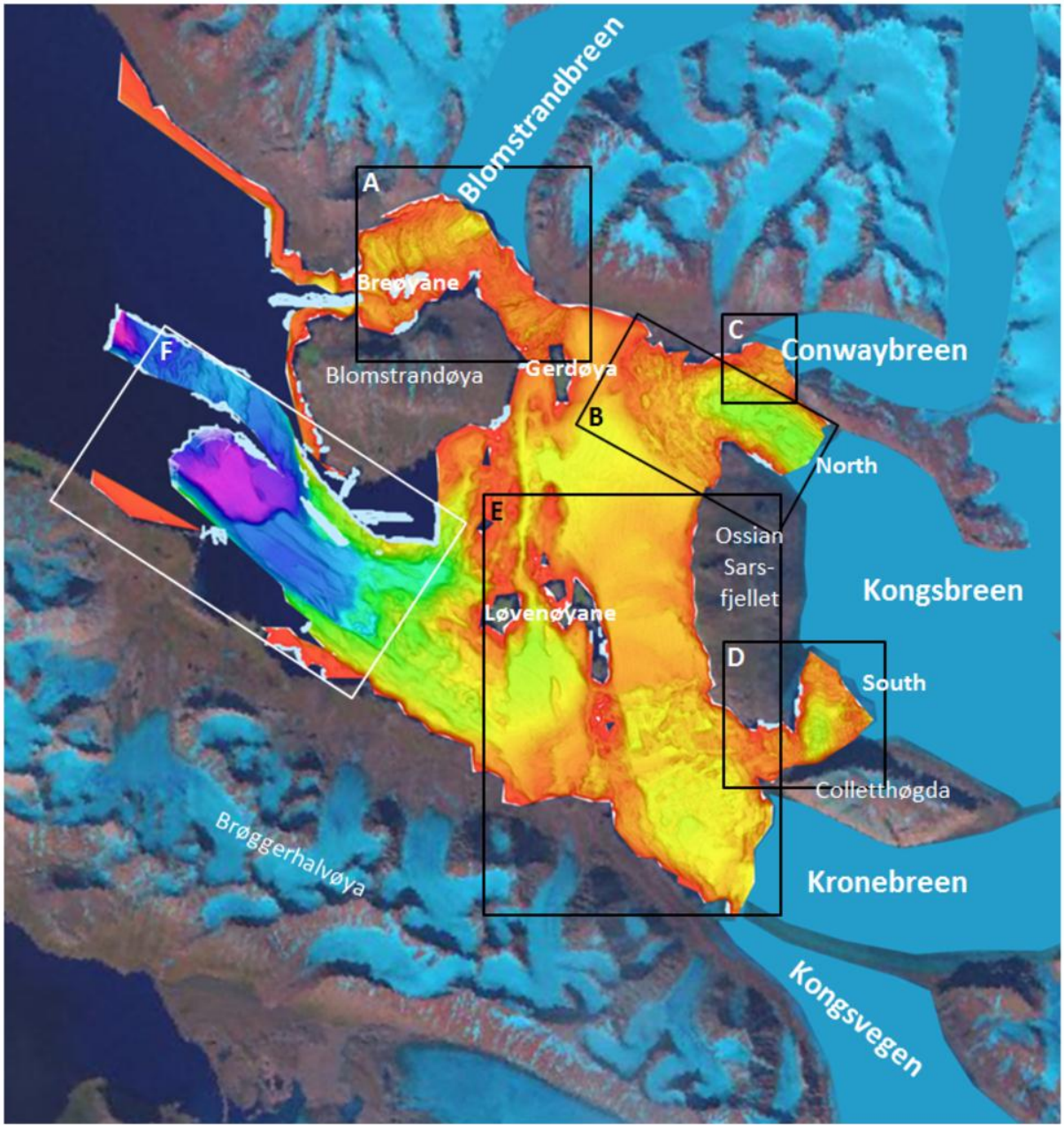

Figure 7.1: Overview over the study area and the six areas showing landforms characteristic of glacial advance.

In this chapter the results presented and interpreted so far will be evaluated and discussed. Firstly, a conceptual model for the landform assemblages in Kongsfjorden will be introduced, which comprises the recurring geomorphic features presented in chapter 4. The model is based on the acoustic data and is derived from the five areas outlined in Figure 7.1 (A, B, C, D, E). Aside from the spatial component the model also includes a temporal component, which clarifies the assumed relative age of deposition for each landform (Figure 7.2).

The majority of the landforms displayed in this model occur in front of several glaciers and a main formation mechanism will be described for each feature. However, in some cases, there are several processes that could have generated the landforms. These will be evaluated throughout this chapter. The evaluation is divided into two parts: one for the surge-induced landforms generated directly by the glaciers, and one for the sedimentary processes following a surge.

Towards the end of the chapter the model proposed for Kongsfjorden will be compared to similar landform models from marine and terrestrial settings to assess the major differences and similarities. A model for landform assemblages of fast-flowing ice streams will also be presented and compared to the geomorphic features documented from outer Kongsfjorden (Figure 7.1, F; Howe et al., 2003; Ottesen et al., 2007; MacLachlan et al., 2010).

7.1 Conceptual Model

Based on the acoustic and lithological data the submarine landforms in inner Kongsfjorden are inferred to be of glacigenic origin. Their characteristics and distribution clearly indicate that they are formed by one of the five tidewater glaciers in the study area.

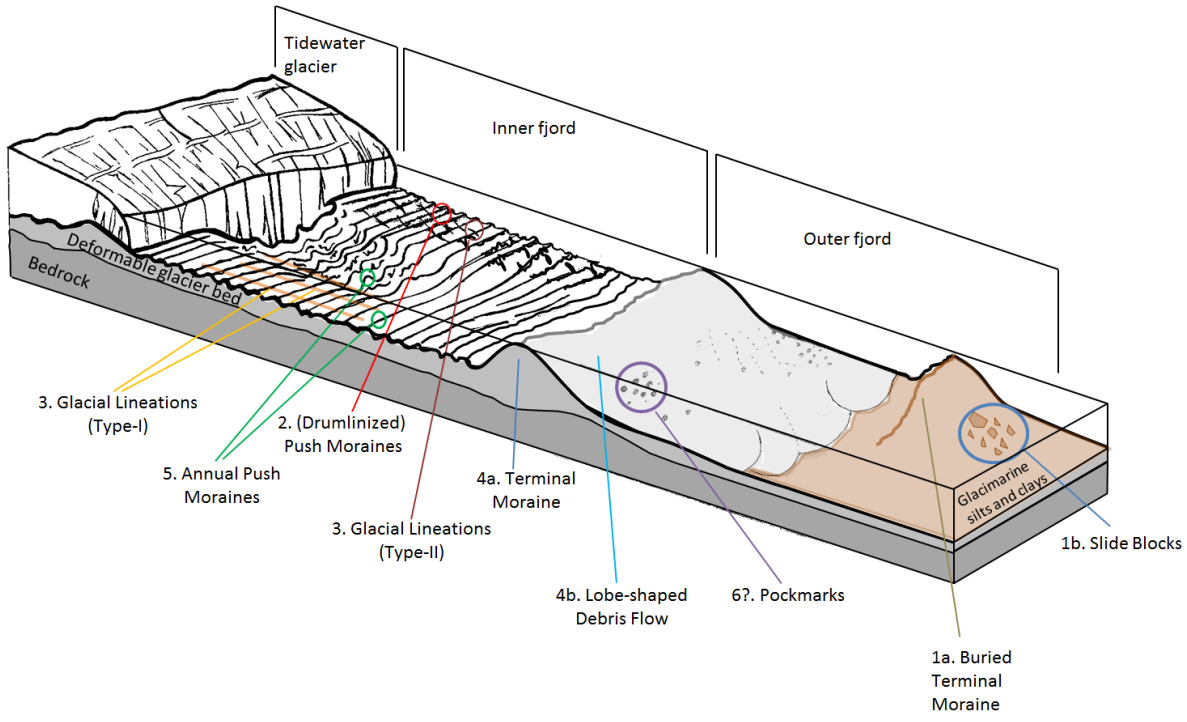

Figure 7.2: Conceptual model for the landforms generated by surge-type glaciers in Kongsfjorden. Numbering is according to relative age of deposition with 1 being the oldest and 6 the youngest.

The landforms found in Kongsfjorden are summarized in the conceptual landform assemblage model shown in Figure 7.2. As all of the landforms occur in front of at least one of the three surging glaciers in the area (Kongsvegen, Kronebreen, Blomstrandbreen), the model can be used as a basis to infer

typical landforms resulting from glacier surges on Svalbard. Nevertheless, it is important to keep in mind, that the model is a generalization. Due to the many different circumstances (glacier dynamics, glacier's thermal structure, frequency of surges etc.) no glacier behaves exactly the same and a standardized model may not always be applicable.

The landforms presented in Figure 7.2 are numbered according to their assumed relative age of deposition. The buried terminal moraine marked as 1a) is inferred to be the oldest feature, created during a previous advance of the glacier, either related to climatic cooling during the Little Ice Age or a surge. A landslide triggered at the moraine's top may have generated slide blocks (1b). Both features were subsequently buried by post-surge sediments (see section 7.3). When the glacier retreated after this ice advance, push moraines were deposited during frequent stagnations of the ice front (Figure 7.2**,** 2). These push moraines were drumlinized by the overriding, surging glacier during a subsequent advance, leaving behind a set of drumlinoid features / glacial lineations (3). At the end of the surge, the terminal moraine (4a) was deposited, marking the maximum ice extent of this, most recent, surge event. The overload of sedimentary material during ice front stagnation led to the triggering of a mass-transport event, resulting in the deposition of lobe-shaped debris flows (Figure 7.2, 4b) across and at the base of the terminal moraine's distal flank. During the quiescent phase of the surge-cycle the grounded glacier slowly retreated and deposited push moraines (5), most probably marking the annual positions of ice stagnation. The pockmarks (6?) on the surface of the lobe-shaped debris flows are inferred to be the youngest landforms; however they could be generated before or at the same time as the annual push moraines.

The processes forming this particular landform assemblage will be discussed in the following paragraphs. Note that the buried terminal moraine is derived to be generated by the same mechanisms as the other, newer, exposed, moraines. This feature will therefore be described together with the rest in section 7.2.2.

7.2 Surge-induced landforms

7.2.1 Drumlinoid Features / Glacial Lineations

Two types of glacial lineations appear in Kongsfjorden (section 4.1). Pairs of parallel elongated grooves and ridges extend along the fjord in front of Blomstrandbreen, Conwaybreen and across two very small areas in front of Kongsbreen South (Type-I-Lineations, Figure 7.1, areas A, C, and D respectively). Given their orientation to the main fjord axis, these features are believed to be aligned parallel to the past ice flow direction.

The lineations in Kongsfjorden are very similar to other glacial lineations observed in previously glaciated areas (mega-scale glacial lineations, e.g. Clark, 1994; Ó Cofaigh et al., 2002; Ottesen et al., 2008; Baeten et al., 2010), which are closely associated with fast-flowing ice streams (e.g. Clark et al., 1993; Stokes & Clark, 2002; Ottesen et al., 2005; Ottesen & Dowdeswell, 2006; Andreassen et al., 2007; Ottesen et al., 2008; King et al., 2009). Common mega-scale glacial lineations have been described to be typically between 8 and 70 km long, between 200 and 1300 m wide and spaced at distances between 300 and 5000 m (Clark et al., 1993). Their main criterion is the elongation ratio, which is larger than 10:1 for mega-scale glacial lineations and smaller for "normal" glacial lineations (Stokes & Clark, 2002). Although the grooves and ridges in Kongsfjorden are much shorter with maximum lengths of around 3 km, much closer together with average spacings of around 150 m, and much narrower with widths between 50 and 100 m, their elongation ratios still exceed the one defined by Stokes & Clark (2002) with a minimum of 10:1 and a maximum of 50:1.
This first type of glacial lineations observed in Kongsfjorden may be much smaller than typical mega-scale glacial lineations, but are very similar to glacial lineations described for other Spitsbergen fjords regarding length, width, height and spacing (e.g. Ottesen & Dowdeswell, 2006; Ottesen et al., 2008). This is why they are believed to be generated by the same processes: during the, in this case surge-induced, advance of a glacier, the fast flowing grounded glacier deforms the soft sediments at its base and excavates or redistributes this material in the typical streamlined fashion (compare with e.g Tulaczyk et al., 2001; Ó Cofaigh et al., 2005; Ottesen et al., 2008). This process is sketched out in Figure 7.3 (A).

The drumlinoid features (see section 4.1) were interpreted to be a second type of glacial lineation (Type-II-Lineations). Even though different to other glacial lineations observed in front of surging glaciers (e.g. drumlins, flutes, mega-flutes), their streamlined character also suggests relatively fast ice flow. Due to their parallel orientation to the main fjord axis, these small ridges are also believed to be indicative of the direction of past ice movement (Figure 7.3, B). Drumlinoid landforms occur in front of Kongsbreen North and in front of the shared ice margin of Kongsvegen and Kronebreen (Figure 7.1, areas B and E, respectively).

The different types of glacial lineations in Kongsfjorden are believed to derive from the “shape” of the seafloor prior to rapid ice movement (Figure 7.3). Glaciers with their last activity during the Late Weichselian as part of a large, fast-flowing ice stream will have generally retreated since then, exposing the landforms created during the LGM. Their burial by a more or less constant settling of glacimarine or (glaci-)fluvial sediments then led to a relatively smooth, soft seafloor in the fjords adjacent to the glaciers. This makes the seafloor prone to deformation when subject to stress, i.e. under the influence of a rapidly advancing glacier. This is believed to be the case for the proximal

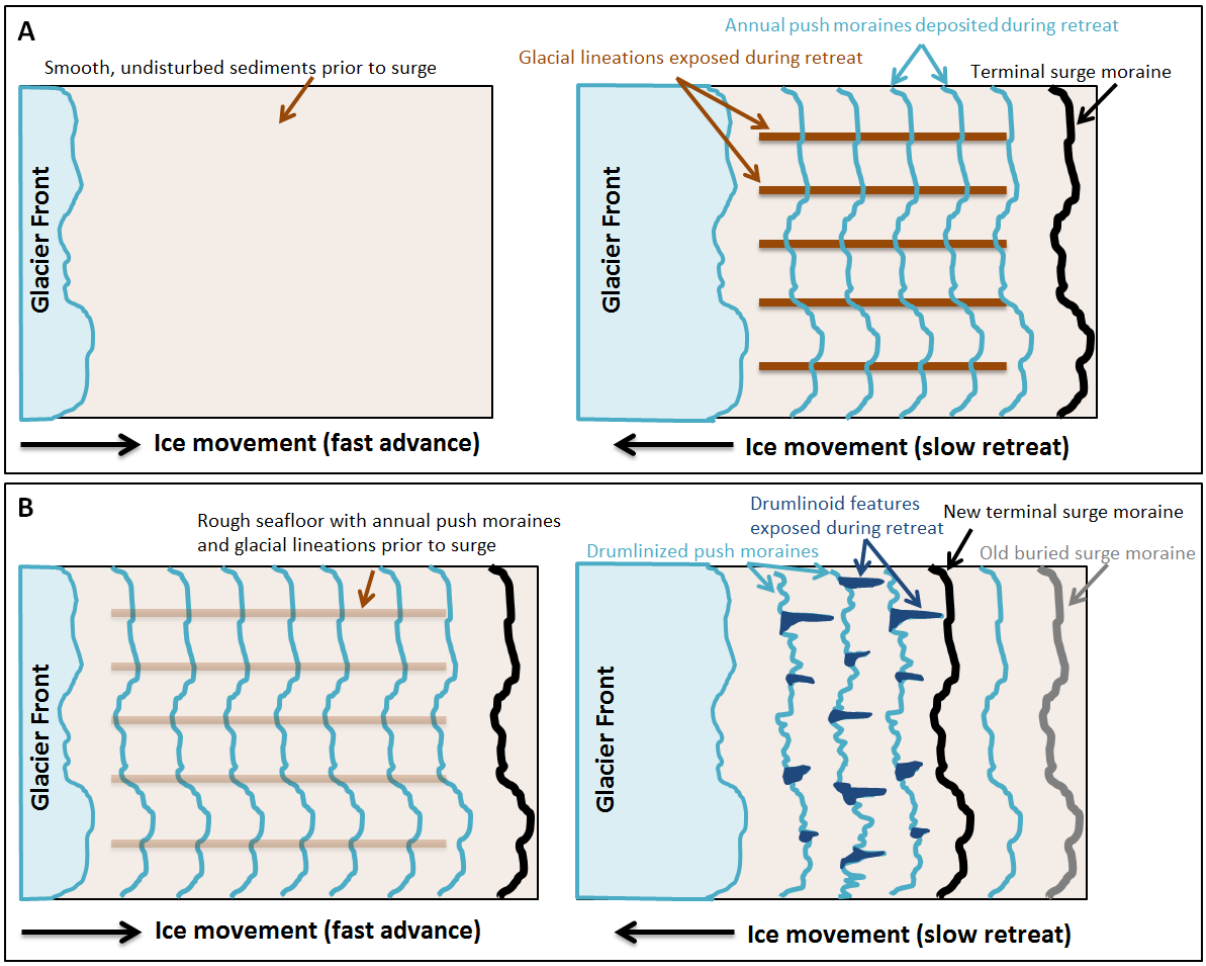

Figure 7.3: Sketch of the processes generating glacial lineations in Kongsfjorden. A: Type-I-glaciations similar to mega-scale glacial lineations, B: Type-2-glaciations (drumlinoid features).

region of Blomstrandbreen (Figure 7.1, A).

The formation process believed to generate the drumlinoid features is best explained using a direct example from the study area (Figure 4.9; Figure 7.1, area E). The Kongsvegen / Kronebreen complex has surged at least once before the last surge of 1948 (e.g. Liestøl, 1988; Hagen et al., 1993). This previous surge event (in 1869) is believed to have left the characteristic landform assemblage described in the conceptual model in section 7.1. As the ice advance related to this previous surge is assumed to be much more extensive than the advance related to the 1948 surge, the terminal moraine from the earlier surge event would not be affected by a second, smaller advance. However, the annual push moraines probably generated inside the surge limit after 1869 would give the seafloor the typically rough character, serving as obstacles to any glacier readvancing at a later time. The drumlinoid features are therefore believed to reflect parts of these small, transverse push moraines, which were streamlined by the force of the renewed (rapid) movement of ice. This process is sketched out in the lower part of Figure 7.3

The distribution pattern of the lineations off Conwaybreen and Kongsbreen is more complicated (Figure 7.1, areas B, C, D). Especially peculiar is the appearance of the Type-I-lineations in front of Conwaybreen and Kongsbreen South, but not in front of Kongsbreen North, where the drumlinoid

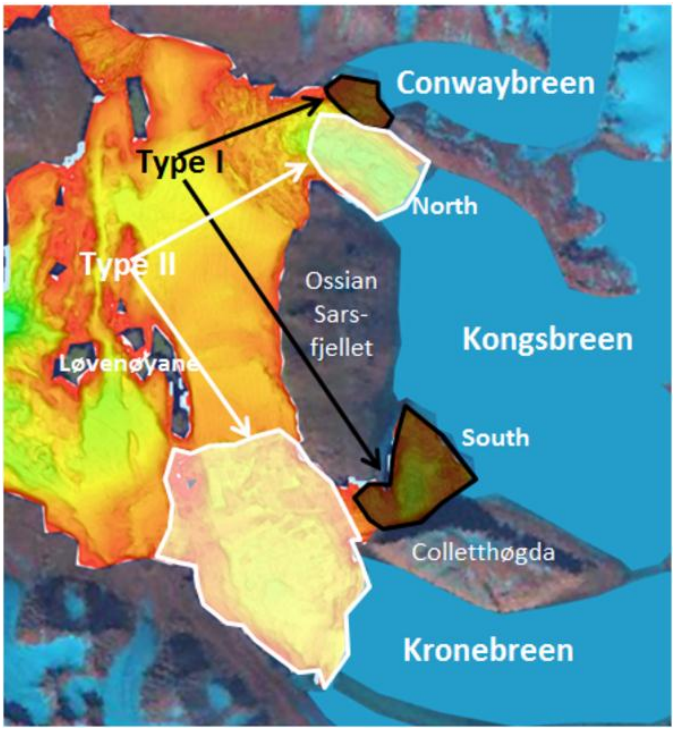

Figure 7.4: Overview over the occurrence of Type-I and Type-II glacial lineations in the east of Kongsfjorden.

features (Type-II) prevail (Figure 7.4). One possible scenario is explained in the following**.** Note that Kongsbreen most probably surged in 1897 as will be shown in section 7.2.2, below.

Kongsbreen South, Kronebreen and Kongsvegen were probably connected (compare with Figure 7.5) and, thus, advanced as a single ice front during the surge initiated by Kronebreen in 1869 (or by Kongsbreen in 1897). Due to fast ice flow the soft glacimarine sediments of the fjord floor in front of Kongsbreen South (and probably also in front of Kronebreen and Kongsvegen) were moulded into glacial lineations of Type I (Figure 7.5). At the end of the surge the glaciers stagnated, deposited a terminal moraine and retreated, while depositing larger recessional moraines, or small annual push moraines. Kronebreen and Kongsvegen retreated to the point where the first drumlinized push moraine can be found on the seafloor today (close to the terminus position of 2010, Figure 7.5). Because of its connection to Kronebreen, Kongsbreen South stagnated, depositing a large moraine at the mouth of the outlet (Figure 7.5, RC2) but no annual push moraines inside the small basin between Colletthøgda and Ossian

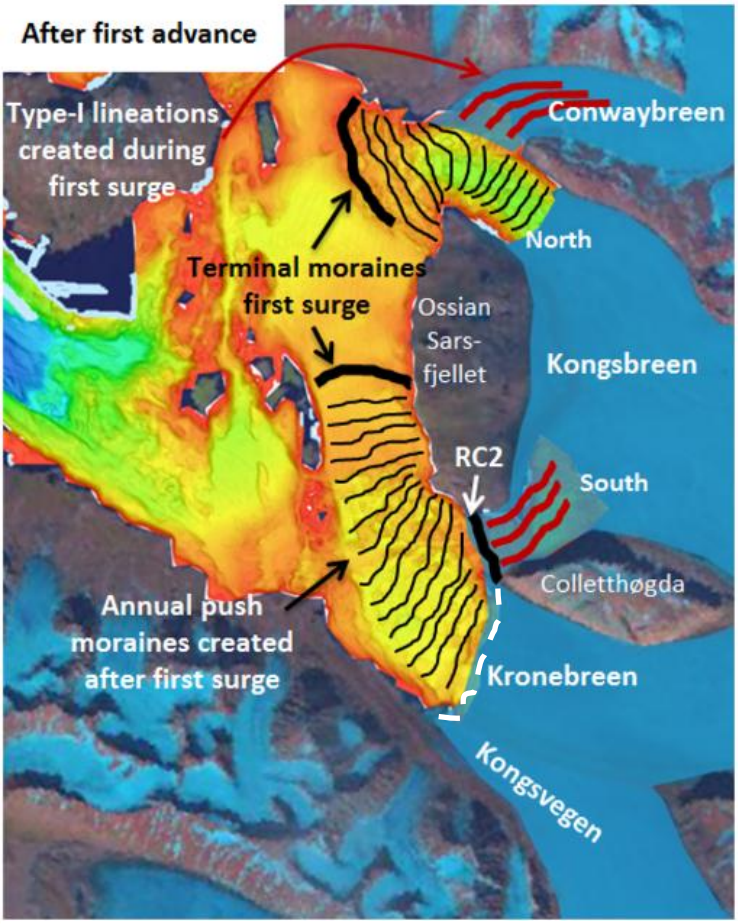

Figure 7.5: Possible configuration of the glacier fronts and landforms after an earlier surge event (most likely 1869 or 1897). Glacial Lineations of Type-I were generated during advance, annual push moraines during retreat. The white dashed line shows the glacier front position in 2010. RC 2 was described in section 4.2 and represents a large transverse ridge.

Sarsfjellet. As Kongsbreen South did not retreat any further than the mouth of the outlet, the previously created Type-I glacial lineations were preserved. In 1948 a second surge was initiated, this time by Kongsvegen. All three fronts advanced again, drumlinizing the push moraines in front of Kongsvegen / Kronebreen. The Type-I glacial lineations in front of Kongsbreen South were preserved. After the second surge the glaciers retreated again, this time further and Kongsbreen South deposited the unmodified annual retreat moraines found in the area today.

The drumlinoid features (Type-II) in front of Kongsbreen North (Figure 7.4) also indicate more than one advance. The reason for this is not entirely certain, as Kongsbreen has originally been classified as a non-surge type glacier (e.g. Hagen et al., 1993). Conwaybreen on the other hand shows Type-I lineations (Figure 7.4), which is peculiar given the connection between the two glaciers up until at least 1976 (Hagen et al., 1993; compare with Figure 7.6, p. 101). Again, a solution to the two different landforms in such close proximity is not obvious, but the following scenario is suggested. If the drumlinoid features in front of Kongsbreen North formed as postulated above (Figure 7.3), an earlier advance created landforms on the seafloor, which were drumlinized during a later readvance. Although Kongsbreen North may have advanced as a response to its own surge, it is considered more likely that the front advanced as a response to a surge involving all of Kongsbreen. It is assumed that such a surge event happened in 1897 (compare with section 7.2.2, below). It is not entirely clear which processes caused another advance, but new investigations have recently suggested that surges already took place in Spitsbergen fjords before the Little Ice Age (e.g. Kempf et al., subm.). Assuming that this was also the case for the tidewater glaciers in Kongsfjorden, it is possible that Kongsbreen surged at least once before 1897.

The fast flow velocities during the first surge probably caused Conwaybreen, and possibly also Kongsbreen North, to form Type-I glacial lineations. When the glaciers retreated, Kongsbreen North retreated at a much faster rate than Conwaybreen. This is based on two assumptions: 1) Conwaybreen today has a much lower calving rate than Kongsbreen (0.029 $km^3\ a^{-1}$ compared to either 0.225 or 0.086 $km^3\ a^{-1}$ according to Blaszczyk et al. (2009[1]), and 2) calving rates tend to increase linearly with water depth (Benn & Evans, 2010). The deep water in front of Kongsbreen North (up to 140 m) may therefore encourage increased calving and fast retreat. Kongsbreen North retreated as far as in 2010, depositing annual push moraines (Figure 7.5). When it readvanced at a later time these push moraines were drumlinized. Conwaybreen on the other hand probably retreated very slowly after the first advance, so that the Type-I glacial lineations were still "protected" by the overlying ice. Another advance would not affect the lineations then. The favoured

[1] Blaszczyk et al. (2009) gave values on the calving rate for Kronebreen 1 and Kronebreen 2 without clarifying which glacier is where. Based on the terminology problem mentioned in section 2.4, it is assumed that one of the two values represents Kongsbreen

possibility however, is that Conwaybreen did not advance a second time. If the rapidly advancing northern front of Kongsbreen pushes aside Conwaybreen and, because of their oblique orientation towards each other, “cuts off” any further advance of Conwaybreen, the glacial lineations would also remain unmodified.

The air photographs used by Liestøl (1988) seem to suggest that especially Kongsbreen, Kronebreen, and Kongsvegen did not retreat as far as assumed here, and that especially the surge from 1948 only caused a small advance (see also Figure 7.14, p. 110). This may indicate some uncertainties in the scenario suggested here. However, as no alternative models have been proposed so far, the formation processes discussed here appear to be the most plausible.

7.2.2 Terminal Moraines

All large, transverse ridges described in section 4.2 are inferred to be terminal moraines marking a maximum ice extent. Howe et al. (2003), Ottesen et al. (2007), and MacLachlan et al. (2010) found glacial landforms (e.g. transverse moraine ridges, (mega-scale) glacial lineations, and lateral ice-stream moraines) in the outer parts of Kongsfjorden, which are dating back to the Last Glacial Maximum or the Late Weichselian deglaciation period (see section 7.4.4, below). The well-preserved character as well as the proximal location of the features described for inner Kongsfjorden indicates a more recent deposition. They are suggested to be either terminal (surge) moraines or terminal moraines indicating the maximum ice extent related to climatic cooling during the Little Ice Age.

Most glaciers enclosing the study area have been recorded to have surged at least once since the early 1800s (compare Hagen et al., 1993). The terminal moraine would in these cases indicate the position of the ice front at maximum ice advance after the active phase of the surge cycle. This first possibility is in contrast to the second one which would indicate the age of the moraines to be about 100 years, a time at which Svalbard was subjected to a short, but fairly significant cold period termed “Little Ice Age” (LIA, Liestøl, 1976; Sexton et al., 1992). The glaciers and ice fields in the area readvanced, leading to the deposition of push-moraines in front of the glacier termini (e.g. Boulton et al., 1996; Plassen et al., 2004; Ottesen & Dowdeswell, 2006).

Although there is no evidence against deposition during the LIA, the terminal moraines in the study area are believed to be surge moraines. This theory is supported by several factors which will be discussed throughout the following paragraphs. Surge moraines contain dislodged sediment masses from beneath the glacier. The unconsolidated sediments at a glacier bed are unable to withhold the large stress gradients they are subjected to during a surge, and eventually fail (Bennett, 2001). The heterogeneous and unsorted material is hence inferred to be pushed up, faulted, folded and thrusted by the glacier (Solheim, 1991). The moraines are deposited at the end of the surge when the

glacier front stops and continuing high sediment discharge from the glacier shapes the more gradual distal flank (Solheim, 1991). When the glacier begins its retreat and changes into its quiescent phase the landforms are exposed.

This interpretation is based on a number of facts: 1) characteristics such as height, asymmetry, and their location with respect to the modern glacier front (e.g. Solheim, 1991; Bennett, 2001; Ottesen & Dowdeswell, 2006); 2) the occurrence of debris flows on the distal flank (see Kristensen et al., 2009); 3) their function as a border between the rough proximal seafloor and the distal smooth and undisturbed parts (see also Solheim, 1991); 4) in some cases the number of annual push moraines within the surge limit and their accordance with surge years proposed by Hagen et al. (1993), and 5) the correlation of their location with maps of past ice front positions provided by Liestøl (1988). The interpretation of the terminal moraines as surge moraines is furthermore in accordance with Svendsen et al. (2002), who postulated that, "as in the case of Kongsbreen, the maximum extent of glaciers may result from surge dynamics" in the Kongsfjorden area.

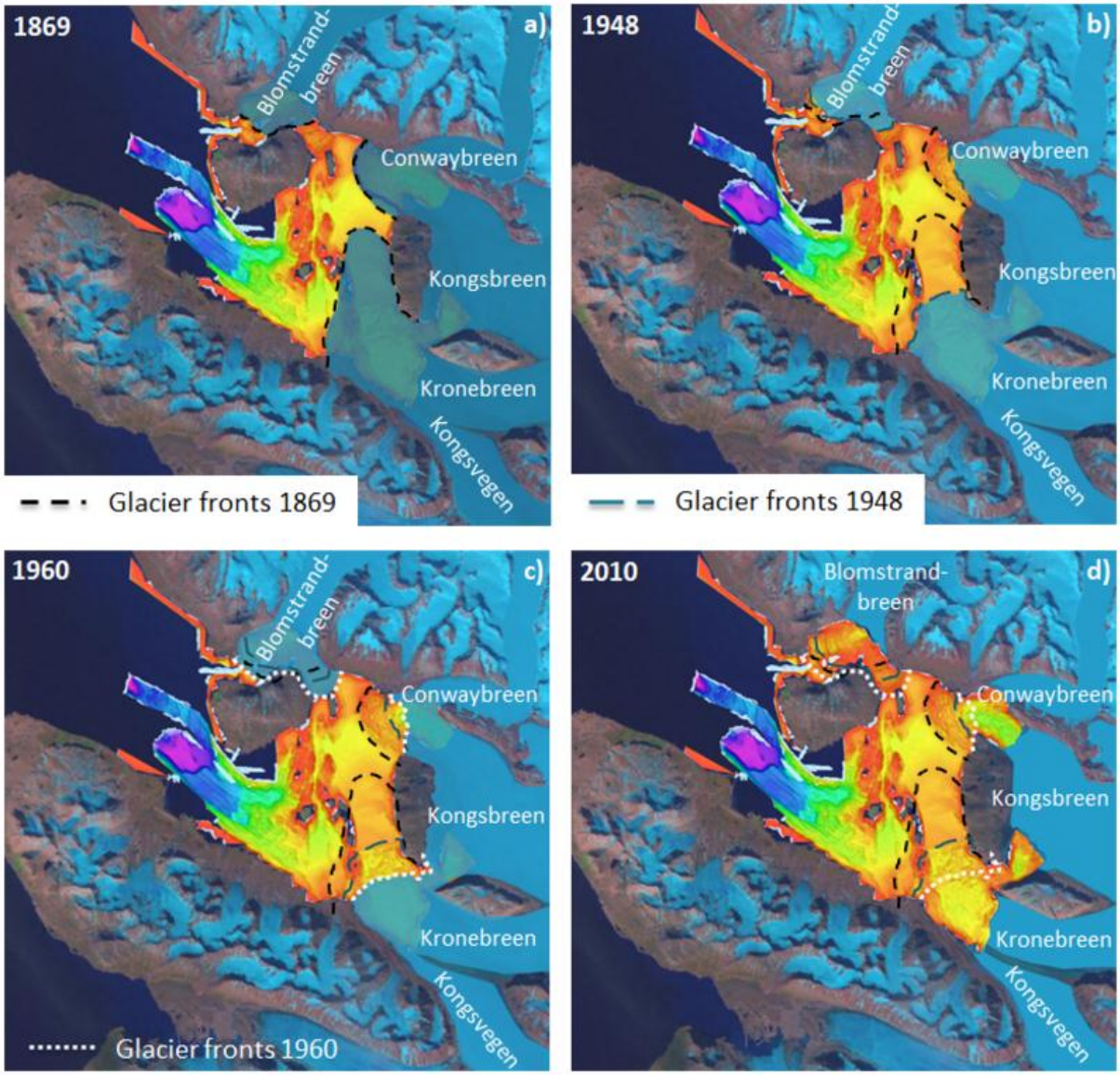

Figure 7.6: Appearance of terminal moraines in the study area and inferred positions of glacier termini during respective surges (1869, Kronebreen; 1948, Kongsvegen; 1960, Blomstrandbreen, based on Liestøl, 1988). Glacier fronts of 2010 are displayed for comparison.

It was mentioned above that Liestøl (1988) provided a map of the different ice front positions in Kongsfjorden for specific years. The positions of the glacier termini during the "key years" fit nicely with the positions of the terminal moraines observed on the acoustic data from 2010 (Figure 7.6). The Kongsvegen / Kronebreen glaciers advanced furthest during the Kronebreen surge of 1869 with their ice front very close to the outermost buried terminal moraine described in section 4.4 (Figure 7.6a). In 1948 the two glaciers advanced again, presumably triggered by a surge event of Kongsvegen. Again, the ice front position mapped by Liestøl (1988) is in almost the same position as the in section 4.4 inferred surge moraine for 1948 (Figure 7.6b). This is also true for the surge moraine from 1960 (see section 4.2), when Blomstrandbreen was at its maximum position (Figure 7.6c). The three terminal moraines described for Blomstrandbreen are believed to be deposited simultaneously, marking the maximum extent of the surge in 1960. It is likely, that the terminal ridges extend over or the glacier deposited a certain amount of material up against the islands in the area (Blomstrandøya, Gerdøya and Breøyane, compare with Boulton et al., 1996). The hypothesis of a simultaneous deposition of actual terminal surge moraines is supported by the work of Liestøl (1988; Figure 7.6c) and the number of the annual push moraines in the area. This latter issue is further addressed in section 7.2.4, below.

Inferred from the landforms described previously, the Kronebreen surge of 1869 advanced mainly in a northward direction, as indicated in Figure 7.7. Given the shape of the presumed glacier extent at that time, it is possible, that the terminal moraine described on the west of today's glacier front is, in fact, a lateral moraine, generated along the side of the stagnating glacier. Similar landforms have been described for many glaciers and have also been documented for Kongsfjorden and the Kongsfjorden Trough (e.g. Bennett et al., 1999; Ottesen et al., 2007). The lack of geomorphic features indicating westward movement on the basin floor in front of Kronebreen / Kongsvegen supports the idea of a lateral moraine. Nevertheless, the part of the glacier generating this moraine must have behaved like a glacier front in some way: the extensive lobe-shaped debris flows on the distal side of the moraine,

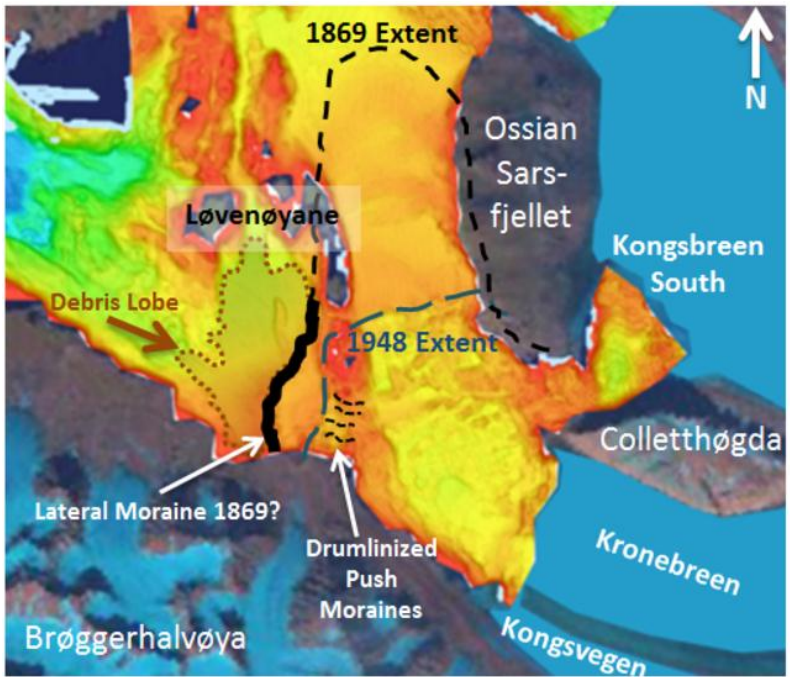

Figure 7.7: Overview over the landforms in front of Kronebreen and Kongsvegen and respective glacier front positions during surge years, as mentioned in the text.

as well as the drumlinized annual retreat moraines just before the terminal moraine (Figure 7.7) suggest regular retreat in an eastward direction rather than a southward retreat after the surge maximum was reached.

The more likely possibility is an advance of Kongsvegen and Kronebreen as a result of the surge, but in different directions. This scenario is sketched out in Figure 7.8. With a shared ice margin just one of the glaciers surging may initiate the simultaneous advance of both glacier termini. Assuming that Kronebreen was the surging glacier in 1869 (Hagen et al., 1993), it would respond to its own internal imbalance by advancing. Kongsvegen, in turn, may have just responded to the advance of the Kronebreen ice margin without any internal imbalance of its own. This would probably cause Kongsvegen to advance only as far as its ice front is still intimately linked with the Kronebreen front, creating its own terminal moraine (Figure 7.8). Kronebreen on the other hand would advance until reaching internal equilibrium again, marking the end of the surge by a terminal moraine (Figure 7.8). If Kronebreen advances in a northward direction, its influence on Kongsvegen would decrease with increasing distance of advance. This would explain why the 1869 surge appears to have reached so far northwards but has a comparably small westward extent. This is also favoured by the local bathymetry, forcing Kronebreen into a sort of trough towards the north (e.g. Figure 7.8). The lack of landforms indicating westward movement may then be explained by a very narrow outlet of Kongsvegen. Today Kongsvegen only contributes a 400 m wide ice cliff to the shared ice front. During a surge of Kronebreen Kongsvegen is probably "pushed" against the mountains along the coast by the force of the rapidly advancing Kronebreen and its outlet becomes even narrower (Figure 7.8). When the stress from Kronebreen decreases, either because the surge wave propagated too far northwards or because the small island group Løvenøyane separated Kongsvegen from Kronebreen, Kongsvegen has more space again, and its ice front can extend and deposit a wide terminal moraine (Figure 7.8). The theory of an adjacent glacier being "pushed aside" by a surging neighbour has also been discussed by Liestøl (1988), who, based on sketches from Kongsvegen and Kronebreen, observed changing locations of the small moraine separating Kronebreen and Kongsvegen. This shift in position was ascribed to changing surge activity of the two glaciers, with the moraine pressed towards the south by a more active Kronebreen and towards the North when Kongsvegen was more active. Accordingly, the moraine was observed in a more southern position after 1869, but pushed northwards by Kongsvegen in 1948.

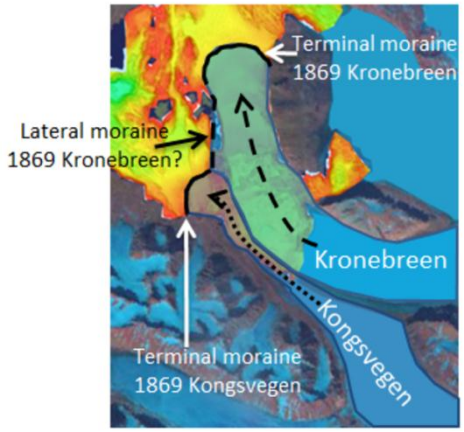

Figure 7.8: Possible glacier configuration during the Kronebreen surge in 1869.

It is interesting that the two glacier fronts of Kongsbreen North and Conwaybreen exhibit signs of surge behaviour as well, even though they were not classified as surge-type glaciers (Liestøl, 1988; Hagen et al., 1993). Figure 7.6 showed the variations of the glacier front positions according to the surges of Kronebreen and Kongsvegen, leaving distinct imprints on the seafloor, at least from 1869. There are two possible scenarios that might have led to the deposition of the landform assemblage in the northeastern part of the study area: 1) a surge of Kongsbreen, or 2) a surge of Kronebreen, assuming that Kongsbreen is in fact, part of Kronebreen (see also section 2.3.4).

1) It is possible that Kongsbreen is of surge-type and caused an advance of its two ice fronts at one point (Figure 7.9). This could have been before 1869 or before 1948 so that any features left by the advance of the southern ice front would have been overridden by later surges of Kronebreen or Kongsvegen. As Liestøl (1988) mapped a maximum ice extent of the northern Kongsbreen ice margin to the year 1897 (Figure 7.9), it might be that Kongsbreen surged then. This would fit very well with the geomorphology, as the terminal moraines in front of Kongsbreen North just mark a maximum ice extent, but do not yield any information on when they were deposited. Furthermore, as described in section 4.4 the bathymetry in front of Kronebreen and Kongsbreen South is characterized by the occurrence of three large transverse ridges: two buried (Figure 7.10, Ridge 2 and 3), where the outermost was interpreted to be from the Kronebreen surge of 1869, and one exposed, proximal moraine, which was derived to be from 1948 (Figure 7.10, Ridge 1). The moraine in the middle must therefore either be a moraine deposited during the recession of Kronebreen after the surge in 1869, or during a separate surge from Kongsbreen. The latter would be in accordance with Liestøl (1988) who mapped the ice front position of either Kongsvegen, Kronebreen, or Kongsbreen South to be more or less at the position of this second ridge. As no other mechanism would explain the occurrence of the middle

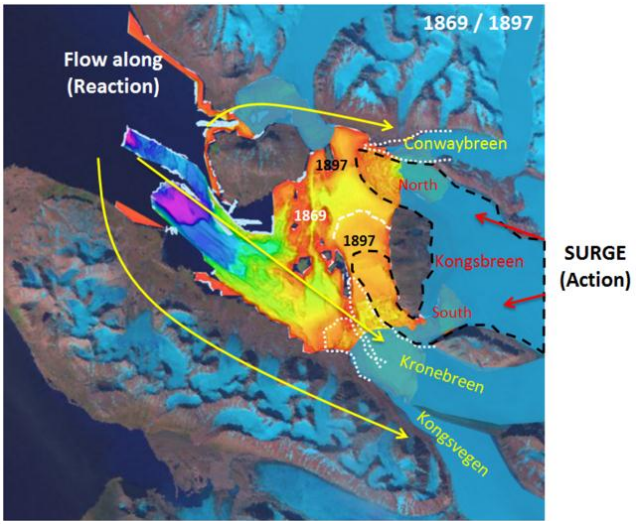

Figure 7.9: Possible extent of a Kongsbreen surge in 1897 and effects on adjacent glaciers. Yellow areas show which glaciers reacted to the surge by advancing, whereas the dashed black lines mark the probable maximum ice extent of a Kongsbreen surge. Dotted white lines indicate the extent of the reactive glaciers.

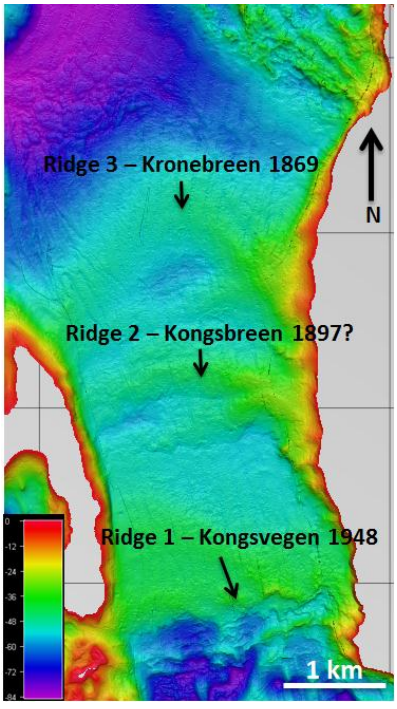

Figure 7.10: Large transverse ridges in front of Kongsbreen South, Kronebreen and Kongsvegen, interpreted to be three terminal moraines from respective surges.

moraine (Figure 7.10, Ridge 2) as satisfactorily, a third surge triggered by Kongsbreen in 1897 is the favoured scenario.

Nevertheless, possibility 2) is also likely. Due to the unambiguous naming of the glaciers at the head of the fjord (compare section 2.3.4) it is difficult to find definite information on surges, calving rates, areas etc. As the majority of sources, including the Norwegian Polar Institute, have referred to Kongsbreen as a separate glacier (Liestøl, 1988; Boulton, 1990; Dowdeswell & Forsberg, 1992; Svendsen et al., 2002; Howe et al., 2003; MacLachlan et al., 2010; Trusel et al., 2010) this terminology has been chosen for this thesis. However, almost as many sources have considered Kongsbreen North and South to be a northern and central front of Kronebreen (Hagen et al., 1993; Lefauconnier et al., 1994; Bennett et al., 1996; 1999; Glasser et al., 2001; Kehrl et al., 2011). As Hagen et al. (1993) is one of the standard sources for registered surges on Svalbard, it may be possible that Kongsbreen South and North are really part of Kronebreen (Figure 7.11). Provided that Kronebreen really is of surge-type (see Bennett et al., 1999), the surge of 1869 might lead to exactly the geomorphology found in Kongsfjorden (Figure 7.11). This is due to the fact that probably all three fronts of Kronebreen would be affected by a surge. The deposition of a terminal surge moraine in front of the northernmost ice front of Kronebreen (so far referred to as Kongsbreen North) would hence be the logical consequence. However, again, the uncertainty about the nature of Kronebreen glacier and the inconsistent use of names do not permit a definite conclusion.

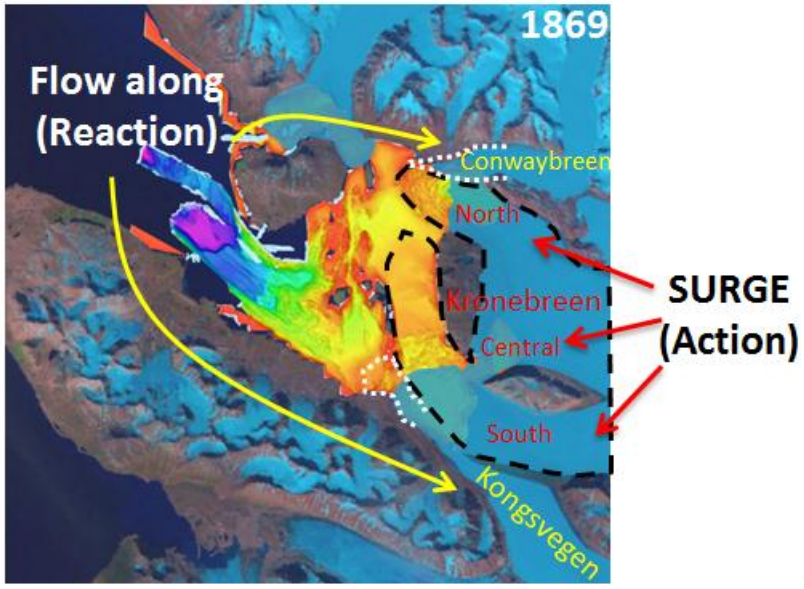

Figure 7.11: Effects of a surge of Kronebreen if Kronebreen incorporates Kongsbreen and is made up of a northern, central, and southern front (as suggested by e.g. Bennett et al., 1999). Yellow arrows show reactive glaciers and white dotted lines their probable extent.

7.2.3 Lobe-Shaped Debris Flows and Slide Blocks

Debris lobes are frequently associated with glacier surges (e.g. Boulton et al., 1996; Plassen et al., 2004; Ottesen & Dowdeswell, 2006; Ottesen et al., 2008; Kristensen et al., 2009) where enhanced sediment supply at the glacier terminus leads to the triggering of a mass flow event (e.g. Ottesen et al., 2008). The debris lobes found in front of many surging glaciers on Svalbard are similar to those

representing grounding line deposits of Pleistocene continental shelf moraines (King et al., 1991; Kristensen et al., 2009).

The overload of material can be related to the discharge from subglacial, englacial or supraglacial meltwater streams, which represents one of several sediment sources. Nevertheless, a number of different sources have been discussed in the literature (e.g. Alley et al., 1989; King et al., 1991; Boulton et al, 1996; Hald et al., 2001; Ottesen et al., 2008). Sediments can derive subglacially representing parts of the deformable glacier bed that were extruded at the glacier's grounding line (Alley et al., 1989; Boulton et al., 1996; Hald et al., 2001). King et al., (1991) proposed the possibility of the debris flows deriving from subglacial sediment meltout of material-laden glacier ice. Ottesen et al. (2008) suggested the failure of the surge moraine's distal slope as a result of oversteepening. However, three main factors may contribute to a decrease in slope stability and subsequent failure: (1) earth quakes, (2) higher pore pressures and (3) a significant increase in sediment supply, often related to glacial activity (Forwick & Vorren, 2007). The lobes with particularly undisturbed surfaces were interpreted to result from turbidity or water-rich debris flows, specifically by meltwater runoff from the front of an active glacier. This is assumed to be the main triggering mechanism in Kongsfjorden, where glacial activity was distinctly higher during surge events of some of the local glaciers. As all of the glaciers with debris lobes on their terminal moraines are believed to have surged, it is assumed, that the lobes with an unperturbed sediment surface are in fact related to subglacial meltwater flow and subsequent outwash at the glacier front, directly after the maximum ice extent of the advance was reached (e.g. Ottesen & Dowdeswell, 2006; Kristensen et al., 2009).

Superficial channel-like features occur on some of the sediment lobes (see section 4.3). These are inferred to be related to water flow across the lobes' surfaces after deposition. Similar features have been described by Boulton et al. (1996) and Kristensen et al. (2009) and may be produced in two ways: 1) meltwater from the glacier surface incising into the soft sediments, or 2) dewatering of the sediment lobes as a consequence of consolidation. This, in turn, would significantly decrease the available pore spaces and result in the expulsion of large water masses (Boulton et al., 1996). The gradually dipping slope of the terminal moraine would facilitate downward flow as a result of gravity. As the superficial features in Kongsfjorden appear only on the lower parts of the debris lobes, this second possibility is considered the more likely.

Larger blocks appear at the foot of one of the buried terminal moraines (see Figure 4.24, and Figure 7.2). Their transitions to the sea floor are not sharp but blurred, which leads to the conclusion that the blocks have been buried by deposits from suspension settling. The chirp data confirmed this (Figure 4.25). As landslides originate from slope failure and are a kind of mass transport event, it is believed that a landslide was triggered at the end of or shortly after the 1869 surge of Kronebreen,

releasing large debris blocks from the grounding line and redepositing them at the foot of the moraine's distal flank. The sedimentary cover of approximately 10 m supports the theory that the blocks were deposited in 1869 and buried gradually over the following 141 years.

7.2.4 Annual Push Moraines

The regularly spaced small, transverse ridges found in Kongsfjorden have been interpreted to be small push moraines produced at annual intervals at the ice margin. The ridges are common in the submarine fore-field of glaciers (e.g. Sharp, 1984; Boulton, 1986; Bennett et al., 2001; Ottesen & Dowdeswell, 2006; Ottesen et al., 2008, Baeten et al., 2010) and their formation has been ascribed to different processes. Among these are squeeze-out of subglacial till at the ice margin, the melting out of englacially trapped debris, bulldozing by the glacier pushing up the sediments in front of it and the deposition of supraglacially transported material (e.g. Sharp, 1984, Boulton, 1986). Even though the formation of these moraines may often involve a combination of different processes, consensus for the formation of annual push moraines on Svalbard seems to be the presence of sea ice at the glacier front during winter, inhibiting calving and therefore momentarily stopping the glacier's overall retreat (e.g. Boulton, 1986; Ottesen & Dowdeswell, 2006; Dowdeswell et al., 2008; Ottesen et al., 2008). The glacier front then stagnates or readvances, leading to the deposition of the moraines. Depending on winter temperatures, glacier velocity, and calving rates, these push moraines may be created once a year, as expected for Kongsfjorden based on the very regular spacing, or less frequently.

The character of the push moraines described from Kongsfjorden varies from linear transverse to very curvy with different orientations. As the more irregular features are confined to water depths exceeding 50 m, the changing shapes are ascribed to the difference in water depth: Deeper water allows for subaqueous calving, breaking away pieces from the grounded ice margin. The more pervasive this calving process, the more irregular the shape of the ice front. In shallower waters subaqueous calving is suppressed or less pronounced giving the ice margin the more regular front resulting in the deposition of the continuous, curvilinear ridges (Benn, pers. comm.).

Assuming the push moraines are in fact created every year, they can be used to reconstruct the age of some geomorphic features. In Kongsfjorden it could be possible to reconstruct the surges of the respective glaciers, trying to confirm whether the recorded years fit with the geomorphology. This is possible for Blomstrandbreen, whose surge limit (the area between the glacier margin and the terminal moraine) is characterized by a set of very regularly spaced annual push moraines (Figure 7.12). As the data for this thesis was gathered in 2010, the occurrence of 50 annual push moraines in

the fjord arm southeast of the glacier (Figure 7.12) suggests the terminal moraine to be from 1960, which fits exactly with the recorded surge (Hagen et al., 1993). However, the push moraines in the southwest of the glacier only add up to roughly 47 (Figure 7.12). There are two options: 1) the southwestern branch of the glacier reached its maximum position three years after the southeastern, or 2) both fronts reached their maximum extents simultaneously, but the southwestern branch retreated three years later than the southeastern. Both are possible, assuming that the glacier's imbalance was more pronounced in the western part of the glacier, that advance was prevented by the geomorphology, or that retreat was inhibited after the deposition of the terminal moraines. Considering the small moraines' irregular character in the deeper parts, however, it is more likely that single moraines could not always be distinguished properly, or that deposition was not as regular as once a year. This is especially probable if subaqueous calving is involved: if the main mechanism causing the deposition of annual push moraines is the presence of shore-fast sea ice, subaqueous calving should not be inhibited during winter, as sea ice should rarely penetrate the entire 50 m depth of the fjord. It is therefore still considered most likely, that all terminal moraines around Blomstrandbreen were deposited at the same time and as a result of the 1960 surge (Figure 7.12). It is also likely that the annual push moraines were deposited more or less at the same time. As mentioned, both fjord arms in front of Blomstrandbreen are characterized by a very similar amount of such push moraines. As remnants of such moraines have also been found on top of Blomstrandøya (Whittington et al., 1997), it is assumed that the ridges are in fact of the same age and may even be connected across the island (Figure 7.12).

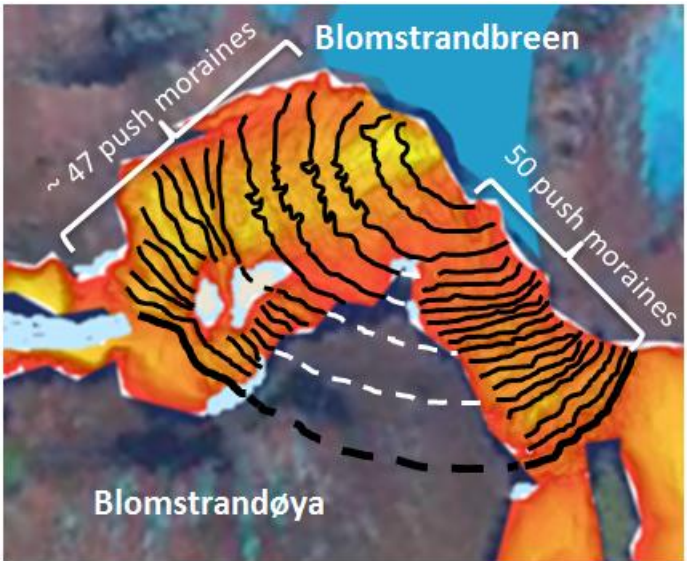

Figure 7.12: Push moraines in front of Blomstrandbreen and their possible connection across Blomstrandøya.

Push moraines in front of Kongsbreen North are distinct, but discontinuous. As drumlinoid features are also present, either the annual push moraines were created during a previous advance and drumlinized throughout the most recent advance. Or the annual push moraines were formed during the latest retreat by an only partly grounded ice margin. Because the moraines are very well-preserved along the sides but missing in the central part of the fjord, the latter possibility is considered more likely. It was described previously, that the fjord in front of Kongsbreen North is characterized by a fairly deep, elongated basin reaching water depths of 140 m. Moraines only occur

until a water depth of 120 m. With probable subaqueous calving it seems likely that the glacier sole can be "hollowed out" in the deeper fjord, resulting in a partly ungrounded glacier.

The 26 annual push moraines in front of Kongsbreen South occur between the glacier margin and the terminal moraine described in section 4.2 (RC2, see Figure 4.15, Figure 7.13). The latter is located north of the western tip of Colletthøgda (Figure 7.13) and thereby marks the point of confluence between Kronebreen and Kongsbreen South. It is considered likely that Kongsbreen South generated more than 26 annual push moraines during retreat, especially during its presumed surge in 1897 (see section 7.2). But, the later readvance of the Kronebreen / Kongsvegen ice margin probably overrode any such features. Nevertheless, after being connected for most of the recent history (compare Liestøl, 1988 and Figure 7.13) and up until at least 1976 (Hagen et al., 1993), the 26 push moraines may indicate that the southern front of Kongsbreen became separated from Kronebreen in 1984 (26 years before 2010).

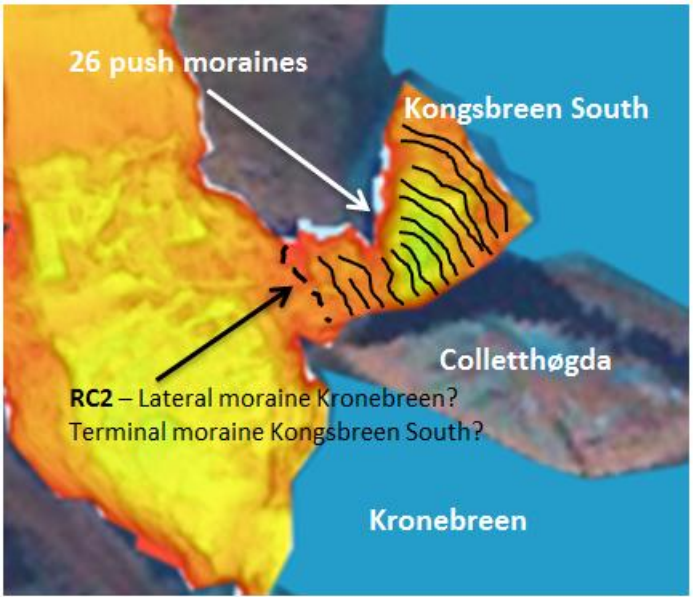

Figure 7.13: Push moraines in front of Kongsbreen South. RC2 is the large transverse ridge found at the mouth of the small outlet (see section 4.2).

Although the small push moraines occur in front of most of the glaciers in Kongsfjorden, they are not always equally well-preserved or equally distinct. However, they are well-developed and spaced fairly regularly in front of Blomstrandbreen, Conwaybreen and Kongsbreen South. Whereas the distance between the terminal moraine in front of Blomstrandbreen deposited in 1960 and the glacier front is approximately 2.6 km, and thus suggests an average annual retreat rate of the grounding line of ~ 52 m, average spacing between the small push moraines in front of Blomstrandbreen suggests a retreat rate of 40 – 60 m a^{-1}. However, the smaller (10 m) and larger spacing between a few individual moraines indicates probable temporal variations in retreat rate.

The push moraines in front of Conwaybreen are well-developed but their distances vary between 20 and 100 m. However, assuming that the 12 most proximal moraines were deposited annually, a tentative retreat rate of 61 m a^{-1} can be calculated. As Conwaybreen has a slightly higher calving volume than Blomstrandbreen (0.029 compared to 0.00137 km^3 a^{-1}, respectively, Blaszczyk et al., 2009), this estimation should be fairly reasonable.

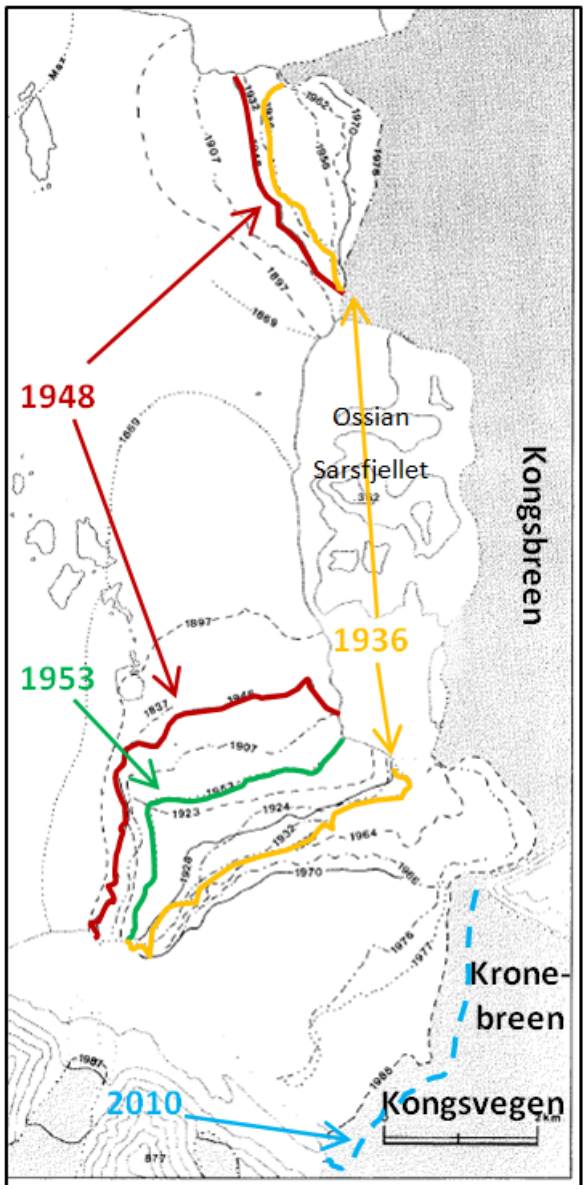

Figure 7.14: Ice front positions for Kongsbreen, Kronebreen and Kongsvegen, inferred from aerial photographs (modified after Liestøl, 1988).

In front of Kongsbreen North the small ridges are not well-developed, mainly because they are missing in the central part of the trough, as explained previously. Some ridges indicate variable retreat rates between 30 and 100 m a^{-1}, which are probably unreliable due to enhanced subaqueous calving in this area. Nevertheless, assuming a constant rate of the grounding line, the distance of roughly 5 km between the surge moraine from 1897 and the ice front yields an average retreat rate of 44 m a^{-1}. Based on a small advance between 1936 and 1948 not only for Kongsbreen South, Kronebreen and Kongsvegen, but also for Kongsbreen North (Liestøl, 1988; Figure 7.14) this rate is most probably unreliable. Based on the distance between the grounding line positions of 1948 and 2010, a more reasonable rate of approximately 57 m a^{-1} was calculated.

The annual push moraines in front of Kongsbreen South are much better developed than for the northern front. They suggest a retreat rate around 130 m a^{-1} in the deeper parts and a decrease to 90 m a^{-1} in the vicinity of the present ice front. This fits well with the results of Benn et al. (2007) and Kehrl et al. (2011) who showed that glaciers tend to stabilize at “pinning points” such as shallow water or fjord narrowings. Aside from the fact that the fjord basin in front of Kongsbreen South becomes increasingly shallower towards the glacier front, the presence of Ossian Sarsfjellet at the eastern side of Kongsfjorden forces both Kongsbreen outlets to be channelled in relatively narrow passages (e.g. Figure 7.1). This could explain the relatively low retreat rate and also the differences between the two ice fronts. Nevertheless, as the fjord in front of Kongsbreen North is much deeper than in the south, theoretically retreat should be even faster than 90 m a^{-1} for the former. This would fit with the higher calving rates reported for Kongsbreen (presumably either 0.0856 or 0.2247 km^3 a^{-1}; Blaszczyk et al., 2009), but does not fit well with the geomorphology. Therefore it is difficult to estimate an accurate retreat rate for Kongsbreen.

Dividing the total distance between the glacier front and the terminal moraine (in the case of Blomstrandbreen) or between the glacier front and the outermost retreat moraine (in the case of Conwaybreen) by the number of years elapsed since deposition seems to yield fairly reasonable results. As there are no annual push moraines in front of Kongsvegen and Kronebreen, a very tentative estimation of the retreat rate can be attempted by employing this method. Considering that a distance of 4.5 km of seafloor has been exposed between the respective terminal moraines from 1948 and the modern ice margin, Kronebreen and Kongsvegen should have retreated with a rate of 73 m a^{-1}. As Kronebreen is considered the fastest-flowing glacier on Svalbard, this rate seems extremely low, especially when compared to the retreat rates suggested in the literature (785 m a^{-1} in the period between 1964 and 1986, Lefauconnier et al., 1994, and 600-800 m a^{-1} between 1999 and 2002, Blaszczyk et al., 2009). Had Kronebreen receded at that rate it should have uncovered between 37 and 50 km of seafloor since 1948. However, a lower rate of 250 m a^{-1} has been implied by Melvold & Hagen (1998) for the time period between 1948 and 1993, which was based on the 4 km of seafloor uncovered since retreat began. This rate still is significantly higher than the one suggested here, but it is possible that once again the assumption of a linear retreat rate underestimates the actual flow velocity. It has been discussed by Kehrl et al. (2011) that the high sedimentation rates in front of the Kronebreen / Kongsvegen margin have a large effect on glacier stability. Because of the relationship between calving rate and water depths, the high sediment input could cause Kronebreen to stabilize and retreat more and more slowly. This could indicate fast retreat directly after the surge but increasingly slower flow over time. However, assuming the retreat rate to be 600 m a^{-1} right after the surge, this would mean that Kronebreen would have reached its present ice front position around 1955 and should have stagnated since then. Even though stabilization effects may be strong, it is considered highly unlikely that the sediment input in front of Kronebreen and Kongsvegen could be high enough to cause the fastest-flowing glacier on Svalbard to suddenly stop retreating. Furthermore the aerial photographs used by Liestøl (1988) show that the ice front in the 1950s was still located close to the maximum position of 1948 (Figure 7.14). Another possibility for the slower retreat rate is that Kronebreen is or has been entering its quiescent phase flow over the recent decades. As mentioned previously, it was discussed by Bennett et al. (1999) whether Kronebreen was of surge-type, because it did not experience quiescent phase flow. Nevertheless, observations made by Voigt (1965) suggested that Kronebreen is of surge-type and that it contributed to an equal part to the surge in 1948, originally only ascribed to Kongsvegen (Liestøl, 1988; Hagen et al., 1993). Although it would be considerably later than usual, it could be that Kronebreen has been experiencing increasingly lower retreat since then as a response to the passive phase of the surge cycle. However, as there is no evidence for that it is impossible to say exactly why Kronebreen has been retreating so slowly.

Kongsvegen on the other hand is classified as one of the slowest glaciers on Svalbard with velocities between 1.4 and 3.6 m a^{-1} (Blasczcyk et al., 2009). The increasing stabilization proposed by Kehrl et al. (2011) should currently decrease this velocity even further. Based on this retreat rate there should be between approximately 90 and 225 m of exposed seafloor (instead of 4500) between the terminal moraine from 1948 and today's ice front. Assuming fast flow of Kronebreen and the intimate connection of the two ice fronts it could be that Kongsvegen was dragged back with Kronebreen after the surge, thereby retreating much faster than its own internal behaviour would have allowed for. The stabilization as a response to the water depth could then account for the very slow retreat rates today. However, as the retreat rate of Kronebreen is so uncertain, this cannot be confirmed.

The push moraines, which have been described as Group 3 ridges (section 4.5) were inferred to be drumlinized push moraines. Assuming each glacier in the area leaves behind a set of transverse recessional moraines according to the number of years it has been retreating, the formation of drumlinized push moraines is inferred to happen as a consequence of a renewed ice advance after the original push moraines' deposition. The fast grounded ice would override the previously created ridges, ripping up parts of the moraines in the movement and redeposit them as small streamlined ridges (drumlinoid features) orientated parallel to the main fjord axis.
This is believed to have happened in front of Kronebreen, Kongsvegen, where a set of chaotically distributed ridges characterize the seafloor. The preferred orientations of the very discontinuous ridges are either perpendicular or parallel to the direction of past ice flow. Perpendicular ridges are interpreted to be parts of larger and smaller recessional moraines produced during a retreat following one of the earlier surges (either Kronebreen in 1869, or Kongsbreen in 1897), whereas the parallel features are believed to be glacial lineations (section 7.2.1). Drumlinization of the features would have happened during the most recent ice advance, when Kongsvegen surged in 1948.

Another possibility could be that the randomly orientated ridges of Group 3 are crevasse-fill-ridges, resulting from the squeezing of soft subglacial sediments into crevasses at the base of the glacier (e.g. Sharp, 1985; Ottesen & Dowdeswell, 2006). Their small heights of some of the ridges and their random orientation would allow for this interpretation, as these characteristics partly fit with observations made for surging glaciers (e.g. Sharp, 1985; Evans & Rea, 1999; Ottesen & Dowdeswell, 2006; Ottesen et al., 2008). Although Kongsvegen has been reported to be smooth without many crevasses, Kronebreen is heavily crevassed from the glacier front until much further inland (Blaszczyk et al., 2009) and could easily produce the ridges. However, the characteristic rhombohedral pattern lacks in Kongsfjorden. Based on this, the varying heights and the orientation of many of the features parallel to past ice flow, it is thought to be more likely, that the small ridges in front of Kongsvegen

and Kronebreen are a mixture of glacial lineations (drumlinoid features) and drumlinized recessional moraines.

7.3 (Post-Surge) Sedimentary Processes

The main sedimentary processes in Kongsfjorden today are unrelated to surges but dependent on glacial activity. These are deposition from sediment-laden meltwater streams entering the fjord at the glacier terminus, and sediment melt-out from icebergs or floes. However, glacimarine environments are characterized by a number of sedimentary processes, which include sedimentation at the contact line between glacier and fjord, sediment input from rivers and the dumping of sediments along the coast line as a result of mass wasting. Sedimentary processes prevailing in a glaciated fjord are summarized in Figure 7.15.

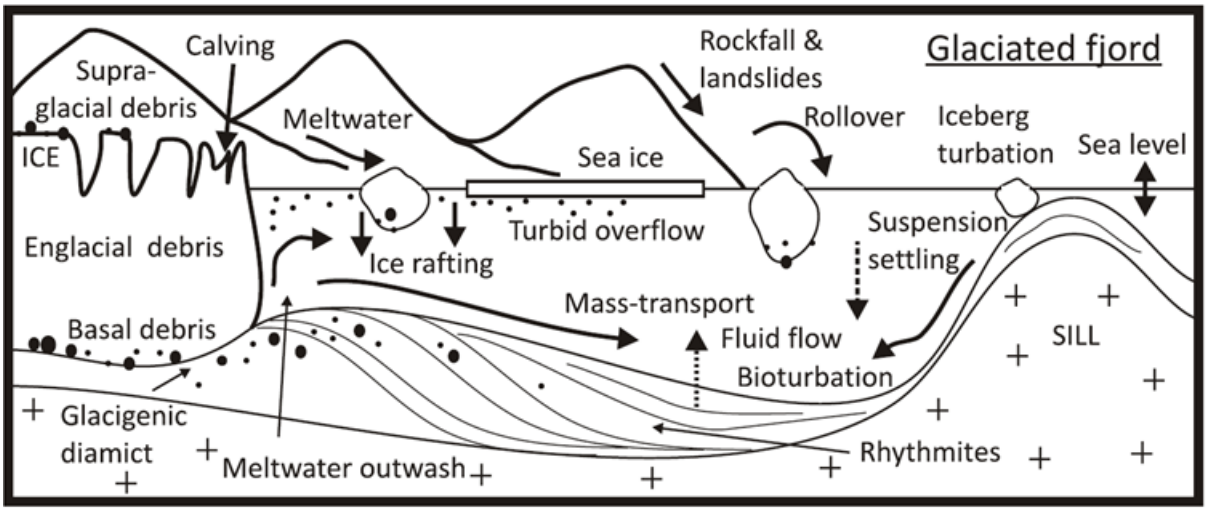

Figure 7.15: Principle processes and deposits of sedimentation in a glacial fjord (Howe et al., 2010).

The importance of the different processes changes with increasing distance from the glacier terminus and will be discussed in the following paragraphs.

7.3.1 Sedimentation at the Glacier Margin

The importance of sedimentary overload at the glacier margin regarding debris lobes and outwash fans has already been discussed in section 7.2.3. As mentioned before, sedimentation can happen at the ice-contact line by several processes, including the settling from rivers or meltwater streams, the squeezing-out of subglacial debris or the melt-out of debris from the glacier front. Furthermore, basal debris is often pushed up and deposited as a ridge (sections 7.2.2, 7.2.4) or transported supraglacially to the edge of the ice cliff and dumped.

7.3.2 Deposition from Meltwater Streams and Rivers

The deposition of sediment transported by meltwater streams is considered the primary source for the finer sediments in glacial fjords (Hoskin et al., 1972). Nevertheless, as meltwater streams can reach considerable flow velocities, the transport of coarser material is also common. When the confined meltwater stream enters the fjord it dramatically slows down. The flow velocity then does not suffice to carry pebbles and sand, causing them to be deposited, often as submarine outwash fans (Boulton, 1990) in front of the glacier (see Figure 5.7). According to Kehrl et al. (2011) around 90 % of the total sediment provided by a glacier is deposited within the first 400 m of the glacier front, causing extremely high sedimentation rates in the proximal areas. With increasing distance from the glacier terminus the meltwater streams will have slowed down to the point, where only suspension load can be transported (Figure 5.7, Figure 7.16). This is why suspension settling is the dominant process in more distal areas (Fig. 7.16). With increasing distance from the glacier more of the fine sediments will have settled from suspension and the meltwater streams lose their sedimentary load. In the areas not reached by the meltwater plumes the meltout of ice-rafted debris dominates, as icebergs and floes can be transported long distances according to wind and water currents (Elverhøi et al., 1980; 1983; Boulton, 1990).

Figure 7.16: Distribution of suspension load in the waters of Kongsfjorden in July 2004. Input is very high close to the glacier margins (mainly Kongsvegen and Kronebreen) and decreases towards the outer fjord (from NASA, Modis Gallery, 2013).

The stratified sediments in the two sediment cores analysed for this thesis are assumed to originate from the “suspension settling zone”. The rain-out of silt and clay from the water column requires little energy, causing the sediments to be deposited in an undisturbed, stratified and controlled fashion. The coarser layers may derive from icebergs or floes depositing their transported debris as they melt.

Similar processes as described for the meltwater streams apply to the sediment input from rivers. Rivers are abundant around Kongsfjorden and may hence reflect an important sediment source.

However, input is restricted to the summer months (June to September), as rivers are frozen in winter (Killingtveit et al., 2003; Plassen et al., 2004).

7.3.3 Ice Rafting

The transport of debris by icebergs and ice floes can be an important sediment source to a fjord. Icebergs incorporate glacial debris and can transport a range of grain sizes that can be deposited in the fjord as a consequence of melt-out, rain-out or the overturning of icebergs dumping the carried material (e.g. Vorren et al., 1983). In fact, icebergs are the most important mechanism bringing coarser sediments into the deep ocean (Dowdeswell et al., 1998). Ice floes usually originate from sea ice breaking up during spring and can transport beach sediments in the case of shore-fast sea ice, or suspended sediments frozen into the ice from the water column (Dowdeswell, 1989; Gilbert, 1990).

Ice rafting can influence the entire fjord from the glacier terminus to the open sea. However, its influence is largely dependent on the availability of icebergs and sea ice, which vary as a consequence of calving intensity of the glaciers and climate or water currents. Debris rafting by icebergs is expected to be small in Kongsfjorden as the calving intensity of the five tidewater glaciers adds up to an estimated 0.35 $km^3 yr^{-1}$ (Blaszczyk et al., 2009) compared to, for example, 15 $km^3 a^{-1}$ for a fjord system in East Greenland (Dowdeswell et al., 1998). Influence is inferred to be greatest in front of Kongsbreen and Kronebreen, which together compensate for 87.8 % of the total calving volume in Kongsfjorden. Nevertheless, relative to the sediment input from meltwater, the effects of ice-rafted debris on the sedimentation in Spitsbergen fjords are very small (Dowdeswell et al., 1998). In inner Kongsfjorden, iceberg rafting contributes to the sedimentary environment with a deposition rate of 5 to 8 mm a^{-1} (Dowdeswell et al., 1992).

The influence of ice-rafting on sedimentation increases away from the glacier margin (Boulton, 1990). This is mainly due to the fact that in more proximal areas other processes (e.g. suspension settling from rivers and glacial meltwater) overshadow the comparably small input of ice-rafted debris (IRD, e.g. Dowdeswell & Dowdeswell, 1989; Plassen et al., 2004). This is consistent with the lithological data described in chapter 5: Coarser layers representing IRD may occur, but are rare in comparison to the stratified glacimarine muds derived from suspension settling.

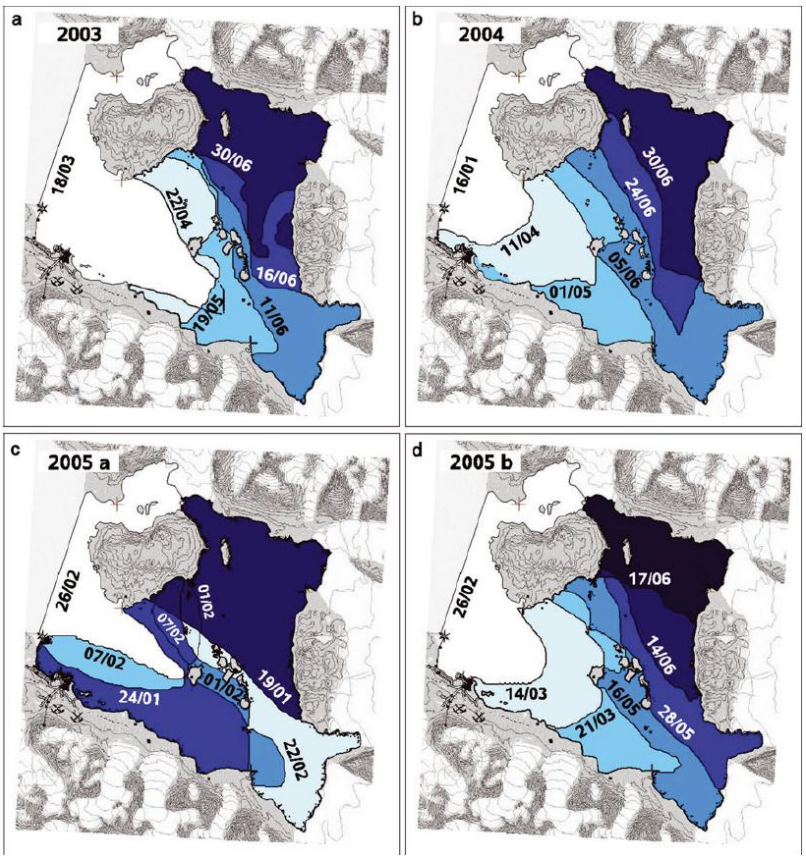

Figure 7.17: Sea ice extent in Kongsfjorden for 2003, 2004 and 2005. Dates are given in day/month (Gerland & Renner, 2007).

Based on the well-developed annual push moraines deposited in front of Blomstrandbreen, it is considered probable that sea ice is common in Kongsfjorden. This is in accordance with Svendsen et al. (2002) who regarded the lack of sea ice during winter and spring to be an "exceptional case" for Kongsfjorden. Furthermore Gerland & Renner (2007) documented that the inner part of Kongsfjorden is normally covered by shore-fast sea ice, which is < 1 m thick and forms in winter (December to March). Due to changing climatic conditions and the prevuiously mentioned highly variable inflow of Atlantic Water (e.g. Cottier et al., 2007; Jernas et al., in prep.) the formation of sea ice is subject to interannual variability. Nevertheless observations have shown that the sea ice extent is usually very similar for early May (Figure 7.17; e.g. Gerland & Hall, 2006; Gerland & Renner, 2007). This is partly due to the coastline of and islands in Kongsfjorden, which favour the formation of sea ice in the protected inner basin (Gerland & Renner, 2007). However, again, the input of ice-rafted debris is considered to be small in comparison to the meltwater concentrations close to the ice margins.

7.3.4 Accumulation Rates

As meltwater plumes are the primary source for the sediments supplied to Kongsfjorden, accumulation rates are particularly high close to the ice margin. Elverhøi et al. (1983), Trusel et al. (2010), and Kehrl et al. (2011) determined sedimentation rates of 100 mm a^{-1}, > 0.6 m a^{-1}, and > 1 m a^{-1}, respectively, directly in front of Kongsvegen / Kronebreen. Accumulation rates may vary over time, because the input of meltwater depends on a glacier's hydrology, which, in turn, may change as a response to different parameters (e.g. climate, sliding velocity etc.). However, even though this could explain the very different rates found in the literature, it is more likely that results vary as a

consequence of different measuring techniques, different locations etc. (Kehrl et al., 2011). A meltwater plume exiting the glacier at the terminus, for example, may change its location frequently in response to wind or the Coriolis effect (Forwick et al., 2010), which may drastically change sedimentation rates from one location.

Accumulation rates decrease significantly away from the glacier margin. As mentioned before suspension settling is the main mechanism in more distal areas and contributes to the sediments in the fjord with a rate of 55 mm a^{-1} 10 km away from the Kongsvegen / Kronebreen margin (Elverhøi et al., 1983). In the outer fjords accumulation rates are lowest (0.4 mm a^{-1}, Elverhøi et al., 1983).

As rates of accumulation for Kongsfjorden are debated, additional accumulation rates are suggested here based on calculations from the acoustic and lithological data.

As shown in chapters 5 and 6 the lowermost 76 cm of the sediment core 10JM-GlaciBar-GC01 represent a debris lobe inferred to be deposited during the surge of 1948. Based on the assumption that the uppermost limit of the lobe was 62 years old in 2010 and that it is covered by a sediment thickness of approximately 2.25 m (calculated from 3 ms reflection thickness and an average p-wave velocity of 1497.86 m s^{-1}), at 7.2 km from the glacier margin the sedimentation rate would be 36.24 mm a^{-1} (33.87 mm a^{-1} with the sediment cover of 2.1 m derived from the core log). This is much lower than originally proposed by Elverhøi et al. (1983). However, as their accumulation rates were determined in 1983, the glacier front was presumably further inside the fjord than in 2010. This means, that at a distance of 10 km away from the ice margin, the higher accumulation rate could have been influenced by additional sediment input from Kongsbreen North and Conwaybreen. This is based on the fact that the terminal moraine of Kongsbreen North was only at a distance of 11 km from Kongsvegen and Kronebreen in 2010.

The debris blocks at a distance of 10 km are covered by 7 ms thick laminated reflections. Using the same p-wave velocity as before, this yields a sediment thickness of 5.24 m. If the blocks really were generated during a landslide in 1869, the 5.24 m should respond to an accumulation rate of 37.18 mm a^{-1}. This indicates an increase of accumulation rate between at least 7.2 and roughly 10 km away from Kronebreen and Kongsvegen, which should confirm the additional input of Conwaybreen and or Kongsbreen North.

Approximately 500 m off the margins of Kronebreen and Kongsvegen the laminated reflections are between 4 and 6 ms thick. Calculated on a base of 62 years the sedimentation rate would be between 48.32 and 72.48 mm a^{-1}. However, as areas so close to the glacier were probably only exposed recently, it is likely that the sediments only accumulated a few years ago. If the retreat rate of 600 m a^{-1} suggested by Blaszczyk et al. (2009) is true, it would mean that the approximately 7.5 m of sediment (4 - 6 ms) accumulated in less than a year. This is considered highly unlikely, as even the

most recent studies by Kehrl et al. (2011) revealed much lower accumulation rates (> 1 m a^{-1}). This, together with the much lower retreat rate calculated from the distance between the 1948 surge moraine and the present position of the glacier terminus strongly suggests that the retreat rate of Kronebreen is much lower than 600 m a^{-1}.

As all calculations in this section are based on acoustic data and the lithological boundary between the mass-transport deposit and the laminated sediments is not entirely clear (see chapter 5), the accumulation rates may not be very exact. However, they serve as a rough estimate and confirm that even 10 km from the ice margin suspension settling may still be effective (see also Figure 7.16).

7.3.5 Sediment Distribution

As discussed in the previous paragraphs sediment distribution may be influenced by a number of factors. Particularly thick sediments may be found close to the ice margins where sediment input and accumulation rates are high, and in basins, whereas thinner deposits should be expected towards the distal regions and / or in shallower areas (Forwick et al., 2010; Forwick & Vorren, 2010). However, based on the different processes contributing to the sedimentation in Kongsfjorden, sediment distribution may not be as straight-forward. Firstly, sediments may be redistributed after initial deposition by mass-transport events (along-slope transport of coarse and fine sediments, section 7.3.6, below), geostrophic currents (along-slope transport of fine sediments with velocities < 10 cm s^{-1}, Svendsen et al., 2002), or iceberg-ploughing (coarse and fine sediments, section 7.3.8, below). Secondly, wave and wind energy during spring and summer may lead to the reworking of sediments in shallow waters (Howe et al., 2003). Thirdly, fjord morphology may favour or influence the distribution of sedimentation (i.e. ridges / basins, e.g. Forwick & Vorren, 2010). And finally, the Coriolis Effect may lead to the redeposition of sediments (e.g. Vorren & Plassen, 2002). As all movement is deflected to the right in the northern hemisphere, the inflow of Atlantic Water will be encouraged along the southern coast of Kongsfjorden, possibly eroding the local sediments. The outflow of sediment-laden waters (as a result of glacimarine sedimentation and possibly erosion) on the other hand would follow the northern shore leading to thicker sediments along that side of the fjord (see also Howe et al., 2003).

7.3.6 Mass Wasting

As discussed previously mass-transport events are triggered by slope failure as a response to increased sediment input, earthquakes, or increased pore pressures (Forwick & Vorren, 2007). Mass wasting can rework more than 50 % of the sediments in some fjords (e.g. Holtedahl, 1975, Forwick & Vorren, 2002; 2011). As shown in Figure 7.15, mass wasting along the steep fjord walls may locally increase the sediment input, when coastal sediments are dumped into the fjord as a result of e.g. a

landslide. This process may favour thicker sediments along the coast. Furthermore, the debris lobes discussed in sections 4.3 and 7.2.3 lead to sediment thickening along the distal flanks of the terminal moraines. Depending on the sloping of the local bathymetry a triggering of a mass-transport event is also possible in distal areas. This may be as a consequence of the steady sediment input on top of a very pointy ridge, for example, where a mass flow is triggered when the angle of slope stability is exceeded. This process also favours thicker sediments in basins and channels, and thinner sediments on ridge crests, which is confirmed by the acoustic data shown in this thesis (e.g. Figure 4.14 A, B, C; Forwick & Vorren, 2011).

7.3.7 Consolidation and Dewatering

Depending on sediment load and quality, sediments may consolidate after deposition as a result of increased burial. Sediments with very high permeabilities may incorporate large amounts of water, which will be forced out of the sediments during consolidation (Boulton, 1996; Kristensen et al., 2009). The escaped water will most likely follow gravity and flow along the surface of these sediments, which can lead to the incision of channels (see section 4.3). Furthermore, pockmarks can result from the dewatering of the sediments, i.e. the migration of pore fluids (Ottesen et al., 2008; Forwick et al., 2009). Mass transport deposits are deposited under high energy conditions and are often unsorted with high permeabilities, which makes the occurrence of pockmarks especially likely along the fjord walls and on the debris lobes deposited at the foot of the terminal moraines (see section 4.6 and Figure 7.2). Even though the distribution of pockmarks can be controlled by other factors (i.e. lithological boundaries, underlying permeable bedrock, tectonic lineaments, and buried channels (Forwick et al., 2009 and references therein), the distribution of pockmarks in Kongsfjorden is believed to be mainly controlled by the occurrence of mass-transport deposits. Furthermore, the dewatering of those sediments is assumed to be the main formation mechanism, although pockmarks may also result from e.g. earthquakes and tsunamis. This is based on the studies of pockmarks in other Spitsbergen fjords (e.g. Ottesen et al., 2008; Forwick et al., 2009).

As the formation of pockmarks can happen slowly or rapidly (Forwick et al., 2009 and references therein), it is difficult to date such processes. The pockmarks generated in Kongsfjorden can hence have been generated immediately after deposition or years later and cannot be clearly identified as the youngest features in the landform model (Figure 7.2).

7.3.8 Iceberg Ploughing

Redistribution of sediments can also happen by grounded keels of icebergs, ploughing the sediment along the seafloor (Dowdeswell & Forsberg, 1992). This effect is believed to be negligible in Kongsfjorden, though, as water depths are rarely below 40 m, a depth which Dowdeswell & Forsberg (1992) defined to be the limit for iceberg ploughing in the study area. This was based on the

observation that the keels of icebergs in Kongsfjorden are not large enough to cut into seafloor deeper than 40 m. This was confirmed by Howe et al. (2003), who found that especially the Kongsvegen / Kronebreen glaciers, which are only 20 m high, cannot calve off icebergs large enough to scour the seafloor.

7.4 Landform Models – A Comparison

Different types of models have been proposed to generalize the glacigenic landforms at a glacier terminus and / or the processes creating them (e.g. Sharp et al., 1985; Solheim, 1991; Evans et al., 1999; 2009; Evans & Rea, 1999; 2003; Evans & Twigg, 2002; Ottesen & Dowdeswell, 2006; Ottesen et al., 2008). Models similar to the one described above were developed by Evans & Twigg (2002) for temperate glaciers in Iceland, by Evans & Rea (1999; 2003) for surging glaciers in Iceland, by Ottesen & Dowdeswell (2006) and Ottesen et al. (2008) for tidewater glaciers on Svalbard, most of surge-type, and by Ó Cofaigh et al. (2008), Ottesen & Dowdeswell (2009), and Andreassen et al. (subm.) for fast-flowing ice streams. As all models are partly applicable to Kongsfjorden, a selection will be introduced here and compared with the model suggested for Kongsfjorden (Figure 7.2).

7.4.1 Models for Surge-Type Glacier Landform Assemblages – Submarine Setting

The model developed by Ottesen et al. (2008) for tidewater glaciers surging into Van Keulenfjorden and Rindersbukta on Svalbard (Figure 7.18) was presented and described shortly in section 1.3.2. Another model was suggested by Ottesen & Dowdeswell (2006) for three tidewater glaciers

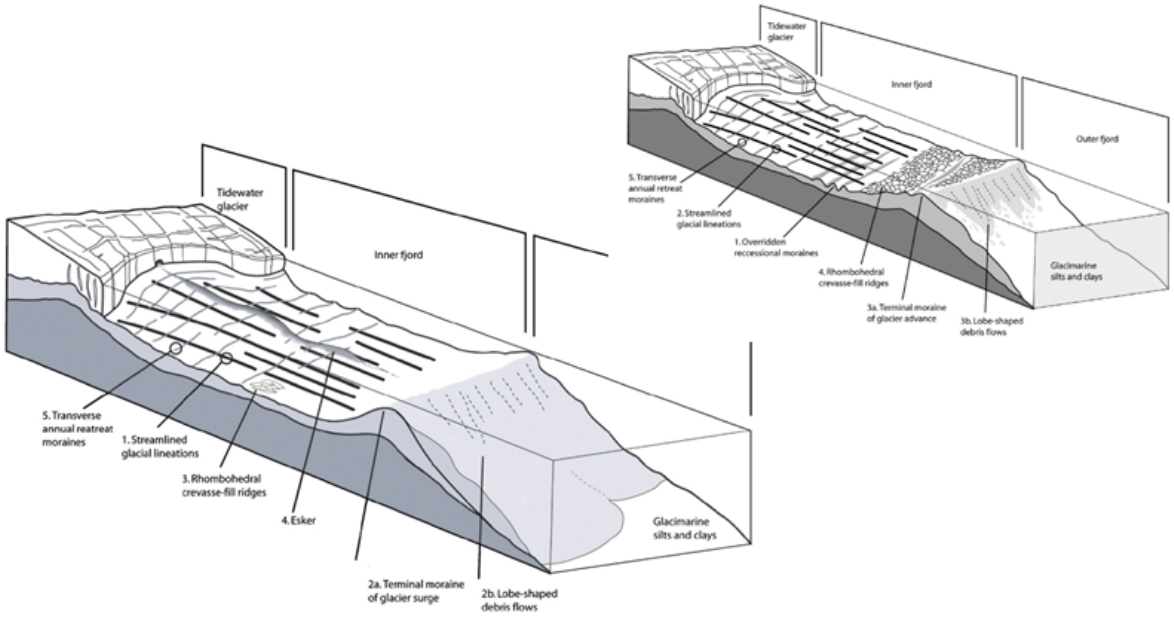

Figure 7.18: Models proposed for the landform assemblages of (surging) tidewater glaciers in Spitsbergen fjords (Ottesen & Dowdeswell, 2006; Ottesen et al., 2008).

terminating into Isfjorden (Borebukta and Yoldiabukta), Svalbard, two of which are recorded to have surged (Figure 7.18). The observations in the latter study area fit well with the landforms recorded for Austfonna on Nordaustlandet, NE-Svalbard (Ottesen & Dowdeswell, 2006).

The main difference between the two models is the occurrence of eskers and the spatially limited distribution of rhombohedral ridges in the surge-type model from Van Keulenfjorden and Rindersbukta. The eskers are larger with heights between 5 and 40 m in Rindersbukta and Van Keulenfjorden, where they are also more common than in Isfjorden. On the contrary the data from Borebukta only showed one small esker with a height < 20 m. Rhombohedral ridges inferred to be crevasse-fill ridges are limited to a small area of < 0.5 km² in Van Keulenfjorden and Rinderbukta, but present across extensive areas in both, Borebukta and Yoldiabukta.

All study areas revealed at least one terminal moraine per glacier marking the maximum ice extent during the LIA or a surge. A lobe-shaped debris flow indicative of a mass-transport event was found on each of these terminal moraines. Furthermore, streamlined glacial lineations extend over distances of several kilometres and are inferred to be indicative of fast-flowing ice. Transverse retreat moraines are regularly spaced and interpreted to be generated annually during small winter readvances of the glacier terminus. They extend between the terminal moraines and the modern glacier front. Even though the features displayed in the surge-type model can be found in front of many surging glaciers on Svalbard, it has been discussed by Ottesen & Dowdeswell (2006) that the only landforms characteristic of surge-activity may be the rhombohedral crevasse-fill ridges, generated by the squeezing of soft sediments into the abundant crevasses at the base of the glacier (Van der Veen, 1998). This was based on the fact that terminal moraines, debris lobes, glacial lineations and annual retreat moraines have also been reported for non-surge type glaciers (Ottesen & Dowdeswell, 2006).

7.4.2 Models for Surge-Type Glacier Landform Assemblages – Terrestrial Setting

Similar to the models proposed by Ottesen & Dowdeswell (2006) and Ottesen et al. (2008), Evans & Rea (1999; 2003) refined a landform model for surging glaciers in terrestrial settings, which was originally proposed by Sharp (1985; Figure 7.19). High-energy reworking often modifies the deposited landforms in terrestrial settings, causing a variety of features.

The outer zone of the landform assemblage in front of terrestrial surge-type glaciers is characterized by a thrust-block moraine, inferred to be generated from the excavation and push-up of proglacial sediments into composite ridges, and a proglacial outwash fan derived from glacifluvial processes (Figure 7.19; e.g. Boulton, 1986; Boulton et al., 1999). The intermediate zone contains hummocky moraines (Figure 7.19). Crevasse-fill ridges, flutings or lineations, and eskers characterize the inner

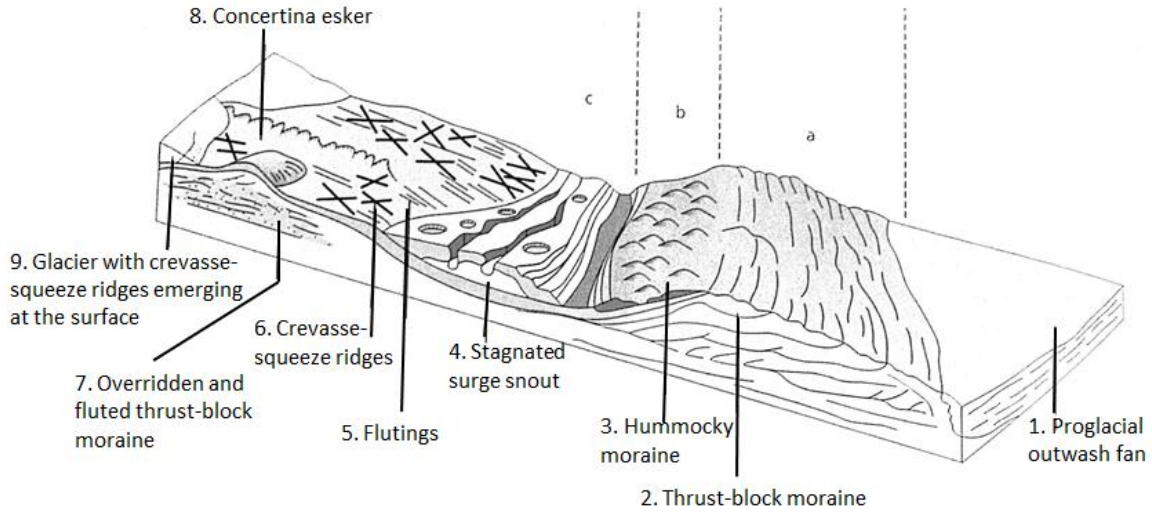

Figure 7.19: Conceptual model for surging glaciers in terrestrial settings. A) Outer zone of proglacially thrust pre-surge sediment, which may grade into small push moraines in areas of thin sediment cover. B) Zone of weakly developed chaotic hummocky moraine located on the down-ice sides of topographic depressions. C) Zone of flutings, crevasse squeeze ridges and concertina eskers (modified from Benn & Evans, 2010; based on Evans & Rea, 1999; 2003).

zone, but overridden thrust-block moraines and a stagnated surge snout, which is covered by pitted and channelled outwash may also occur (Fig. 4.18).

7.4.3 Models for Landform Assemblages Produced by (Fast-Flowing) Ice Streams

The model proposed by Ottesen & Dowdeswell (2009) for the landforms formed by fast-flowing ice streams (Figure 7.20) is very similar to other models (e.g. Ó Cofaigh et al., 2008; Andreassen et al., subm.). All landform assemblages include the formation of mega-scale glacial lineations, glacigenic debris flows, grounding-zone wedges, and small transverse ridges, although Ó Cofaigh et al. (2008) suggested a dependence of the latter two on the velocity of retreat. Rapid retreat would not form grounding-zone wedges or annual push moraines, which were inferred to be a product of slow recession. Furthermore, Ottesen et al. (2009) suggests the occurrence of lateral moraines, larger transverse ridges, and iceberg ploughmarks (Figure 7.20). Andreassen et al. (subm.) confirm the iceberg ploughmarks and report the

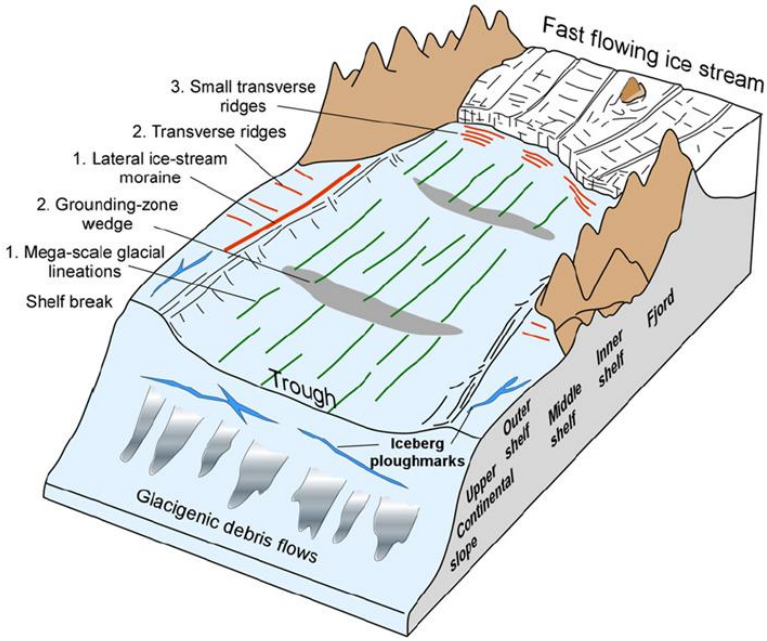

Figure 7.20: Model for the landform assemblage produced by fast-flowing ice streams (Ingólfsson& Landvik, 2013, modified from Ottesen& Dowdeswell, 2009).

occurrence of rhombohedral crevasse-squeeze ridges. The differences may mainly occur from the different study areas. While Ó Cofaigh et al. (2008) focussed on Antarctic ice streams, Ottesen et al. (2009) and Andreassen et al. (subm.) described landforms from ice streams draining the Barents Sea Ice Sheet during the Late Weichselian.

7.4.4 Comparison

All models described above are partly applicable to Kongsfjorden. The models describing the landform assemblages inferred to be typical of glacier surges (Evans & Rea, 1999; 2003; Ottesen & Dowdeswell, 2006; Ottesen et al., 2008; sections 7.4.1 and 7.4.2) are very similar to the model proposed for the glacier-proximal regions of inner Kongsfjorden. The outer fjord on the other hand is characterized by mega-scale glacial lineations (section 4.1), which are believed to originate from the glaciation period, when a fast-flowing ice stream modified the soft, subglacial sediments accordingly. For this part of the fjord, the ice-stream model presented in section 7.4.3 (Ottesen & Dowdeswell, 2009) is more applicable.

The main differences between terrestrial and submarine settings are 1) the lack of high-energy reworking of previously deposited landforms, and 2) the occurrence of annual retreat moraines in submarine settings. The former leads to a generally better preservation of submarine features (e.g. Ottesen & Dowdeswell, 2006). The latter is absent in terrestrial environments as a consequence of in-situ downwasting of the stagnating glacier tongues (Benn & Evans, 2010). Apart from these two main differences both models are fairly similar with the occurrence of an outermost push moraine and outwash fan, and crevasse-fill-ridges, glacial lineations, and eskers in the inner zone (Evans & Rea, 1999; 2003; Ottesen & Dowdeswell, 2006; 2008). The model proposed for Kongsfjorden (Figure 7.2) represents very well the main similarities between the two settings. Terminal thrust moraines and outwash fans mark the outer fjord in the Kongsfjorden model as well as in the two others. Furthermore, annual push moraines are indicative of the submarine setting in the inner fjord. Glacial lineations in Kongsfjorden are of two types, with Type-I reflected by the submarine landform model (Ottesen & Dowdeswell, 2006; Ottesen et al., 2008). Type-II glacial lineations occurring in Kongsfjorden have not been reported from other Spitsbergen fjords. Neither do they appear in landform models for surging glaciers on land. However, as derived in section 7.2.1, they are thought to be formed by the repeated advances and retreats of the glacier front as a result of several surge events, which deform the original landforms into glacial lineations. This may be comparable to the overridden and fluted thrust moraines appearing in terrestrial settings (Evans & Rea, 1999; 2003). The buried thrust moraine included in the landform assemblage of terrestrial glacier surges is believed to reflect the overridden and buried terminal moraine described for Kongsvegen / Kronebreen (Figure 7.2 (1); sections 4.4; 7.2.2). Peculiarly, rhombohedral crevasse-fill ridges and

eskers found in the two other models are absent in Kongsfjorden. As both features are the product of sediment being squeezed into glacial cavities, it is assumed, that the pressure was not high enough to fill the cavities, or that sediment was not soft enough. Like other surging glaciers Kronebreen, Kongsbreen, and Blomstrandbreen have been recorded to be heavily crevassed in their terminal zone (Blaszczyk et al., 2009), which is why the absence of crevasse-fill ridges cannot be explained by a lack of cavities either. It may be possible that either there was not sufficient coarse sediment within the conduits to allow deposition or that the pressure was too high, so that all the sediment was transported out of the conduit. However, as glacier beds are generally inaccessible, it is not possible to define an unambiguous solution.

Since the occurrence of crevasse-fill ridges has been suggested to be the only characteristic for a surge-type glacier landform assemblage (Sharp, 1985b; Van der Veen, 1998; Ottesen & Dowdeswell, 2006) it could be argued, that contrary to common belief none of the tidewater glaciers around Kongsfjorden are actually of surge-type. Because terminal moraines, debris lobes, glacial lineations, and annual push moraines have been documented for non-surge type glaciers as well, it is possible that the terminal moraines in Kongsfjorden merely represent the maximum ice extent of each glacier during the Little Ice Age. This is considered unlikely, however, as Hagen et al. (1993) defined the surge years based on aerial photography showing the glacier front positions during respective years. Thus derived ice front positions (Liestøl, 1988) clearly indicate an advance of Kongsbreen, Kronebreen, and Kongsvegen between 1936 and 1948 and of Blomstrandbreen between 1956 and 1966 (Figure 7.14). If the tentative line representing the Kongsvegen / Kronebreen / Kongsbreen South extent of 1837 is true, another advance can be inferred for the glacier complex between 1837 and 1869. Such glacier behaviour cannot be explained by a single advance during the LIA, mainly because this cold period influenced Svalbard much earlier than the registered surge-related advances (at least for most glaciers), and because retreat should have happened constantly in that case.

Including the work of Howe et al. (2003), Ottesen et al. (2007) and MacLachlan et al. (2010) it can be shown that almost all of the features proposed by Ottesen & Dowdeswell (2009) for the ice-stream model occur in outer Kongsfjorden (Figure 7.21). The terminal and lateral moraines, the mega-scale glacial lineations, the grounding-zone wedge, and the transverse retreat ridges are all indicative of a fast-flowing ice stream (Ottesen & Dowdeswell, 2009). The relict subglacial crag and tail ridges and glacial channels (Figure 7.21; Howe et al., 2003; MacLachlan et al., 2010) are not part of the model but are also inferred to be indicative of the past glaciation of the outer fjord. This confirms the assumption that landforms in the outer fjord were formed during the Late Weichselian as a result of a fast-flowing ice stream draining through Kongsfjorden, whereas the ice-proximal features are the result of local glacial activity and ice front oscillations.

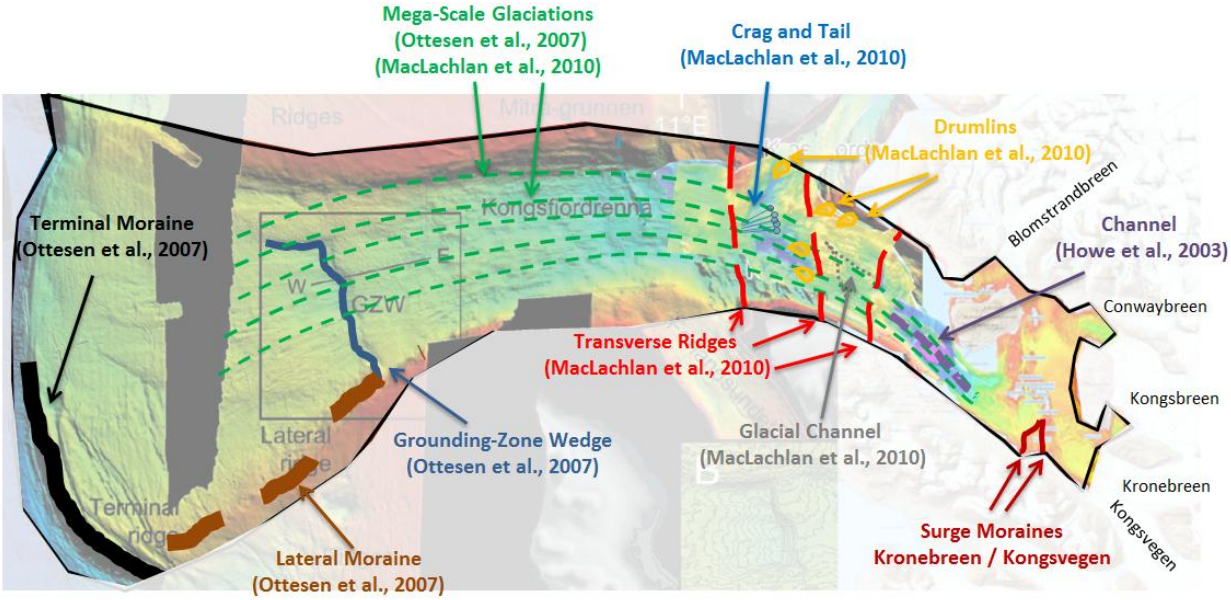

Figure 7.21: Compilation of the bathymetry and landforms reported from inner and outer Kongsfjorden, including Kongsfjordrenna (modified after Howe et al., 2003; Ottesen et al., 2007; MacLachlan et al., 2010).

8. Summary and Conclusions

With the purpose of reconstructing the glacial activity in inner Kongsfjorden, analyses of swath bathymetry, chirp profiles and sediment cores were integrated to map glacigenic landforms and to study the sedimentary processes in the study area. The main conclusions are:

- Kongsfjorden shows a characteristic landform assemblage that served as a good base to develop a conceptual model.
- The landform assemblage in Kongsfjorden includes glacial lineations of two types: 1) groove-ridge features, which are inferred to be created when soft basal sediments are deformed as a consequence of a rapidly advancing glacier, and 2) Glacier readvances may lead to the deformation of previous landforms, creating small, drumlinoid ridges aligned parallel to the past-ice flow direction. Large transverse ridges mark the maximum extent during a surge event. The distal flanks of these terminal moraines are characterized by the occurrence of lobe-shaped debris flows, deposited from a mass –transport event. The latter is inferred to be triggered by the increased sedimentary load to the glacier front when the ice advance stopped and the glacier stagnated. During retreat after a surge some of the Kongsfjorden glaciers deposited small push moraines, interpreted to indicate minor annual readvances during winter.
- The groove-ridge glacial lineations, the terminal moraines with their debris lobes, and the annual push moraines are very similar to landform assemblages documented for surging glaciers in submarine settings, especially in Spitsbergen fjords. The absence of eskers and crevasse-fill ridges is the main difference. Although annual push moraines and the groove-ridge features are lacking in the terrestrial environment, the terminal moraines and debris lobes also occur on land. Drumlinized push moraines may be comparable to overridden and fluted thrust moraines from terrestrial settings, but have not been reported for tidewater glaciers.
- Today, glacial activity in Kongsfjorden is generally decreasing. However, the landforms in inner Kongsfjorden are the products of recent glacial activity, and most of them formed during the last 150 years as a consequence of climatically-independent rapid advances of the tidewater glaciers (surges).
- The acoustic data confirms a surge of Blomstrandbreen in 1960, as well as surges of Kronebreen and Kongsvegen in 1869 and 1948, respectively. As the two latter glaciers share an ice margin, a surge from one of the two triggered a geometrical response of the other, leading to a simultaneous advance.

- In addition to two terminal moraines indicating the maximum ice advance of Kronebreen and Kongsvegen during the 1869 and the 1948 surges, a third terminal moraine is inferred to reflect the maximum extent of Kongsbreen after a surge in 1897. This may indicate that Kongsbreen, currently regarded as a non-surge type glacier (Hagen et al., 1993) is, in fact, of surge-type.
- A debris lobe 7 km from the Kronebreen / Kongsvegen ice margin comprises reworked glacimarine sediments that were bulldozed and / or remoulded by the surging Kongsvegen. The lobe was deposited in or shortly after 1948 and is composed of a massive silty-clayey matrix with clasts.
- The absence of iceberg ploughmarks in the entire study area suggests iceberg keels to be shallower than 40 m for all of the five tidewater glaciers calving into Kongsfjorden.
- Post-surge sedimentary processes include sediment settling from turbid waters emanating from subglacial meltwater channels. Sedimentation rates are highest close to the glacier front. Suspension settling is the dominant process in the inner fjord and leads to the deposition of finely stratified glacimarine mud. During spring and summer temperatures may also permit sediment supply from rivers. Mass-wasting and bottom currents may lead to along-slope redistribution of already deposited sediments. Iceberg rafting becomes more important towards the outer fjord.
- Sediment input into the inner fjord basin is dominated by two glaciers: Kongsvegen and Kronebreen. Whereas sediments emanating from Kongsvegen are characterized by relatively high Ca-contents, sediments deriving from Kronebreen have higher Fe-contents. Fluctuations of these element contents within the sediment column are suggested to reflect temporal variations in sediment supply from the glaciers to the fjord.
- Pockmarks are abundant in Kongsfjorden and are mostly associated with rapid dewatering of mass-transport deposits.

References

Alley, R., Blankenship, D., Bentley, C., & Rooney, S. (1989). Till beneath ice stream B, 4. Till deformation: evidence and implications. *Journal of Geophysical Research, 92*, 8921–8929.

Andreassen, K., Nilssen, E., & Ødegaard, C. (2007). Analysis of shallow gas and fluid migration within the Plio-Pleistocene sedimentary succession of the SW Barents Sea continental margin using 3D seismic data. *Geo-Mar Lett, 27*, 155-171.

Andreassen, K., Winsborrow, M., Bjarnadóttir, L., & Rüther, D. (subm.). Landform assemblage from the collapse of the Bjørnøyrenna Palaeoice.

Baeten, N., Forwick, M., Vogt, C., & Vorren, T. (2010). Late Weichselian and Holocene sedimentary environments and glacial activity in Billefjorden, Svalbard. *Fjord Systems and Archives, 344*, 207-223. (J. Howe, W. Austin, M. Forwick, & M. Paetzel, Eds.) Geological Society London, Special Publications.

Benn, D., & Clapperton, C. (2000). Pleistocene glacitectonic landforms and sediments around central Magellan Strait, southernmost Chile: evidence for fast outlet glaciers with cold-based margins. *Quaternary Science Reviews, 19*(6), 591-612.

Benn, D., & Evans, D. (2010). *Glaciers and Glaciation* (2 ed.). London: Hodder Education.

Benn, D., Warren, C., & Mottram, R. (2007). Calving processes and the dynamics of calving glaciers. *Earth-Science Reviews*(3-4), pp. 143-179.

Bennett, M. (2001). The morphology, structural evolution and significance of push moraines. *Earth-Science Reviews*(53), pp. 197-236.

Bennett, M., Hambrey, M., Huddart, D., & Ghienne, J. (1996). The formation of a geometrical ridge network by the surge-type glacier Kongsvegen, Svalbard. *Journal of Quaternary Science*(11), pp. 437-449.

Bennett, M., Hambrey, M., Huddart, D., & Glasser, N. &. (1999). The landform and sediment assemblage produced by a tidewater glacier surge in Kongsfjorden, Svalbard. *Quaternary Science Reviews, 18*, 1213-1246.

Bergh, S., Maher, H., & Braathen, A. (2000). Tertiary divergent thrust directions from partitioned transpression, Brøggerhalvøya, Spitsbergen. *Norsk Geologisk Tidsskrift*(80), pp. 63-82.

Birks, H., Paus, A., Svendsen, J., Alm, T., Mangerud, J., & Landvik, J. (1994). Late Weichselian environmental change in Norway, including Svalbard. *Journal of Quaternary Science, 9*(2), 133-145.

Björnsson, H., Pálsson, F., Sigurðsson, O., & Flowers, G. (2003). Surges of glaciers in Iceland. *Annals of Glaciology, 36*(1), 82-90.

Blaszczyk, M., Jania, J., & Hagen, J. (2009). Tidewater glaciers of Svalbard: recent changes and estimates of calving fluxes. *Polish Polar Research, 30*(2), 85-182.

Blatter, H., & Hutter, K. (1991). Polythermal conditions in arctic glaciers. *Journal of Glaciology, 37*, 261-269.

Boulton, G. (1976). The Origin of glacially-fluted surfaces: observations and theory. *Journal of Glaciology, 17*, 287-301.

Boulton, G. (1979). Glacial history of the Spitsbergen archipelago and the problem of a Barents Sea ice sheet. *Boreas, 8*(1), 31-57.

Boulton, G. (1986). Push-Moraines and Glacier-Contact Fans in Marine and Terrestrial Environments. *Sedimentology*(33), pp. 667-698.

Boulton, G. (1990). Sedimentary and sea level changes during glacial cycles and their control on glacimarine facies architecture. *Glacimarine Environments: Processes and Sediments, 53*, 15-52. (J. Dowdeswell, & J. Scourse, Eds.) Geological Society Special Publication.

Boulton, G., Smith, G., Jones, A., & Newsome, J. (1985). Glacial geology and glaciology of the last mid-latitude ice sheets. *Journal of the Geological Society, London, 142*, 447-474.

Boulton, G., Van Der Meer, J., Beets, D., Hart, J., & Ruegg, G. (1999). The sedimentary and structural evolution of a recent push moraine complex: Holmstrømbreen, Spitsbergen. *Quaternary Science Reviews, 18*, 339-371.

Boulton, G., Van Der Meer, J., Hart, J., Beets, D., Ruegg, G., Van Der Watern, F., et al. (1996). Till and Moraine Emplacement in a Deforming Bed Surge - an Example from a Marine Environment. *Quaternary Science Reviews*(15), pp. 961-987.

Chapman, W., & Walsh, J. (1993). Recent variations of sea ice and air temperature in high latitudes. *Bulletin American Meteorological Society*, 33-47.

Clark, C. (1993). Mega-scale glacial lineations and cross-cutting ice-flow landforms. *Earth Surface Processes and Landforms*(1), pp. 1-29.

Clark, C. D. (1994). Large-scale ice-moulding: A discussion of genesis and glaciological significance. *Sed. Geol, 91*, 253-268.

Clark, C., Tulaczyk, S., Stokes, C., & Canals, M. (2003). A groove-ploughing theory for the production of mega-scale glacial lineations, and implications for ice-stream mechanics. *Journal of Glaciology, 49*(165), 240-256.

Cottier, F., Nilsen, F., Inall, M., Gerland, S., Tverberg, V., & Svendsen, H. (2007). Wintertime warming of an Arctic shelf in response to large-scale atmospheric. *Geophysical Research Letters, 34*.

Cottier, F., Nilsen, F., Skogseth, R., Tverberg, V., Skardhamar, J., & Svendsen, H. (2010). Arctid fjords: a review of the oceanographic environment and dominant physical processes. *Geological Society London, Special Publications, 344*, 35-50.

Dallmann, W., Ohta, Y., Elvevold, S., & Blomeier, D. (2002). Bedrock map of Svalbard and. *Norsk Polarinstitutt Temakart No. 33*.

Dowdeswell, J. (1989). On the nature of Svalbard icebergs. *Journal of Glaciology*(35), pp. 224-234.

Dowdeswell, J., & Dowdeswell, E. (1989). Debris in icebergs and rates of glaci-marine sedimentation: Observations from Spitsbergen and a simple model. *The Journal of Geology, 97*(2), 221-231.

Dowdeswell, J., & Forsberg, C. (1992). The size and frequency of icebergs and bergy bits derived from tidewater glaciers in Kongsfjorden, northwest Spitsbergen. *Polar Research*(2), pp. 81-91.

Dowdeswell, J., Elverhøi, A., & Spielhagen, R. (1998). Glacimarine sedimentary processes and facies on the polar North Atlantic margins. *Quaternary Science Reviews, 17*(1-3), 243-272.

Dowdeswell, J., Hagen, J., Björnsson, H., Glazovsky, A., Harrison, W., Holmlund, P., et al. (1997). The mass balanceof circum-Arctic glaciers and recent climate change. *Quaternary Research, 48*, 1-14.

Dowdeswell, J., Hamilton, G., & Hagen, J. (1991). The duration of the active phase of surge-type glaciers: Contrast between Svalbard and other regions. *Journal of Glaciology, 37*, 86-98.

Dowdeswell, J., Hodgkins, R., Nuttall, A.-M., Hagen, J., & Hamilton, G. (1995). Mass balance change as a control on the frequency and occurrence of glacier surges in Svalbard, Norwegian High Arctic. *Geophysical Research Letters, 22*(21), 2909-2912.

Dowdeswell, J., Hogan, K., Evans, J., Noormets, R., Ó Cofaigh, C., & Ottesen, D. (2010). Past ice-sheet flow east of Svalbard inferred from streamlined subglacial landforms. *Geology, 38*(2), 163-166.

Dowdeswell, J., Ó Cofaigh, C., & Pudsey, C. (2004). Thickness and extent of the subglacial till layer beneath an Antarctic paleo-ice stream. *Geology, 32*(1), 13-16.

Dowdeswell, J., Ottesen, D., Evans, J., & C.Ó. Cofaigh, J. A. (2008). Submarine glacial landforms and rates of ice-stream collapse. *Geology*(36), pp. 819-822.

Elverhøi, A., Andersen, E., Dokken, T., Hebbeln, D., Spielhagen, R., Svendsen, J., et al. (1995). The growth and decay of the Late Weichselian Ice Sheet in western Svalbard and adjacent areas based on provenance studies of marine sediments. *Quaternary Research, 44*, 303-316.

Elverhøi, A., Liestøl, O., & Nagy, J. (1980). Glacial erosion, sedimentation and microfauna in the inner part of Kongsfjorden, Spitsbergen. *Norsk Polarinstitutt Skrifter, 172*, 33-58.

Elverhøi, A., Lønne, Ø., & Seland, R. (1983). Glaciomarine sedimentation in a modern fjord environment, Spitsbergen. *Polar Research*(1), pp. 127-149.

Evans, D., & Lemmen, D. R. (n.d.). Glacial landsystems of the Southwest Laurentide Ice Sheet: modern Icelandic analogues. *Journal of Quaternary Science, 14*, 673-691.

Evans, D., & Rea, B. (1999). Geomorphology and sedimentology of surging glaciers: a landsystem approach. *Annals of Glaciology, 28*, 75-82.

Evans, D., & Rea, B. (2003). Surging glacier landsystem. *Glacial Landsystems*, 259-288. (D. Evans, Ed.) London: Arnold.

Evans, D., & Twigg, D. (2002). The active temperate glacial landsystem: a model based on Breidamerkurjokull and Fjallsjokull, Iceland. *Quaternary Science Reviews, 21*, 2143-2177.

Evans, D., Twigg, D., Rea, B., & Orton, C. (2009). Surging glacier landsystem of Tungnaárjökull, Iceland. *Journal of Maps, 5*(1), 134-151.

Forman, S., & Miller, G. (1984). Time-Dependent Soil Morphologies and Pedogenic Processes on Raised Beaches, Bröggerhalvöya, Spitsbergen, Svalbard Archipelago. *Arctic and Alpine Research, 16*(4), 381-394.

Forwick, M., & Vorren, T. (2002). Deglaciation history and postglacial sedimentation in Balsfjord (North Norway). *Polar Research, 21*(2), 259-266.

Forwick, M., & Vorren, T. (2007). Holocene mass-transport activity and climate in outer Isfjorden, Spitsbergen: marine and subsurface evidence. *The Holocene, 17*(6), 707-716.

Forwick, M., & Vorren, T. (2009). Late Weichselian and Holocene sedimentary environments and ice rafting in Isfjorden, Spitsbergen. *Paleogeography, Paleoclimatology, Paleoecology, 280*, 258-274.

Forwick, M., & Vorren, T. (2010). Stratigraphy and deglaciation of the Isfjorden area, Spitsbergen. *Norwegian Journal of Geology, 90*, 163-179.

Forwick, M., & Vorren, T. (2011). Submarine mass-wasting in Isfjorden, Spitsbergen. In Y. Yamada, *Submarine Mass Movements and Their Consequences* (Vol. 31, pp. 711-722). Advances in Natural and Technological Hazards Research.

Forwick, M., Baeten, N., & Vorren, T. (2009). Pockmarks in Spitsbergen fjords. *Norwegian Journal of Geology, 89*, 65-77.

Forwick, M., Vorren, T., Hald, M., Korsun, S., Roh, Y., Vogt, C., et al. (2010). Spatial and temporal influence of glaciers and rivers on the sedimentary environment in Sassenfjorden and Tempelfjorden, Spitsbergen. *Fjord Systems and Archives, 344*, 163-193. (J. Howe, W. Austin, M. Forwick, & M. Paetzel, Eds.) Geological Society, London, Special Publications.

Førland, E., Benestad, R., Flatøy, F., Hanssen-Bauer, I., Haugen, J., Isaksen, K., et al. (2009). Climate development in North Norway and the Svalbard region during 1900-2100. *Norsk Polarinstitutt Rapportserie, 128*.

GEOTEK. (2000). Geotek Multi-Sensor Core Logger (MSCL) Manual.

Gerland, S., & Hall, R. (2006). Variability of fast-ice thickness in Spitsbergen fjords. *Annals of Glaciology, 44*, 231-239.

Gerland, S., & Renner, A. (2007). Sea-ice mass-balance monitoring in an Arctic fjord. *Annals of Glaciology, 46*, 435-442.

Gilbert, R. (1990). Rafting in glacimarine environments. *Geological Society, London, Special Publications, 53*, 105-120.

Gilbert, R., Nielsen, N., Möller, H., Desloges, J., & Rasch, M. (2002). Glacimarine sedimentation in Kangerdluk (Disko Fjord), West Greenland, in response to a surging glacier. *Marine Geology, 191*, 1-18.

Glasser, N., & Hambrey, M. (2001). Tidewater glacier beds: insights from iceberg debris in Kongsfjorden, Svalbard. *Journal of Glaciology, 47*(157).

Hagen, J., Liestøl, O., Roland, E., & Jørgensen, T. (1993). Glacier Atlas of Svalbard and Jan Mayen. *Middelelser* (129).

Hald, M. H. (1998). Early Preboreal cooling in the Nordic seas region triggered by. *Geology, 26*, 615-618.

Hald, M., Dahlgren, T., Olsen, T.-E., & Lebesbye, E. (n.d.). Late Holocene paleoceanography in Van Mijenfjorden, Svalbard. *Polar Research, 20*(1), 23-35.

Hald, M., Ebbesen, H., Forwick, M., Godtliebsen, F., Khomenko, L., Korsun, S., et al. (2004). Holocene paeloceanography and glacial history of the West Spitsbergen area, Euro-Arctic margin. *Quaternary Science Reviews, 23*, 2075-2088.

Hamilton, G., & Dowdeswell, J. (1996). Controls of glacier surging in Svalbard. *Journal of Glaciology, 42*, 157-168.

Hjulström, F. (1935). *Studies of the morphological activity of rivers as illustrated by the River Fyris. Inaugural dissertation.* Uppsala: Almkvist & Wiksells.

Holtedahl, H. (1975). The geology of the Hardangerfjord, West Norway. *Norges Geologiske Undersøkelse, 323*.

Hoskin, C., & Burrell, D. (1972). Sediment transport and accumulation in a fjord basin, Glacier Bay, Alaska. *Journal of Geology, 80*, 359-551.

Hovland, M., Heggland, R., De Vries, M., & Tjelta, T. (2010). Unit-pockmarks and their potential significance for predicting fluid flow. *Marine and Petroleum Geology, 27*(6), 1190-1199.

Howe, J., Austin, W., Forwick, M., Paetzel, M., Harland, R., & Cage, A. (2010). Fjord systems and archives: a review. (J. Howe, W. Austin, M. Forwick, & M. Paetzel, Eds.) *Geological Society, London, Special Publications, 344*, 5-15.

Howe, J., Moreton, S., Morri, C., & Morris, P. (2003). Multibeam bathymetry and the depositional environments of Kongsfjorden and Krossfjorden, western Spitsbergen, Svalbard. *Polar Research*(22 (2)), pp. 301-316.

Ingólfsson, Ó., & Landvik, J. (2013). The Svalbard-Barents Sea ice-sheet - Historical, current and future perspectives. *Quaternary Science Reviews, 64*, 33-60.

Ito, H., & Kudoh, S. (1997). Characteristics of water in Kongsfjorden, Svalbard. (T. National Institute of Polar Research, Ed.) *Proc. NIPR Symp. Polar Meterol. Glaciol.*(11), pp. 211-232.

J.A., D., Drewry, D., Liestøl, 0., & Orheim, 0. (1984). Airborne radio echo sounding of sub-polar glaciers in Spitsbergen. *Norsk Polarinstitutt Skrifter, 182*, 41.

Jernas, P., Klitgaard-Kristensen, D., Husum, K., Koç, N., Tverberg, V., Loubere, P., et al. (In prep.). Response of modern Arctic benthic foraminiferal fauna to annual environmental changes; evidence from Kongsfjorden, Svalbard.

Jessen, S., Rasmussen, T., Nielsen, T., & Solheim, A. (2010). A new Late Weichselian and Holocene marine chronology for the western Svalbard slope 30000-0 cal years BP. *Quaternary Science Reviews*(29), pp. 1301-1312.

Kehrl, L., Hawley, R., Powell, R., & Brigham-Grette, J. (2011). Glacimarine sedimentation processes at Kronebreen and Kongsvegen, Svalbard. *Journal of Glaciology*(57), pp. 841-847.

Kempf, P., Forwick, M., Laberg, J., & Vorren, T. (subm.). Late Weichselian – Holocene sedimentary palaeoenvironment and glacial activity in the high-Arctic van Keulenfjorden, Spitsbergen. Submitted to "The Holocene".

Killingtveit, Å., Pettersson, L.-E., & Sand, K. (2003). Water-balance investigations in Svalbard. *Polar Research, 22*(2), 161-174.

King, E., Hindmarsh, R., & Stokes, C. (2009). Formation of mega-scale glacial lineations observed beneath a West Antarctic ice stream. *Nature Geoscience, 2*, 585-588.

King, L., Rokoengen, K., Fader, G., & Gunleiksrud, T. (1991). Till-tongue stratigraphy. *The Geological Society of America, Bulletin, 103*(5), 637-659.

Kohler, J., James, T. D., Murray, T., Nuth, C., Brandt, O., Barrand, N. E., et al. (2007). Acceleration in thinning rate on western Svalbard glaciers. *Geophysical Research Letters*(34).

Kristensen, L., Benn, D., Hormes, A., & Ottesen, D. (2009). Mud aprons in front of Svalbard surge moraines. Evidence of subglacial deforming layers or proglacial glaciotectonics? *Geomorphology, 111*, 206-221.

Lamb, H. (1977). *Climate: present, past and future.* London: Methuen.

Landvik, J., Bondevik, S., Elverhøi, A., Fjeldskaar, W., Mangerud, J., Salvigsen, O., et al. (1998). Last Glacial Maximum of Svalbard and the Barents Sea Area: Ice Sheet Extent and Configuration. *Quaternary Science Reviews*(17), pp. 43-75.

Landvik, J., Ingólfsson, Ó., Mienert, J., Lehman, S., Solheim, A., Elverhøi, A., et al. (2005). Rethinking Late Weichselian ice-sheet dynamics in coastal NW-Svalbard. *Boreas*(34), pp. 7-24.

Lefauconnier, B., Hagen, J., & Rudant, J. (1994). Flow speed and calving rate of Kongsbreen glacier, Svalbard, using SPOT images. *Polar Research, 11*, 59-65.

Lehman, S., & Forman, S. (1992). Late Weichselian glacier retreat in Kongsfjorden, West Spitsbergen, Svalbard. *Quaternary Research, 37*, 139-154.

Liestøl, O. (1975). Glaciological work in 1975. *Norsk Polarinstitutt*, 147-158.

Liestøl, O. (1976). Årsmorener foran Nathorstbreen? *Aarb. Nor. Polarinst.*, 361– 363.

Liestøl, O. (1988). The glaciers in the Kongsfjorden area, Spitsbergen. *Norsk geogr. Tidsskr., 42*, 231-238.

Maclachlan, S., Howe, J., & Vardy, M. (2010). Morphodynamic evolution of Kongsfjorden-Krossfjorde, Svalbard, during the Late Weichselian and the Holocene. (J. Howe, W. Austin, M. Forwick, & M. Paetzel, Eds.) *Geological Society, London, Special Publications, Fjord Systems and Archives*(344), pp. 195-205.

Mangerud, J., & Landvik, J. (2007). Younger Dryas cirque glaciers in western Spitsbergen: smaller than during the Little Ice Age. *Boreas, 36*, 278-285.

Mangerud, J., Bolstad, M., Elgersma, A., Helliksen, D., Landvik, J., Lønne, I., et al. (1992). The Last Glacial Maximum on Spitsbergen. *Quaternary Research, 38*, 1-31.

Meier, M., & Post, A. (1969). What are Glacier Surges? *Can. J. Earth Sci.*(6), pp. 807-817.

Meier, M., & Post, A. (1987). Fast tidewater glaciers. *Journal of Geophysical Research: Solid Earth, 92*(B9), 9051-9058.

Melvold, K., & Hagen, J. (1998). Evolution of a surge-type glacier in its quiescent phase: Kongsvegen, Spitsbergen, 1964-95. *Journal of Glaciology, 44*, 394-404.

Menzies, J. (1979). A review of the literature on the formation and location of drumlins. *Earth Science Review, 14*, 315-359.

Menzies, J., & Rose, J. (1989). Subglacial bedforms - drumlins, rogen moraine, and associated subglacial bedforms. *Sedimentary Geology (special issue), 62*, 214.

Mercer, J. (1961). The response of fjord glaciers to changes in the firn limit. *Journal of Glaciology, 3*, 850-858.

Murray, T., Strozzi, T., Luckman, A., Jiskoot, H., & Christakos, P. (2003). Is there a single surge mechanism? Contrasts in dynamics between glacier surges in Svalbard and other regions. *Journal of Geophysical Research: Solid Earth, 108*(B5).

Murray, T., Stuart, G., Miller, P., Woodward, J., Smith, A., Porter, P., et al. (2000). Glacier surge propagation by thermal evolution at the bed. *Journal of Geophysical Research: Solid Earth, 105*(B6), 13491-13507.

Nesje, A., Jansen, E., Birks, H., Bjune, A., Bakke, J., Andersson, C., et al. (2005). Holocene climate variability in the Northern North Atlantic Region: a review of terrestrial and marine evidence. *The Nordic seas: an integrated perspective, geophysical monograph, 158*, 289-322. (H. Drange, T. Dokken, T. Furevik, R. Gerdes, & W. Berger, Eds.) Washington: American Geophysical Union.

Ó Cofaigh, C., Dowdeswell, J., Allen, C., Hiemstra, J., Pudsey, C., Evans, J., et al. (2005). Flow dynamics and till genesis associated with a marine-based Antarctic paleo-ice stream. *Quaternary Science Reviews, 24*, 709-740.

Ó Cofaigh, C., Dowdeswell, J., Evans, J., & Larter, R. (2008). Geological constraints on Antarctic paleo-ice-stream retreat. *Earth Surface Processes and Landforms, 33*(4), 513-525.

Ó Cofaigh, C., Pudsey, C., Dowdeswell, J., & Morris, P. (2002). Evolution of subglacial bedforms along a paleo-ice stream, Antarctic Peninsula continental shelf. *Geophysical Research Letters*(8), pp. 1-41.

Ottesen, D., & Dowdeswell, J. (2006). Assemblages of submarine landforms produced by tidewater glaciers in Svalbard. *Journal of Geophysical Research*(111), p. F01016.

Ottesen, D., & Dowdeswell, J. (2009). An inter-ice stream glaciated margin: submarine landforms and a geomorphic model based on marine-geophysical data from Svalbard. *Geological Society of America Bulletin, 121*(11/12), 1647-1665.

Ottesen, D., Dowdeswell, J., & Rise, L. (2005). Submarine landforms and the reconstruction of fast-flowing ice streams within a large Quaternary ice sheet: the 2500-km-long Norwegian-Svalbard margin (57° - 80° N). *Geological Society of America Bulletin*(117), pp. 1033-1050.

Ottesen, D., Dowdeswell, J., Benn, D., Kristensen, L., Christiansen, H., Christensen, O., et al. (2008). Submarine landforms characteristic of glacier surges in two Spitsbergen fjords. *Quaternary Science Reviews*(27), pp. 1583-1599.

Ottesen, D., Dowdeswell, J., Landvik, J., & Mienert, J. (2007). Dynamics of the Late-Weichselian ice sheet on Svalbard inferred from high-resolution sea-floor morphology. *Boreas, 36*, 286-306.

Ottesen, R., Bogen, J., Finne, T., Andersson, M., Dallman, W., Eggen, O., et al. (2010). *Geochemical atlas of Norway. Part 2: Geochemical atlas of Spitsbergen: Chemical composition of overbank sediments.* Trondheim: Geological Survey of Norway.

Pettersson, R. (2004). *Dynamics of the cold surface layer of polythermal Storglaciären, Sweden.* Stockholm: Doctoral dissertation.

Plassen, L., Vorren, T., & Forwick, M. (2004). Integrated acoustic and coring investigations of glacigenic deposits in Spitsbergen fjords. *Polar Research, 23*(1), 89-110.

Potts, P. (2003). *Handbook of Rock Analysis.* Viridian.

Prest, V., Grant, D., & Rampton, V. (1968). Glacial Map of Canada, Map 1253A. *Geological Survey of Canada*.

Quinn, R., Bull, J., & Dix, J. (1998). Optimal Processing of Marine High-Resolution Seismic Reflection (Chirp) Data. *Marine Geophysical Researches, 20*, 13-20.

Rasmussen, S., Vinther, B., Clausen, H., & Andersen, K. (2007). Early Holocene climate oscillations recorded in three Greenland ice cores. *Quaternary Science Reviews, 26*, 1907-1914.

Raymond, C. (1987). How do glaciers surge? A review. *92*(B9), 9121-9134.

Sexton, D., Dowdeswell, J. S., & Elverhøi, A. (1992). Seismic architecture and sedimentation in northwest Spitsbergen fjords. *Marine Geology, 103*, 53-68.

Sharp, M. (1984). Annual moraine ridges at Skálafellsjökull, south-east Iceland. *Journal of Glaciology, 30*(104).

Sharp, M. (1985). Crevasse-Fill-Ridges - a landform type characteristic of surging glaciers? *Geografiska Annaler. Series A. Physical Geography, 67*(3/4), 213-220.

Sharp, M. (1988). Surging glaciers: behaviour and mechanisms. *Progress in Physical Geography, 12*(3), 349-370.

Skirbekk, K., Kristensen, D., Rasmussen, T., Koc, N., & Forwick, M. (2010). Holocene climate variations at the entrance to a warm Arctic fjord: evidence from Kongsfjorden trough, Svalbard. *Fjord Systems and Archives, 344*, 289-304. (J. Howe, W. Austin, M. Forwick, & M. Paetzel, Eds.) Geological Society, London, Special Publications.

Solheim, A. (1991). *The depositional environment of surging sub-polar tidewater glaciers: a case study of the morphology, sedimentation and sediment properties in a surge-affected marine basin outside Nordaustlandet, Northern Barents Sea* (Vol. 194). Oslo: Norsk Polarinstitutt Skrifter.

Solheim, A., & Pfirman, S. (1985). Sea-floor morphology outside a grounded, surging glacier; Bråsvellbreen, Svalbard. *Marine Geology, 65*, 127-143.

Solheim, A., Andersen, E., Elverhøi, A., & Fiedler, A. (1996). LAte Cenozoic depositional history of the western Svalbard continental shelf, controlled by subsidence and climate. *Global and Planetary Change*(12), pp. 135-148.

Stokes, C., & Clark, C. (2002). Are long subglacial bedforms indicative of fast ice flow? *Boreas, 31*(3), 239-249.

Strahler, A., & Strahler, A. (2005). *Physische Geographie (Modern Physical Geography)* (3 ed.). Stuttgart: Verlag Eugen Ulmer.

Sundborg, Å. (1967). Some Aspects on Fluvial Sediments and Fluvial Morphology I. General Views and Graphic Methods. *Geografiska Annaler. Series A, Physical Geography, 49*(2/4), 333-343.

Svendsen, H., Beszczynska-Møller, A., Hagen, J., Lefauconnier, B., Tverberg, V., Gerland, S., et al. (2002). The physical environment of Kongsfjorden-Krossfjorden, an Arctic fjord system in Svalbard. *Polar Research, 21*(1), 133-166.

Svendsen, J., & Mangerud, J. (1997). Holocene glacial and climatic variations on Spitsbergen, Svalbard. *The Holocene, 7*(1), 45-57.

Svendsen, J., Elverhøi, A., & Mangerud, J. (1996). The retreat of the Barents Sea Ice Sheet on the western Svalbard margin. *Boreas, 25*, 244-256.

Tjallingii, R., Röhl, U., Kölling, M., & Bickert, T. (2007). Influence of the water content on X-ray fluorescence core-scanning measurements in soft marine sediments. *Geochem., Geophys., Geosyst., 8*.

Trusel, L., Powell, R., Cumpston, R., & Brigham-Grette, J. (2010). Modern glacimarine processes and potential future behaviour of Kronebreen and Kongsvegen polythermal tidewater glaciers, Kongsfjorden, Svalbard. *Geological Spciety of London Special Publications*(344), pp. 89-102.

Tulaczyk, S., Scherer, R., & Clark, C. (2001). A ploughing model for the origin of weak tills beneath ice streams: a qualitative treatment. *Quaternary Internationals, 86*, 59-70.

Van Der Veen, C. (1998). Fracture mechanic approach to penetration of bottom crevasses on glaciers. *Cold Reg. Sci. Technol., 27*, 213-223.

Vorren, T., & Plassen, L. (2002). Deglaciation and paleoclimate of the Andfjord-Vågsfjord area, North Norway. *Boreas, 31*, 97-125.

Vorren, T., Hald, M., Edvardsen, M., & Lind-Hansen, O.-W. (1983). Glacigenic sediments and sedimentary environments on continental shelves: General principles with a case study from the Norwegian shelf. *Glacial deposits in north-west Europe*, 61-73. (J. Ehlers, Ed.) Rotterdam: Balkema.

Weber, M., Niessen, F., Kuhn, G., & Wiedicke, M. (1997). Calibration and application of marine sedimentary physical properties using a multi-sensor core logger. *Marine Geology, 136*(3-4), 151-172.

Wellner, J., Lowe, A., Shipp, S., & Anderson, J. (2001). Distribution of glacial geomorphic features on the Antarctic continental shelf and correlation with substrate: implications for ice behaviour. *Journal of Glaciology, 47*(158), 397-411.

Weltje, G., & Tjallingii, R. (2008). Calibration of XRF core scanners for quantitative geochemical logging of sediment cores: Theory and application. *Earth and Planetary Science Letters, 274*, 423-438.

Whittington, R., Forsberg, C., & Dowdeswell, J. (1997). Seismic and side-scan investigations of recent sedimentation in an ice-proximal glacimarine setting, Kongsfjorden, north-west Spitsbergen. In T. D. al. (Ed.), *Acoustic images of glaciated continental margins* (pp. 175-178). London.


UNIVERSITY
OF TROMSØ